



University of **HUDDERSFIELD**

University of Huddersfield Repository

Clayton, Kate

Novel Polythiophenes for Biosensor Applications

Original Citation

Clayton, Kate (2011) Novel Polythiophenes for Biosensor Applications. Doctoral thesis, University of Huddersfield.

This version is available at <http://eprints.hud.ac.uk/id/eprint/11677/>

The University Repository is a digital collection of the research output of the University, available on Open Access. Copyright and Moral Rights for the items on this site are retained by the individual author and/or other copyright owners. Users may access full items free of charge; copies of full text items generally can be reproduced, displayed or performed and given to third parties in any format or medium for personal research or study, educational or not-for-profit purposes without prior permission or charge, provided:

- The authors, title and full bibliographic details is credited in any copy;
- A hyperlink and/or URL is included for the original metadata page; and
- The content is not changed in any way.

For more information, including our policy and submission procedure, please contact the Repository Team at: E.mailbox@hud.ac.uk.

<http://eprints.hud.ac.uk/>



University of
HUDDERSFIELD

Novel Polythiophenes for Biosensor Applications

Kate L. Clayton

Supervisors Dr Carl Hall and Dr Gareth Parkes

Thesis submitted in accordance with the requirements of the
University of Huddersfield for the degree of Doctor of Philosophy

February 2011

Copyright Statement

- i. The author of this thesis (including any appendices and/or schedules to this thesis) owns any copyright in it (the “Copyright”) and s/he has given The University of Huddersfield the right to use such Copyright for any administrative, promotional, educational and/or teaching purposes.
- ii. Copies of this thesis, either in full or in extracts, may be made only in accordance with the regulations of the University Library. Details of these regulations may be obtained from the Librarian. This page must form part of any such copies made.
- iii. The ownership of any patents, designs, trade marks and any and all other intellectual property rights except for the Copyright (the “Intellectual Property Rights”) and any reproductions of copyright works, for example graphs and tables (“Reproductions”), which may be described in this thesis, may not be owned by the author and may be owned by third parties. Such Intellectual Property Rights and Reproductions cannot and must not be made available for use without the prior written permission of the owner(s) of the relevant Intellectual Property Rights and/or Reproductions.

Acknowledgements

I would like to acknowledge Dr Carl Hall for the opportunity to work on this project and for his supervision.

I would also like to acknowledge Dr Gareth Parkes, Professor Roger Jewsbury and Professor Rob Brown for their encouragement and help throughout this project.

Many members of staff in the department have contributed their support and therefore I would like to thank the stores team, the technicians Margret Scott, Ibrahim George, Natasha Reed, Ian Johnson, Felix Owusu-Kwarteng and Neil Mclay.

Many people have helped me along the way and I thank them all but it is the love, support and encouragement from my husband, Steven Clayton, my close friends Katie Hewson, Alison Langley, Simone Swift and especially Natalie Duncalf and my family Maria, Brian, Stephen Wilson and my cousin Dr David Hales that has made the completion and success of this project possible.

Abstract

Novel Polythiophenes for Biosensor Applications

Kate L. Clayton

The development of an enzyme biosensor employing a novel functionalised polythiophene matrix is presented. The research upon conducting polymer platforms for biological immobilisation is extensive but by no means exhaustive and therefore this investigation contributes to the field of glucose detection with covalently immobilised glucose oxidase upon novel copolymers of N-succinimido thiophene-3-acetate/3-methylthiophene (STA-MT), trans-3-(3-thienyl) acetic acid/3-methylthiophene (TTA-MT) and N-succinimido trans-3-(3-thienyl) acetate/3-methylthiophene STTA-MT.

Polymer characterisation was performed using electrochemical techniques, primarily cyclic voltammetry. The examination of various substituted conducting polymers from the polythiophene family was performed where 3-methylthiophene was selected for copolymerisation due to its low oxidation potential and redox behaviour. Copolymerisation of the novel monomers provided reversible and stable films and succeeded in generating a range of copolymer ratios characterised by cyclic voltammetry with the available binding sites calculated using SEM-EDX. Film morphology and dopant intercalation were investigated, providing supporting evidence for the successful copolymerisation of novel monomers with 3-methylthiophene.

Optimisation of the biosensor format was investigated through analysis of film thickness, copolymer ratio and enzyme immobilisation time. A film thickness generated with 50 mC provided a stable film with good response to glucose over a wide range of immobilisation times and was employed for all other biosensor investigations. A 10% functional monomer content provided enhanced current signals upon glucose addition which supported the findings of Kuwahara *et al* where a 10% thiophene-3-acetic acid content within a thiophene-3-acetic acid/3-methylthiophene copolymer demonstrated enhanced biosensor behaviour. All studies were compared against the thiophene-3-acetic acid and 3-methylthiophene system generated under the optimised conditions of the novel copolymer films.

The evaluation of the immobilised glucose oxidase as an amperometric biosensor within a mediated system employing *p*-benzoquinone was performed generating fast response times within 4 seconds, good stability and excellent current response to glucose between 1.4 and 1.9 mA/cm² after the addition of 15 mM of glucose. All three novel biosensor systems exhibit good analytical performance demonstrating excellent repeatability typically over 90%, reproducibility of over 80% and shelf-life stability of 85-96% over a seven day analysis and between 50-78% after 1 month.

Abbreviations and Acronyms

MeCN	Acetonitrile
$(\text{NH}_4)_2\text{S}_2\text{O}_8$	Ammonium persulfate
BTA	Tert-butyl thiophene-3-carboxylate
CP	Conducting polymer
CE	Counter electrode
CV	Cyclic voltammogram
DCM	Dichloromethane
DCC	Dicyclohexylcarbodiimide
DIC	Diisopropylcarbodiimide
EL	Electroluminescence
EMI	Electromagnetic interference
EDX	Electron Diffraction X-ray
FTIR	Fourier Transform Infra Red
Gox	Glucose oxidase
g	Gram
HOMO	Highest Occupied Molecular Orbital
hr	Hour
i	Current (Amperes)
ICP	Intrinsically conducting polymer
ITO	Indium-tin Oxide
FeCl_3	Iron chloride
LED	Light Emitting Diode
LiClO_4	Lithium perchlorate
LUMO	Lowest Unoccupied Molecular Orbital
MS	Mass spectrometry
MT	3-Methylthiophene
mmol	Millimole
M	Molar
mol	Mole
ME	Molecular electronics
MoCl_5	Molybdenum chloride
NHS	N-Hydroxysuccinimide
STA	N-succinimido thiophene-3-acetate*
STTA	N-succinimido trans-3-(3-thienyl) acetate
NMR	Nuclear Magnetic Resonance (spectroscopy)
ppm	Parts per million
PAT	Poly(alkylthiophene)
PBT	Poly(bithiophene)
PDDT	Poly(3-dodecylthiophene)
PEDOT	Poly(3,4-ethylenedioxythiophene)
PLED	Polymer light emitting diode
POT	Poly(3-octylthiophene)
E	Potential (V)
PC	Propylene carbonate
PT	Polythiophene
PTS	<i>p</i> -toluene sulfonate
RE	Reference Electrode

SCE	Saturated Calomel Electrode
SEM	Scanning electron microscopy
S	Siemens
σ	Sigma
TBAClO ₄	Tetrabutylammonium perchlorate
TBATFB	Tetrabutylammonium tetrafluoroborate
T3AA	Thiophene-3-acetic acid
TCA	3-Thiophene carboxylic acid
TMA	3-Thiophenemalonic acid
TTA	Trans-3-(3-thienyl) acrylic acid
BFEE	Trifluoroborate–ethyl ether
SO ₃ CF ₃	Trifluoromethyl sulfonate
UV	Ultra violet
UV-Vis	Ultra violet -Visible spectrometry
Vis	Visible
V	Volts
λ	Wavelength (nm)
cm ⁻¹	Wavenumber
WE	Working Electrode
XRD	X-Ray Diffraction

*IUPAC; (2,5-dioxopyrrolidin-1-yl) thiophene-3-carboxylate known and referenced in this thesis as N-succinimido thiophene-3-acetate¹³⁷

Table of Contents

Acknowledgements	ii
Abstract	iii
Abbreviations and Acronyms	iv
Table of Contents	vi
List of Tables	x
 CHAPTER 1 INTRODUCTION	 1
1.0. The Discovery of Conducting Polymers	1
1.1. What are Conducting Polymers	2
1.2. Conducting Polymers	2
1.3. Conductivity in Conducting Polymers	3
1.3.1. Atomic Structure and Bonding	5
1.3.2. Hybridisation and Conjugation	5
1.3.3. Conductivity in Metals	6
1.3.4. Doping of Conducting Polymers	6
1.4. Polythiophenes	8
1.4.1. Substituted Thiophenes	9
1.4.2. Solvent	14
1.4.3. Dopant Species	14
1.5. Polythiophene Polymerisation	15
1.5.1. Oxidative Polymerisation	15
1.5.2. Electrochemical Polymerisation	16
1.6. Regioregular Poly(alkylthiophenes)	17
1.7. Electrochemistry	19
1.7.1. Cyclic Voltammetry	19
1.7.2. Electrochromism	25
1.8. Applications	27
1.9. History of Biosensors	28
1.10. What are Biosensors?	28
1.11. Transduction	29
1.11.1. Amperometric Biosensors	29

1.12. Electron Transfer Mechanisms	29
1.13. Biological Elements	31
1.13.1. Glucose Oxidase	32
1.14. Immobilisation of the Biological Component	33
1.14.1. Enzyme activity	33
1.14.2. Enzyme Kinetics	34
1.14.3. Michaelis-Menten Equation	34
1.14.4. Immobilised Enzyme Kinetics	37
1.14.5. Conformational Changes	37
1.14.6. Partitioning Effects	38
1.14.7. Diffusion Limitations	38
1.15. Immobilisation Matrices	38
1.16. Enzyme Immobilisation Techniques	39
1.16.1. Physical Adsorption	40
1.16.2. Physical Entrapment	40
1.16.3. Affinity Binding	41
1.16.4. Covalent Immobilisation	41
1.16.5. Carbodiimide coupling	42
1.17. Factors Influencing Sensor Response	43
1.17.1. Optimising the Sensor Response	43
1.17.2. Signal Reproducibility	44
1.17.3. Sensor Response Time	44
1.17.3.1. Diffusion Effects	44
1.17.3.2. Substrate and Enzyme Concentration	45
1.17.3.3. Effect of pH and Temperature	45
1.17.3.4. Matrix Thickness and Dialysis Membrane Effects	45
1.18. Polythiophenes for Biosensor Applications	46
CHAPTER 2 MATERIALS AND METHODS	52
2.0. Synthetic Procedures	55
2.0.1. Synthesis of Methyl thiophene-3-carboxylate	55
2.0.2. Synthesis of Tert-butyl thiophene-3-carboxylate	56
2.0.3. Synthesis of N-succinimido thiophene-3-acetate	58
2.0.4. Synthesis of N-succinimido trans-3-(3-thienyl) acetate	59
2.1. Polymer Generation	60
2.1.1. Chemical Polymerisation	60
2.1.2. Electrochemical Polymerisation	61
2.2. Film Characterisation	61

2.3. Atomic Absorption Spectroscopy	62
2.4. Scanning Electron Microscopy with Elemental Detection	63
2.4.1. Elemental Analysis	64
2.5. Fourier Transform Infra Red Spectroscopy (FTIR)	65
2.6. Nuclear Magnetic Resonance (NMR)	65
2.7. Biosensor Analysis	65
2.7.1. Film Preparation	65
2.7.2. Enzyme Immobilisation	66
2.7.3. Response to Glucose	66
2.8. UV Spectroscopy	67
CHAPTER 3 ELECTROCHEMISTRY OF POLYTHIOPHENE MATERIALS	69
3.0. Electrochemistry of Poly(thiophenes)	70
3.0.1. Electrochemical Polymerisation of Bithiophene	70
3.0.2. Stability of Poly(bithiophene) during Cycling	74
3.0.3. Electrochemical Characterisation of Bithiophene	76
3.0.4. Influence of Solvent and Dopant upon Bithiophene Growth	77
3.0.5. Investigating Different Dopants within Film Growth and Characterisation	80
3.0.6. Effects of Scan Rate upon Poly(bithiophene)	84
3.1. Alkyl Thiophene Analogues	85
3.1.1. Electrochemistry of Poly(3-methylthiophene)	86
3.1.2. Electrochemistry of Thin Film Poly(3-octylthiophene)	90
3.1.3. Electrochemistry of Thin Film Poly(3-dodecyl thiophene)	92
3.1.4. Electrochemistry of Thin Film Poly(3-octadecylthiophene)	93
3.2. Acid Substituted Thiophene Monomers	94
3.2.1. Chemical Polymerisation	95
3.2.2. Electrochemistry of 3-Thiophenecarboxylic acid	96
3.2.3. Electrochemistry of 3-Thiophenemalonic acid	98
3.2.4. Electrochemistry of Thiophene-3-acetic acid	98
3.2.5. Electrochemistry of Trans-3-(3-thienyl) acrylic acid	101
3.3. Electrochemical Investigation of the Activated Ester Compounds	103
3.3.1. Electrochemical Investigation of Tert-butyl thiophene-3-carboxylate	104
3.3.2. Electrochemical Investigation of N-succinimido thiophene-3-acetate	107
3.4. Copolymerisation	109
CHAPTER 4 POLYMER FILM CHARACTERISATION	118
4.0. Techniques Investigated for Functional Monomer Content	122

4.1. Infrared Spectroscopy	122
4.2. Atomic Absorption Spectroscopy	124
4.3. Scanning Electron Microscopy with Energy-Dispersive X-ray Analysis (SEM-EDX)	125
4.4. Surface Coverage using Electrochemistry	130
4.5. Film Morphology	136
 CHAPTER 5 BIOSENSOR ANALYSIS	 157
5.0. Sensor Response in a Non-Mediated Environment	159
5.0.1. Investigation of The Novel N-succinimido thiophene-3-acetate and 3-Methylthiophene Copolymer	159
5.0.1.1. Reproducibility	160
5.0.1.2. Investigation of Length of Enzyme Exposure upon Sensor Response	161
5.0.1.3. Examination of Copolymer Thickness	163
5.0.1.4. Investigation of Analyte Diffusion	164
5.1. Sensor Response in a Mediated Environment	165
5.1.1. Investigation of The Novel N-Succinimido thiophene-3-acetate and 3-Methylthiophene Copolymer	165
5.1.1.1. Altering Potential Binding Sites through Copolymerisation	166
5.1.1.2. Determination of Film Thickness versus Enzyme Exposure	170
5.1.1.3. Repeatability and Reproducibility	177
5.1.1.4. Investigation of Buffer Exposure Time upon Current Response	181
5.1.1.5. Stability Over 72 Hours	182
5.1.1.6. Stability Over Four Weeks	187
5.1.2. Investigation of the Thiophene-3-acetic acid and 3-Methylthiophene Copolymer	189
5.1.2.1. Repeatability and Reproducibility	191
5.1.2.2. Stability Over 72 Hours	191
5.1.2.3. Stability Over Four Weeks Stored at 4 °C	193
5.1.3. Investigation of the Novel Trans-3-(3-thienyl) acrylic acid and 3-Methylthiophene Copolymer	195
5.1.3.1. Repeatability and Reproducibility	195
5.1.3.2. Stability Over 72 Hours	196
5.1.3.3. Stability Over Four weeks	197
5.1.4. Investigation of The Novel N-succinimido trans-3-(3-thienyl) acetate and 3-Methylthiophene Copolymer	198
5.1.4.1. Repeatability and Reproducibility	198
5.1.4.2. Stability Over 72 Hours	199
5.1.4.3. Stability Over Four Weeks	201
5.1.5. Data Comparison of Each Biosensor System	202
5.1.6. Effect of Temperature and pH upon the Sensor Response	206
 CHAPTER 6 CONCLUSIONS	 207
 REFERENCES	 207

Thesis word count 49,155

List of Tables

Table 1.1. Oxidation Potentials of Thiophene Monomers	11
Table 1.2. Applications of Conducting Polymers	27
Table 2.1. Reagents and Purity	53
Table 2.2. ¹ H nmr (500 MHz) Data in CDCl ₃	56
Table 2.3. ¹³ C nmr (500 MHz) Data in CDCl ₃	56
Table 2.4. ¹ H nmr (500 MHz) Data in CDCl ₃	57
Table 2.5. ¹³ C nmr (500 MHz) Data in CDCl ₃	57
Table 2.6. ¹ H nmr (500 MHz) Data in CDCl ₃	58
Table 2.7. ¹³ C nmr (500 MHz) Data in CDCl ₃	59
Table 2.8. ¹ H nmr (500 MHz) Data in CDCl ₃	60
Table 2.9. ¹³ C nmr (500 MHz) Data in CDCl ₃	60
Table 2.10. Various electrolyte and solvents used within the project	61
Table 2.11. Absorbance Readings Taken from an Enzyme Assay and Blank Solution	67
Table 3.1. Potentiostatic Polymerisation of Bithiophene (SCE)	71
Table 3.2. Polymer Growth Data for Different Solvent and Electrolyte systems	79
Table 3.3. Data Produced from Various Dopants Employed for Both Growth and Characterisation. ...	84
Table 3.4. Carboxylic Acid Substituted Thiophenes.	95
Table 3.5. T3AA-MT Molar Ratio and Percentage Functional Monomer Content.	112
Table 3.6. STA-MT Molar Ratio and Percentage Functional Monomer Content	113
Table 3.7. Redox Data for 3-Methylthiophene and the Copolymer Materials	114
Table 4.1. Absorbance Data from the Carbonyl Species Present in Ten Polymer Films	123
Table 4.2. Elemental Data Representing Percentage Atomic Weight.	127
Table 5.1. Kinetic Data for Different Enzyme Immobilisation Times.	163
Table 5.2. Kinetic Data for Increasing Polymer Thickness.	164
Table 5.3. Comparison of current generated at 0.4 V to the average current obtained upon biosensor analysis for the copolymers with different ester content.	168
Table 5.4. Kinetic Data Associated with a Varying Monomer Ratio.	170
Table 5.5. Maximum Response Determined after 15 mM	177
Table 5.6. Kinetic Data for Film Thickness and Enzyme Exposure Time.	177
Table 5.7. Error Associated with Each Set of Sensors for Various Buffer Soak Times.	182
Table 5.8. Percentage Signal Retained Over 72 Hours	186
Table 5.9. Stability of the N-succinimido thiophene-3-acetate Copolymer Sensors Analysed over Four Weeks.	189
Table 5.10. Stability of the 3-thiophene acetic acid Copolymer Sensors Analysed over Four Weeks.	194
Table 5.11. Stability of the Trans-3-(3-thienyl) acrylic acid Copolymer Sensors Analysed over Four Weeks.	198
Table 5.12. Stability of the N-succinimido trans-3-(3-thienyl) acetate Copolymer	202
Sensors Analysed over Four Weeks.	202
Table 5.13. Examination of Data Obtained from a 10% Functional Monomer Content.	202

Chapter 1 Introduction

1.0. The Discovery of Conducting Polymers

Prior to the discovery of conducting polyacetylene, polymer materials were generally utilised for their insulating properties. It was the birth of a new genre of research when enhanced electrical conductivity was produced through polyacetylene by Shirakawa *et al.* in 1977¹. The way was paved and the direction was set for conducting polymer research, which led to Nobel Prize achievements in Chemistry for Hideki Shirakawa, Alan McDiarmid and Alan Heeger in 2000 “for the discovery and development of electrically conductive polymers”. An awareness of the advantages surrounding such materials began the surge forward for potential applications.

“In the field of observation, chance favours only the prepared mind” Louis Pasteur lecture 1854

Like most great discoveries the conducting properties of polymers were pursued due to acts of unintentional practice. Although deemed merely accidental, the highly conductive form of polyacetylene was not discovered by an untrained mind.

Polyacetylene was first noted for its ability to carry an electric current in 1961 by Hatano². Although displaying only semi-conductive properties of 7×10^{-11} to $7 \times 10^{-3} \text{ Sm}^{-1}$ its true potential would soon be discovered. However it was not the only polymer to be examined for electrical qualities through this period. In 1968 “pyrrole black” was identified as a conductive material when it was electrochemically polymerised, producing a brittle film using a variety of oxidising agents³. Whilst it is the conducting nature of the materials that is of particular interest the precluding synthesis of polyacetylene and polypyrrole has been established in some detail since 1958 when polyacetylene was first synthesised by Natta *et al*⁴⁻⁵ as an intractable, air sensitive black powder and in 1916 for the chemical polymerisation of pyrrole⁶.

In 1967 the unfolding of Shirakawa’s achievement commenced at the Tokyo Institute of Technology. A researcher visiting Shirakawa’s group was attempting to synthesise polyacetylene in which a silvery material was produced contrary to the previous black powdered polymer usually obtained. This substance was the result of miscalculation and in fact 1000 times the normal amount of Zeigler-Natter catalyst had been

introduced into the reaction. The film was investigated and conductivities were found to demonstrate semi-conducting materials. A separate investigation led to the “doping” of polyacetylene which involved a chemical process exposing the films to halogens. The result was a film demonstrating conductivity similar to a metal a billion times more conductive than the 1961 findings of Hatano *et al*¹. The semiconducting silvery film represents an undoped form of polyacetylene intractable, insoluble and air sensitive⁷ and when doped with the halogen, iodine, becomes weakly oxidised, green in colour and possesses a high conductivity⁸ of 10^4 Sm^{-1} .

1.1. What are Conducting Polymers

Intrinsically conducting polymers (ICP) are organic polymers that have been termed “synthetic metals”. They are a different class of polymeric materials that possess the electrical, electronic, magnetic and optical properties of a metal while retaining the associated characteristics of common plastics such as mechanical properties, solubility and processibility⁹. The metal associated properties are inherent to the doped form reaching conductivities of 1 to 10^4 Scm^{-1} , although some range from poor conductivity 10^{-15} to 10^{-5} Scm^{-1} towards semi-conducting values¹⁰ of 10^{-6} to 1 Scm^{-1} .

1.2. Conducting Polymers

Conducting polymers differ from typical insulating polymer materials by permitting the movement of electrons through the structure initiating a current flow. The key feature allowing this transfer of charge corresponds to the conjugation present throughout the polymer backbone

Polyacetylene is the simplest conjugated system and is the most studied conducting polymer to date¹¹. However there are significant limitations to this non aromatic polymer including processing difficulties and high instability in air. The effect that this has on the film is described as an initial increase in conductivity followed by a decrease due to irreversible oxidation destroying the conjugated structure¹²⁻¹³.

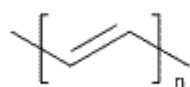
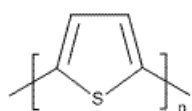
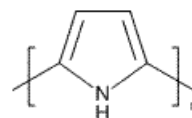


Figure 1.1. Polyacetylene (PA)

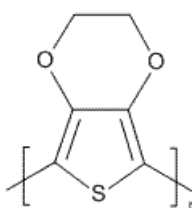
Heterocyclic systems were developed in the 1980s and have become very popular conducting polymers offering increased stability, good conductivities and the ease of synthesis with the option of incorporating substituents into the ring for specific functionality.



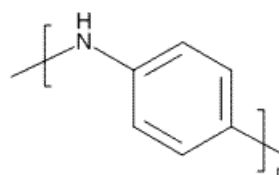
Polythiophene
(PT)



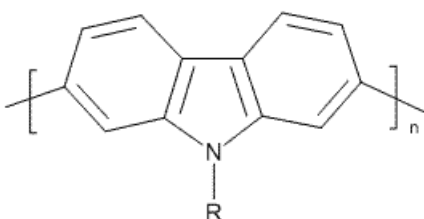
Polypyrrole
(PPy)



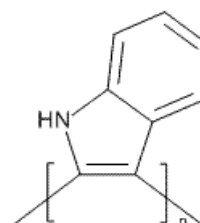
Poly3,4-ethylenedioxythiophene
(PEDOT)



Polyaniline
(PANI)



Polycarbazole
(PCz)



Polyindole
(PI)

Figure 1.2. Structural representation of some conducting polymer units.

1.3. Conductivity in Conducting Polymers

Conductivity is a measure of electrical conduction and is therefore employed to determine the ability of current flow through certain materials. Generally materials with conductivities less than 10^{-8} S/cm are considered insulators, measurements of 10^{-8} through to 10^3 S/cm are categorised as semi-conductors and values greater than 10^3 are classed as conductors¹¹.

Conductivity within a conducting polymer is influenced by a number of parameters. The extent of doping within the polymer is of great value to the level of conductivity achievable¹⁴, as well as the degree of strain acting upon the polymer backbone through the presence of substituents affecting conjugation length¹⁵⁻¹⁷. Such factors provide a very complex assignment to the mechanistic interpretation of conductivity and as a result this translation is avoided and explanation is founded on the band theory.

Conducting polymers exhibit intrinsic conductivity between 10^{-14} and 10^2 Scm^{-1} and the band theory is often used to explain the conductivity observed¹³. The simplest model describes the three different categories materials can be classified under: insulating, semi conducting or conducting.

Polymers in their general function are insulators which are associated with a large energy gap between the conduction and the valence band. Conducting materials such as metals possess a continuous band with no gap as seen in figure 1.3. The space acting to separate these two groups is known as the band gap and is associated with a specific energy which is determined by the materials molecular structure.

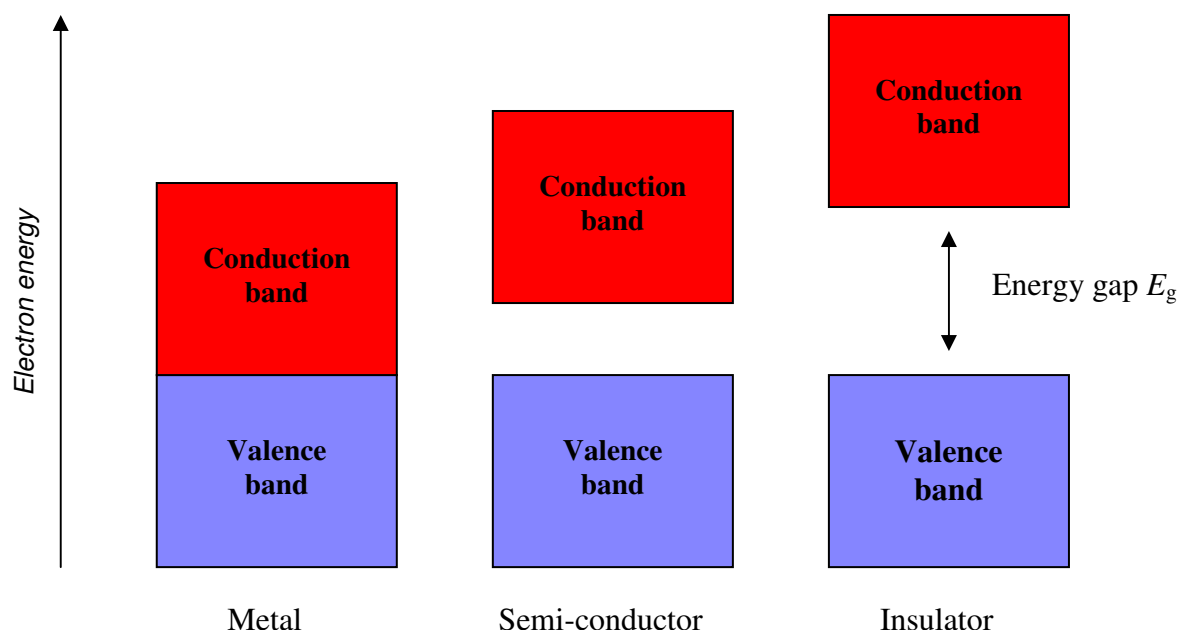


Figure 1.3. Band theory diagram

1.3.1. Atomic Structure and Bonding

The conduction and valence bands, displayed as simple energy blocks, refer to a more complicated system. The valence band is associated with lower energy compared to the conduction band and serves as the highest occupied molecular orbital (HOMO). In the ground state the HOMO or the bonding molecular orbital is fully occupied by electrons, which are observed in the case of insulating and semi-conducting materials. The lowest unoccupied molecular orbital (LUMO) remains empty in the ground state which functions as the conduction band. When an external energy is applied to the system the molecules can be represented in their excited state in which electrons will be found in the anti-bonding region approaching a level of conductivity.

Molecular orbitals are generated by the bonding of two or more atoms. Covalent bonding arises when atomic orbitals of the individual atoms overlap allowing the electrons to interact and become associated to one another. A new orbital is then created with the two electrons being shared across both atoms. Bonding occurs so that lower energy molecular orbitals can be generated, however a higher energy molecular orbital exists, known as the anti-bonding molecular orbital¹⁹.

1.3.2. Hybridisation and Conjugation

Hybridisation of carbon atoms into sp^2 orbitals allows pi-bond formation with the interaction of one sigma (σ) and two pi (π) bonds. By definition conjugated hydrocarbon polymers contain a sequence of linked sp^2 hybridized carbons¹⁹⁻²⁰. Polyacetylene demonstrates this linkage and therefore the acetylene molecule is linear. If the axis between the molecules is not parallel π bonding will not result and conductivity of the molecule through the conjugated backbone will be severely disrupted. As alternating double and single bonds are introduced the available electrons in the π orbitals become delocalised across the conjugated system affecting the energy state of the molecule. The associated energy is lower compared to systems without conjugation and therefore is thermodynamically stable (less reactive)²¹. The HOMO-LUMO gap is reduced through conjugation² and so less energy is needed to overcome the band gap and therefore electrons are more easily promoted to the conduction band.

1.3.3. Conductivity in Metals

The band theory diagram (figure 1.3) demonstrates the metallic structure as a continuous energy band due to the large number of overlapping molecular orbitals significantly reducing the energy of the band gap. The electrons available for metallic bonding do not completely fill the molecular orbitals and this is what gives rise to the characteristic metallic properties. Unoccupied molecular orbitals permit the passage of excited electrons which require only a small quantity of energy such as an applied electrical potential or an input of thermal energy. The electrons are then free to move through the lattice initiating electrical and thermal conductivity²².

The band gap associated with conducting materials represents an energy barrier below 0.2 eV and insulating properties occur with very large band gaps typically greater than 3 eV²³. Semi-conducting materials are somewhere in between with a band gap sufficient enough to prevent high conductivity but low enough to allow some electrons to jump the gap through the application of energy.

Conducting polymers generally fit in the class of semi-conductors. It is their alternating single and double bonds that provide the extended π conjugated system and allows the process of conductivity. Various parameters influence the band gap value such as regioregularity, the doping level and the extent of the conjugation in the system. However conducting polymers cannot remain in their neutral state for conductivity to be established as they require doping before they can imitate the metallic state. Polythiophene band gap values have been reported to range from 2.2 eV in the undoped state to 1.7-1.8 eV²⁴ within a regioregular format and can hypothetically reach 0.14 eV upon a doping level of 100 %²⁰.

1.3.4. Doping of Conducting Polymers

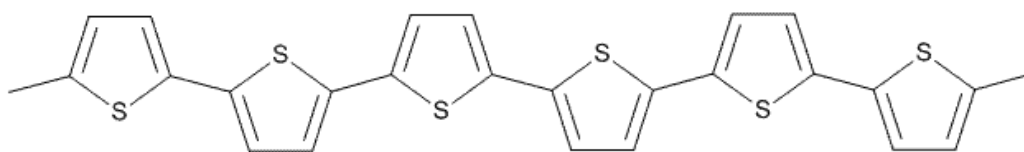
Doping of the polymer systems can be introduced through either chemical or electrochemical processes. Doping is considered a redox reaction and so oxidation or reduction of the molecules produces the corresponding polycations and polyanions. This involves either the injection of an electron (n-doping) or the expulsion of an electron (p-doping). Semi-conductors can be doped producing p- and n-type mechanisms by the addition of atoms such as boron or arsenic. The doping in such systems provides either a partially filled valence band or excess electrons that

populate the LUMO. This is not the case for conducting polymers as an alternative method for storing charge across the polymer chain propagates conductivity through the backbone.

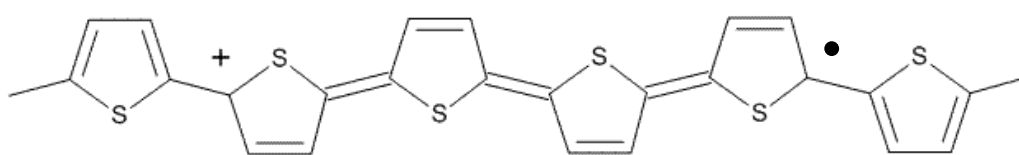
Upon oxidation of a conducting polymer system such as polypyrrole an electron is lost from the delocalised arrangement and a radical cation is formed. The radical and cation species are linked and this creates a polaron. By localising the charge, geometric modifications appear through the polymer system and lead to the appearance of electronic states in the band gap. Although the energy of the system is increased it is able to accommodate the newly produced charge within a quinoid formation and remains lower in energy. The formation of the defects is limited and in the case of polythiophenes is extended over two to four thiophene rings^{20,25-26}.

A bipolaron is formed upon further oxidation whereby the unpaired electron is removed which is favoured by a lower energy system. Continued oxidation gradually extends the bipolaron shells into overlapping bands, extending the upper valence and lower conduction limits to induce conductivity through partially filled electronic shells providing a semi-conducting state.

Neutral Polymer


 $-e$

Polaron


 $-e$

Bipolaron

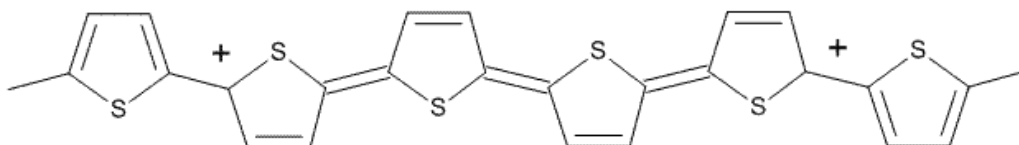


Figure 1.4. Charge localisation through the polymer backbone.

1.4. Polythiophenes

Thiophene belongs to a family of heterocycles that can undergo polymerisation through both chemical and electrochemical methods. From the brittle polypyrrole film produced by Dall'Olio to the free standing pyrrole film developed by Diaz in 1979²⁷ investigations into an extended range of monomers was initiated. These included thiophene²⁸⁻²⁹, furan, indole²⁹, carbazole, azulene, pyrene³⁰, benzene³¹ and polyaniline^{9,32}. These aromatic compounds all polymerise to produce polymers with differing qualities; however polythiophene is of particular interest due to its stability exhibited in both doped and reduced forms.

Polythiophene produced from the simple thiophene unit generates a polymer that is insoluble and difficult to process and characterise leading to little use in any potential application. Manipulation of the thiophene ring through chemical synthesis creates derivatives that present additional qualities associated with the polymerised compound influencing solubility, processability and functionality.

Substituted thiophenes presents a large area for investigation as the change in ring structure will influence many aspects including polymerisation, morphology, conductivity, stability and the opto-electronic properties associated with conducting polymer materials. Adaptation of the thiophene monomer represents one feature available for variation. Additional variables that have a direct effect upon the quality of the film are the solvent and dopant inclusive of the polymerisation process and of course the method of polymerisation itself.

1.4.1. Substituted Thiophenes

Polymerisation generally occurs through the α -positions on the thiophene monomer which is also true of pyrrole. From the examination of the π electron density at each carbon atom in the ring it is the α -positions of the neutral monomer that retain the highest π electron density and therefore would be mostly reactive in these locations³³⁻³⁴. By the incorporation of various substituents in the β -positions 2,4' linkages can be minimised providing mainly the desirable 2,5' couplings with possible head to tail arrangement.

Polymerisation of β -substituted thiophenes provides enhancement of regioregularity through electrochemical methods with head to tail linkages being predominant. Chemical oxidation however leads to the incorporation of defects³⁵ and affects the planarity of the polymer structure causing loss of conductivity. Alternative methods include organometallic chemistry.

The nature of the substituent bonded at the β -position can influence the polymerisation process and also affect the properties associated with the resulting film. Steric hindrance and inductive effects are the principle factors dominating the onset of polymerisation and the overall structure of the resulting film. Steric factors

remain an obstacle for polymerisation as it is the large bulky shape of the substituent that shields the reactive sites at the α -carbons.

Inductive or electronic effects of the substituent are more subtle in effect than the obvious obstruction anticipated with bulky groups, nevertheless they exert a strong influence upon the electronegativity of the ring. As it is the electron density that determines the reactive centres, the inductive effects of the side groups is of great importance for initiation of chain propagation. Strongly electron donating groups and electron withdrawing groups insert a push pull effect upon the thiophene aromatic system³⁶. Electron density is either increased at the α -positions or minimised advancing or impeding the polymerisation reaction³⁷⁻³⁸.

Strongly electron withdrawing species include nitro $-\text{NO}_2$ and cyanide $-\text{CN}$ groups with carboxylic acid $-\text{COOH}$ demonstrating electron withdrawing effects to a lesser extent. These side groups are able to pull electron density away from the ring structure destabilising the thiophene monomer. The monomer undergoes a one electron loss upon reaching the oxidation potential and due to the destabilised species, monomer or radical cation polymerisation is ineffective. As the reactivity of the radical cation intermediate increases, the chemical selectivity is decreased and as a result indiscriminate reactions with the solvent or other nucleophilic species within the vicinity of the electrode surface are produced³⁹.

The prevention of the polymerisation process can in some cases be overcome by the alteration of the electrochemical reaction conditions. As the HOMO energy of the neutral species is lowered through the attachment of these electron withdrawing groups an increase in oxidation potential is required to initiate polymer growth. However the resulting polymer represents dark brittle intractable materials due to the high potentials employed which is reported to introduce over oxidation into the electrosynthesised polymer system⁴⁰⁻⁴³. Further manipulation to the reaction conditions involves monomer concentration. A higher concentration of the monomeric polymerisation solution is necessary to obtain a conducting film demonstrated with the electropolymerisation of thiophene-3-acetic acid⁴⁴⁻⁴⁵. Introducing increased monomer content enhances the probability of radical-monomer

reactions not radical-solvent interactions and therefore reduces the dissipation of short chain oligomers into the bulk solution.

On the contrary electron donating groups such as methyl, ethyl and benzyl release electronegativity into the ring causing an increase of electron density found at the alpha positions which act to introduce stability to the system. In this case the energy associated with the HOMO is increased enabling polymerisation to occur through a lower oxidation potential as seen with methyl substituted thiophene.

Table 1.1. Oxidation Potentials of Thiophene Monomers³⁶. (* Experimental data)

Compound	E _{pa} (V) vs. SCE	
	monomer	polymer
Thiophene	2.06	0.96
2,2'-Bithiophene	1.32	1.00
3-Methylthiophene	1.86	0.72
Thiophene-3-acetic acid	1.94 / 1.7*	1.9*
3-Thiophenemalonic acid	2.02	
3-Bromothiophene	2.10	1.06
3-Thiopheneacetonitrile	2.22	1.12
3-Thiophenecarboxylic acid	2.28	
3-Cyanothiophene	2.46	
3-Nitrothiophene	2.69	

Steric and negative inductive factors oppress propagation of the polymer chain reaction and therefore require more concentrated monomer starting solutions and increased oxidation potentials to maintain the polymerisation rate⁴⁶. An additional negative effect upon polymerisation is reported by Li *et al* which again refers to the substituent bound to the ring⁴⁷. The nucleophilic character of certain side groups results in the attack of the species upon radical cation intermediates during the electrochemical polymerisation process. The substituents that can potentially facilitate nucleophilic attack provide the capability of enhancing the functional properties of the polymer and therefore have the potential to realise a variety of applications. The range of functional groups -NH₂, -OH and -COOH can be used in the covalent

immobilisation of enzymes⁴⁸⁻⁴⁹. The carboxylic acid group commonly incorporated for this purpose⁵⁰⁻⁵⁵ has the ability to immobilise biological compounds and once adapted can be utilised within a biosensor device due to the specificity provided to the polymer by the biological entity. To effectively utilise the available functionality these monomers need to either be copolymerised with the corresponding unsubstituted heterocycle or protected so polymerisation can be facilitated. A simple and effective way for functional group protection is to react the acid group with an alcohol to produce an ester⁵⁶.

Functionality through the extension of the alkyl chain at the β -position has been utilised for the modification of a range of properties. Not only does the solubility of the corresponding polymer increase but steric factors that affect the polymerisation of the monomer can be resolved.

3-Methylthiophene is associated with the simplest alkyl species and generates improved conductivity over the unsubstituted monomer and remains highly conductive through the addition of longer alkyl groups. Methyl, ethyl and propyl thiophene demonstrate very compact films with extension up to nine carbons increasing the mean conjugation⁵⁷. Longer alkyl chains approaching 14 and 18 carbons show a decrease in conductivity due to the presence of a higher proportion of the insulating hydrocarbon chain and provide a less regular and more porous structure⁴⁶. Increased solubility is a desirable property due to the ability to process the materials and is advantageous for a number of characterisation techniques that cannot be employed for insoluble materials. Several groups have reported increased solubility with the extension of the alkyl chain⁵⁸⁻⁶¹.

Relieving the impedance of bulky side groups is accomplished through the addition of linear alkyl chains. Roncali *et al* proved the necessity of inserting at least two methylene groups to separate the branched chain from the ring structure. The addition of the spacer link enabled polymerisation to proceed where it was not possible with the isopropyl branched group directly attached to the β -position and incorporating one methylene link required overoxidation to initiate polymerisation demonstrating the persistence of steric factors. The thickness of the prepared films for monomers that proved difficult to electropolymerise were thicker suggesting the production of a more

disordered film whereas neutralising the steric effects with the spacer methylene groups provided a film of relatively comparable thickness due to the facile arrangement generated by the longer alkyl chains.

Further adaptation of the thiophene monomer has been produced with one monomer in particular displaying enhanced qualities in terms of electrochemical and thermal stability⁴⁰ and exhibiting high electronic conductivity⁶². The monomer 3,4-ethylenedioxythiophene (EDOT) is polymerisable at only the α -positions due to fully occupied β -sites on the ring. This leads to a homogenous planar structure with no defects that are potentially possible with single β -substituted thiophenes and therefore produces higher conductivities. It is a water soluble monomer and so biological entities can be stabilised within the same medium for immobilisation purposes.

For polymerisation to occur under lower oxidation potentials and therefore maintaining the integrity of the film dimerisation and further oligomerisation of thiophene monomers and their derivatives have been produced. Terthiophene is a common oligomer employed as a starting monomer to introduce mainly α - α linkages through the film and so improve regularity and therefore the extent of conjugation of the backbone. This method was employed by Vignali *et al* to establish high conductivity in polymer films for photovoltaic applications⁶³. Modification of the terthiophenes has been encountered to introduce additional properties or to overcome the inflexibility and insolubility that the films demonstrate⁵⁹. Ballarin *et al* constructed a tetramer with two hexamethylenic methoxy side chains and was successful in lowering the oxidation potential in comparison to other poly(3-alkylthiophene)s bearing monothiophenic repeating units⁶⁴, similarly tetramers of alkylthio-substituted thiophene aid the decrease of the oxidation potential⁶⁵. Beneficial effects upon polymer solubility were established due to the oxygen containing alkyl chains increasing the polarity with no steric contribution and a film was grown which offered enhanced electronic properties and facile film preparation. Terthiophenes with carboxylic functionality have been prepared⁶⁶⁻⁶⁷ which compensates for the difficulty associated with the polymerisation of carboxylic acid bearing monomers. However as the functionality is entrapped within the oligomer, customisation of optimum groups for biomolecule immobilisation cannot be realised.

1.4.2. Solvent

The effect of solvent upon the resulting polymer films shows varied results. Different solvents can be employed within the polymerisation process that produces differences in film formation, material quality and resulting conductivity.

Facilitating polymerisation by stabilising the generated radical cations is essential for the formation of longer polymer chains. Radical-radical couplings lead to short oligomeric chains and typically a coloured solution is observed due to the high solubility of low weight polymer material. Acetonitrile comprises nucleophilic character and favours the stabilisation of the radical intermediates⁶⁴. This effect is detrimental to monomer species that have increased instability such as the influence of electronegative groups upon the destabilisation of the radical cation causing side reactions and inhibiting polymerisation. Many monomer species that are important to the structure of the polymeric film require this solvent support which general solvent systems such as acetonitrile can provide.

Chen *et al* demonstrated that it is not a direct effect of the solvent that causes the properties of the polymer to alter, it is the ability of the solvent to facilitate the onset of polymerisation at lower potentials⁶⁸. Due to the polythiophene paradox^{41-43,57,64} in which a higher potential is required for the polymerisation of the thiophene monomer (1.6 V / Ag/AgCl) compared to the redox potential of the polymer (0.8 V Ag/AgCl) the films become overoxidised resulting in brittle intractable and insoluble films. In order to solve the problem of high oxidation potential a lewis acid, trifluoroborate-ethyl ether (BFEE), solvent system is employed and forms a complex with the heterocyclic monomer through the lone pairs on the sulphur, lowering the electrochemical polymerisation potential due to the strong electrophilic property of BF₃, catalysing the deprotonation of thiophene on the electrode. This was proposed by Dietrich *et al* in which oxidation potentials of 1.0 V can be employed and overoxidation is not reached at 1.45-1.55 V producing high quality films with improved mechanical properties and conductivities⁴⁰.

1.4.3. Dopant Species

The choice of dopant ion can lead to interesting morphological changes where polymer colour is affected, this is known as ionochromism⁶⁹. McCullough *et al*

demonstrated colour change with varying counterion size upon regioregular polythiophenes with differing alkyl chain length and pendant carboxylic acid functionality. Small cations maintained the stacked nature of the film appearing purple whilst larger cations interrupted the backbone alignment producing twisted polymer chains producing a yellow colour. This was evident with polythiophenes containing short alkyl chains whereas the longer alkyl groups could accommodate the larger ions producing little colour variation. 3-methylthiophene is another monomer when polymerised with a specific anion results in a diverse morphological structure⁷⁰. A helicoidal arrangement is determined through XRD (X-ray diffraction) and UV-Vis (UV-Visible spectrometry) techniques with the incorporation of the anion SO_3CF_3^- . The interpretation of the developed structure is rationalised by structural parameters in which the anion size fits perfectly between adjacent thiophene units providing anchorage and secondly electronic effects support the polymer-dopant interactions due to charge delocalisation through the polymer to the electron withdrawing SO_3CF_3^- ion.

The extent of doping within the polymer also affects the structure shape and size. Undoped polythiophene and its derivatives are observed as a “noodle”-like assembly and when doped to 25% the fibrillar diameter increases in size⁷¹. Higher doping levels have been reported to increase conductivity of the polymer^{14,72} however contrasting results from Waltman *et al* have also been reported³⁶ which could be explained by different electrochemical parameters, electrode surface and the monomer purity.

1.5. Polythiophene Polymerisation

There are three general synthetic methods for polythiophene formation. Catalysed coupling of Grignard reagents or dihalothiophene monomers, electrochemical polymerisation and oxidative polymerisation⁷³. Each method offers different benefits such as planar structures, efficient scale up and area controlled growth.

1.5.1. Oxidative Polymerisation

Widely used chemical oxidants include ammonium persulfate ($(\text{NH}_4)_2\text{S}_2\text{O}_8$) and iron chloride (FeCl_3)⁷⁴. Molybdenum chloride (MoCl_5) can also be employed as a stronger oxidising reagent however many other chemicals can be utilised such as hydrogen peroxide and transition metal salts. Oxidative polymerisation is a process of choice

where large scale production is intended and the resulting product is usually in powder form or a colloidal dispersion. The chemicals used are relatively inexpensive and the polymerisation is performed in a simple one step reaction generating high molecular weight polymer. The difficulty arises with the extraction of the oxidant and regioregularity within the material is considered poor. The mechanism of polymerisation can be followed from the electrochemical process outlined below, as it is generally assumed to be comparable.

1.5.2. Electrochemical Polymerisation

Oxidation of the monomer solution by the application of a voltage yields a polymer grown upon the surface of an electrode. Electropolymerisation of heterocyclic monomers other than thiophene follow the same general mechanism below.

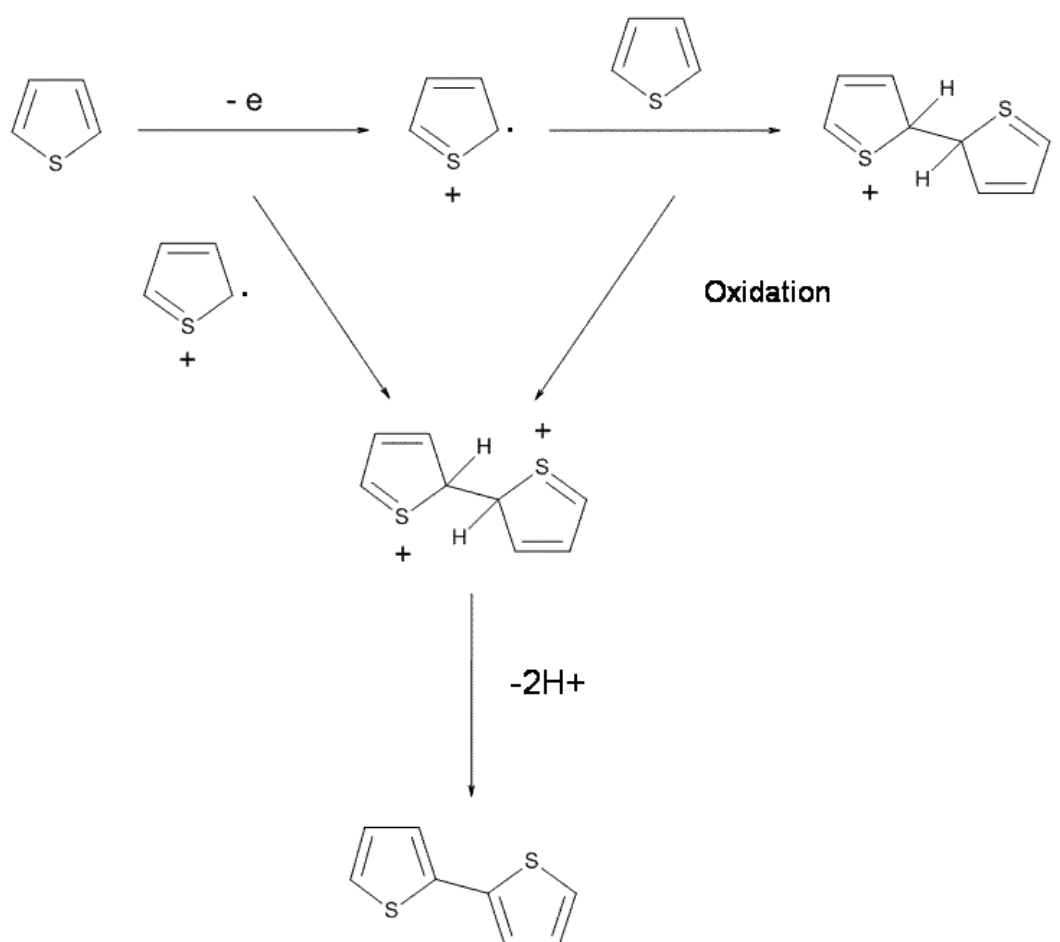


Figure 1.5. Electrochemical polymerisation mechanism.

Upon reaching the oxidation potential of the specific monomer an electron is lost from the ring and a radical cation is produced. Radical cations react together to form a dimer. Protons are lost from the structure to leave a neutral dimer. The dimer is again oxidised due to the constant potential and forms another radical cation which in turn reacts with another radical cation to eventually produce an oxidised conducting polymer.

The neutral monomer requires a higher oxidation potential than the corresponding dimer and higher molecular weight oligomers as coupling of monomers reduces the energy needed for oxidation. Thiophene requires a potential of +1.6 V / SCE to initiate polymerisation whereas only +1.1 V / SCE is needed for the oxidation of the polymer.

The removal of electrons through the material directly initiates anion movement into the polymer to counteract the positive charge. Each molecule loses 2.25-2.50 electrons creating 0.25 to 0.5 cation centres per heterocyclic unit therefore charge is stored over three sulphur rings⁷⁵⁻⁷⁶.

1.6. Regioregular Poly(alkylthiophenes)

The band gap is the central dynamic function that is responsible for the levels of conductivities achievable and the colours obtainable from the conducting polymeric materials. The band gap can be altered by changes to the monomer units such as side chain addition or copolymerisation and the process of polymer doping.

To ensure the band gap remains small regioregularity is required. Conducting polymers are generally adapted through the ring structure to activate necessary functions specific to the materials purpose. Flexible, soluble and durable films are essential for characterisation and processing for possible applications and consequently derivatives of these materials allow such qualities. A typical monosubstituted thiophene is shown in figure 1.6 with the α -positions denoting the reaction sites however polymerisation can also occur through α - β and β - β linkages seriously disrupting the π -orbital overlap between the monomer units. Further disruption arises from steric factors due to side chain interactions¹⁵⁻¹⁷. Additional groups present on the ring cause the repulsion of the monomer units forcing the

conjugated backbone to twist and lead to a disordered π -orbital arrangement. Due to the asymmetry of the substituted thiophene the side bearing the substituted group is denoted as the head (H) and the opposite side of the monomer represents the tail (T).

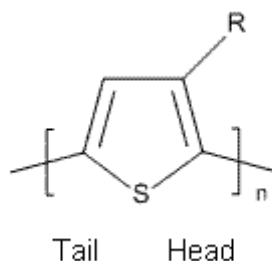


Figure 1.6. Denotation of head and tail arrangement in poly(alkylthiophene).

The head to tail (HT) conformation reduces steric hindrance between the units as the groups are furthest apart from the neighbouring thiophene units whereas the other three possible arrangements cause loss of conductivity.

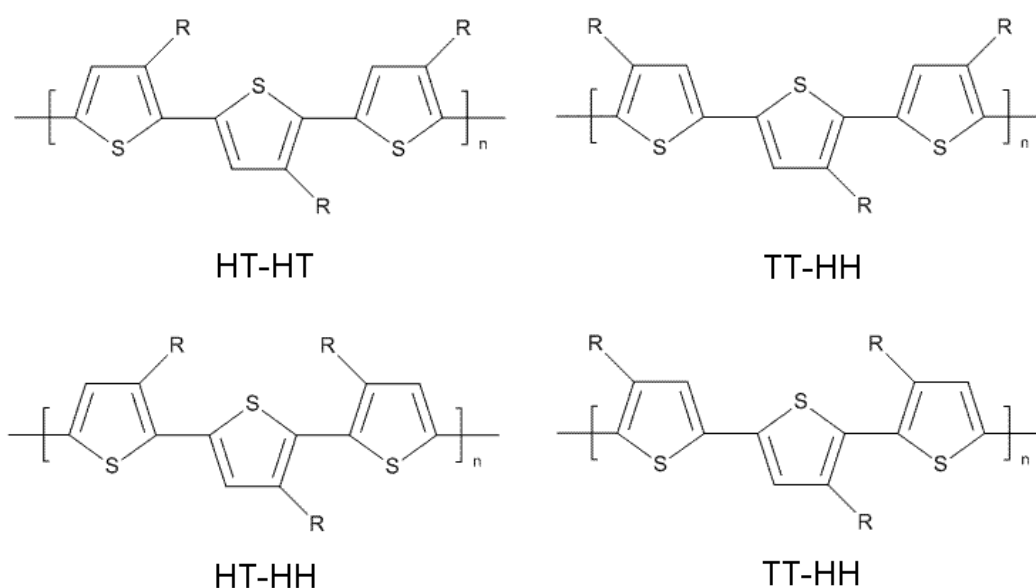


Figure 1.7. Possible head to tail arrangement in poly(alkylthiophene).

Loss of conductivity due to the polymer alignment can be prevented through specific polymerisation routes which can produce almost exclusively head to tail couplings however increased cost and problematic scale-up are the compromise. Improved conductivity can be accomplished without complete regioregularity incorporating reduced vacuum annealing and copolymerisation⁷⁷⁻⁷⁸.

1.7. Electrochemistry

1.7.1. Cyclic Voltammetry

Cyclic voltammetry is one of the most common electrochemical techniques for acquiring qualitative information about electrochemical reactions⁷⁹ and for the determination of redox potentials, detection of chemical reactions that precede or follow the electrochemical reaction and evaluation of electron transfer kinetics⁸⁰. The technique employs a set potential window with data collected through forward and reverse scans monitoring the change in current. Cyclic voltammetry can offer many desirable advantages such as high sensitivity with detection limits reported at 10^{-5} M, selectivity towards electroactive species, a wide linear range, portable and low cost instrumentation and the use of a wide variety of electrodes⁷⁹.

To initiate the experiment a potential is employed to the system where no electrochemistry is detected V_1 . The potential is then controlled at a set rate (v) to a potential limit encompassing electrochemical activity V_2 . Upon reaching V_2 the potential is reversed and both redox processes are recorded. During the potential sweep electron transfer reactions are activated due to the specific potential values (redox potentials) and the potentiostat measures a current signal resulting from this process⁷⁹. The current generated is related to the rate at which the electrons have transported across the electrode-solution interface. The typical waveform for cyclic voltammetry is displayed as a triangular potential waveform.

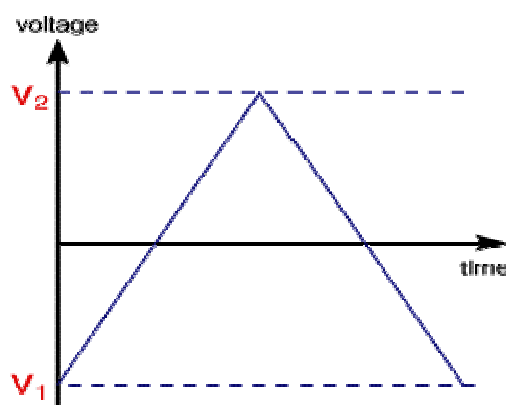


Figure 1.8. triangular potential waveform⁸¹.

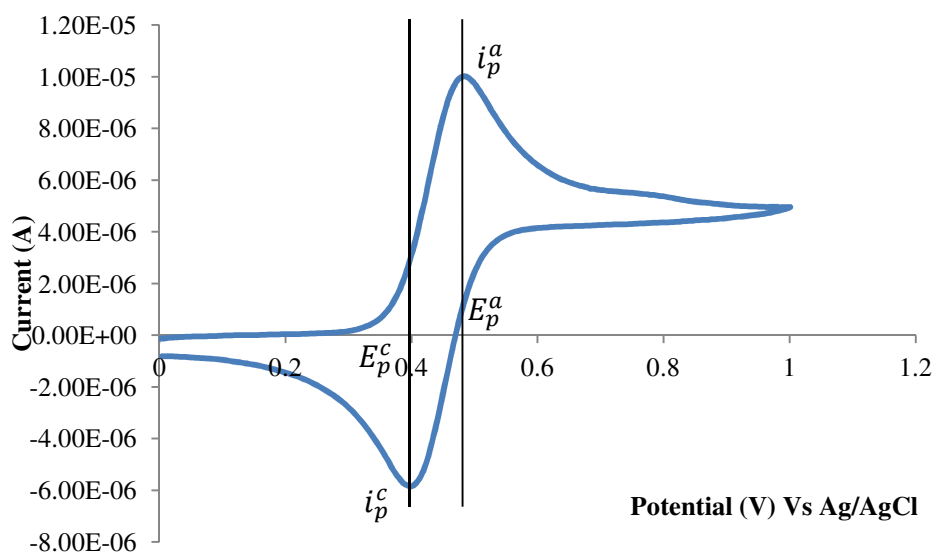


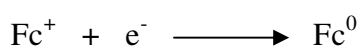
Figure 1.9. Typical cyclic voltammogram demonstrating a reversible single electron transfer for the ferrocene / ferrocenium $\text{Fc}^{0/+}$ system displaying extractable analytical data.

Figure 1.9 demonstrates a simple single electron transfer maintained under diffusion control in which the solution initially contained the ferrocene compound in the neutral state (Fc^0) and therefore the cathodic and anodic responses correspond to the following reactions;

Oxidation observed as the anodic response



Reduction observed as the cathodic response



The current is produced from the above oxidation (positive current response) and reduction (negative current response) processes of the electroactive species Fe and is termed the Faradaic current as it obeys Faraday's law. Faraday's law states that the reaction of 1 mol of substance involves a change of $n \times 96,487 \text{ C}$ (n corresponds to the number of electrons involved in the reaction and $96,487 \text{ C}$ is the Faraday constant in coulombs). The current is also directly related to the concentration of the analyte that is under the redox process and therefore by determining the redox potential the

concentration of the electroactive species at the surface can be established according to the Nernst equation.

$$E = E^{\theta} + \frac{RT}{nF} \ln \frac{[Fe^{3+}]}{[Fe^{2+}]} \quad \text{Eq 1.1}$$

Where E is the applied potential difference, E^{θ} is the standard electrode potential for the redox reaction, R is the universal gas constant ($8.314 \text{ JK}^{-1} \text{ mol}^{-1}$) and T is the temperature in Kelvin. For current to be detected electron transfer from the electrode to the surface species has to occur. The Faradaic current measured is therefore dependent upon two factors: the kinetics of electron transfer and the rate at which the redox species diffuses to the surface⁸². The rate of such reactions is determined by the slowest step⁷⁹ in which simple reactions such as the single electron transfer system of the $\text{Fc}^{0/+}$ redox couple involve only the mass transport of the species, electron transfer across the interface and transport of the product back to the bulk solution⁷⁹ whereas more complicated systems can include additional chemical processes such as chemical electrochemical (CE) mechanisms or electrochemical chemical (EC) systems depending upon the sequence of such steps. For a reaction in which the slowest step involves mass transport to the electrode surface the kinetics of the electron transfer is therefore fast and the current is said to be mass-transfer limited. These reactions are said to be Nernstian or reversible, which describes the $\text{Fc}^{0/+}$ system.

All reversible voltammograms display the same general shape and can be both qualitatively and quantitatively rationalised by considering the voltage and mass transport effects⁸¹. In the case of the $\text{Fc}^{0/+}$ system the ferrocene compound is initially present in the neutral state (0) therefore at $t = 0$ the bulk concentration consists of only the neutral form Fc^0 and no concentration gradient exists. The potential window employed (0-1-0 V) starts at a potential where no redox processes are initiated ensuring there is no flow of current, this is represented by the initial flat portion of the trace. As positive potentials are reached the concentration of the neutral form Fc^0 at the electrode surface begins to decrease due to the formation of the oxidised species Fc^+ . During this process a high concentration gradient is generated due to the lower concentration of Fc^0 at the

electrode surface. This in turn produces more flux of Fc^0 to the surface creating a higher anodic current this is therefore represented by the increasing positive peak on the voltammogram as more Fc^+ is generated.

Assuming that the electron transfer rate is rapid due to Nernstian behaviour as the potential is decreased the measurable current, i , will be directly related to the diffusion rate (the flux) of the oxidised species to the electrode surface⁸².

$$i = nFAJ \quad \text{Eq 1.2}^{82}$$

Where n is the number of electrons, F is Faraday's constant, A is the electrode surface area and J is the flux of the oxidised species to the surface.

The peak occurs as the potential continues to increase. The concentration of Fc^0 depletes as the oxidised form Fc^+ predominates therefore as the concentration gradient begins to diminish a growing diffusion layer becomes more abundant limiting the flux to the surface and therefore a decrease in current can be seen.

Once the switching potential is reached the process occurs in the reverse direction. The bulk of the species around the electrode is now composed of Fc^+ and when the standard potential is applied a concentration gradient is generated in which this time the cathodic current dominates and Fc^+ is reduced back to Fc^0 .

The cyclic voltammogram in figure 1.9 displays four important measurable factors E_p^a and E_p^c anodic peak potential and cathodic peak potentials respectively and i_p^a and i_p^c peak currents for the anodic and cathodic responses. Such extractable information can be used as diagnostic tests for the reversibility of the system known as the Nicholson and Shain criteria.

For a reversible system the peak separation between E_p^a and E_p^c should be around 59 mV for a single electron transfer (59/n mV).

E_p is independent of scan rate which is expected within a Nernstian system in which the varying scan rates provide the same E_p values for both the anodic peak current (E_p^a) and the cathodic peak current (E_p^c). E^0 which is the standard potential for the redox reaction can be determined by the average of both the E_p^a and E_p^c . $E^0 = (E_p^a + E_p^c) / 2$

The peak currents for both the anodic and cathodic responses should be equal $i_p^c = i_p^a$ in which i_p is proportional to the square root of the scan rate^{80,83} and is also directly proportional to the concentration as seen with the Randle-Sevcik equation:

$$I_p = -(2.69 \times 10^5) n^{\frac{3}{2}} D^{\frac{1}{2}} C_0^\infty V^{\frac{1}{2}} \quad \text{Eq 1.3}^{83}$$

The scan rate is the rate of change of potential with time and has the units Vs^{-1} or mVs^{-1} . By increasing the scan rate the current signal becomes greater. Therefore the scans below in figure 5 demonstrate that peak current is scan rate dependent.

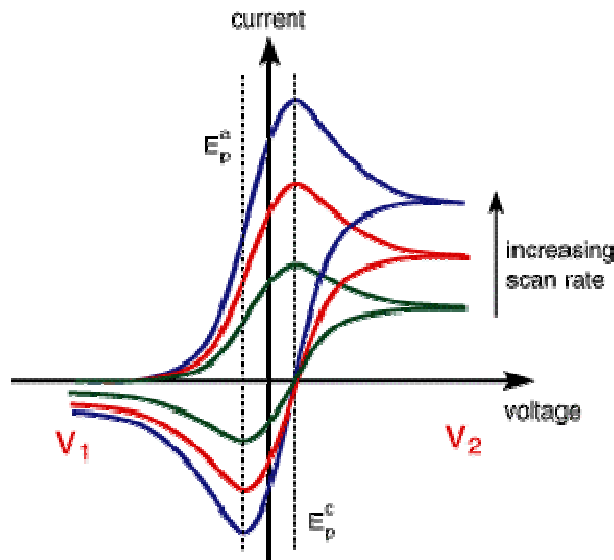


Figure 1.10. Influence of voltage scan rate upon current response⁸¹

The combination of two important equations can be used to explain the voltammograms current reduction.

$$i = nFAJ \quad \text{Eq 1.2}$$

$$J = -D \left(\frac{dC}{dx} \right) \quad \text{Eq 1.4}^{79}$$

Flux is related to the concentration gradient multiplied by the diffusion coefficient. The two equations provide the general expression for current response:

$$i = nFAD \left(\frac{dC}{dx} \right) \quad \text{Eq 1.5}^{79}$$

Where D is the diffusion coefficient (cm^2/s), (dC/dx) is the concentration gradient at the surface (C concentration and x corresponds to a particular distance).

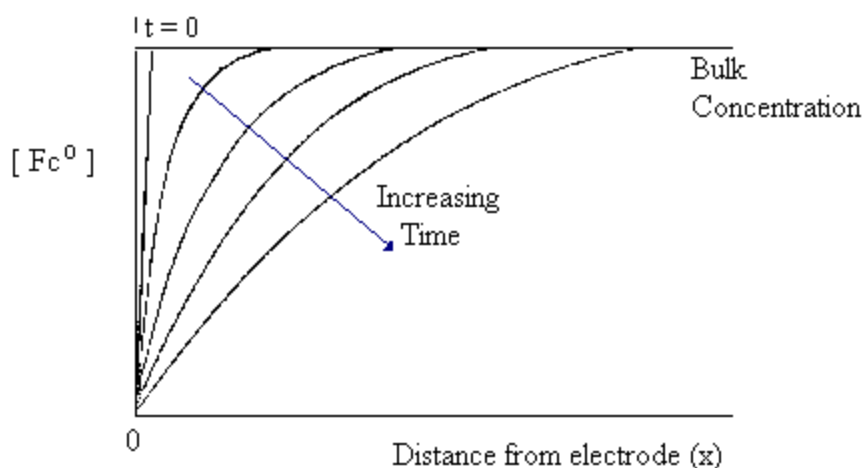


Figure 1.11. Fc^0 concentration profiles for varying electron transfer rates⁸⁴.

From the above equations a simple relationship can be determined. As diffusion is the movement across a concentration gradient the rate of diffusion (the flux) is directly proportional to the slope in Fick's first law therefore a greater concentration gradient will produce greater flux of the electroactive species to the surface which in turn increases the current response. Thin depletion produces a steep concentration gradient as seen in figure 1.11 above and is caused by a fast rate of electron transfer k in which $k > 10^{-2} \text{ cm/s}$ corresponds to reversible systems. In contrast the slower scans in figure 1.11 provide greater depletion at the surface causing the gentle gradients above which in turn generate less current.

Extremely slow electron transfer rates that correspond to $k < 5 \times 10^{-3}$ cm/s are indicative of irreversible behaviour. In fact irreversibility, quasi-reversible behaviour and other non-ideal processes such as additional chemical reactions are usually of greatest chemical interest in which cyclic voltammetry provides useful information.

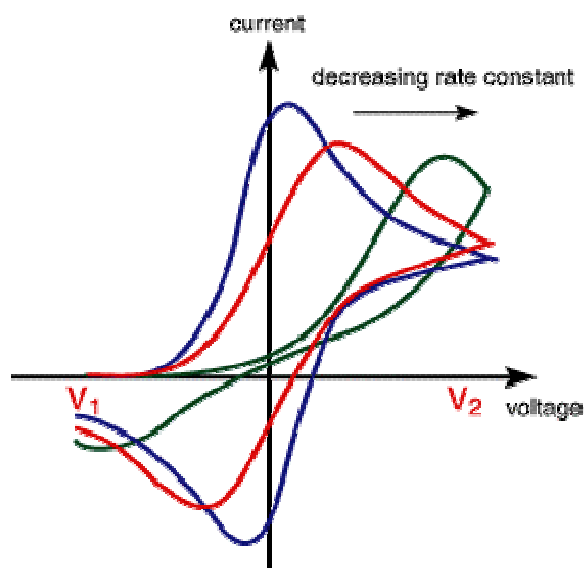


Figure 1.12. quasi-reversible reaction⁸¹.

Figure 1.12 demonstrates quasi reversible behaviour in which electron transfer is slow compared to the rate of mass transport. The rate constants are varied in the above diagram in which k is gradually lowered and the corresponding redox responses shift increasing the peak separation. For non-reversible behaviour peak separation varies as a function of scan rate and peak current is now independent of the square root of the scan rate. For complete irreversibility the rate constant reaches values as low as $k < 5 \times 10^{-3}$ cm/s in which more distortion of the responses are seen and current becomes depleted.

1.7.2. Electrochromism

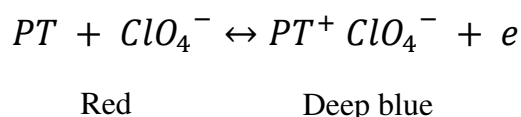
Electrochromism can be defined by the ability of a material to reversibly change colour under the influence of an applied electric current or field⁸⁵.

Many conducting polymers display chromatic changes whilst undergoing electrochemical oxidation and reduction. Electrochromism is an inherent property shared by many conducting polymers in which the colour of the material is

manipulated by the modification of the electronic structure. Through induced redox processes anion insertion and exertion causes the polymer backbone to morphologically alter. The twist and bend produced in the polymer accommodates the counter ion presence important for neutralising the film. Whilst doped, charge carriers are introduced producing new electronic states in the band gap therefore new electronic transitions are produced which cause the colour changing properties of the material. The band gap can be manipulated in several ways as a method for colour control⁸⁶.

Polythiophene conducting polymers generally display chromatic changes from blue in which the film is doped to red when the film is reduced.

The electrochemical process for polythiophene electrochromism is displayed below;



Regioregularity and the incorporation of pendant side groups can be introduced by synthetic procedures and are key features in the chromic properties of polythiophenes⁸⁷.

Electrochromism encompasses only one avenue for inducing colour change; many conducting polymers exhibit chromism through a wide variety of external effects.

Polythiophenes can exhibit an optical response to changes in temperature⁸⁸ solvent, counter ion size⁶⁹, pressure and light exposure due to the structural alteration of the film and will respond with a colour change through the detection of chemical and biological moieties as the film is oxidised or reduced.

Considering the capabilities these materials hold, they have the propensity to operate in many devices. Electrochromism is a response that can be measured for use within sensor applications however amperometric detection is the response typically monitored whereby electrochromic effects are the accompanying feature. This is

generally the case for conducting polymers within biosensor formats. However the colour change is a nice addition to the detection process and provides opportunity to develop the sensor based on the two different approaches.

1.8. Applications

Conducting polymers have the potential to be utilised within a wide variety of applications due to their inherent properties and ease of manipulation. With the potential to achieve semi conducting and metallic states, colour transitions, biological compatibility, increased stability and processability conducting polymer materials are frequently reported within many areas of research and are therefore employed within many applications⁸⁹.

Table 1.2. Applications of Conducting Polymers

Conducting Polymer Material	Application
poly (N-3-aminopropyl pyrrole-co-pyrrole) ⁴⁹ polypyrrole ⁹⁰ polyaniline ⁴⁸ 3-methylthiophene/thiophene-3-acetic acid copolymer ⁵⁰⁻⁵⁴ poly(3,4-ethylenedioxythiophene) ⁹¹⁻⁹²	Biosensors
poly(3-methylthiophene) and poly(dibenzo-18-crown-6) ⁹³ polypyrrole ⁹⁴	Ion-Selective Electrodes
polyaniline, polypyrrole, polyhexylthiophene and poly(3,4-ethylenedioxythiophene) ⁹⁵ polyaniline/PPS ⁹⁶	Gas Sensors
Polyaniline ⁹⁷⁻⁹⁸ Polypyrrole ⁹⁹	Electromagnetic Shielding
Poly(vinyl pyrrolidone) (PVP) ¹⁰⁰ poly(3,4-ethylenedioxythiophene) ¹⁰¹	Battery Applications
poly(bis-terthiophene) ¹⁰² porphyrin/oligothiophene hybrid monomer ¹⁰³ oligo(3-hexylthiophenes)-perylene-oligothiophene ¹⁰⁴	Photovoltaic devices
3-methylthiophene/thiophene-3-acetic acid copolymer ¹⁰⁵⁻¹⁰⁶	Fuel Cell
octanoic acid 2-thiophen-3-yl-ethyl ester ¹⁰⁷ poly(3,4-ethylenedioxythiophene) ¹⁰⁸	Electrochromic Devices

1.9. History of Biosensors

Biosensor systems were first developed for analytical measurement by Clarke and Lyon in 1962 which became known as the enzyme electrode¹⁰⁹. Glucose oxidase was incorporated with an amperometric transduction mechanism in the form of an oxygen electrode. Oxygen was the monitored species as it exhibited a concentration change when the reaction was initialised. The consumption of oxygen responded to the catalytic oxidation of glucose and was proportional to the concentration of the analyte.

The biosensor term was not recognised until further developments were made utilising biological functions and physical transduction platforms. In 1977 this partnership was eventually established through the immobilisation of living microorganisms at an electrode surface. Rechnitz *et al* developed a gas sensing ammonia electrode for the selective determination of the amino acid arginine¹¹⁰. This device was described as a bio-selective sensor and was eventually shortened and widely regarded as a biosensor.

1.10. What are Biosensors?

A biosensor can be explained as the combination of two critical parts the bioselector / receptor and the transducer. The receptor is very specific enabling only the analyte of interest to be detected and therefore producing a reaction or response in acknowledgement to the analyte. The transducer detects the physiochemical change produced by the bioselector and converts the biochemical signal into a quantifiable electrical signal. The high specificity is created by the biological nature of the receptor which can include antibodies, enzymes, nucleic acid, microorganisms or cells.

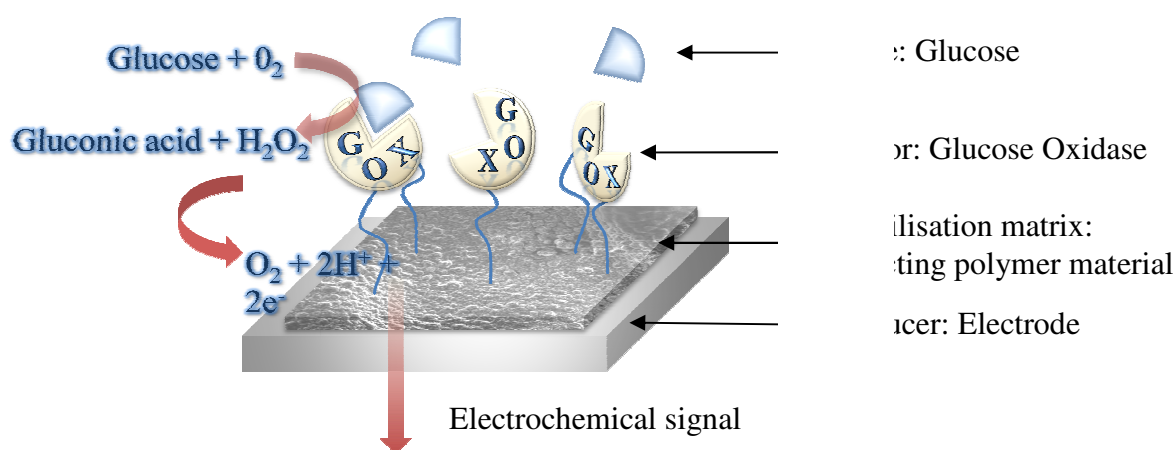


Figure 1.13. Biosensor schematic for glucose detection

1.11. Transduction

The transduction element of the biosensor monitors the physiochemical change that occurs between the analyte and complementary receptor. The transducer can monitor the physiochemical change in various ways and the biosensor is classified accordingly. Therefore biosensors can be defined as being electrochemical, optical, thermal or piezoelectric. Piezoelectric, optical and thermal biosensors monitor the change in mass, light and temperature whereas measurements of current, potential and conductance relate to amperometric, potentiometric and conductimetric transduction systems respectively and are electrochemical in nature. The most common transducers within this field are electrochemical where current and potential are the measured parameters¹¹. Amperometric transducers or biosensors were the first of their type developed by Clarke and Lyon and are still a distinguished method of choice today.

1.11.1. Amperometric Biosensors

Amperometry employs the oxidation and reduction capabilities of chemical or biological species. Detection is achieved at the surface of a metal electrode where the redox reactions take place. The exchange of electrons generates an electric current which can be measured. Accessing the redox reaction directly from the receptor is difficult therefore the amperometric response is usually produced by an electroactive species generated from the reaction. Hydrogen peroxide is an electroactive species that is commonly formed through the oxidation of a redox enzyme and can be detected at the electrode surface provided that the oxidation potential is reached. The current signal produced is proportional to the concentration of analyte present therefore enabling quantitative determination through indirect measurement.

1.12. Electron Transfer Mechanisms

There are two main categories of electron transfer, direct and non-direct. Whichever the method of choice, the objective is simple; to deliver facile, rapid communication between the biological entity and the electrode surface. Immobilisation media represents a common intervention of this essential process and therefore an obvious approach would be to immobilise the enzyme/protein directly upon the bare electrode surface. The possibility of enhanced electron transfer relating to this theory is however unsuccessful as demonstrated by Wen *et al*¹². The biological molecule is incompatible with the inorganic surface and therefore attachment of a biocatalyst

upon an unsustainable environment causes denaturation of the biological recognition element and consequently, the bioactivity of the enzyme/protein is lost. However, as this method constitutes what is referred to as a third generation biosensor, research into the novel enzyme electrode structures have continued and advances in this area have been positive. A third generation biosensor utilises electron transfer directly from the source of the redox biomolecule, typically an enzyme belonging to the oxidoreductase family providing high sensitivity to the system and eliminating complicated diffusion effects as a result of immobilisation media. Wang *et al* utilised highly oriented pyrolytic graphite as an electrode that supported the biological nature of glucose oxidase¹¹³. The enzyme was electrostatically adsorbed onto the surface and the signals observed could be associated with the FAD/FADH₂ redox couple. Furthermore Lu *et al* describes a polypyrrole conducting polymer with electrostatic hemoglobin (Hb) adsorption where direct electron transfer is established through the Fe²⁺ / Fe³⁺ redox couple associated with the heme protein¹¹⁴.

Indirect electron transfer is commonly the method adapted as the materials and techniques employed within the biosensor format have been studied in depth over time providing the knowledge and understanding required for biosensor advancement. Such research has determined the advantages of electroactive compounds incorporated within immobilisation matrices. These particular compounds are known as mediators and operate to shuttle electrons across the immobilisation matrix electrode interface. Ferrocene and *p*-benzoquinone are common examples of electron mediators^{50-51,54-55, 115-116} allowing facile electron transfer by accepting electrons from the biological entity and becoming oxidised at the anode. As well as facilitating electron transfer the incorporation of electroactive compounds lower the potential normally required to oxidise hydrogen peroxide generating the amperometric response. The exact potential can be varied by substitution of the ferrocene to fine tune the sensor response. By decreasing the applied potential common interferents that generally contribute to the electrochemical signal at potentials matching hydrogen peroxide oxidation are eliminated. Interferents such as uric acid and ascorbic acid are commonly found in blood which demonstrates a typical biological sample utilised for the analysis of many analytes including glucose.

Indirect electron transfer introduces a more complex system although this is compensated by prolonged biosensor life. Strong covalent linkage to the matrix increases the stability of the biological molecules delivering enhanced resistance against dynamic environments as well as providing protection against inhibitors. The enzyme is less susceptible to interfering species through the existence of the immobilisation matrix¹¹⁷ due to its physical protection and/or the potential to carry charge in order to repel known interferents¹¹⁷. These media are typically polymeric and are favoured for their biological support due to their chemical and physical properties and ease of fabrication¹¹⁵. However slow diffusion through the matrix can limit the electron transfer mechanism as reported with the use of dialysis membranes¹¹⁰. However, manipulation of the matrix thickness and choice of mediator are just a few techniques utilised to overcome potential slow electron transfer. In fact the incorporation of unique immobilisation platforms that encourage electron transport and provide the potential to covalently bind biological species with facile electrochemical generation, biocompatibility and low cost are promising materials and are commonly referred to as intrinsically conducting polymers.

Mediators can be easily incorporated into a conducting polymer matrix by utilising their ability to carry current. As the polymer is generated using electrochemical methods, mediators bearing negatively charged groups can be introduced into the film structure through charge compensation adopted by the electrolyte. Therefore the mediator simulates the roll of the anion providing neutrality to the film and also assisting electron transport. Ferrocene carboxylate is an example used by Iwakura *et al*¹¹⁶.

1.13. Biological Elements

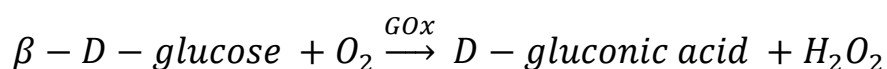
The biological element is the key to providing selectivity to the device and enables its use as a sensor for a specific analyte. The biological species is capable of recognising the presence, activity or concentration of a particular analyte in solution and will react to it in a certain manner. There are many biological entities that can be employed within a biosensor format. Enzymes are commonly integrated into the device although living cells¹¹⁰, antibodies¹¹⁸⁻¹¹⁹ and DNA fragments¹²⁰⁻¹²³ have been investigated. Enzymes are involved in a biocatalytic reaction when in the presence of their

biological counterpart, whereas antibodies, DNA segments and cell receptors undergo a binding process regarded as affinity ligand-based biosensors.

The glucose sensor is a well-known and comprehensively studied biosensor format through its introduction in 1962 by Clarke and Lyon. Glucose oxidase is widely accepted as an analytical reagent in which the catalysed products are utilised within the food and cleaning industries in addition to clinical applications¹²⁴⁻¹²⁵. Glucose oxidase is therefore a heavily studied catalytic method representing a very stable and well-documented enzyme system. Due to its familiarity, cost, stability and high level of activity glucose oxidase is commonly used as a model for the development of biosensors.

1.13.1. Glucose Oxidase

Glucose oxidase (GOx; β -D-glucose:oxygen oxidoreductase) from *Aspergillus niger* is a flavoenzyme and belongs to a family of enzymes known as oxidoreductases. This group of enzymes can be exploited for their redox behaviour within a sensor format. The sensor response is generated through a redox mechanism catalysed by the enzyme in which the depletion of oxygen or the increase of hydrogen peroxide concentration can be monitored to assess the amount of glucose present through electrochemical methods.



Glucose oxidase catalyses the oxidation of β -D-glucose in the presence of molecular oxygen to δ -gluconolactone which represents the reaction intermediate and therefore undergoes rapid hydrolysis to the reaction products gluconic acid and hydrogen peroxide¹²⁶. Its structural conformation represents a homodimer with a molecular mass of 160 kDa¹¹³. The surface of glucose oxidase is covered with thirteen lysine residues¹²⁷ with an isoelectric point of 4.0-5.0¹²⁸ and as a result has a net positive charge below the isoelectric point. Glucose oxidase importantly contains one tightly, noncovalent bound flavin adenine dinucleotide (FAD) cofactor per monomer. The FAD is the reaction centre of the enzyme and is the species that is oxidised and reduced therefore generating the FAD/FADH₂ redox couple. The enzyme activity is determined through the FAD cofactor.

Enzyme activity can be affected due to the influence of extreme conditions such as temperature, pH, and nature of the solution. Additional factors such as measurement environment can also have an impact upon the catalytic activity of the enzyme due to the inhibiting species present within biological specimens such as blood.

Immobilisation of the enzyme is a recognised method that minimises or removes the difficulties and problems associated with free enzyme. An inert matrix is used to retain the enzyme, providing a barrier to obstruct interfering analytes and preserve catalytic activity upon the influence of extreme temperature and pH generating longer sensor lifetime and enabling repetitive analysis.

1.14. Immobilisation of the Biological Component

Immobilisation offers many advantages to the enzyme system, with various immobilisation techniques to choose from. However immobilisation can also introduce changes involving the enzyme environment, possible conformation changes and diffusion effects which all contribute to the apparent activity of the biological element. Recognising the optimum method and conditions is therefore important to avoid denaturation and retain activity as they are paramount to the sensor response.

It is important to maintain two essential factors through the immobilisation of the enzyme, enzyme stability and its biological activity.

1.14.1. Enzyme activity

Enzyme concentration has to be treated differently to common laboratory reagents and materials as the weight of the enzyme does not constitute the quantity involved in the reaction. Therefore only a small amount of the weighed enzyme maybe active and as it is the activity of the enzyme that is essential for the conversion of substrate to product it is important that a different term is identified.

The definition of enzyme activity is associated with the reaction rate and is expressed in enzyme activity units (U). This is the international unit (IU) which signifies that one unit (U) of any enzyme is defined as that amount which will catalyse the transformation of 1 micromole of substrate per minute¹²⁹. Therefore the activity of glucose oxidase can be expressed as the number of μmols of $\beta\text{-D-glucose}$ oxidised to

D-gluconic acid and hydrogen peroxide per minute. The specific activity of an enzyme is expressed as units of enzyme per milligram of protein (U/mg protein)

1.14.2. Enzyme Kinetics

First order kinetics can be determined by the direct relationship between the increase of substrate concentration and the reaction rate for a single component reaction. When substrate concentration is increased an enzyme-substrate complex is formed. This is the basic model developed by Michaelis and Menten¹³⁰.



The model above illustrates the breakdown of the complex generating the products and liberating the enzyme demonstrating a first order reaction.

1.14.3. Michaelis-Menten Equation

Michaelis and Menten developed the enzyme substrate (ES) concept and derived the following equation important to enzyme studies.

$$v_o = \frac{V_{max} \times [S_o]}{K_m + [S_o]} \quad \text{Eq1.6}$$

The equation is important for obtaining K_m which is the Michaelis constant relating to a particular enzyme involved in the reaction and is a measure of the enzyme's activity. The term V_{max} is the maximum velocity of the reaction obtained by a substrate concentration $[S_o]$ where the measured velocity (v_o) no longer increases. A large K_m describes a less active enzyme as its dissociation from the enzyme substrate complex is not as effective as enzymes that are associated with a small Michaelis constant.

Several methods can be employed to obtain the K_m and V_{max} values; these are demonstrated in figure 1.14 and are based upon the Michaelis-Menten equation.

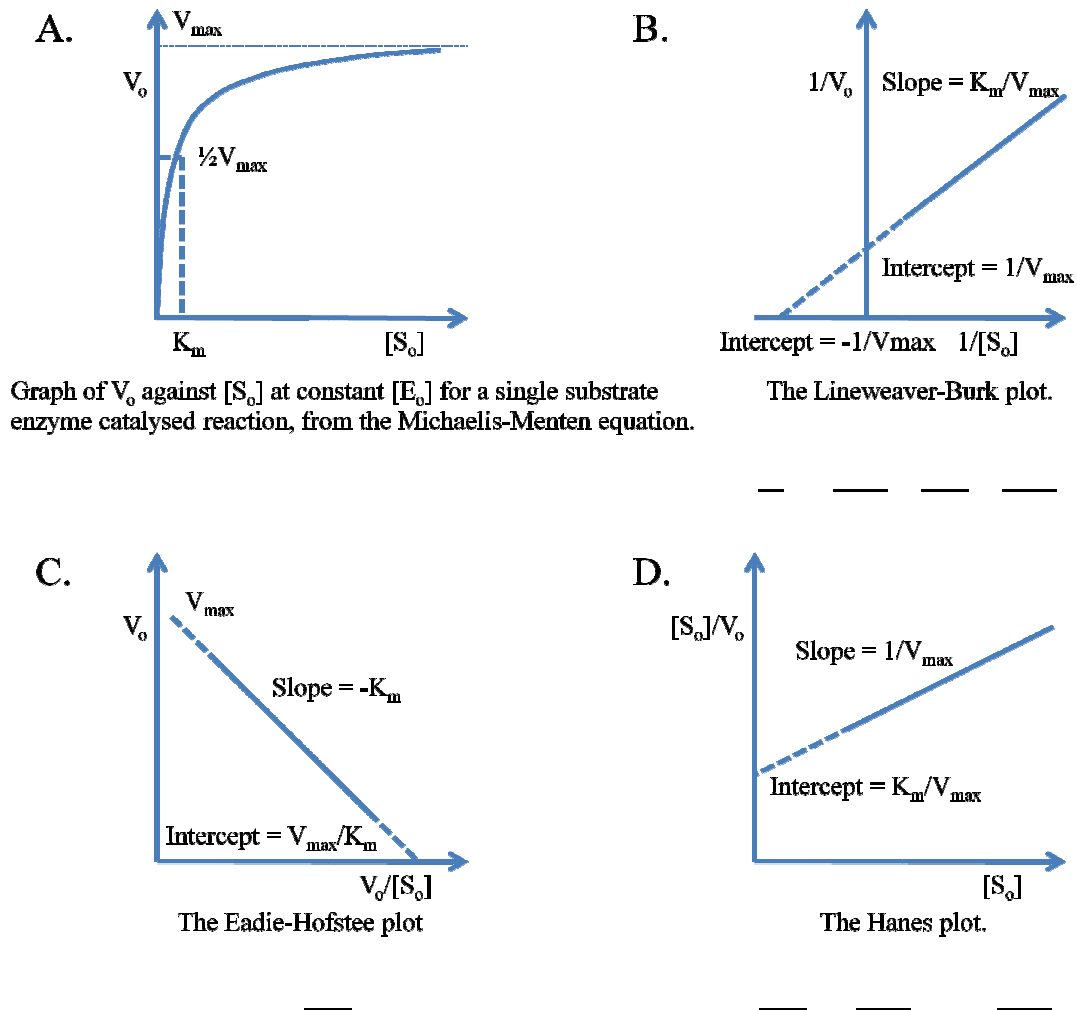


Figure 1.14. Manipulation of the Michaelis-Menten equation to obtain linear plots.

In order to determine the Michaelis constant of an enzyme the enzyme quantity is kept constant and the reaction velocity is monitored with increased substrate concentration. A plot of velocity against substrate concentration is generated producing the typical hyperbolic curve seen in plot A.

Using the plot to obtain the value for half the maximum velocity the substrate concentration can be determined following the relationship of the curve. This concentration is the value corresponding to the Michaelis constant. Although this experimental method produces the K_m value it is not the most accurate determination. Due to the hyperbolic nature of the plot, V_{max} is a value approaching a point of no curvature and therefore is not definitive. By manipulating the data to produce a linear

relationship shown in figure 1.14 plots B-D, K_m and V_{max} are more accurately obtained.

There are however significant errors associated with the linear models such as the Lineweaver-Burk plot as the reciprocal conversion of the data generates the greatest experimental error range¹³¹. Furthermore deviation from linearity is not clearly apparent compared to the Eadie-Hofstee and Hanes plots which is important if a reaction mechanism is under investigation¹³².

The direct linear plot is a more reliable method where a statistical approach is required.

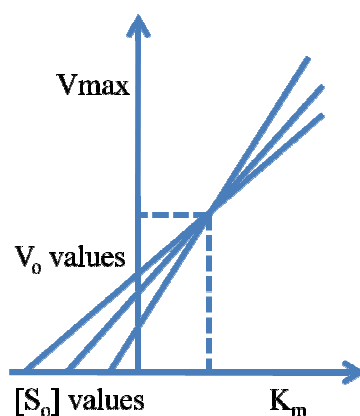


Figure 1.15. Manipulation of enzyme kinetics data forming the direct linear plot.

The direct linear approach involves the velocity and substrate concentration pairs to be plotted upon each axis with the joining of the two points. The lines are then extrapolated to intersect in the V_{max} , K_m region obtaining the values. When the data fits the Michaelis-Menten equation perfectly all the extrapolated plots meet at the same point providing the best-fit values for V_{max} and K_m . As experimental data contain measuring errors several intersections may result in this case the median value is calculated and used for the best-fit data.

There are various methods based upon the Michaelis-Menten equation for the determination of enzyme kinetics. However when considering the rate of enzyme catalytic activity as a function of substrate concentration the important factors to determine are V_{max} and K_m . The K_m value determines the concentration of substrate

needed to achieve a given rate therefore a different enzyme with a lower K_m value provides a higher rate of reaction when subjected to the same substrate concentration.

1.14.4. Immobilised Enzyme Kinetics

The kinetic information previously discussed concerns free enzyme systems. Analytical use of enzymes requires high stability and therefore immobilisation is paramount. Whilst immobilisation is essential the enzyme kinetics are likely to be affected and it is important to maintain the catalytic activity of the enzyme

Although physiological factors remain important they are somewhat alleviated by introducing immobilisation, which increases the biosensor effectiveness over wider pH ranges and at increased temperatures. Influential effects upon enzyme kinetics through immobilisation are thought to result from changes to enzyme conformation and stability, the enzyme microenvironment, and diffusion limitations through the surrounding solution to the film and internal diffusion through the matrix. These factors may provide both beneficial and problematic effects to the system.

1.14.5. Conformational Changes

In order for an enzyme to be effective towards the catalysis of a specific substrate the structure of the enzyme must remain in its natural conformation but must also have the freedom to adjust its spatial arrangement for effective interaction. The Koshland ‘induced fit’ hypothesis¹³³ describes this morphological alteration generating the complete matching of structures. However there may exist a level of strain acting upon the enzyme resulting from the high number of binding sites. This will affect the enzymes ability to align the substrate to the active centre demonstrating non-productive binding. Additionally immobilisation in which the enzyme position is affected can cause blockage of the active site, the enzyme orientation is therefore unfavourable for receiving the substrate. To avoid these adverse effects a suitable immobilisation matrix is required. An environment, which allows the enzyme to take up its natural conformation, is essential with an optimum level of anchorage points to provide sufficient enzyme loading with minimal structural constraint.

1.14.6. Partitioning Effects

Two regions are classified within an immobilised enzymatic system, the micro environment which is the thin solution layer surrounding the enzyme and the macro environment representing the bulk of the solution. The micro environment is influenced by the surface properties of the enzyme which include temperature, pH and ionic character; these may be altered by the immobilisation procedure. If there is a significant influence upon these properties through immobilisation two different environments will result causing partitioning. Not only do partitioning effects originate from the enzyme properties but also the immobilisation matrix can contribute to the surrounding changes. Ionic character between the support and the solute can cause substrate accumulation or reduced concentration depending if the charged matrix acts to attract or repel additionally charged substrate material.

1.14.7. Diffusion Limitations

Diffusion of the substrate through the bulk solution to the immobilised enzyme is regarded as the external diffusion barrier and product diffusion through the support material toward the electrode exists as the internal diffusion barrier¹³⁴.

The rate of mass transfer is different in the two environments with transport across the liquid solid interface decreasing and therefore creating an accumulation of solute at the boundary. The solute has to cross this barrier to reach the immobilised enzyme and can be influenced by mechanical agitation of the solution. By stirring the bulk solution the rate of external diffusion is increased, penetrating the barrier into the matrix where internal diffusion now exists as the limiting factor. Internal diffusion is affected by the porosity of the support material and has an effect upon the substrate diffusion. If the catalytic action upon the substrate is faster than its diffusion to the enzyme, substrate depletion will occur within the vicinity of the enzyme and reaction velocity will decrease. Subsequently product formed will generate a concentration gradient leading to enhanced linear responses and elevated apparent K_m values.

1.15. Immobilisation Matrices

Biosensor construction offers diverse possibilities due to the several matrix platforms available for the integration of the biological moiety. With the various matrices there are important considerations to be made. Relevance to their use in industrial processes

and cost especially if the sensor is only designed for single use. Issues regarding the nature of the support are pertinent for realisation of biological properties such as activity and reaction kinetics and most importantly the biocompatibility between the biological component and the material of choice. Ideally the matrix should be cheap, inert, physically strong and provide efficient and stable immobilisation of the biological species easily accessible to the substrate¹³⁵. Sepharose, cellulose, glutaraldehyde, hexamethyl diisocyanate and glass substrates can be used to support the choice of biomolecule following chemical modification and enables covalent and cross linking attachment. Acrylamide gels and cellulose acetate fibres can provide supports for cross-linking and entrapment and membrane confinement introduces a different concept of securing the analyte and allowing access through a semipermeable seal.

Conducting polymers are associated with a number of important advantages regarding their use in biomedical applications. Biocompatibility, the ability to immobilise the recognition element through a number of methods including entrapment, adsorption, covalent linkage and affinity binding, efficient electron transfer from the biochemical reaction to the electrode and the adaptable nature of the polymer material through copolymerisation or facile chemical modification to specifically tailor the electrical and physical properties of the support. The amount of material produced can be controlled by simply disconnecting the power supplied to the system and the area of conducting polymer produced is dictated by the size of the electrode surface. Such methods provide invaluable advantages where miniaturisation is an essential aspect of the final product and where specific control of material deployment is fundamental. Biosensor devices have the ability to take advantage of such techniques and therefore bimolecular immobilisation employing conducting polymers is of great interest

1.16. Enzyme Immobilisation Techniques

Enzyme immobilisation is a critical part of the biosensor construction; it is the key to enzyme stability, which is not only necessary for the function of the device but also to maintain enzyme activity and to achieve increased lifetime. The attachment of biological species onto the polymer substrate can occur through various methods of which there are two main categories covalent or non covalent immobilisation.

1.16.1. Physical Adsorption

The incorporation of the enzyme into the polymer matrix proceeds through electrostatic forces. The static interactions arise from the positive charge negotiated within the polymer film due to its electrochemical oxidation and the overall negative charge upon the enzyme produced through the solution pH¹³⁶⁻¹³⁸. The positive and negative effect causes the attraction of the species into the polymer material.

The solution pH needs to be carefully maintained to achieve adsorption of the enzyme however molecular interactions are considerably weak causing major disadvantages associated with this simple method. The non-covalent attachment of the biological species renders the recognition element unstable and biomolecule loss (desorption) is inevitable over time^{49,118}. Adsorption only produces a single monolayer at the polymer surface¹³⁸ further increasing the potential of the species to leach out into the sample solution during measurements and therefore causing loss of longevity of the enzyme electrode and poor sensitivity. In addition controlling the concentration of the immobilised compound is difficult and random biomolecule orientations further increase the problematic nature of this technique.

Glutaraldehyde can be used to crosslink the enzyme to the polymer reducing leaching and supporting a more direct electron transfer to the electrode aiding the sensing performance. Increased response times are generated but stability is compromised due to denaturisation of the enzyme¹³⁸.

1.16.2. Physical Entrapment

Physical entrapment is a quick and simple way to immobilise biological species throughout the structure of the film. This therefore overcomes the monolayer limits seen by physical adsorption and so a larger concentration of the recognition element can be incorporated. The enzyme is entrapped during the polymerisation of the conducting material due to the enzymes partial negative charge and the positive polymer generated through oxidation. It is possible that the enzyme takes the role of the anion balancing the charge created during polymerisation. This method incorporates the two processes in one simple function avoiding time implications associated with the other methods such as adsorption, affinity binding and covalent immobilisation.

The limitations of this method include the mild conditions required to sustain the enzyme whilst it is entrapped this therefore limits the choice of starting monomer as it needs to be water soluble and easily oxidised. The produced polymer is likely to be hydrophobic which will affect the structure of the protein possibly leading to decreased biological activity. Hydrophilic properties can be imparted to the material through a synthetic approach, however this would then implement a more time consuming technique and remove the simplicity of a single-pot procedure. Additional problems involve high enzyme concentration, increased cost and potential difficulty surrounding substrate-enzyme accessibility⁴⁹ which is essential to processes such as affinity complex formation (antibody-antigen and hybridization of nucleotides) and so other methods of immobilisation may be more beneficial.

1.16.3. Affinity Binding

This technique concentrates upon the attachment of the sensing element to the surface of the conducting polymer. It involves strong non-covalent interactions to secure the compound, which can provide minimal loss of biomolecule activity. Complexes that demonstrate this high obtainable affinity include the avidin-biotin interaction and DNA single strand pairing through a intercalator molecule¹³⁹. The method offers good control over the molecule “orientation” important for the facilitation of the analyte “interaction” and therefore high accessibility to the bound substrate.

1.16.4. Covalent Immobilisation

The immobilisation technique that far surpasses the methods mentioned so far in terms of binding strength is covalent attachment. Functionality imparted to the polymer backbone provides the covalent bond producing strong and efficient immobilisation generating a very robust and stable system under adverse conditions and subsequently improves the biosensor lifetime⁴⁹.

The disadvantages surrounding this method are; the increased complexity in comparison to the other techniques and the unsuitable reaction conditions that are unfavourable to biological species.

In most cases commercially available functionalised monomers are utilised and if they cannot be obtained synthetic routes provide an option. Functionalised polymer

materials with aldehyde⁵³ and carboxylic acid groups^{50-55,67,137,140-141} have been used for covalent immobilisation following different strategies. The use of carboxylic acid groups for covalent linkage is popular as there are commercially available monomers of this type and generation of the peptide linkage occurs through a well established reaction method. The difficulty associated in generating polymers with this particular species is due to the electron withdrawing effect it causes upon the starting monomer, therefore polymerisation can be problematic. The protection of these groups through esterification has been explored^{56,137,144-147} and eliminates polymerisation difficulties due to inductive effects although steric hindrance is likely to then constitute the limiting factor⁵⁶. Activated esters assist the generation of covalent peptide linkage between the monomer and the biomolecule bearing amine groups. Such activated esters include *p*-nitrophenol, pentafluorophenol, 1-hydroxy benzotriazole, 3-hydroxy-4-oxo benzotriazine and N-hydroxysuccinimide where commonly a carboxylic acid group has been protected and functionalised to react with the amine groups under mild conditions¹³⁸⁻¹³⁹.

1.16.5. Carbodiimide coupling

Carbodiimides are extensively used in the formation of peptide amide bonds from carboxylic acids and amines¹⁵⁰. The condensation reaction has been employed for the modification of conducting polymer substrates^{48,51-55,67,140-141,151-152}. Various carbodiimide coupling reagents exist and can be implemented within aqueous or organic reaction environments.

The carboxylic acid groups are esterified by the carbodiimide producing the very reactive intermediate O-acyl isourea¹⁴⁹. Amine species located in protein molecules can then attach through the carbonyl carbon forcing electron rearrangement and the subsequent elimination of the carbodiimide reagent with oxygen attachment.

A second approach is to activate the carboxylic acid function on the monomer unit^{56,137,145-147} therefore ensuring all modified monomers have the potential to initiate biological binding followed by polymerisation into an activated matrix. This reaction can be performed within organic media as the protein is not introduced at this stage. This method generates a more complex web of side reactions through influential parameters such as the incorporation of bases or nucleophiles, reagent ratio¹⁵³, solvent

polarity and pH¹⁵⁴. The instability of the reaction intermediate O-acyl isourea causes the isolation of this compound to be extremely problematic. Therefore isolated O-acyl isourea compounds are uncommon and are mainly witnessed as intermediates as their instability forces racemisation to occur generating the more stable N-acyl isourea conformation which does not facilitate biological linkage¹⁵⁵.

The way to resolve this difficulty is to introduce an additive into the reaction solution that has the direct purpose of “trapping” and stabilising the reactive intermediate. By stabilising the species required for the amide coupling, peptide bonding can proceed through the formation of an activated ester. The main coupling catalysts used for this purpose are N-hydroxysuccinimide (HOSu) and N-hydroxybenzotriazole (HOBt).

1.17. Factors Influencing Sensor Response

Sensor response encompasses several areas that determine the overall effectiveness of an enzyme electrode. Optimising the response capability and maintaining signal reproducibility are important when developing the sensor. Equally rapid response times influence efficiency and enable glucose determination for practical analysis.

1.17.1. Optimising the Sensor Response

A major influence on sensor response is enzyme activity. The choice of enzyme determines the maximum rate of conversion for the substrate so a higher enzyme activity is favourable. To achieve optimum activity pH and temperature can be altered. Enzymes typically have a pH range over which they are operational however an optimum pH will exist where activity will be highest. Immobilised enzymes are likely to exhibit a pH range shift compared to soluble enzyme due to the different environment introduced, however activity is likely to be lost at pH values <3 and >9¹⁵⁶. Increasing the temperature generally sees a higher reaction rate as a 10 degree rise will approximately double the rate of reaction. Immobilisation benefits the enzyme when increased temperature is unavoidable as increased stability is imparted to the biological element. Room temperature is frequently employed, which is accepted as 25 degrees; however many countries with warmer climates employ higher limits as clinical measurements are performed in this environment. Enzyme loading is a commonly explored variable, as the amount of catalytic reagent deployed will affect the amount of product generated. The optimum quantity is dependent upon the

enzyme electrode structure including immobilisation matrix thickness and composition. Too much enzyme may decrease the matrix porosity obstructing diffusion channels and too little may lead to small signals.

1.17.2. Signal Reproducibility

Generating the optimum response is important but if it cannot be maintained then the sensor has little value for repeated analysis and therefore must conform to a single use disposable biosensor system. Stability of the response can be increased primarily through the immobilisation technique used to support the enzyme. Through the three commonly practised methods covalent attachment delivers the greatest stability to the system concerning enzyme leaching. The strong irreversible linkages improve the sensor's long term stability and provide increased reproducibility where non covalent methods suffer from loss of enzyme. It is generally observed that biosensor longevity is associated with immobilisation efficiency and follows the order chemical attachment > physically bound > solubilised¹⁵⁶. The prepared enzyme electrodes should be stored in buffer solution when not in use and although room temperature is generally accepted, lower temperatures of 4 degrees and therefore refrigerator storage is recommended. Integrating a dialysis membrane or cellophane film aids stability of the system especially where chemical immobilisation is not practiced. The membrane permeability restricts passage of the enzyme but permits diffusion of the analyte into the film for detection. The dialysis membrane also prevents bacteria entering the polymer/enzyme matrix during storage.

1.17.3. Sensor Response Time

A wide range of factors that include diffusion effects, substrate and enzyme concentration, pH and temperature of the system, the membrane thickness and the potential to include additional membranes in the device affect sensor response time. It is important to generate a relatively quick response as biosensors are generally marketed on their "real time use" within environmental and clinical applications. Therefore all the variables must be considered and investigated to determine an effective response time.

1.17.3.1. Diffusion Effects

Sensors developed for analytical use are devoid of diffusion effects through a liquid surround as they are reagentless systems. In contrast experimental set ups employ

mechanical stirring and therefore mass transport must be considered. The rate of substrate movement is dependent upon the stirring rate of the solution therefore a faster stirring setting will afford a quicker response. Therefore it is important to fix the stirring setting at a constant rate to ensure response times are influenced through other factors. The analyte of interest is therefore directly in contact with the supporting enzyme matrix; therefore internal diffusion is the limiting diffusion factor.

1.17.3.2. Substrate and Enzyme Concentration

In general the higher the concentration of the substrate the greater the rate of reaction and therefore the faster the response time as more enzyme activity will increase the rate of conversion from start reagents to product. However there exists an enzyme loading limit as increasing the available activity also increases the supporting matrix thickness¹⁵⁷. Increasing the thickness introduces an extended diffusion barrier and it is reported that when the limit is approached response times dramatically increase. Therefore depending upon the material used an optimal enzyme load versus thickness exists and must be investigated. It is recommended that a thin support material be employed with the highest enzyme activity incorporated into the matrix for obtaining rapid enzyme kinetics and hence rapid responses.

1.17.3.3. Effect of pH and Temperature

Achieving maximum enzyme activity requires optimal pH and temperature conditions; however the different environment produced through immobilisation causes a shift from their reported optimum values. Glucose oxidase has an optimum pH value of 5.5 within a solution environment whereas once immobilised shifts to encompass a possible range of pH 5.8-8.0¹⁵⁸. Therefore to achieve the fastest responses the optimum pH should be utilised. However the sensor electrode may not demonstrate the same optimal behaviour as the immobilised enzyme and a compromise is therefore required. Extreme temperature differences can either denature the enzyme or significantly reduce the reaction rate and therefore room temperature is employed as the biosensor device will be used within this environment.

1.17.3.4. Matrix Thickness and Dialysis Membrane Effects

Stable measurements are governed by the diffusion rate of the substrate through the film to the enzyme and the diffusion of the catalysed products through the matrix to

the electrode surface. Matrix composition such as thickness and porosity contribute to the diffusion rate¹⁵⁹ which affects the reaction rate to generate equation 1.7.

$$V = \frac{K_3 E_0 d^2}{DK_m} \quad \text{Eq 1.7}$$

Membrane thickness d , diffusion coefficient D , the Michaelis constant K_m , and the maximum velocity of the enzyme reaction V_{\max} are related to provide V in which an increasing value indicates a higher rate of enzyme catalysis compared to the diffusion of the species. Where the rate of the enzyme reaction is faster than the rate of diffusion the process is referred to as diffusion controlled. In the opposite case where the enzyme reaction is the rate limiting step the process is reaction controlled. Diffusion controlled reactions provide advantages to the system where sensitivity is independent of enzyme activity and concentration, including inhibitors and pH variation. Temperature effects are minimal as diffusion is less affected than the enzyme reaction. Extended linear range and greater functional stability are also gained through diffusion limited biosensors however the major disadvantage corresponds inevitably to slower response times due to larger film thickness.

Incorporating a membrane secures the enzyme within the matrix and discourages microorganism growth however the speed of response can be affected with thicker membranes although this can be avoided if small scale membranes are employed.

1.18. Polythiophenes for Biosensor Applications

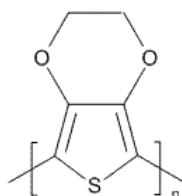
Many materials within the conducting polymer family have been investigated for potential use within a biosensor format however there still remains opportunity to potentially improve areas of the biosensor design.

Polythiophene is a conducting polymer that has a largely untapped potential use in biosensor systems. With the exception of poly(3,4-ethylenedioxythiophene) (PEDOT), polythiophenes have not been exploited in biosensors as they lack aqueous solubility. However post polymerisation treatment can allow enzyme immobilisation through a carbodiimide coupling reaction. Therefore various materials and analytes that require very diverse environments can function in one biosensor device.

The aim of this project is to produce a biosensor capable of facile analyte detection based upon the well documented glucose oxidase system. By tailoring the thiophene monomer to incorporate the functionality for covalent enzyme immobilisation the overall process for the biosensor construction can be simplified without loss of sensitivity.

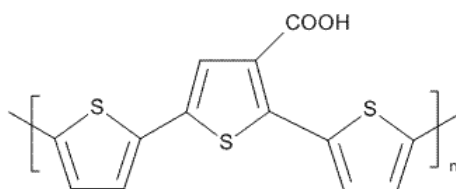
Recent polythiophene biosensor research has seen the use of a range of polymer structures. A water soluble thiophene has been employed to produce poly(3,4-ethylenedioxythiophene), PEDOT (compound 1)⁹¹⁻⁹². This material entraps the enzyme within the polymer matrix during the polymerisation stage and this can lead to some variability in the final sensor response due to enzyme leakage.

Compound 1

Poly(3,4-ethylenedioxy
thiophene) (PEDOT)

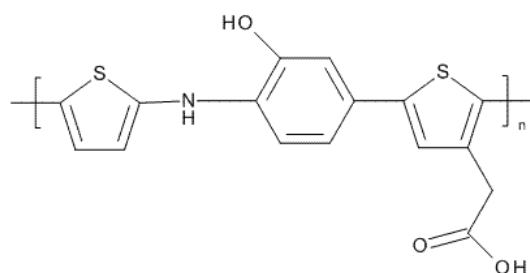
Korean researchers in 2005 produced poly(terthiophene-3'-carboxylic acid)¹⁶⁰, compound 2. Whilst this material seems to be very reproducible in a biosensor format it does provide a fixed ratio of binding sites on the polymer layer which may, or may not be the optimum required.

Compound 2

Poly(terthiophene-3'-
carboxylic acid)
(PTTCA)

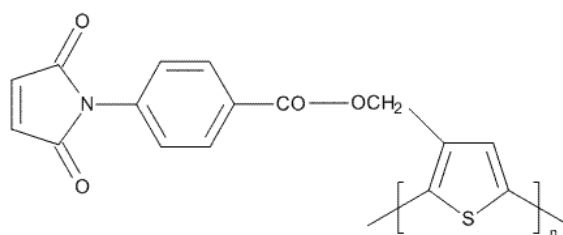
Additional thiophene analogues demonstrated below show extended monomer systems for the incorporation of enzyme moieties.

Compound 3



poly(thiophene-2-aminophenol-thiophene-3-acetic acid) (PTAPTAA)

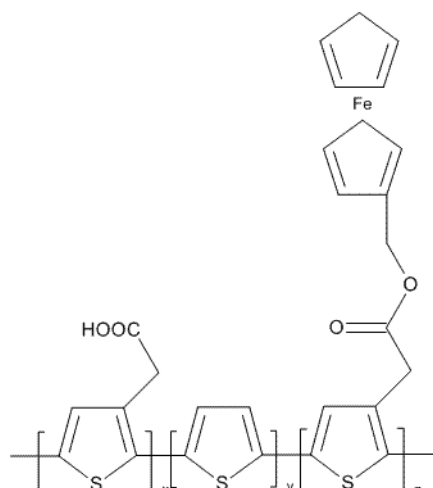
Compound 4



n-(4-(3-thienyl methylene)-oxycarbonylphenyl) maleimide (MBThi)

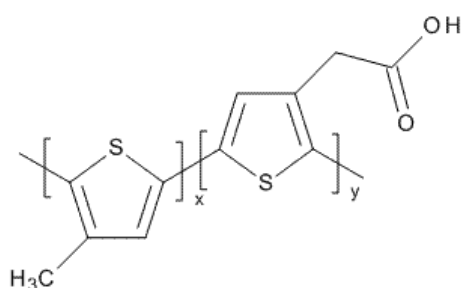
The development of poly(thiophene-2-aminophenol-thiophene-3-acetic acid)¹⁶¹ by Kim *et al* maintains the use of the carboxylic acid functional group for successful immobilisation. However such a diverse and complicated system offers no additional advantages over simplified thiophene films and therefore attracts little attention for future research towards biosensor applications. Similarly the Middle East Technical University in Turkey prepared an extensive thiophene monomer n-(4-(3-thienyl methylene)-oxycarbonylphenyl) maleimide (MBThi)¹⁶² for the copolymerisation with pyrrole and styrene¹⁶²⁻¹⁶³. The copolymer was designed for the entrapment of enzymes, incorporating various organic units for their rigidity within the polymer backbone providing the polymer with superior mechanical and thermal stability. Although the stability of the polymer material is important it is the stability of the biological compound that offers long term use of the biosensor. Immobilisation of the biological species through entrapment is known to offer limited stability and therefore is not ideal for a multiuse biosensor device.

Compound 5



thiophene-3-
acetic acid, thiophene and
dicyclopentadienyl iron-
1,4-dienylmethyl-
2-(thiophen-3-yl)acetate
copolymer
(T3AA-T-TFc)

Compound 6

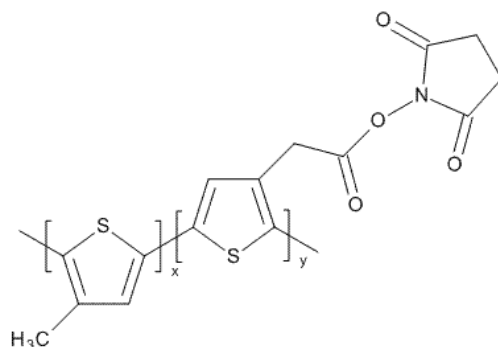


Thiophene-3-acetic
acid/3-methylthiophene
copolymer
(T3AA-MT)

Compound 5 demonstrates a polymer matrix with a covalently bound mediator this is an advantage as the mediator would normally be introduced separately. The data for reproducibility and biosensor stability is not reported for this biosensor format which is important for such devices and therefore its performance is unclear¹⁶⁴. A common polythiophene format for biosensor applications that is prepared under organic conditions is displayed as compound 6 and is a copolymer of thiophene-3-acetic acid and 3-methylthiophene. It is a simple and well documented functional copolymer capable of covalent attachment through the carboxylic acid substituent. The optimum composition has been determined requiring only 10% T3AA groups for potential enzyme attachment. Generation of the film upon a platinum electrode employing electrochemical techniques is typical using acetonitrile and dopants such as tetrabutylammonium tetrafluoroborate and tetraethylammonium perchlorate (TEAP)⁵³. Differences are observed for the film thickness (6 mC/cm^2 - 800 mC/cm^2) influencing enzyme loading^{51,54}. Enzyme attachment generally proceeds through a two step process with activation of the carboxylic acid groups using a carbodiimide reagent in

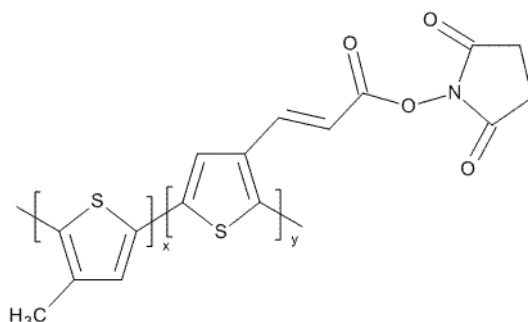
which a stabilising agent can be used. Enzyme immobilisation then follows in a buffered solution, with varied reaction times (1-24 hrs) at each stage⁴⁸.

Compound 7



N-succinimido
thiophene-3-
acetate/3-
methylthiophene
copolymer
(STA-MT)

Compound 8



N-succinimido trans-
3-(3-thienyl) acetate/
3-methylthiophene
copolymer
(STTA-MT)

The proposed biosensor system that will be investigated for its amperometric response to glucose will incorporate an activated ester thiophene monomer. The two activated monomers will be investigated and synthesised from their corresponding starting compounds of thiophene-3-acetic acid and trans-3-(3-thienyl) acrylic acid which are inexpensive and commercially available. To enable activation of the carboxylic acid functional group N-hydroxysuccinimide will be used in combination with a condensation reagent of the carbodiimide family^{48,51-55,67,140-141,151-152}. It is envisaged that the prepared monomer will represent the primed species generated within the preparation of the simple T3AA-MT copolymer films creating a thiophene monomer ready for enzyme immobilisation. By introducing the activated species directly into the copolymer film enzyme immobilisation should proceed readily under controlled conditions through the use of a single buffered enzyme solution eliminating further preparation and simplifying the immobilisation process. Generating the film electrochemically with the incorporation of 3-methylthiophene will allow a range of

copolymers to be produced with the direct intention to quantify the content of the activated monomer specifically to optimise enzyme loading. Through the introduction of a spatially diverse monomer and a complete conjugated system seen in compound 8, changes to the film structure will be expected and subsequently the films may acquire modified properties. The characteristics of the films will be probed using cyclic voltammetry with FTIR and elemental analysis to determine the copolymer ratio. Further characterisation will include morphological studies upon the copolymers to generate information regarding porosity and film structure. Analysis of the dopant content for a range of copolymer compositions will be undertaken to gain an understanding of the film deposition process. In conjunction with the analysis of the activated copolymer systems the thiophene-3-acetic acid/3-methylthiophene and trans-3-(3-thienyl) acrylic acid/3-methylthiophene copolymers will be investigated for comparative studies.

This project is directed towards the successful development of a novel copolymer capable of covalently binding biological species for specific recognition of its complementary counterpart. Preliminary studies provide the foundation of this investigation exploring the electrochemistry of various polythiophene monomers to gain an understanding of the redox properties of the various polymer systems. By probing a range of thiophene monomers conclusions can be drawn regarding the changes to the monomer structure that can help elucidate potential problems and gain an insight into the properties required for successful polymerisation. It is also important to maintain the functionality needed to support the biological compound and consider the effects of electron transport through manipulation of the thiophene ring and copolymer ratio.

Chapter 2 Materials and Methods

Table 2.1. Reagents and Purity

Reagent name	Purity	Company
Thiophene Monomers		
2,2'-Bithiophene	97%	Aldrich
Tert-butyl thiophene-3-carboxylate		Synthesised
3-Dodecylthiophene		Synthesised ¹⁶⁵
3-Methylthiophene	98%	Aldrich
Methyl thiophene-3-carboxylate		Synthesised
N-succinimido thiophene-3-acetate		Synthesised
N-succinimido trans-3-(3-thienyl) acetate		Synthesised
3-Octadecylthiopene		Synthesised ¹⁶⁵
3-Octylthiophene		Synthesised ¹⁶⁵
Thiophene-3-acetic acid	98%	Aldrich
3-Thiophenecarboxylic acid	99%	Acros Organics
3-Thiophenemalonic acid	97%	Aldrich
Trans-3-(3-thienyl) acrylic acid	97 %	Sigma-Aldrich
Electrolytes		
Lithium perchlorate	99.99%	Aldrich
Tetrabutylammonium perchlorate	99%	Acros Organics
Tetrabutylammonium tetrafluoroborate	99%	Aldrich
Tetraethylammonium <i>p</i> -toluene sulfonate		Aldrich
Electrodes		
Glassy carbon 3 mm diameter		Bioanalytical Systems Inc
Gold electrode 1.6 mm diameter		Bioanalytical Systems Inc
Indium tin oxide glass slides		Aldrich
Platinum electrode 1.6 mm diameter		Bioanalytical Systems Inc
Platinum wire 5 cm, 0.5 mm diameter	99.9%	Fisher Scientific
Saturated calomel electrode		Sentek
Silver-Silver Chloride		Bioanalytical Systems Inc
Materials for Maintaining Electrodes and System		
Aluminium oxide	99.98%	Alfa Aesar
Ferrocene (dicyclopentadienyl iron)		Sigma

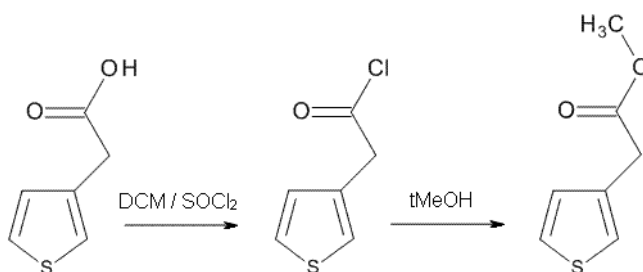
Felt (for polishing)		Bioanalytical Systems Inc
Reagents for Synthesis Procedures		
<i>Tert</i> -Butanol (anhydrous)	99.5%	Sigma-Aldrich
1,3-Dicyclohexylcarbodiimide	99%	Aldrich
N,N'-Diisopropylcarbodiimide	99%	Sigma-Aldrich
N-Hydroxysuccinimide	98%	Aldrich
Iron (III) chloride anhydrous		Lancaster Synthesis
Methanol (anhydrous)	99.8%	Sigma-Aldrich
Molybdenum(V) chloride	95%	Aldrich
Silica TLC cards		Fluka
Thionyl chloride	99.0%	Fluka
Reagents for Biosensor Investigation		
Glucose		Sigma-Aldrich
Glucose Oxidase (EC 1.1.3.4, type X-S 155 U/mg from <i>Aspergillus niger</i>)		Sigma-Aldrich
Potassium dihydrogenphosphate	99%	Aldrich
Potassium chloride	99.5%	AnalaR BDH
Sodium chloride	99.0%	Sigma-Aldrich
Solvents		
Acetonitrile HPLC grade		Fisher Scientific
Dichloromethane laboratory reagent grade		Fisher Scientific
Deuterated chloroform	99.8%	Cambridge Isotope Laboratories, Inc
Ethyl acetate laboratory reagent grade		Fisher Scientific
Petroleum ether laboratory reagent grade		Fisher Scientific
Propylene carbonate	99%	Aldrich

2.0. Synthetic Procedures

Several thiophene monomers were chemically synthesised to investigate electrochemical polymerisation techniques. Esterification employing thiophene-3-acetic acid as the starting reagent was the focus for each synthetic procedure.

2.0.1. Synthesis of Methyl thiophene-3-carboxylate

The synthesis of simple thiophene esters are described in schemes 2.1 and 2.2. The method followed the procedure from Ruff and Abenas¹⁶⁶ and Ganapathy *et al*¹⁶⁷ with the formation of the acid chloride from the addition of dichloromethane and thionyl chloride.



Scheme 2.1. Synthesis of methyl thiophene-3-carboxylate

Thionyl chloride was added in excess to a solution of thiophene-3-acetic acid (0.5 g) dichloromethane (50 ml) and toluene (20 ml). The reaction mixture was heated under reflux for 5 hours, cooled and the solvent was removed under reduced pressure. Dry dichloromethane (40 ml) was added and the reaction vessel was placed under nitrogen. Anhydrous methanol (5 ml) was added under nitrogen and the reaction was left to stir for 1 hour in which the progress of the reaction was monitored using TLC. Purification was performed upon silica gel column chromatography using a ratio of 2:1 ethyl acetate and petroleum ether solvent system. The fractions were collected and the solvent was removed leaving an off-white solid material which was determined to be the methyl thiophene-3-carboxylate with a yield of 51.5%.

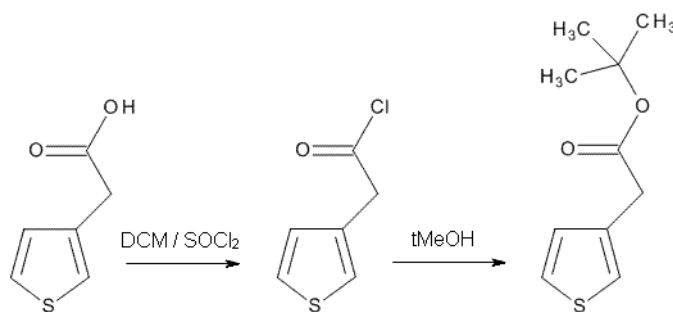
Table 2.2. ^1H nmr (500 MHz) Data in CDCl_3

Chemical Shift (δ)	Multiplicity	No. of H	Assignment
7.31-7.28	m	1	H-position 4
7.17-7.16	d,d	1	H-position 2
7.07-7.05	d,d	1	H-position 5
3.73	s	3	$\text{CH}_2\text{COOCH}_3$
3.69	s	2	$\text{CH}_2\text{COOCH}_3$

Table 2.3. ^{13}C nmr (500 MHz) Data in CDCl_3

Chemical Shift (δ)	Assignment
171.57	$\text{CH}_2\text{COOCH}_3$
133.58	CHSCHCHCCH_2
129.07-128.26	Thiophene ring carbons
125.78	
122.91-122.55	
52.06	$\text{CH}_2\text{COOCH}_3$
35.65	$\text{CH}_2\text{COOCH}_3$

IR Data

C=O st.(ester) 1735 cm^{-1} C-O st. (ester) 1216 cm^{-1} and 1154 cm^{-1} C-H st. (alkene C=C-H) (Ar-H) $2904\text{-}3097\text{ cm}^{-1}$ **2.0.2. Synthesis of Tert-butyl thiophene-3-carboxylate**

Scheme 2.2. Synthesis of tert-butyl thiophene-3-carboxylate

The same method was employed for the synthesis of tert-butyl thiophene-3-carboxylate where the methyl alcohol was substituted for the butyl alcohol reagent (0.5 ml). The yield obtained was 54.9%.

Table 2.4. ^1H nmr (500 MHz) Data in CDCl_3

Chemical Shift (δ)	Multiplicity	No. of H	Assignment
7.31-7.29	m	1	H-position 4
7.16-7.15	d,d	1	H-position 2
7.07-7.06	d,d	1	H-position 5
3.59	s	2	$\text{CH}_2\text{COOC}(\text{CH}_3)_3$
1.49	s	9	$\text{CH}_2\text{COOC}(\text{CH}_3)_3$

Table 2.5. ^{13}C nmr (500 MHz) Data in CDCl_3

Chemical Shift (δ)	Assignment
170.4	$\text{CH}_2\text{COOC}(\text{CH}_3)_3$
134.3	CHSCHCHCCH_2
128.5	Thiophene ring carbons
125.4	
122.4	
81	$\text{CH}_2\text{COOC}(\text{CH}_3)_3$
37.1	$\text{CH}_2\text{COOC}(\text{CH}_3)_3$
28.0	$\text{CH}_2\text{COOC}(\text{CH}_3)_3$

IR Data

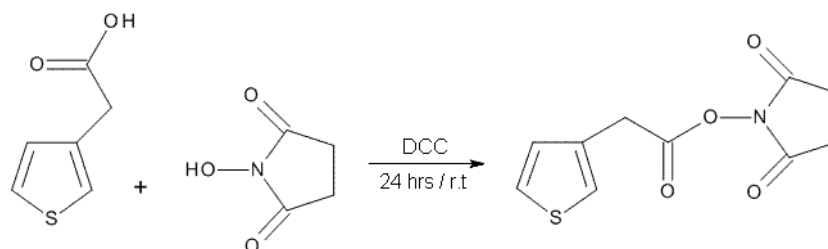
C=O st.(ester) 1733 cm^{-1}

C-O st. (ester) 1141 cm^{-1} and 1080 cm^{-1}

C-H st. (alkene C=C-H) (Ar-H) $2929\text{-}3107\text{ cm}^{-1}$

2.0.3. Synthesis of N-succinimido thiophene-3-acetate

N-succinimido thiophene-3-acetate was prepared from thiophene-3-acetic acid using dicyclohexylcarbodiimide (DCC) as coupling reagent detailed in scheme 2.3.



Scheme 2.3. Synthesis of N-succinimido thiophene-3-acetate

The general procedure for the synthesis is as follows: Thiophene-3-acetic acid (1.86 g), DCC (2.7 g) and N-hydroxysuccinimide (1.5 g) in an equal mole ratio were combined with 90 ml of acetonitrile. The reaction was stirred for 24 hours at room temperature and monitored through TLC. When the reaction had reached completion it was filtered and the solvent was reduced under pressure. The reaction mixture was purified upon a silica column with ethyl acetate and petroleum ether at a ratio of 1:1. The product was collected as an off white solid material which was determined as N-succinimido thiophene-3-acetate with a yield of 66.0 %.

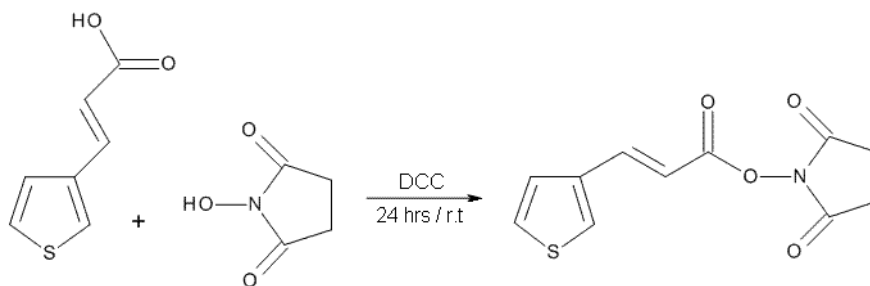
Table 2.6. ^1H nmr (500 MHz) Data in CDCl_3

Chemical Shift (δ)	Multiplicity	No. of H	Assignment
7.35-7.34	m	1	H-position 4
7.32-7.29	d,d	1	H-position 2
7.11-7.10	d,d	1	H-position 5
3.99	s	2	$\text{CH}_2\text{COOC}(\text{CH}_3)_3$
2.84	s	4	$\text{CH}_2\text{COOC}(\text{CH}_3)_3$

Table 2.7. ^{13}C nmr (500 MHz) Data in CDCl_3

Chemical Shift (δ)	Assignment
168.98	$\text{CH}_2\text{COON}(\text{CO})_2(\text{CH}_2)_2$
166.25	$\text{CH}_2\text{COON}(\text{CO})_2(\text{CH}_2)_2$
130.62	CHSCHCHCCH_2
123.26	Thiophene ring carbons
126.25	
128.10	
32.31	CHSCHCHCCH_2
25.25	$\text{CH}_2\text{COON}(\text{CO})_2(\text{CH}_2)_2$

IR Data

C=O st. (ester) 1724 cm^{-1} C=O st. (Saturated anhydride $-\text{CO}-\text{N}-\text{CO}-$) 1781 cm^{-1} and 1823 cm^{-1} C-O st. 1198 cm^{-1} and 1253 cm^{-1} C-H st. (alkene $\text{C}=\text{C}-\text{H}$), (Ar-H) $2849\text{--}3095\text{ cm}^{-1}$ **2.0.4. Synthesis of N-succinimido trans-3-(3-thienyl) acetate**

Scheme 2.4. Synthesis of N-succinimido trans-3-(3-thienyl) acetate

Equal mole ratios of all reagents were used to synthesise N-succinimido trans-3-(3-thienyl) acetate. Trans-3-(3-thienyl) acrylic acid (67.1 mg) was prepared with the same method for the synthesis of N-succinimido thiophene-3-acetate in scheme 2.3. N-succinimido trans-3-(3-thienyl) acetate was obtained with a yield of 59.8 %.

Table 2.8. ^1H nmr (500 MHz) Data in CDCl_3

Chemical Shift (δ)	Multiplicity	No. of H	Assignment
7.85-7.81-	d	1	$\text{CHCHCOON}(\text{CO})_2(\text{CH}_2)_2$
7.57-7.56	d,d	1	H-position 5
7.33-7.31	m	1	H-position 4
7.28-7.26	d,d	1	H-position 2
6.40-5.97	d	1	$\text{CHCHCOON}(\text{CO})_2(\text{CH}_2)_2$
2.82-2.81	s	4	$\text{CHCHCOON}(\text{CO})_2(\text{CH}_2)_2$

Table 2.9. ^{13}C nmr (500 MHz) Data in CDCl_3

Chemical Shift (δ)	Assignment
169.36	$\text{CHCHCOON}(\text{CO})_2(\text{CH}_2)_2$
162.32	$\text{CHCHCOON}(\text{CO})_2(\text{CH}_2)_2$
143.21	$\text{CHCHCOON}(\text{CO})_2(\text{CH}_2)_2$
136.82	CHSCHCHCCHCH
127.55	Thiophene ring carbons
125.04	
122.4	
110.95	CHSCHCHCCHCH
25.62	$\text{CH}_2\text{COON}(\text{CO})_2(\text{CH}_2)_2$

IR Data

$\text{C}=\text{O}$ st. (ester) 1724 cm^{-1}

$\text{C}=\text{O}$ st. (Saturated anhydride $-\text{CO}-\text{N}-\text{CO}-$) 1761 cm^{-1} and 1784 cm^{-1}

$\text{C}-\text{O}$ st. 1213 cm^{-1} and 1194 cm^{-1}

$\text{C}-\text{H}$ st. (alkene $\text{C}=\text{C}-\text{H}$), (Ar-H) $2852-3098\text{ cm}^{-1}$

2.1. Polymer Generation

2.1.1. Chemical Polymerisation

Chemical polymerisation was performed upon the three acid substituted monomers 3-thiophenecarboxylic acid, thiophene-3-acetic acid and 3-thiophenemalonic acid along

with thiophene and bithiophene, which were known to polymerise readily. The same quantity of each monomer material (0.5 g) was dissolved in 25 ml of acetonitrile and 1.0 g of anhydrous FeCl_3 was introduced to the mixture as the oxidant. A second set of chemical polymerisation was performed for the same monomers with a more powerful oxidant (MoCl_5).

2.1.2. Electrochemical Polymerisation

Electrochemistry investigations were performed using autolab software with a general-purpose electrochemical system installed with windows version 4.9. A conventional three-electrode set up was employed with a platinum working electrode, platinum wire counter electrode and an $\text{Ag}|\text{AgCl}/\text{KCl}_{\text{sat}}$ reference electrode. A 1 mM ferrocene solution was used for checking the integrity of the system each day and aluminium oxide slurry provided the ideal medium for electrode surface regeneration after subsequent film formation.

Development of the polymer film upon the platinum working electrode surface was typically produced with 0.1 M of monomer in a 0.1 M electrolyte solution of 10 ml solvent. The parameters chosen depended upon the experiment undertaken but included those listed below. Initial studies of polymer growth were performed by cyclic voltammetry and eventually potentiostatic conditions generated thicker films with a passed charge of 800 mC for microscopy and elemental characterisation.

Table 2.10. Various electrolyte and solvents used within the project.

Electrolyte	Solvent
Tetrabutylammonium tetrafluoroborate	Acetonitrile
Lithium perchlorate	Propylene carbonate
Tetrabutylammonium perchlorate	Dichloromethane
Tetraethylammonium <i>p</i> -toluenesulfonate	

2.2. Film Characterisation

The polymer films which remained attached to the electrode surface were washed thoroughly in acetonitrile to remove excess monomer and electrolyte.

Cyclic voltammetry was chosen for the characterisation of the electrochemically-generated polymer incorporating a monomer free solution with 0.1 M electrolyte and 10 ml of organic solvent.

2.3. Atomic Absorption Spectroscopy

Atomic absorption spectroscopy was employed for the quantification of carboxylic acid functional groups within various copolymer ratios by sodium exchange.

Plastic volumetric flasks and beakers were used within the investigation to avoid sodium absorption onto glass and the primary standard sodium chloride was used after oven drying (50 °C overnight) for the sodium exchange and standard preparation for the instrument.

Homopolymers of 0.6 M thiophene-3-acetic acid (2.2 V 800 mC) and 0.1 M 3-methylthiophene (1.7 V 800 mC) were first grown and used at the same weight to determine the accuracy of the method. A five figure analytical balance was used for accurate mass determination in which 0.45 mg films were used and weighed to constant mass.

The films were placed in 2 M Na⁺ solution and agitated for 10 minutes then left overnight. An extensive wash method was employed to eliminate trapped sodium from the material which included three, 30 second vortex of the ion exchanged film in hot ultra pure water followed by 20 minutes of gentle boiling in 40 ml and finally 50 ml of hot ultra pure water washed over the film in a filter using a pipette.

After 30 minutes in the oven to dry at 100 °C the films were placed in epindorff tubes with 1.2 ml of high grade (low sodium content) concentrated HNO₃ and left to completely dissolve.

Calculation for Sodium Ion Content in a 0.45 mg Poly(thiophene-3-acetic acid) Film.

$$Mols = \frac{0.45 \times 10^{-3} g}{142 g mol^{-1}} = 3.17 \times 10^{-6} mol$$

$$\text{Concentration} = \frac{3.17 \times 10^{-6}}{0.0012} = 2.64 \times 10^{-3} \text{ M}$$

$$2.64 \times 10^{-3} \times 23 \times 1000 = 60.72 \text{ ppm of Na}^+$$

From the calculation above a suitable dilution could be determined for the atomic absorption spectrometer as the highest concentration measureable is 1 ppm.

Standards were prepared from a 10 ppm Na⁺ stock solution covering the range 0.1-1 ppm and were run on the instrument using a sodium lamp set at a wavelength of 589 nm. The Standards were prepared fresh each day providing a straight line calibration graph.

2.4. Scanning Electron Microscopy with Elemental Detection

Microscopy enables a pictorial representation of the structure generating morphological information. In this case scanning electron microscopy (SEM) is employed for the visual characterisation of the polymer films.

Scanning electron microscopy forms the images seen by the generation of electrons in contrast to conventional microscopes that utilise light. This approach allows for larger depth of field, greater magnification and higher resolution. The images obtained are created through either secondary or backscattered electrons which are generated when the incident electron beam interacts with the specimen.

Backscattered electrons originate from the incident beam and have been deflected through a circular path around the atoms nucleus. Such electrons that occupy this path have sufficient energy to exit the sample whereas lower energy backscattered electrons have generally passed through smaller angle scattering events to eventually emerge from the material. Due to the differing nuclei within the various atomic species the number of deflected electrons will vary as larger atoms will increase the amount of backscattered electrons.

Secondary electrons can also be used for viewing the image. The electrons detected are outer shell electrons released from the sample atoms by interaction with the

incident beam. They are low in energy and so can only escape from a shallow depth to be detected.

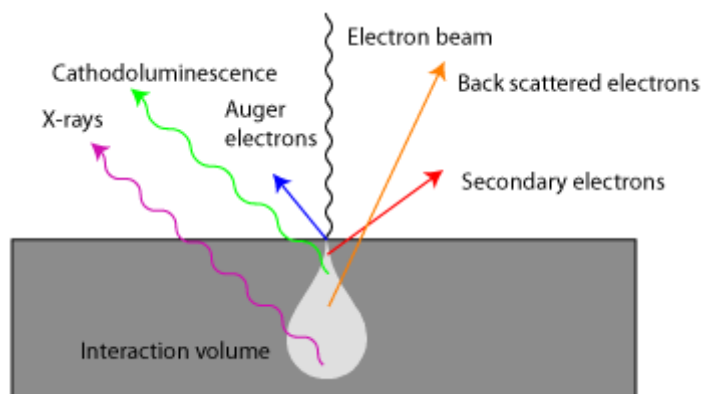


Figure 2.1 Various forms of energy release produced through sample irradiation¹⁶⁹

2.4.1. Elemental Analysis

The scanning electron microscope is equipped with elemental acquisition capabilities in the form of an energy-dispersive x-ray detector. X-rays are the result of the emission of inner core electrons, leaving the atom in an ionised form where stabilisation then occurs by the transition of an outer electron to fill the vacancy with the generation of an x-ray photon. The energy of the emitted x-ray photon is associated with the elements electronic configuration and is therefore unique to the individual element.

Films were grown potentiostatically upon either the platinum working electrode or ITO glass depending upon film thickness and amounts required.

Due to the conducting properties of the polymer materials the samples did not require sputter coating and were therefore peeled away from the electrode surface and mounted upon aluminium stubs for microscopy examination upon the solution side of the electro generated material.

Secondary electron detection was responsible for the images generated. A range of magnifications were employed to establish detailed polymer film topography.

Backscattered electron mode enabled elemental mapping of the samples and x-ray generated signals were used to identify the composition and measure the abundance of

elements in the sample. For reliable elemental data the system recommended a high-energy electron beam set to 20 kV and a working distance of 10 mm. Spot size remained constant at 69 and dead time was recommended to be no lower than 20%. The parameters chosen remained unchanged where elemental information was concerned in order to compile data over several areas of the sample for the generation of average values.

2.5. Fourier Transform Infra Red Spectroscopy (FTIR)

Both monomeric and polymeric material were characterised by infra red spectroscopy. Monomers obtained commercially were analysed along with synthetically produced monomer as a method for identification. Spectra were recorded over the range of 400 cm^{-1} to 4000 cm^{-1} and data provided in absorbance mode for comparison purposes. Copolymer composites were characterised through FTIR for assignment of the carbonyl function group and its intensity.

2.6. Nuclear Magnetic Resonance (NMR)

Commercial and synthetic monomers were analysed on a 500 MHz NMR instrument using both carbon and proton NMR operation for identification and to assess the purity of the synthesised material. The solvent used was CDCl_3 unless otherwise stated.

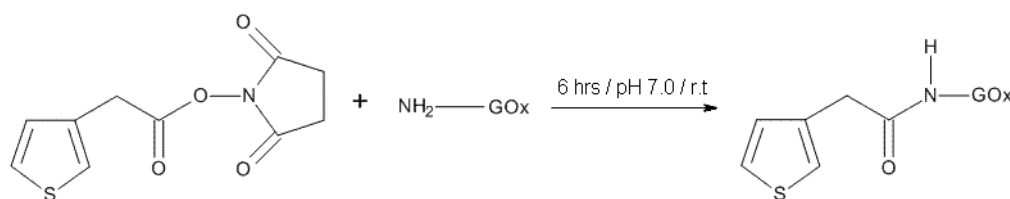
2.7. Biosensor Analysis

Optimum conditions were established for the sensor device in which the methods for the optimised biosensor system are reported here, all other experimental conditions are documented with the results in chapter 5.

2.7.1. Film Preparation

Copolymer films of thiophene-3-acetic acid/3-methylthiophene, trans-3-(3-thienyl) acrylic acid/3-methylthiophene, N-succinimido thiophene-3-acetate/3-methylthiophene and N-succinimido trans-3-(3-thienyl) acetate/3-methylthiophene were grown potentiostatically at 2.2 V until a charge of 50 mC was reached. The electrodes were washed with acetonitrile to remove excess monomer and electrolyte and then left on the bench top for the solvent to evaporate prior to enzyme immobilisation.

2.7.2. Enzyme Immobilisation



Scheme 2.5. Immobilisation of GOx on the polymer film.

Copolymers containing the activated ester (N-succinimido thiophene-3-acetate/ 3-methylthiophene and N-succinimido trans-3-(3-thienyl) acetate/3-methylthiophene) were placed in 0.01 M phosphate buffer solution pH 7.0 with 16 mg /5 ml (153100 Units/G) glucose oxidase (*Aspergillus niger*) for six hours and left to stir gently at room temperature. After six hours the enzyme electrodes were removed from the enzyme solution and rinsed with phosphate buffer solution in which they were then stored and kept at room temperature (unless otherwise stated) until they were analysed.

Copolymers with the carboxylic acid group were immobilised with glucose oxidase (16 mg) in a 0.01 M phosphate buffer solution pH 7.0 with EDC (60 mg) for six hours at room temperature for a direct comparison.

2.7.3. Response to Glucose

A three electrode system was prepared as stated in section 2.1.2. The analysis of the enzyme electrodes were performed in 0.01 M phosphate buffer solution with 0.01 M sodium chloride as the electrolyte under constant stirred conditions. 0.1 M *p*-benzoquinone was employed as a mediator using the same amount stated in the literature⁵⁴ for the generation of reproducible results.

Amperometry was used to monitor the current signal to 0.1 M additions of glucose with an applied potential of 0.45 V with the mediator in solution and 0.70 V when no mediator was used. Sufficient time was allowed upon each glucose addition for the signal to stabilise and an accurate reading to be recorded. All data was displayed as current density against glucose concentration.

2.8. UV Spectroscopy

UV spectroscopy was used to establish whether the glucose oxidase was active prior to its immobilisation¹⁶⁹.

A 16 mM glucose sample was prepared by taking 4 ml of a 0.2 M glucose stock solution and diluting to 50 ml with deionised water. A blank was used containing only deionised water.

An enzyme working solution was also prepared containing 7.50 mM phenol, 2.50 mM 4-aminophenazone, 0.5 IU/mL GOx, and 20 IU/mL HRP in 25 ml of 0.10 M pH 7.0 phosphate buffer.

2 ml of the enzyme working solution was delivered to a cuvette followed by the addition of 0.4 ml of the 16 mM glucose solution. The reaction mixture was shaken and inserted into the spectrometer. The first reading was taken immediately and a stopwatch was started. Absorbance values were then taken every minute for 10 minutes. The same method was followed for the blank and the data was recorded and displayed in table 2.11.

Table 2.11. Absorbance Readings Taken from an Enzyme Assay and Blank Solution

Time (minutes)	Glucose Assay	Blank Assay
0	0.043	0.029
1	0.083	0.026
2	0.112	0.026
3	0.149	0.027
4	0.19	0.026
5	0.228	0.026
6	0.268	0.027
7	0.309	0.027
8	0.346	0.028
9	0.386	0.028
10	0.424	0.029

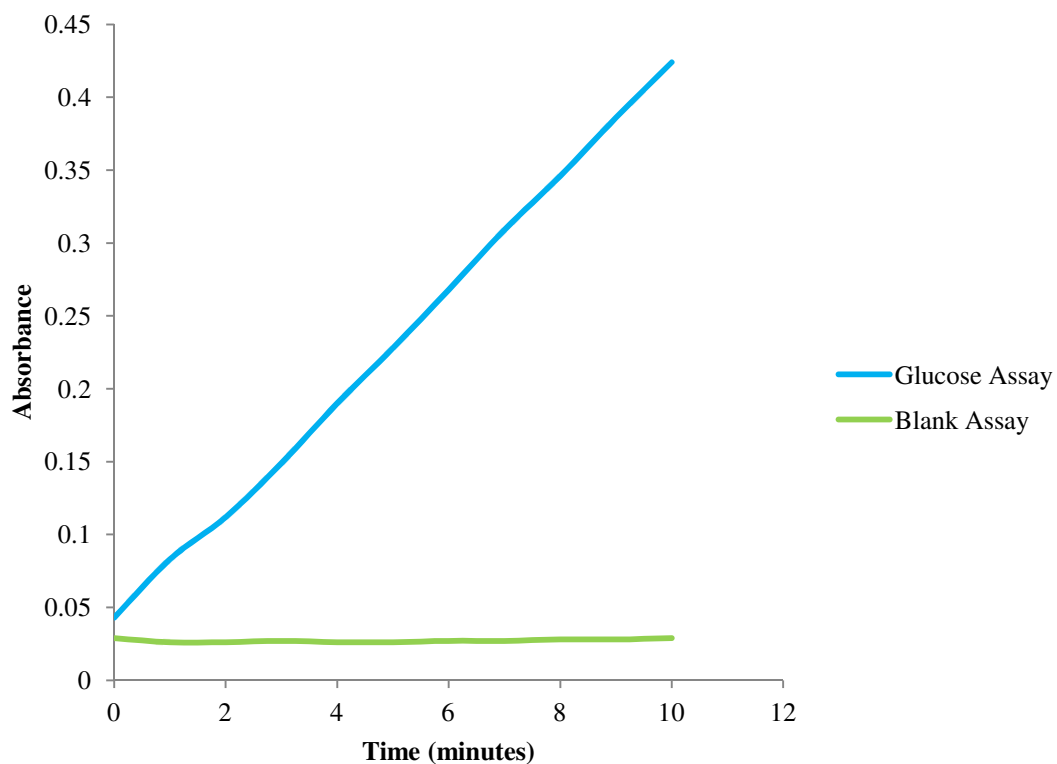


Figure 2.2. Measurement of absorbance as a function of time for glucose oxidase assays with and without glucose.

The increase in absorbance where glucose was present demonstrated that the enzyme was active and therefore was used for immobilisation upon the conducting polymer platforms in chapter 5.

Chapter 3 Electrochemistry of Polythiophene Materials

3.0. Electrochemistry of Polythiophenes

Thiophene compounds were investigated using electrochemical techniques to establish criteria for polymerisation and film stability for their potential use as a substrate to accommodate a biological species. Simple thiophene compounds were explored initially with the dimer 2,2'-bithiophene, chosen as a substitute for the thiophene monomer as thiophene is unsuitable for prolonged use due to its odoriferous effects.

The electrochemistry of simple polythiophene materials has been extensively investigated^{17,24-25,34-35,41,44,170}. The repetition of this work within our own experimental set up is important in order to understand and interpret the subsequent behaviour of novel materials.

3.0.1. Electrochemical Polymerisation of Bithiophene

Polymer film generation is dependent upon several factors such as solvent, potential, and monomer concentration. The potential required to initiate polymerisation is the oxidation potential and can be determined by cycling voltammetry of a monomer / electrolyte solution. The current increase observed indicates polymerisation at the electrode surface with an increase in current through subsequent scans. Cyclic voltammetry is also used to probe the electrochemistry of the resulting film. Typically a large potential sweep is employed for the investigation of new compounds to ensure all the electrochemical data is collected.

Figure 3.1 demonstrates the electrochemical oxidation of bithiophene in a 0.1 M monomer solution using TBATFB as electrolyte. The signal increase at 1.16 V indicates the oxidation of the monomer and is typified by the presence of a hysteresis or nucleation loop characteristic of the polymerisation of conducting polymers^{7,45,65,67,78}. Further extension of the potential towards positive values seen in figure 3.1 introduces over oxidation. It is recommended that over oxidation be avoided due to irreparable damage to the film. Disruption caused along the polymer chain backbone through twisting destroys the conjugative effect that is responsible for film conductivity¹⁵⁻¹⁷.

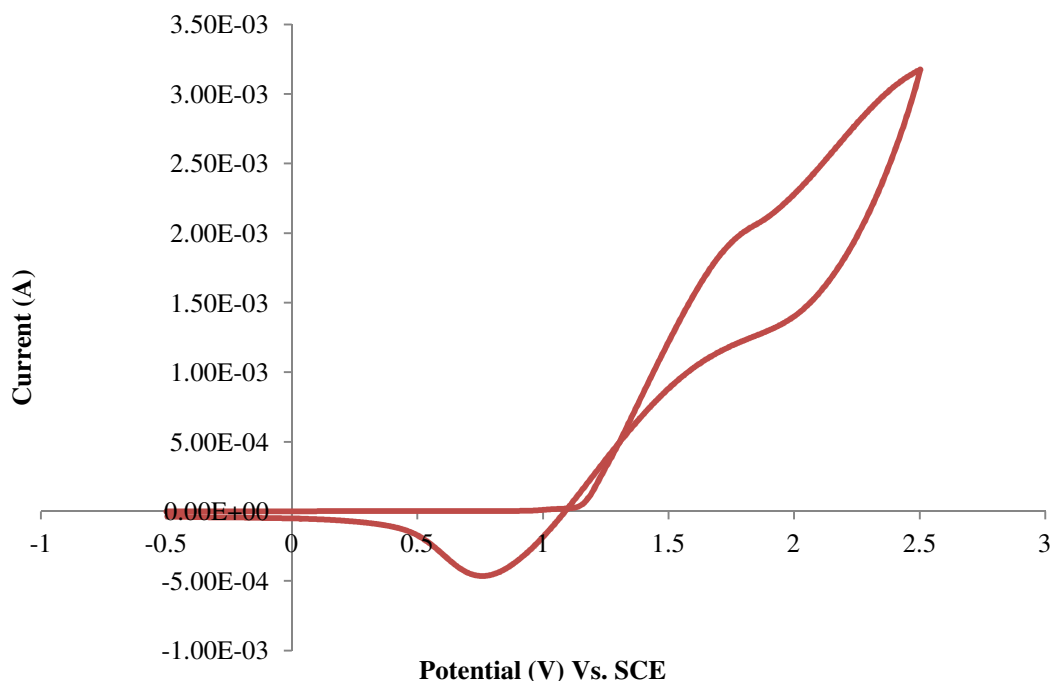


Figure 3.1. A single growth cycle of bithiophene incorporating TBATFB.

Potentiostatic polymerisation was used as a different approach to determine the oxidation potential of bithiophene. A series of experiments employing fixed potentials were performed over 60 s concluding that successful polymerisation does not commence until a sufficiently high potential is applied, determined for bithiophene as 1.2 V. Following all potentiostatic polymerisation experiments visual examination of the electrode surface was the initial method for identification of film formation which was coupled by the more reliable determination by characterisation through cyclic voltammetry.

Table 3.1. Potentiostatic Polymerisation of Bithiophene (SCE)

Potential	Film	Description
0.8 V	No visible film	No redox signals in CV.
0.9 V	No visible film	No redox signals in CV.
1.0 V	No visible film	No redox signals in CV.
1.1 V	Dark yellow film	No redox signals in CV.
1.2 V	Black film produced	Broad redox signals in CV.

Thick films generated by potentiostatic or potential cycling methods are difficult to characterise. The characterisation of a thick film produced by cyclic voltammetry can be seen in figure 3.2.

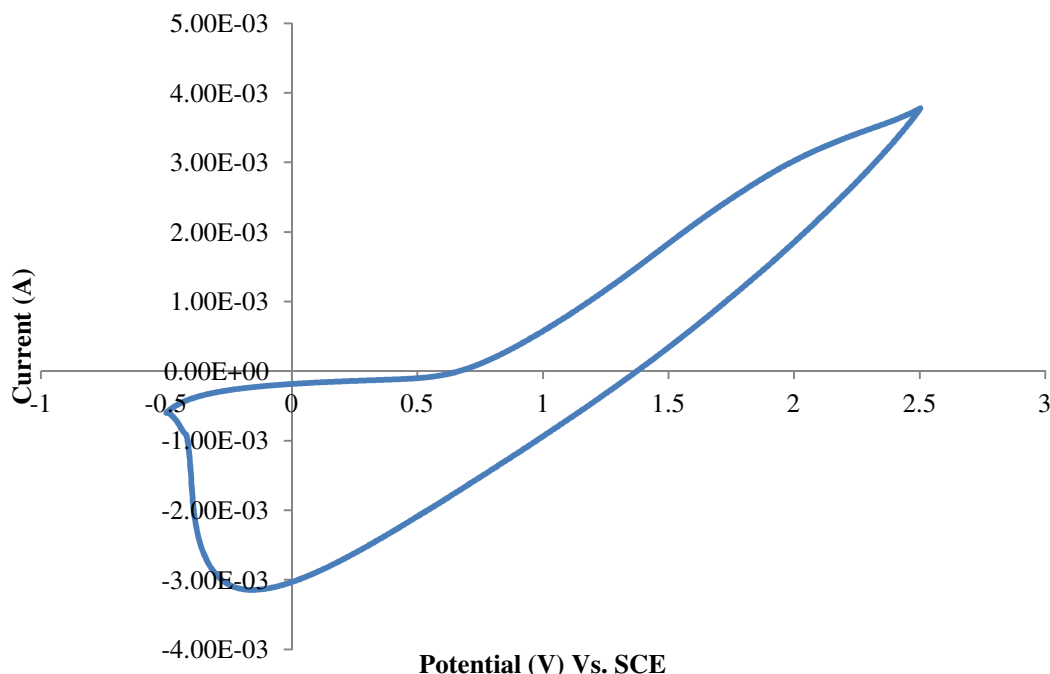


Figure 3.2. Characterisation of poly(bithiophene) utilising a wide potential window.

Broad oxidation from +0.6 V is observed with no clear oxidation peaks and reduction represents a broad peak at around -0.25 V. These ill defined responses are unsuitable in terms of characterising the effects of growth parameter changes and therefore a potentiodynamic method was employed which allowed reliable oxidation and reduction information to be generated by setting the oxidation potential of the monomer as the cycle limit and controlling the amount of cycles passed for film development.

Figure 3.3 displays the typical *i*/*E* curve recorded during polymer potentiodynamic electrogeneration. The potential was cycled from 0 to +1.2 V at a scan rate of 100 mV s⁻¹. The initial scan shows current increase from +1.0 V due to oxidation of the monomer to which a cathodic process occurring at *ca.* + 0.7 V is directly associated.

Oxidation occurs more readily over consecutive cycles compared to the first potential scan. Monomer oxidation requires a larger potential for radical cation formation

compared to the longer polymer chains formed after several cycles. This is evident from the decreasing positive potentials required to oxidise the polymer upon increasing scan number.

The redox responses account for the p-doping and the de-doping of the bithiophene polymer growing upon the electrode. The electrolyte present in the polymerisation solution provides the anions that dope the developing film upon oxidation and de-dope the material through reduction over increasingly negative potentials. Polymer deposition can be indicated by the current signal increase, which is observed through consecutive cycling as the polymer layer thickens effectively increasing the surface area of the electrode.

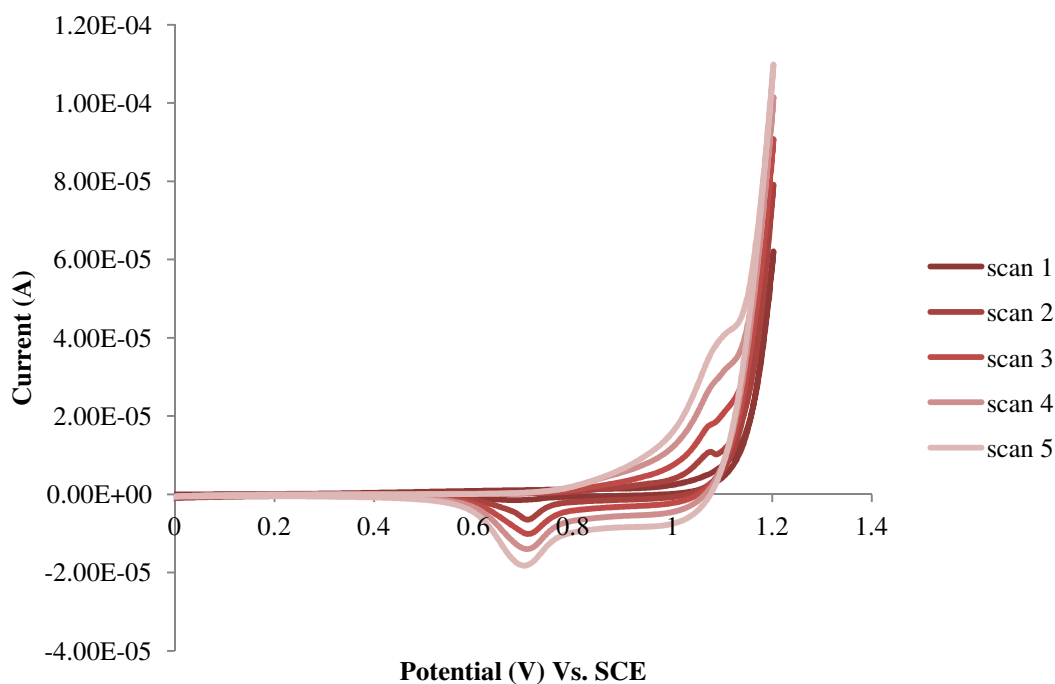


Figure 3.3. Bithiophene polymer growth.

Investigations into the cycle number for film generation concluded that five cycles over the potential range 0 V-1.2 V-0 V produced an even film that covered the electrode surface. Visible electrochromic switching could be detected from dark blue when oxidised to red upon reduction of the film and detailed redox data was provided when characterised through cyclic voltammetry.

3.0.2. Stability of Poly(bithiophene) during Cycling

Narrow potential range and low cycle numbers demonstrate maximum detail in the CV of the resulting poly(bithiophene) material seen in figure 3.4 where a monomer free $\text{CH}_3\text{CN}/\text{TBATFB}$ solution was used and a potential window from 0.0 V to +1.4 V at 100 mV s^{-1} was employed. The first scan demonstrates a clearly defined redox couple occurring at +1.09 V and +0.67 V. A negative shift directly follows upon the anodic response of the second scan which then progressively became more anodic through increased cycles. Signal decrease was evident, and the current fell to less than 40 % of the original anodic response although the rate of decline slowed with each cycle.

The initial large oxidation response is commonly observed with the electrogeneration of conducting polymers¹⁷¹ as it is likely residual monomers or oligomers become trapped in the resulting polymer. The decreasing current throughout the remaining cycles can be explained as a result of the degradation of the pi orbital overlap through the polymer backbone described previously as over oxidation. This was observed through the manifestation of a second oxidation response from +1.2 V to +1.4 V.

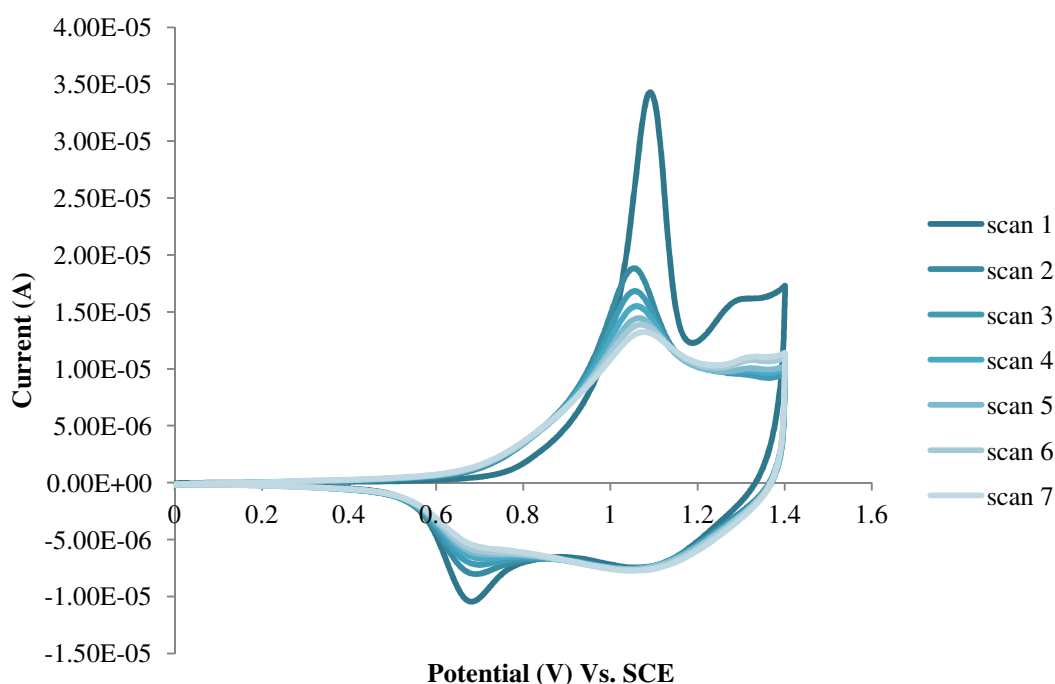


Figure 3.4. Degradation of poly(bithiophene) characterised by cyclic voltammetry.

Characterisation potentials were investigated to establish a cycling limit that would conserve the integrity of the film thereby generating redox responses that would resist current decrease and potential shift.

Poly(bithiophene) films were grown under potentiodynamic conditions to +1.2 V for five consecutive cycles using TBATFB in both the growth and characterisation solutions. Their characterisation utilised three upper potential limits of +1.2, +1.4 and +1.6 V and can be seen below. The effect of higher potentials acting upon the film was clear. A larger second oxidation wave is generated when scanning out to +1.6 V destroying the film and generating minimal reduction on the reverse scan. The same effect was seen by Kabasakaloglu *et al* with polythiophene where redox features are lost and conductivity is destroyed at potentials above +1.4 V⁷².

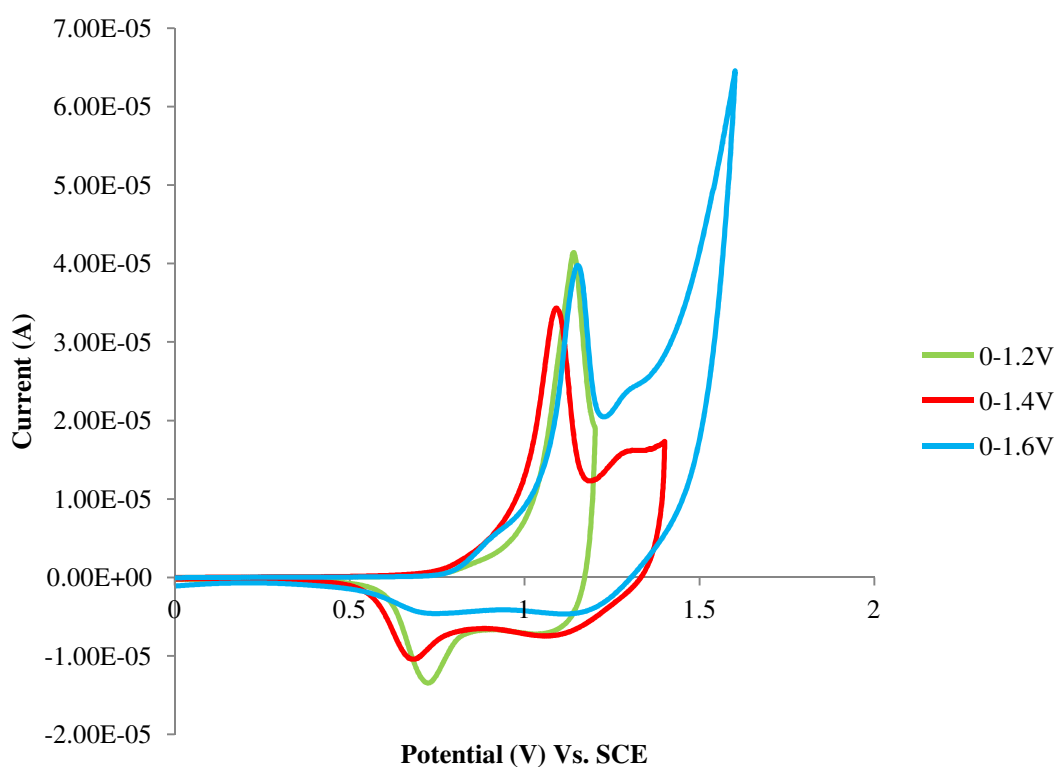


Figure 3.5. Characterisation of bithiophene employing various potentials.

Initialising characterisation at 0 V where there was no electrochemistry and restricting scan potentials to +1.2 V generated a clear redox couple with a sharp anodic peak at +1.14 V followed by reduction at +0.72 V which, over several cycles maintained peak currents indicating a reversible process with high stability as shown in figure 3.6.

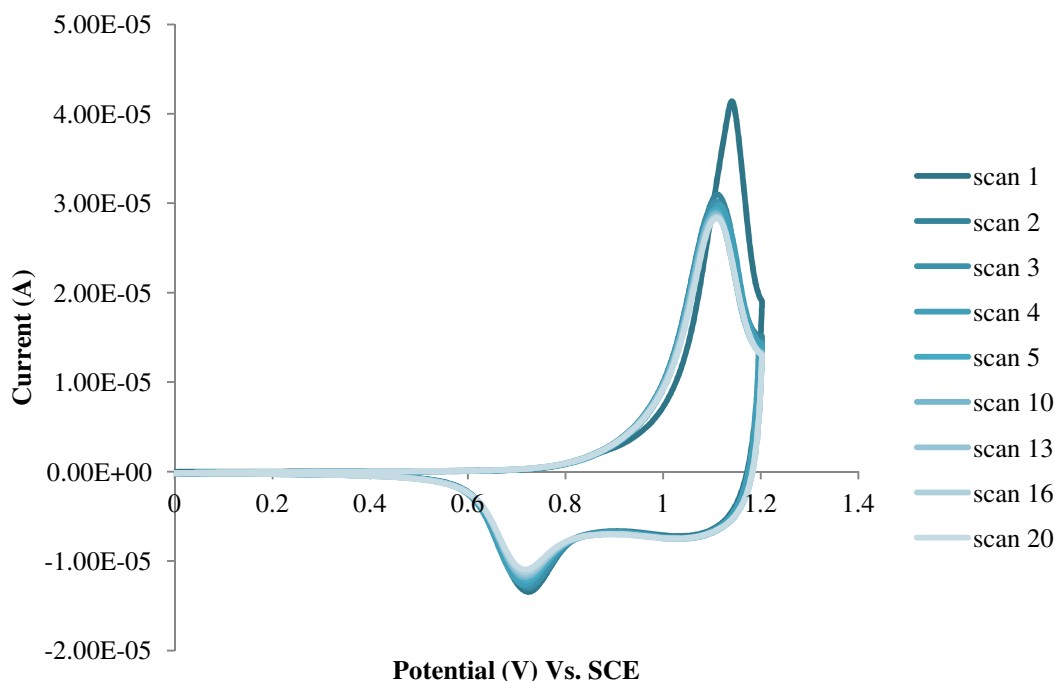


Figure 3.6. 0.1 M Bithiophene demonstrating minimal current decrease after scan 2.

3.0.3. Electrochemical Characterisation of Bithiophene

The shape of the poly(bithiophene) voltammogram was dependent upon the starting potential of the cycle. Initialising polymer characterisation at potentials when the film was electrochemically active induced a much broader voltammogram with two reduction processes compared to starting the cycle at 0.0 V. Due to the broad response a wider potential window was employed to capture the electrochemical data, reducing the film thickness by controlling the cycle number provided additional information upon characterisation. The film generated by a single polymer growth cycle (0-1.2-0 V) clearly contains two redox couples in comparison to the single redox pair observed in the forward mode of characterisation. Oxidation is seen at +1.0 V with an ill defined response at +1.2 V and reduction of the film provides two broad cathodic responses seen at +1.0 V and +0.61 V.

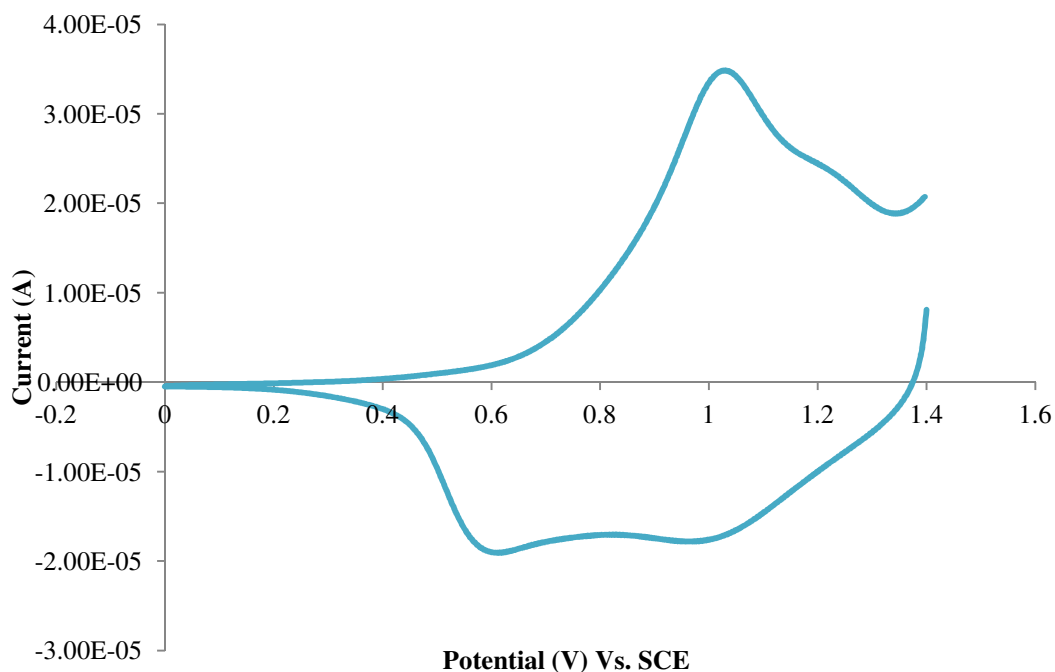


Figure 3.7. Characterisation of thin film bithiophene polymer.

3.0.4. Influence of Solvent and Dopant upon Bithiophene Growth

There exists a range of solvents suitable for electrochemical experiments the relevant solvent properties include solvating power and reactivity^{64,172-174}. Acetonitrile, dichloromethane and propylene carbonate were the three solvents investigated. All offer good solvating power important for ionic character with acetonitrile providing high stability under oxidative and reductive potentials, dichloromethane recommended for oxidative electrochemistry and propylene carbonate effective for use with lithium salts.

According to Roncali⁵⁷ the solvent used to electrogenerate conducting polymers provides influential effects upon the structure and properties associated with the film⁵⁷. It is therefore important to employ a solvent that possess high polarity to ensure the ionic conductivity of the system. Also electrochemical resistance of the solvent is important to enable film generation without suffering extensive decomposition at increased positive potentials¹⁷³.

The support electrolyte is an essential constituent in the electrochemical growth of conducting polymers. The electrochemical oxidation leads to the incorporation of

charge compensating anions into the polymer film. The anions are referred to as the dopant ions and provide conductivity within the conjugated structure upon oxidation. However the film becomes electrically insulating when the dopant is forced out of the polymer through electrochemical reduction. The interaction of specific dopant ions in the polymer has been reported¹⁷⁵⁻¹⁷⁶ with suggested anion involvement occurring mostly within the polymer growth.

The dopant species employed within this investigation were *p*-toluene sulphonate, perchlorate and tetrafluoroborate. Two perchlorate species were studied with Li^+ and TBA^+ as the associated cations.

The three electrolytic solvents have been investigated to monitor the electrochemical behaviour upon the electrodeposition of the conducting film with the intercalation of four different dopants.

The electrochemical responses seen within different solvents demonstrate the facile electropolymerisation of 2,2-bithiophene in acetonitrile. Oxidation at lower potentials is achieved in acetonitrile with the most accumulated charge seen more clearly when five growth cycles had been completed.

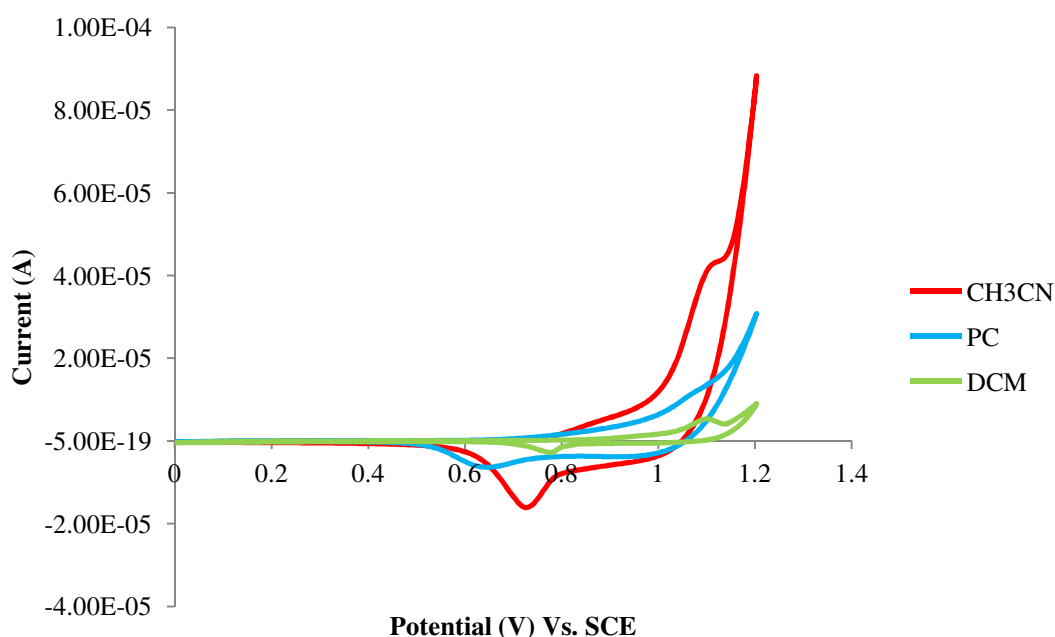


Figure 3.8. The fifth 2,2-bithiophene growth cycle in a range of solvents with TBATFB.

Table 3.2. Polymer Growth Data for Different Solvent and Electrolyte systems.

Solvent	Dopant	Anodic Charge (μC) 1 st Scan	Anodic Charge (μC) 5 th Scan
Acetonitrile	TBATFB	73.82	138.9
	PTS	190.4	136.4
	TBAClO ₄	126.5	359.6
	LiClO ₄	151.8	503.7
Propylene Carbonate	TBATFB	37.85	56.58
	PTS	72.9	65.3
	TBAClO ₄	49.7	86.2
	LiClO ₄	94.5	146.4
Dichloromethane	TBATFB	15.22	14.30
	PTS	49.1	44.2
	TBAClO ₄	28	43.2

From these results the main response observed was clearly the higher current produced when acetonitrile was the solvent. The tabulated data displays the charge accumulated upon the first and fifth scans demonstrating their higher values. Various dopants were employed in the study which emphasized the larger currents obtained in this solvent where figure 3.9 displays the fifth scan of bithiophene grown in the various electrolyte media.

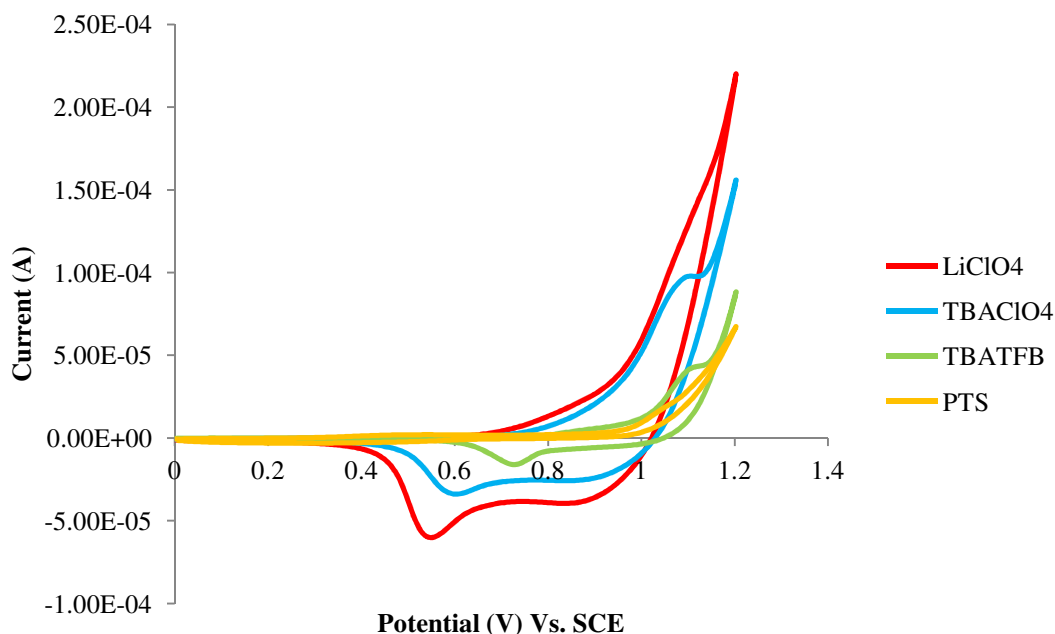


Figure 3.9. Bithiophene growth in acetonitrile incorporating different electrolytes.

It was clear that the perchlorate grown films generated the larger currents with PTS demonstrating limited electrochemical activity. A single weak anodic signal is observed for the PTS incorporated solution with reduction remaining absent. Each electrolyte that produced increasing current signals through successive growth cycles developed the reduced form of the poly(bithiophene) film upon the electrode surface. The PTS electrolyte that did not generate the typical polymer growth response resulted in a yellow film. Therefore the PTS anion does not support polymer growth but passivates the electrode surface forming a yellow non conducting material observed after five potential sweeps.

The large current responses generated by LiClO_4 in acetonitrile can be associated with facile polymerisation in comparison to the other solvents and dopants investigated and therefore will be incorporated in the following electrochemical studies.

3.0.5. Investigating Different Dopants within Film Growth and Characterisation

The electropolymerisation of bithiophene in various solvent and electrolyte systems concluded that LiClO_4 and acetonitrile generated the largest current signals after five growth cycles with good adherent films covering the electrode surface.

The investigation of electrolyte employed for film characterisation is also important as the behaviour of the polymer material during the charge-discharge process is affected by the dopant used¹⁷⁶. Both the anion and cation influence the redox processes and this is generally observed through the shape of the cyclic voltammogram¹⁷⁵⁻¹⁷⁶.

Characterisation of the electrogenerated films were investigated through cyclic voltammetry in which five growth cycles were used to produce the film with the resulting polymer characterised at 50 mV s^{-1} . The slower scan rate enabled more detail to be observed upon the redox signals.

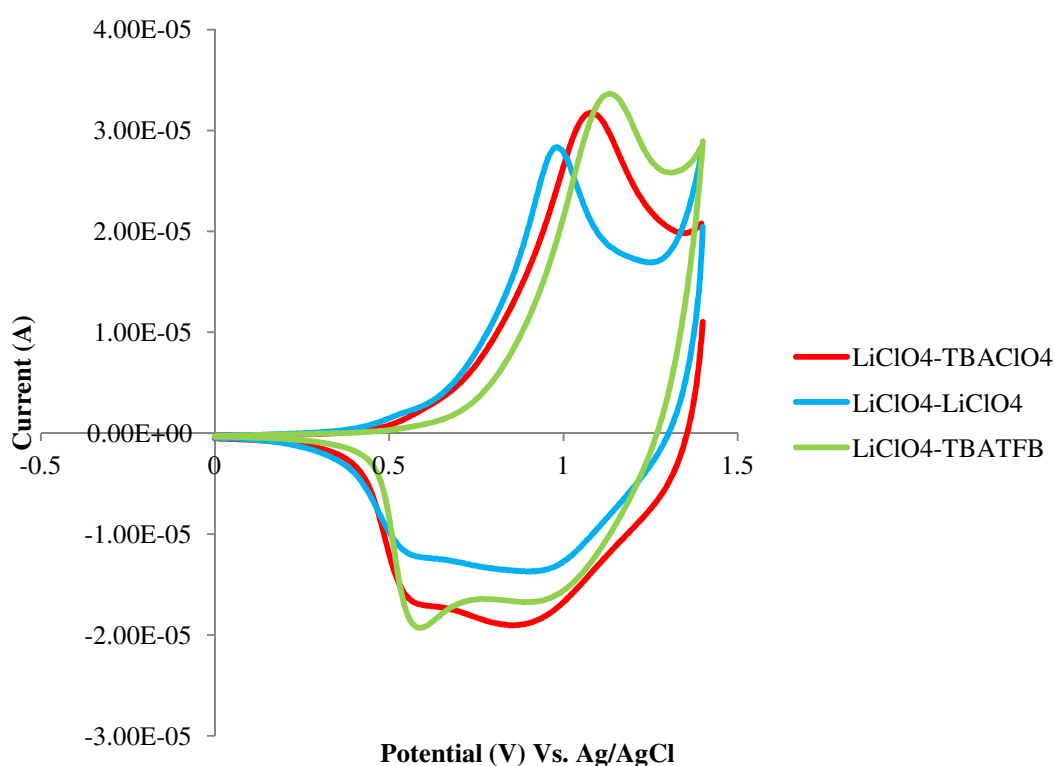


Figure 3.10. Poly(bithiophene) growth in LiClO_4 with characterisation in acetonitrile incorporating different dopant species.

Table 3.3 displays the data for the anodic and cathodic signals generated using three different dopants for characterisation whilst maintaining LiClO_4 as the growth electrolyte. Although the general shape was similar the main differences concerned the peak heights and oxidation potentials. The largest currents were seen with TBATFB however the oxidation potential was more positive at +1.13 V. Each anodic

peak represented a broad response with reduction clearly demonstrating two signals when TBATFB was employed.

Comparing the films produced with LiClO_4 to those grown with TBATFB generated some interesting results.

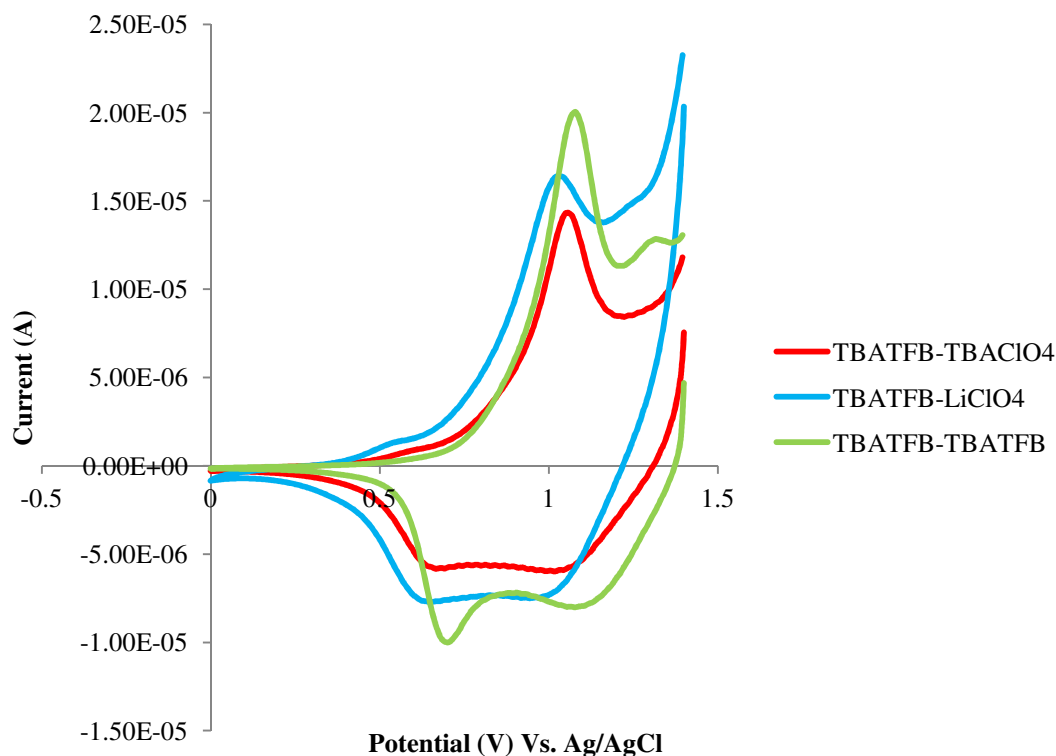


Figure 3.11. Poly(bithiophene) growth employing TBATFB with characterisation in acetonitrile incorporating different dopant species.

General observations could be made which demonstrated some similarities and differences between the two different growth dopants used. Using TBATFB as the electrolyte for polymer generation produced films with decreased anodic peak current response which was on average over 50% lower. Overall the anodic peaks are sharper and the clear reduction responses are again evident with TBATFB employed as the characterisation dopant. This could be directly influenced by the TFB^- anion as TBAClO_4 did not produce such a reduction response.

Pre-peaks are observed mainly when ClO_4^- is the characterisation anion. This is evident within the films formed through TBATFB growth. The voltammogram in figure 3.10 generated with LiClO_4 and characterised with the same dopant also shows

a small pre-peak and it is possible that the LiClO_4 generated film with TBAClO_4 characterisation could present a pre-peak. The identification of the pre peak is difficult as the films generated with LiClO_4 have greater currents and more polymer is produced therefore the thicker films may conceal such details.

The anion is generally associated with achieving charge neutrality of the oxidised polymer^{39,75-76,177} where different anion species have influenced the resulting polymer characterisation demonstrated upon polypyrrole films^{28,175}. However it is reported by Tourillon and Garnier *et al* that the variation of counterion inclusion upon polythiophene conducting polymers show no difference in the cyclic voltammetry traces¹⁷, clearly the dopant investigation in this report does not provide the same outcome. Interestingly the films generated using both LiClO_4 and TBATFB demonstrate decreasing oxidation potentials for the same dopant range used within the characterisation. This can be seen in table 3.3 where polymer oxidation potentials for the various dopants decrease steadily in the following order $\text{TBATFB} > \text{TBAClO}_4 > \text{LiClO}_4$. The cation has been reported to influence the behaviour of the polymer film during the charge discharge process due to the facile removal of the smaller and more mobile Li^+ cation from the oxidised polymer film¹⁷⁶. This could partially explain the lower oxidation potentials associated with the lithium electrolyte. As evidence exists for both doping processes it is difficult to determine the exact charge-discharge mechanism however it is clear to conclude that each voltammogram displays unique redox behaviour. This is also true when the growth electrolyte is kept constant and different dopants are used for characterisation but employ the same anion or cation.

Table 3.3. Data Produced from Various Dopants Employed for Both Growth and Characterisation.

Dopant Polymer Growth	Dopant Characterisation	, (V)		, (μA)		, (V)		, (μA)	
TBATFB	TBATFB	1.08		20.0		1.08	0.70	-8.01	-10.0
	TBAClO ₄	0.61	1.06	0.45	14.3	1.02	0.67	-5.99	-5.84
	LiClO ₄	0.50	1.03	1.03	16.4	0.94	0.65	-7.51	-7.73
LiClO ₄	TBATFB	1.13		33.6		0.87	0.59	-16.7	-19.3
	TBAClO ₄	1.08		31.8		0.86	0.55	-19.0	-17.4
	LiClO ₄	0.99		28.3		0.9	0.61	-13.7	-12.3

3.0.6. Effects of Scan Rate upon Poly(bithiophene)

The investigation of scan rate upon poly(bithiophene) characterisation demonstrates diffusion controlled oxidation, this is deduced from the linearity of the anodic peak current () on the square root of the potential scan rate ($V^{1/2}$).

Figure 3.12. Linear relationship for current Vs $\sqrt{\text{scan rate}}$ for Poly(bithiophene).

The poly(bithiophene) films were generated over five potential cycles and characterised (1.4 V-0 V-1.4 V) with the chosen scan rates of 10, 50, 100, 300 and 500 mV s⁻¹.

Kinetically limiting factors that cause linearity to deviate can be associated with film thickness and polymer chain relaxation⁶⁴. Increasingly thick films become more disordered with the introduction of defects affecting the packing of the polymer^{25,178-179} this then decreases the conductivity of the electrode surface and damages the conjugation preserved within thin films. In addition polymer relaxation through dopant anion expulsion can seriously be affected by sterically hindered species occupying the polymer material. As linearity for the $I_{p,a} V^{1/2}$ plots are preserved for the poly(bithiophene) polymer, film thickness and steric limitations have no bearing upon the kinetics of the oxidation process. Typical factors that cause a non-zero intercept is non-faradaic current generated by high solution resistance and large distance between the reference and working electrode. Such resistance can be minimised by reducing the electrode gap and introducing a large concentration of electrolyte.

Utilising 2,2'-bithiophene for the generation of a conducting polymer film provided a thiophene polymer structure free from substituent groups that could be electrochemically investigated. The simple structure enabled a series of experiments to examine the external influence of dopant and solvent without interference from reactive groups associated with the polymer.

The bithiophene system generated an understanding of the synthesis and electrochemistry of conducting polymer materials this was extended by incorporating linear alkyl chains to the ring structure in order to probe the electrochemical properties of substituted thiophene compounds.

3.1. Alkyl Thiophene Analogues

Probing the electrochemistry of various substituted thiophenes generates important information on their redox behaviour, which can be directly related to the structure of the polymerised film. The presence of differing side groups bonded to the thiophene

ring dramatically alters the electrochemistry observed and therefore provides valuable insight into the properties associated with the polymer^{25,46,57}.

Alkyl substituted thiophene compounds offer many advantageous properties useful for a number of applications. Increased polymer solubility can be generated through the alkyl moiety desirable for processibility and characterisation. Polymer morphology can be controlled to a certain extent where porosity is an important property of the material without introducing steric factors limiting conductivity. 3-Methylthiophene the simplest alkyl thiophene analogue has been shown to demonstrate very desirable qualities and is therefore commonly encountered due to its high conductivity and relative inexpense^{36,176,180}.

3.1.1. Electrochemistry of Poly(3-methylthiophene)

Investigating the electrochemistry of 3-methylthiophene provides a good starting point for probing the properties of hydrocarbon side groups and demonstrates the significant effect that a simple thiophene derivative can produce.

The 3-methylthiophene monomer unit is substituted with a CH₃ (methyl) group located at the beta ring position. Although only a small alkyl chain is introduced many properties of the polymer change. The generation of a lower oxidation potential (+0.8 V) in comparison to unsubstituted thiophene (+1.1 V) is observed however a higher potential is required for polymerisation (+1.35 V) than bithiophene (+1.2 V)¹⁷. Conductivity is reported to increase^{25,46,75} and the redox data provides additional information especially through scan rate variation. An example of 3-methylthiophene polymer growth can be seen below. Current increases through each consecutive sweep incorporating the potential window 0 V-1.7 V-0 V.

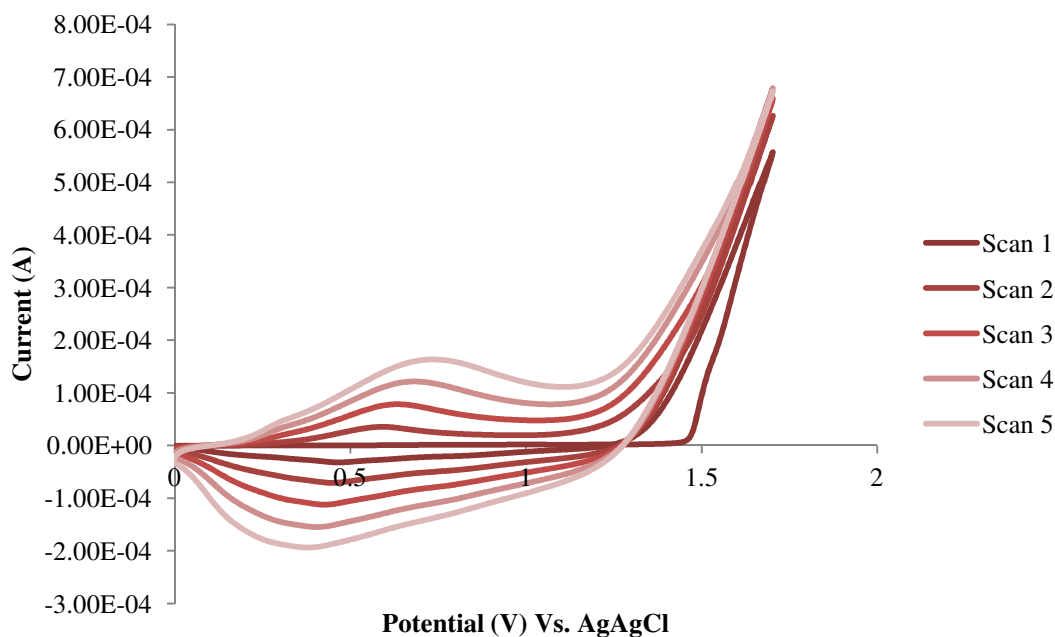


Figure 3.13. Growth of 3-methylthiophene over five scans.

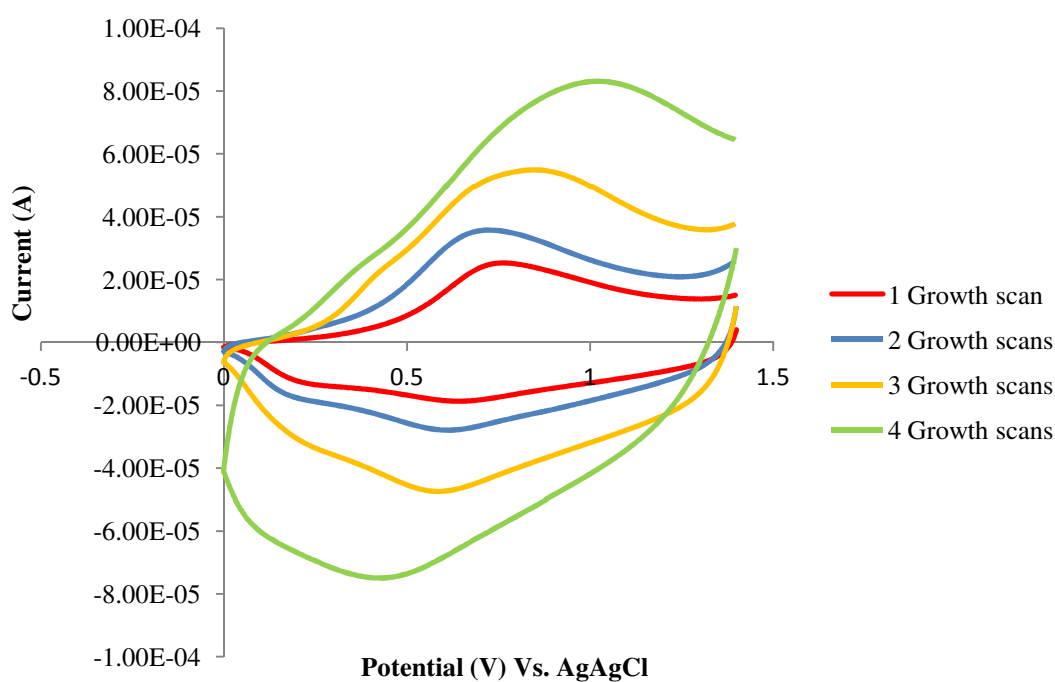


Figure 3.14. Characterisation of poly(3-methylthiophene) with varying thickness.

The thin films of 3-methylthiophene displayed in figure 3.14 represent very similar traces to thin film bithiophene with the broad single oxidation and the two reduction responses. The difference between the characterisation voltammograms at 50 mV s^{-1} is

the oxidation potential where the introduction of a methyl group shifts the peak 300 mV cathodically.

Examination of 3-methylthiophene with increasing growth cycles demonstrates the signal increase as more material is deposited and also the extending potential gap between the redox responses. Over three or more growth cycles the appearance of a pre-peak is visible however upon slower scan rates with a film generated through a single potential cycle the pre-peak is also evident. This suggests that at faster scan rates of 100 mV s^{-1} some of the film details are obscured until enough material is generated for the response to be seen.

The poly(3-methylthiophene) films were grown through 0 V-1.7 V-0 V over five scans at 100 mV s^{-1} . The effect of scan rate upon redox response of the poly(3-methylthiophene) films were investigated over the range $20\text{-}200 \text{ mV s}^{-1}$.

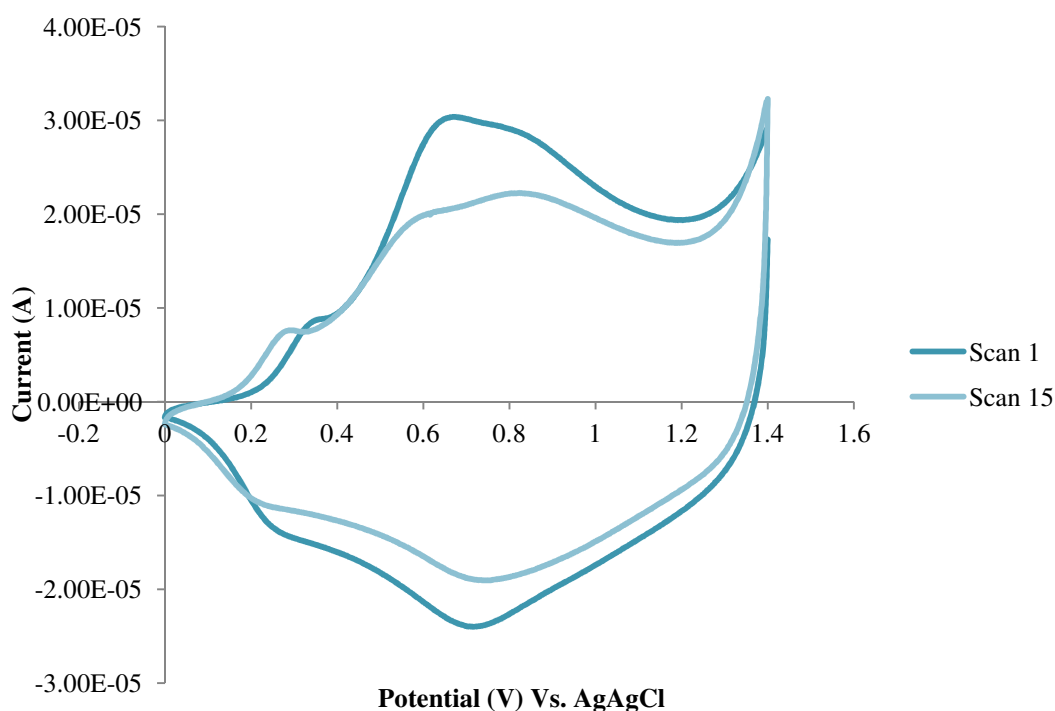


Figure 3.15. Characterisation of poly(3-methylthiophene) at 20 mV s^{-1} .

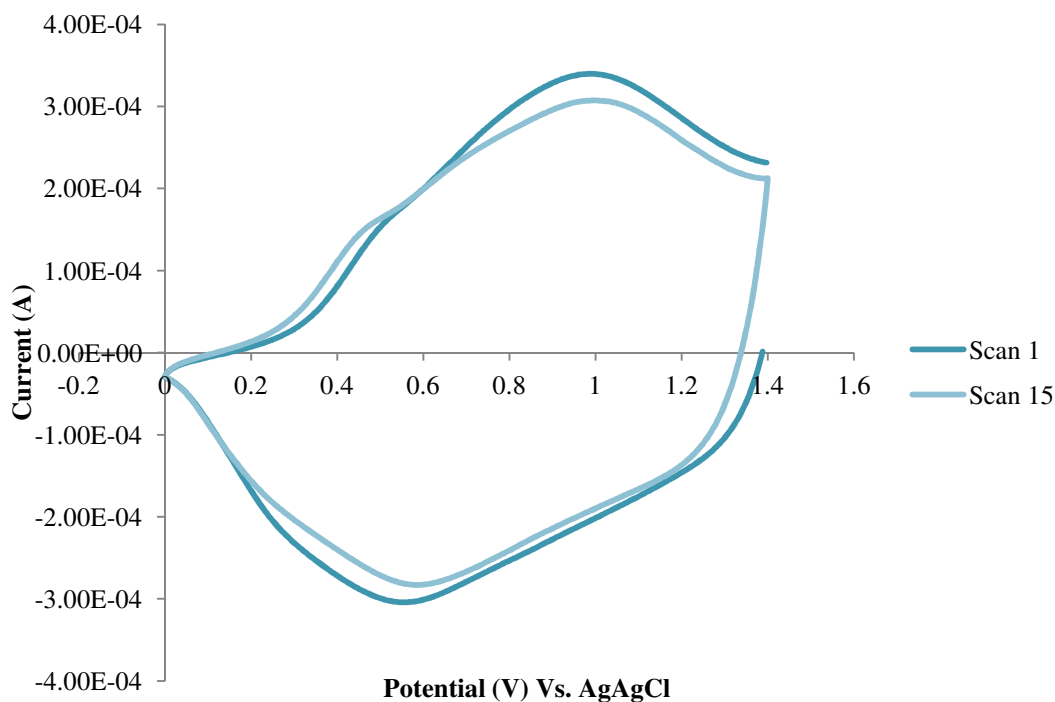


Figure 3.16. Characterisation of poly(3-methylthiophene) at 200 mV s⁻¹.

The pre-peak signal is well defined through slower scan rates. As faster rates are employed the anodic and cathodic signals lose their distinct structure and combine forming broad peaks in which two anodic and one large cathodic peak remains as seen with a 200 mV s⁻¹ scan rate.

Increased detail is generated when a slower sweep rate is used to scan the polymer. Examination of the trace where 20 mV s⁻¹ was used demonstrates the pre-peak location at +0.32 V on the first sweep with the major oxidation peak at +0.63 V and a possible anodic shoulder signal at +0.80 V. The reverse scan shows two reduction responses at +0.74 V and +0.28 V.

The pre-peak seen through the poly(3-methylthiophene) voltammogram series is reported in the literature, and has been attributed to the presence of different conjugation lengths and to the presence of two conformers. Additionally relaxation effects linked to reversible polymer swelling, resistivity changes and electronic structures, relating to bipolaron, polaron plus bipolaron and pi-dimers have all been postulated in the attempt to identify and explain polymer behaviour¹⁸¹⁻¹⁸².

3.1.2. Electrochemistry of Thin Film Poly(3-octylthiophene)

The extension of the hydrocarbon chain from a single methyl group to a hydrocarbon chain comprising of eight carbons exerts only a small effect upon monomer polymerisation seen with a slight increase in polymerisation potential.

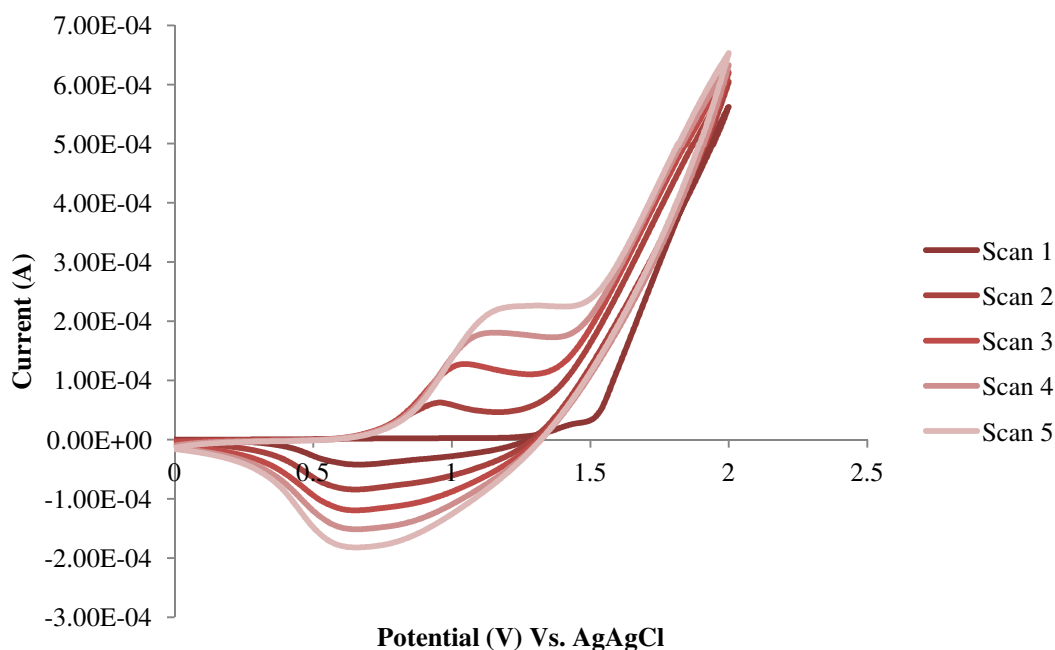


Figure 3.17. Growth of 3-octylthiophene over five scans.

The increasing current through each potential cycle of 0 V-2.0 V-0 V indicates the deployment of polymer film on the electrode surface as seen with 3-methylthiophene. A single polymerisation cycle is used to probe the redox characteristics of the film.

Characterisation of the longer alkyl chain displays two significant effects. Firstly the anodic oxidation potential of the polymer increases to +1.03 V compared to +0.8 V with 3-methylthiophene and secondly the redox features show a very different composition demonstrating a more symmetrical arrangement.

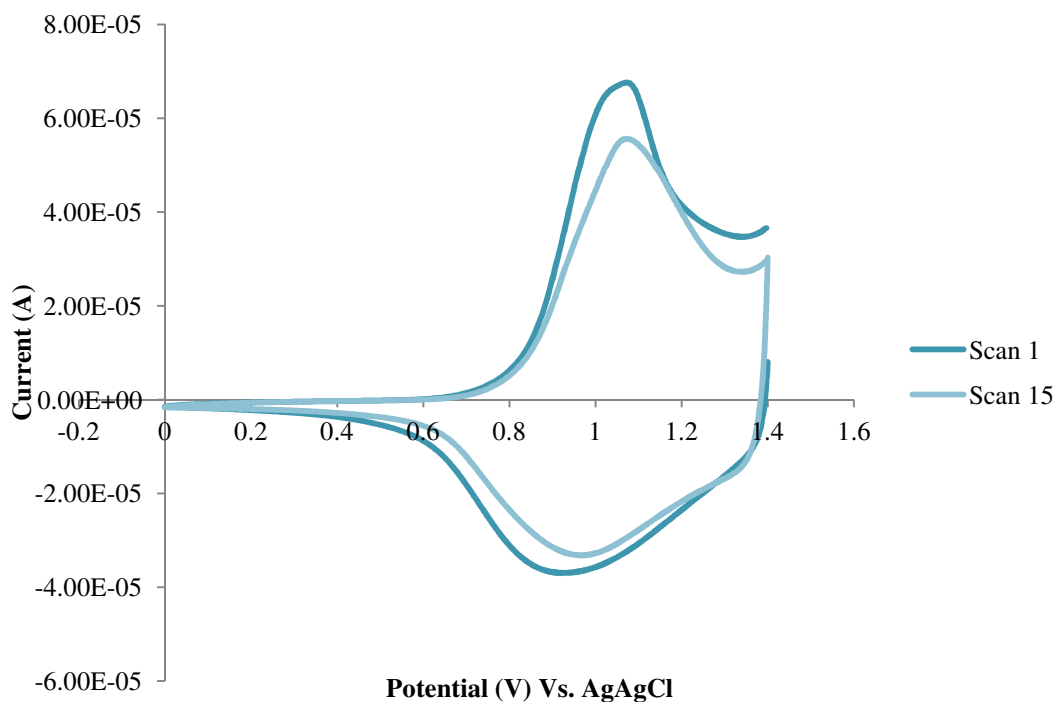


Figure 3.18. Characterisation of poly(3-octylthiophene) at 100 mV s⁻¹.

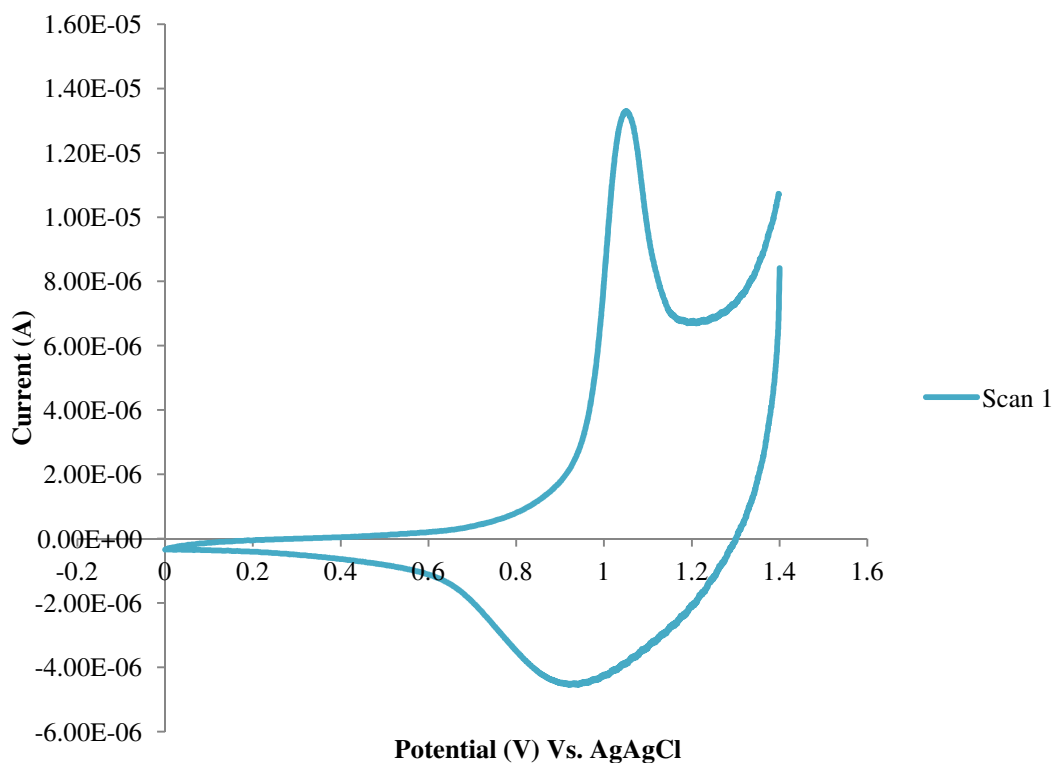


Figure 3.19. Characterisation of poly(3-octylthiophene) at 20 mV s⁻¹.

Examination of the thin film produced by one growth cycle (0.0-2.0-0.0 V) at 20 mV s⁻¹ demonstrates the narrow oxidation at +1.03 V and symmetry of the redox signals

with absence of further anodic response. The anodic and cathodic peaks are separated by a lower potential value of +0.1 V which demonstrates an almost perfect reversible system for surface immobilised species. This suggests that the space generated by the octyl chain allows significantly greater movement of ions through the film facilitating the redox processes compared to bithiophene in figure 3.10 with a separation of +0.4 V. It is reported by Roncali⁵⁷ that increasing the length of the alkyl chain to 7-9 carbons produces the extension of the mean conjugation length and an increase of the electrochemical reversibility which can be observed by the trace symmetry.

3.1.3. Electrochemistry of Thin Film Poly(3-dodecyl thiophene)

3-Dodecyl thiophene is substituted with a 12 carbon chain located at the beta position upon the ring. A higher potential of +2.5 V was needed to stimulate polymerisation owing to the increased monomer size restricting the diffusion rate.

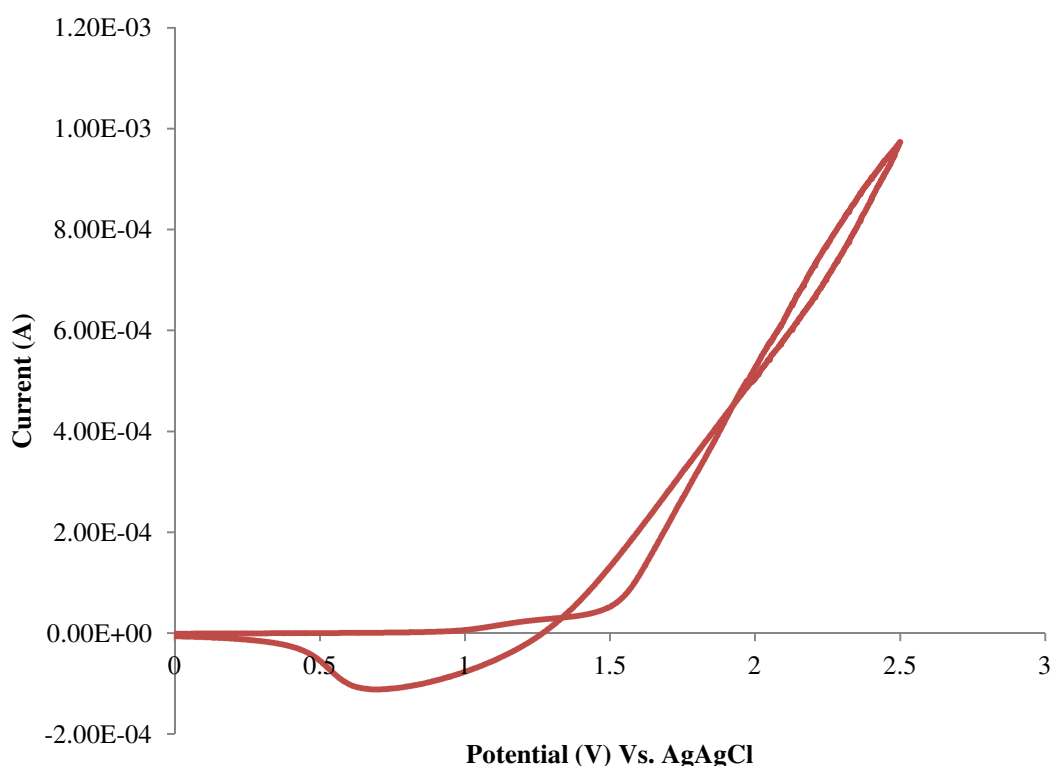


Figure 3.20. Growth of 3-dodecylthiophene over a single scan.

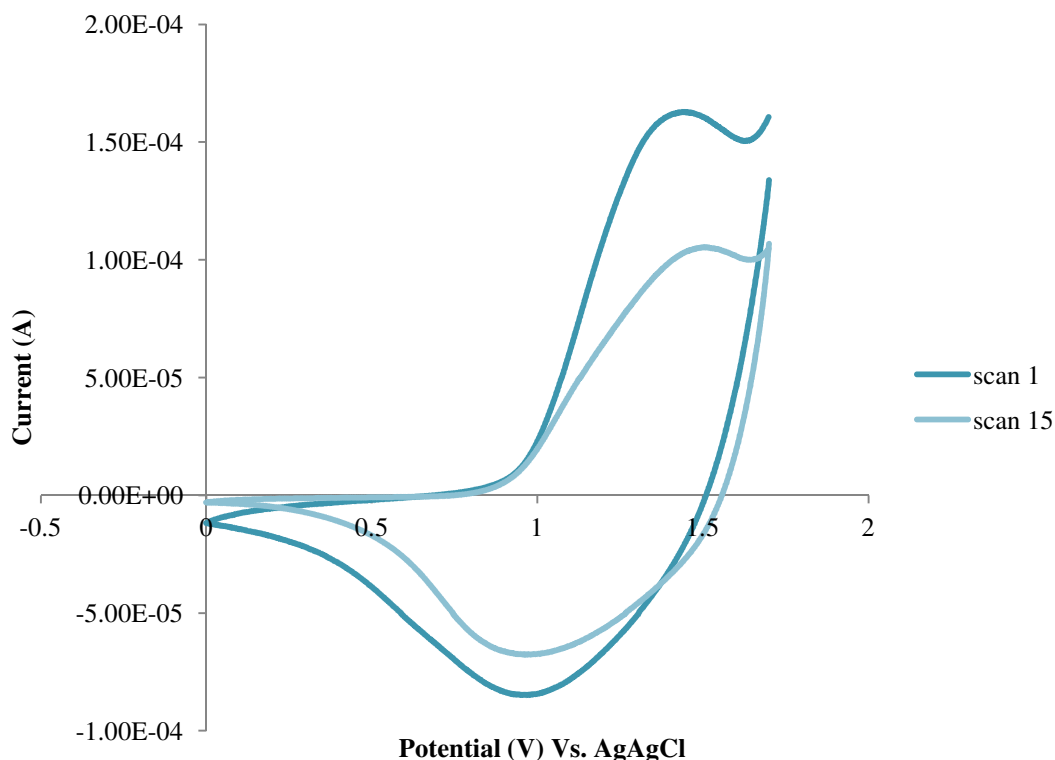


Figure 3.21. Characterisation of poly(3-dodecylthiophene) at 100 mV s^{-1} .

Increasing the carbon chain by four carbons produces a significant effect upon the oxidation potential of the polymer extending the peak to more positive potentials. Oxidation occurs at +1.38 V indicating greater oxidation difficulty, with peak separation increasing from +0.1 V for 3-octylthiophene to +0.38 V producing a more irreversible system.

3.1.4. Electrochemistry of Thin Film Poly(3-octadecylthiophene)

3-Octadecylthiophene has an extended 18 carbon chain. Due to the steric requirements of the large alkyl chain and the solubility of oligomeric materials electrochemical growth only generated very thin films which did not adhere well to the electrode surface. Characterisation generated poor electrochemistry with low current and therefore was not investigated further.

The investigation of thiophene compounds substituted with linear alkyl chains provided a good understanding of the electrochemical properties associated with these materials. Facile polymerisation was generated and good conducting polymer films with low oxidation potential were obtained. To further increase the attractive qualities

associated with these materials introduction of functionality is essential. The polymer films generated could be potentially employed in a device or reaction. For the application of biosensor devices the polymer film is required as an immobilisation platform providing functionality for covalent biological attachment. Such functional species include: carboxylic acid groups, amine groups or activated ester sites.

The electrochemistry of some acid substituted thiophene monomers was therefore investigated to find a suitable monomer that can be further modified to facilitate enzyme immobilisation. The proposed monomer would potentially allow a more efficient immobilisation to occur due to its activated status. This would potentially mean all binding sites would be occupied and therefore enhanced current responses would result. With the monomer in this activated format there would be no requirement for functional priming prior to enzyme immobilisation reducing the uncertainty associated with the amount of sites primed and potentially reducing the overall process with a possible decrease in the time needed for optimum biological attachment.

Polymerisation of this monomer will generate a material with different morphological properties. It is expected that the immobilisation matrix will provide a more porous structure due to the large ester species allowing facile substrate and product diffusion and generate a good sensor response.

The following section describes the electrochemical examination of commercially available acid substituted thiophene compounds. Determination of the reaction conditions needed to generate polymerisation and the investigation of their inherent properties are important for the development of materials with larger functional species such as the activated ester compound.

3.2. Acid Substituted Thiophene Monomers

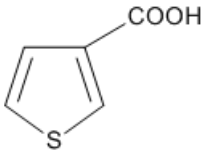
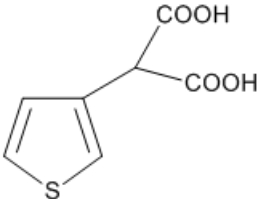
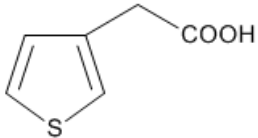
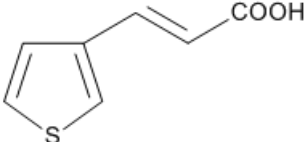
It is well known that the carboxylic acid group is a species that undergoes facile peptide linkage through the loss of water. The reaction can be implemented within organic or aqueous environments for acid substituted thiophene polymers and is relatively simple requiring only a condensation reagent and the biological molecule without the need of advanced conditions. Due to the simple procedure and the varied

approaches available, carboxylic acid substituted monomers are readily utilised for biological attachment within conducting polymer films^{50-55,67,137,140-141}.

3.2.1. Chemical Polymerisation

There are a number of commercially available carboxylic acid substituted thiophene monomers that have the potential to provide covalent attachment to biological species. Four of these are explored through chemical and electrochemical methods to stimulate polymerisation. It is important to investigate the ease of polymerisation for the different monomers as the substituents are likely to exert some influence on the process. Chemical methods employing iron chloride and molybdenum chloride were used to provide a quick indication to the polymerisation capabilities of the thiophene derivatives including non-substituted thiophene and its dimer 2,2'-bithiophene. Once polymerisation was confirmed electrochemical techniques were employed to generate the material upon the electrode surface and characterisation was performed.

Table 3.4. Carboxylic Acid Substituted Thiophenes.

Monomer 1		TCA	3-Thiophenecarboxylic acid
Monomer 2		TMA	3-Thiophenemalonic acid
Monomer 3		TAA	Thiophene-3-acetic acid
Monomer 4		TTA	Trans-3-(3-thienyl) acrylic acid

As expected polymerisation of thiophene and 2,2'-bithiophene occurred readily with both oxidant reagents however the acid substituted monomers did not generate any polymer material with the iron chloride oxidant despite prolonged reaction times. Molybdenum chloride which is a more powerful oxidant was introduced to the acid substituted monomers in which a fine precipitate of both poly(thiophene-3-acetic acid) and poly(trans-3-(3-thienyl) acrylic acid) was generated after several days. 3-thiophenecarboxylic acid and 3-thiophenemalonic acid failed to polymerise.

From the information gathered employing chemical polymerisation upon the various thiophene compounds, it is expected that the acid substituted thiophene monomers will not polymerise readily through electrochemical methods. However adopting electrochemical techniques to generate conducting polymers provides a diverse system and therefore many parameters can be investigated for the successful growth of a functional thiophene film.

3.2.2. Electrochemistry of 3-Thiophenecarboxylic acid

3-Thiophenecarboxylic acid is the simplest of the four carboxylic acid containing monomers, with the functional group directly attached to the thiophene ring. Although the ring structure was associated with the smallest substituent out of the three investigated, electrochemical polymerisation was not successful.

Figure 3.22 demonstrates the falling current signal produced through the attempts to generate a conducting polymer film from the 3-thiophenecarboxylic acid monomer on a glassy carbon electrode. A steady decrease of the anodic response is observed with no hysteresis commonly encountered with the deposition of conducting polymer films. Reduction upon the reverse scan is also absent despite efforts to extend, limit and stabilise the potential employed. Platinum and gold electrode surfaces were also explored but failed to assist polymer deposition. In addition increased monomer concentration was investigated but proved unsuccessful in the generation of a polymer film.

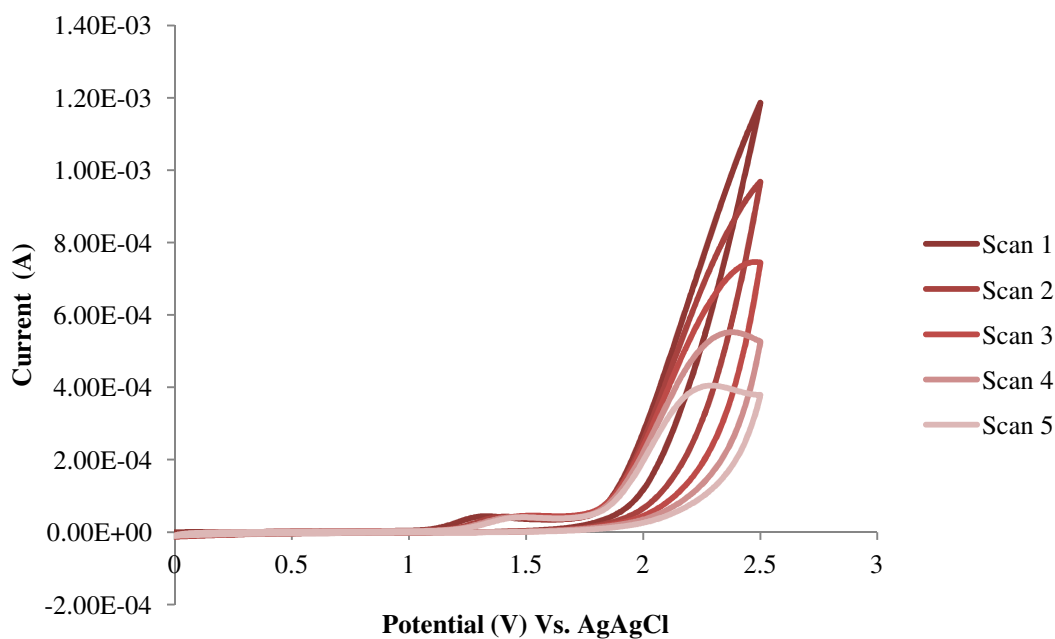


Figure 3.22. Cyclic voltammogram of 3-thiophenecarboxylic acid.

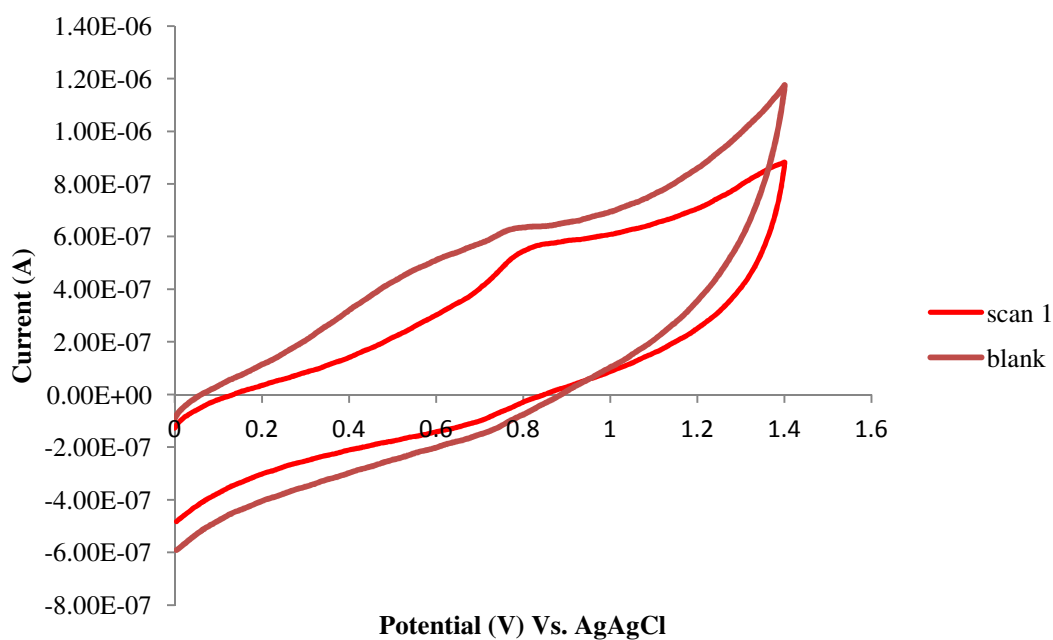


Figure 3.23. Characterisation of poly(3-thiophenecarboxylic acid).

To confirm that polymerisation had not taken place on the electrode surface the electrode was cycled in monomer free solution and compared against a blank run where no polymer growth had been attempted. Figure 3.23 demonstrates the absence of redox signals normally observed with conducting polymer films.

3.2.3. Electrochemistry of 3-Thiophenemalonic acid

3-Thiophenemalonic acid offers an additional carboxylic acid functional group extended away from the immediate vicinity of the thiophene ring by a single methylene spacer. Similarly the voltammogram displays no hysteresis or reduction compared to the 3-thiophenecarboxylic acid monomer and no film formation despite the small anodic peak at +1.9 V observed upon successive cycles. Further investigations monitoring electrode surface, varied potential windows using cyclic voltammetry and fixed potential through potentiometric methods and monomer concentration were again employed with no observed film deposited which was confirmed through characterisation.

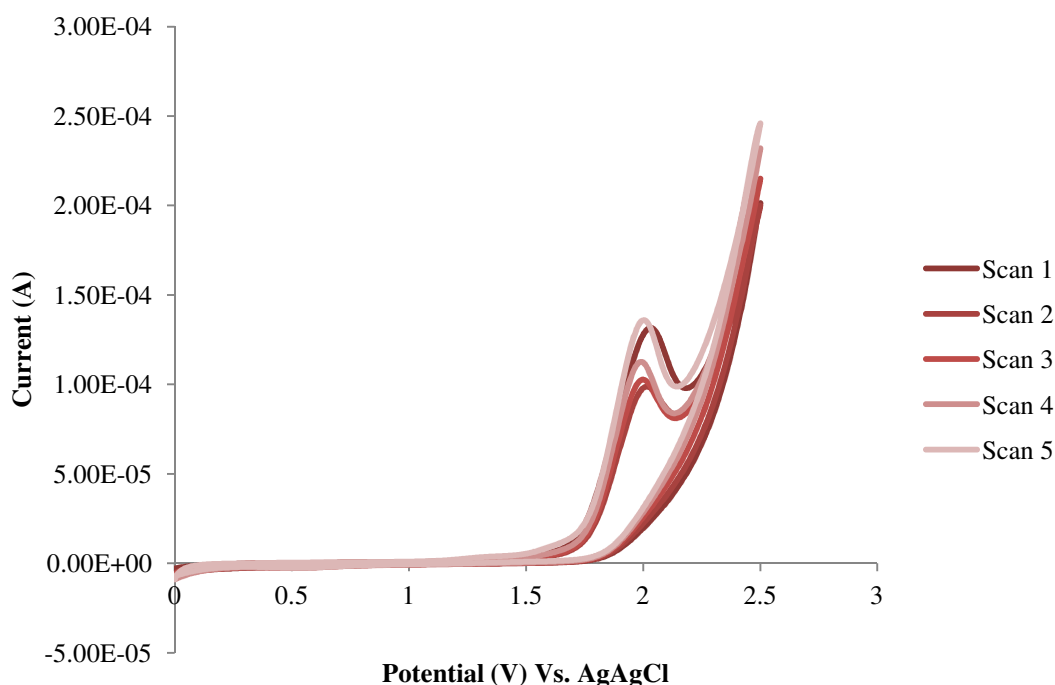


Figure 3.24. Cyclic voltammogram of 3-thiophenemalonic acid.

3.2.4. Electrochemistry of Thiophene-3-acetic acid

Thiophene-3-acetic acid incorporates a methylene spacer between a single carboxylic acid group and the thiophene ring. The same experiments were performed in order to generate a conducting polymer film however all proved unsuccessful except where increased monomer concentrations were employed. Monomer concentrations of 0.1 M were incorporated for the successful polymerisation of 2,2'-bithiophene in the initial studies. The same concentration was initially implemented for the electrochemical investigation of the acid substituted thiophene monomers and then extended. The

particular arrangement of the acetic acid substituent within the structure allows polymerisation to commence under increased concentrations where the other species are shown to inhibit polymer growth.

Figure 3.25 demonstrates the current decrease associated with thiophene-3-acetic acid with low monomer concentration employing a wide potential window. The absence of an electroactive film is established upon the characterisation voltammogram where no redox processes are observed.

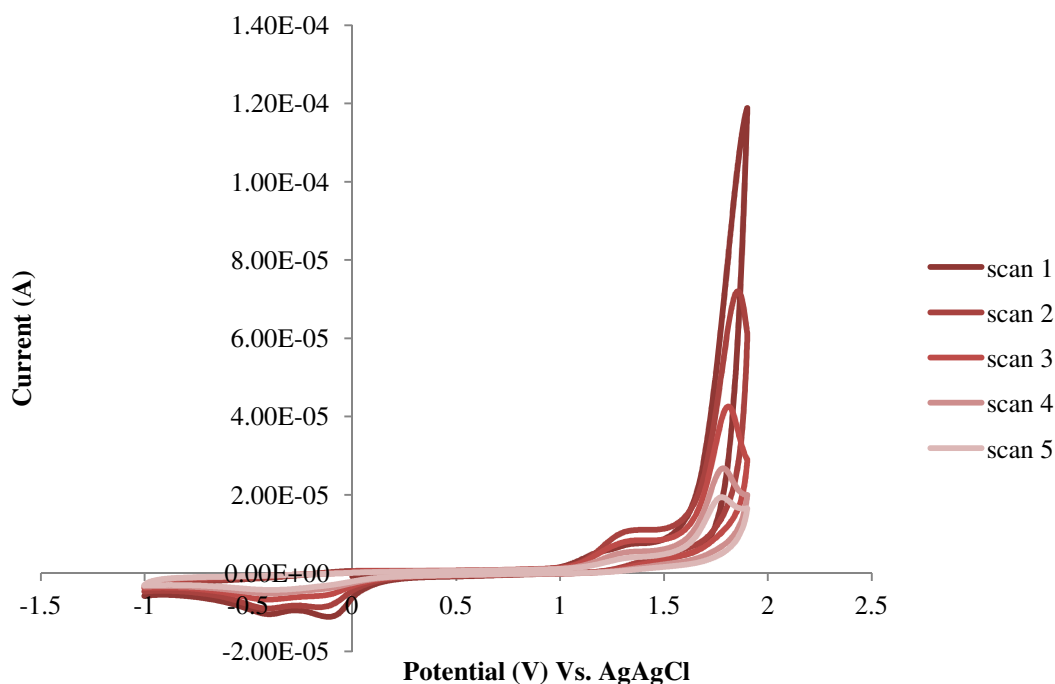


Figure 3.25. Cyclic voltammogram of thiophene-3-acetic acid.

Figure 3.26 clearly demonstrates polymerisation of 0.6 M thiophene-3-acetic acid with characteristic current increase through each completed cycle. Electrochemical polymerisation of thiophene-3-acetic acid was initiated at low monomer concentrations of 0.1 M and further investigated at 0.1 M increments to reach 0.6 M where polymer growth and the corresponding film deposit was detected.

Characterisation of the 0.6 M poly(thiophene-3-acetic acid) demonstrates a rapidly decreasing anodic signal at +2.0 V with a corresponding reduction response disappearing at +0.89 V. The absence of reproducible cycles indicates the difficulty of

the polymer structure to accommodate the movement of dopant during the charge-discharge process.

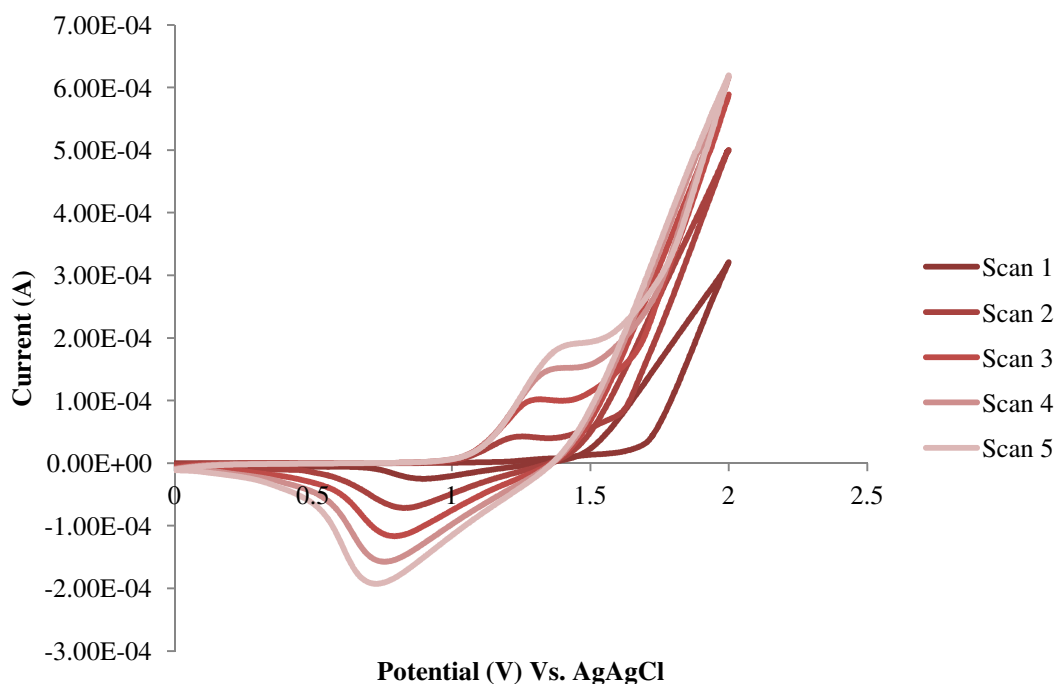


Figure 3.26. Growth of thiophene-3-acetic acid.

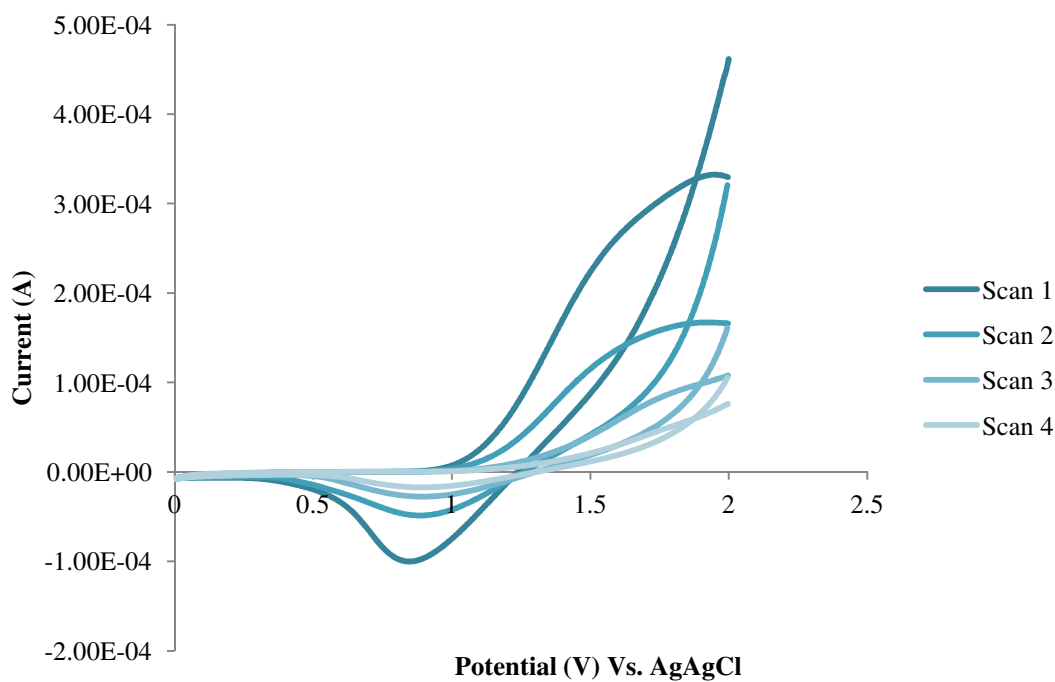


Figure 3.27. Characterisation of poly(thiophene-3-acetic acid) grown using a high monomer concentration of 0.6 M.

Characterisation seen in figure 3.27 clearly displays an unstable system where subsequent cycles fail to fully re oxidise and reduce the polymer leading to decreased current redox responses. Such behaviour supports steric effects which also influence the onset of polymerisation seen within the investigations of 3-thiophenemalonic acid and 3-thiophenecarboxylic acid. Oxidation of these compounds through cyclic voltammetry resulted in the formation of yellow non conducting films which were independent of monomer concentration. As a film is successfully deposited in the case of thiophene-3-acetic acid some characterisation is detected however the substituent causes a disordered monomer structure that restricts anion movement within the film. The polymer needs to be flexible to this movement in order to retain its arrangement otherwise strain on the system will lead to a collapse in conjugation with polymer degradation.

3.2.5. Electrochemistry of Trans-3-(3-thienyl) acrylic acid

The polymerisation of trans-3-(3-thienyl) acrylic acid remained unsuccessful. Standard monomer concentrations of 0.1 M were initially investigated but failed to initiate polymer growth. Thiophene-3-acetic acid polymerisation required high monomer concentrations of 0.6 M and therefore this option was explored. Increasing the concentration introduced solubility problems and the compound would not go into solution despite trying a range of solvents therefore this compound was not investigated any further for the generation of a homopolymer film.

From the examination of the four acid substituted thiophene monomers it is clear that the incorporation of a side group to the ring structure influences the ability of the compound to undergo polymerisation.

3-Thiophenecarboxylic acid demonstrated that the close proximity of the carboxylic substituent to the ring inhibited the polymerisation of the monomer. A yellow discolouration of the electrode surface was evident causing passivation of the electrode. The degeneration of the electrode surface was caused by the formation of a non conducting film through the disturbance of the conjugated system produced by the carboxylic acid species directly attached to the ring and is observed through the current decrease upon subsequent cycles.

3-Thiophenemalonic acid demonstrated the same effect upon the electrode surface as 3-thiophenecarboxylic acid. This result was anticipated, as the structural features of the monomer require a larger spacial distribution and the electronegativity provides greater instability to the polymerisation of the compound. Although the carbon linker offers some steric relief in the system the degree of occupancy imposed by the side group is significant and fails to compensate the steric effect.

Thiophene-3-acetic acid and trans-3-(3-thienyl) acrylic acid also suffered from steric effects rendering polymerisation problematic. The thiophene-3-acetic acid functional group is separated by a single methylene spacer providing some flexibility to the large carboxylic acid group, whereas movement within trans-3-(3-thienyl) acrylic acid is disabled due to the double bond character.

The contribution of steric effects was large as increased solvation affects film generation. Steric influence reduces the chance of cross-linking, imparting less strength to the polymer and with the presence of a dipole between the substituent and the ring within a polar environment polymer chain solvation was adversely supported. In addition it is well documented that due to the requirement of increased positive potentials competition is generated between growth and deactivation of the polymer during the polymerisation process. This was initiated by over oxidation and was dependent upon electrochemical stability of the polymer and the efficiency of the deposition⁴⁴.

The application of large positive potentials and the imbalance associated with the electronegativity of the compound are also responsible for the prevention of chain propagation. The accompanying factors impede the radical cation coupling mechanism due to nucleophilic attack. Potentials equalling +1.2 V or greater are known to induce the oxidation of water. Water will exist within the reaction solution occupying a small percentage but will generate nucleophiles under positive potential influence. The nucleophiles will attack the radical centres of the monomers causing the inhibition of polymerisation at the reactive sites⁷⁵.

The determining factors limiting the polymerisation of thiophene-3-acetic acid and trans-3-(3-thienyl) acrylic acid was therefore a combination of effects. The steric

requirement of the substituent to some extent physically hinders oxidised monomer contact, the substituent polarity increases solubility and the increased potentials employed introduces adverse over oxidation and nucleophilic attack.

However the successful polymerisation of thiophene-3-acetic acid was achieved in which a visible polymer film was produced on the electrode surface. Polymerisation was initiated through the application of greater positive potentials, monomer concentration and reduced steric restraint. The high concentration employed for the growth of thiophene-3-acetic acid is responsible for the sustained radical cation to radical cation interaction allowing a film to be deposited before intermediate reactions prevent chain formation resulting in soluble oligomers.

Increased monomer concentrations for trans-3-(3-thienyl) acrylic acid was not possible because of the restricted solubility of the compound and therefore increased radical cation formation could not be initiated.

3.3. Electrochemical Investigation of the Activated Ester Compounds

The incorporation of substituents on the thiophene ring is generally employed to deliver functionality to the material. Any extension to the thiophene ring structure will impose a number of effects on the resulting polymer. Changes to the structure, morphology chemical and physical features are likely to occur to some extent and may be beneficial to the application of the material. However it is likely that substituents will influence the generation of the polymer and it is important that the compound remains responsive to electrochemical polymerisation.

Small changes to the electrochemistry of alkyl substituents were found in the previous section leading to the determination that the continuous addition of flexible groups up to 12 carbons provided an increase in solubility with little polymerisation difficulties occurring from steric factors. Steric hindrance was evident when the carbon chain was increased to 18 and branched configurations were investigated. This resulted in poor polymer growth with little characterisation data and signal degradation over repeated cycles.

The electrochemical investigation of functional thiophene carboxylic acid monomers presented additional problems with inductive effects leading to destabilisation of the radical cation sites and therefore polymerisation difficulties, however in some cases where steric hindrance was not the dominating factor the onset of polymerisation was successful by increasing monomer concentration.

The spatial bearing of the attached substituent was found to be significant to the film growth and subsequent characterisation. It was therefore expected that the bulky nature of the activated ester groups would present similar difficulties.

Thiophene-3-acetic acid provided the starting compound desirable for further modification. Several aspects were responsible for this choice which included the synthetic approach through the functional COOH terminal, the availability of the compound and its low cost. This compound has the ability to polymerise through an applied voltage due to the presence of the methylene link providing a degree of flexibility and the introduction of elevated concentration.

3.3.1. Electrochemical Investigation of Tert-butyl thiophene-3-carboxylate

The investigation of activated ester substituents starts with simple synthesised thiophene esters incorporating a methyl and a large butyl group to the monomer. By investigating the parameters required to generate a suitable polymer film from the methyl and butyl esters it can be determined if the polymerisation of the activated ester will be successful. Furthermore the established methods can be employed with the activated ester in order to use less of the synthesised material.

Polymerisation of both methyl and butyl ester substituents were investigated initially at a concentration of 0.1 M employing wide potential windows of 0.0 V-2.0 V-0.6V. Polymerisation under these conditions was not successful and resembled the attempts to polymerise 0.1 M thiophene-3-acetic acid.

Employing a higher monomer concentration of 1 M was found to produce both the hysteresis loop commonly generated within electropolymerisation of conducting polymers and significant current increase upon each subsequent growth scan.

Successful polymerisation of poly(*tert*-butyl thiophene-3-carboxylate) can be seen in figure 3.28.

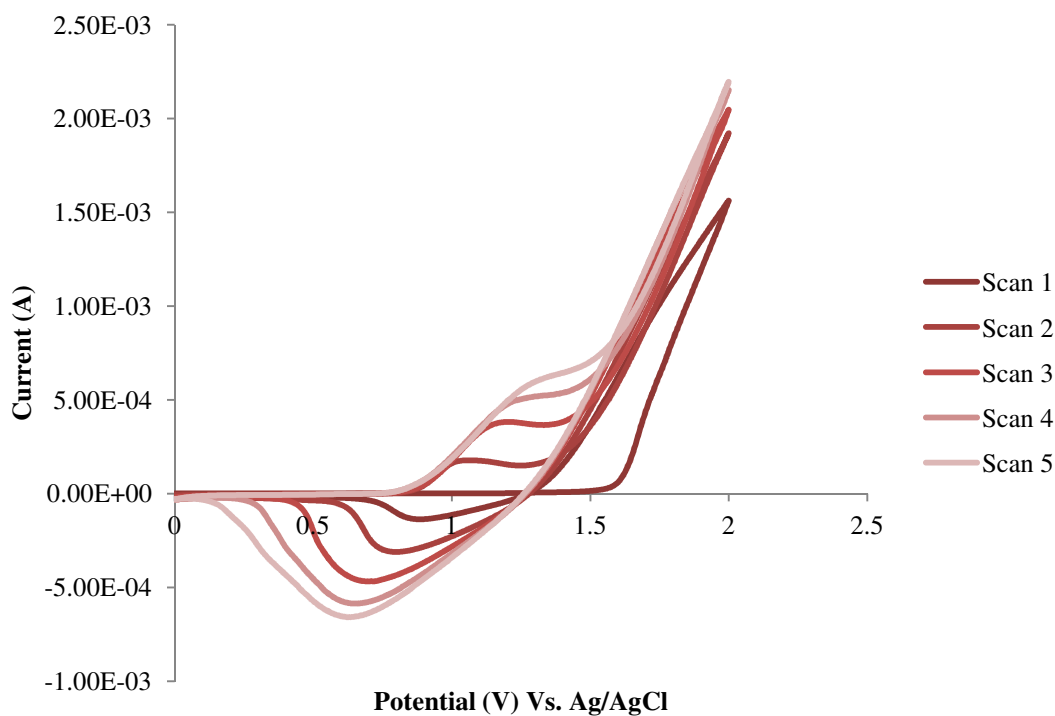


Figure 3.28. Growth of *tert*-butyl thiophene-3-carboxylate.

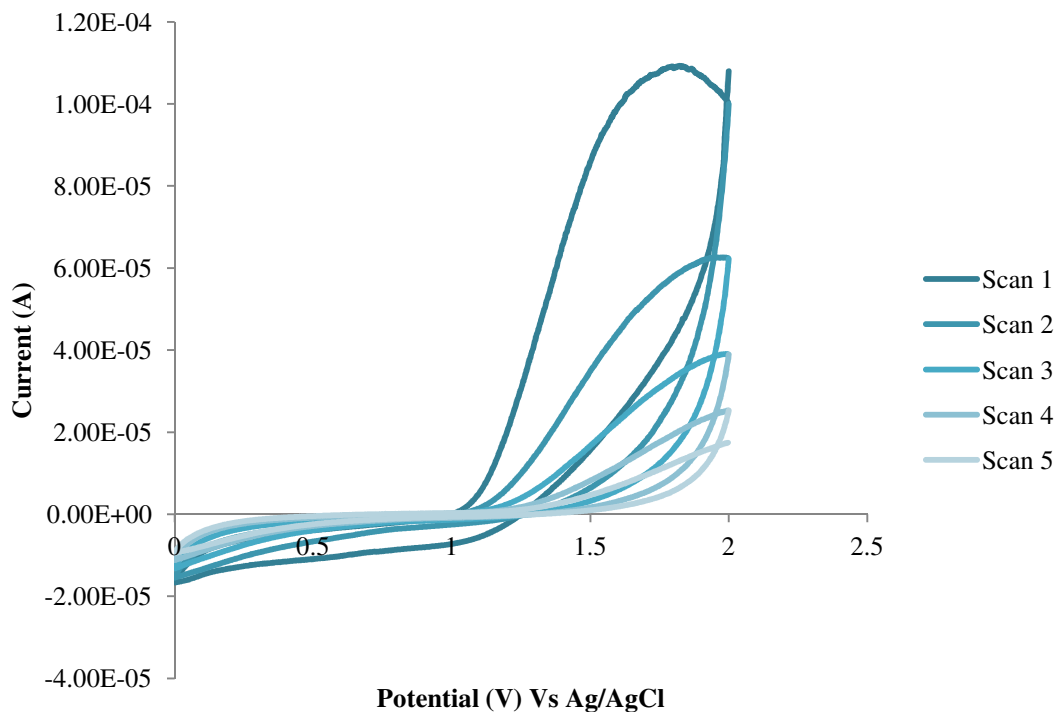


Figure 3.29. Characterisation of poly(*tert*-butyl thiophene-3-carboxylate).

Implementing five growth scans utilising a 1 M monomer solution produced a thick black film. Complete film oxidation was not reached and therefore reduction remained absent. The successive scans continue to show decreasing signals due to the steric properties of the monomer and the thickness generated opposing the intercalation and removal of dopant ions. A thinner film was produced by lowering the number of growth cycles to two. Characterisation of the film seen in figure 3.30 shows both oxidation and reduction peaks generated through the movement of dopant ions. Signal depletion persists through progressive cycles owing to the bulky nature of the side group restraining the flexibility of the polymer which is needed to accommodate dopant migration.

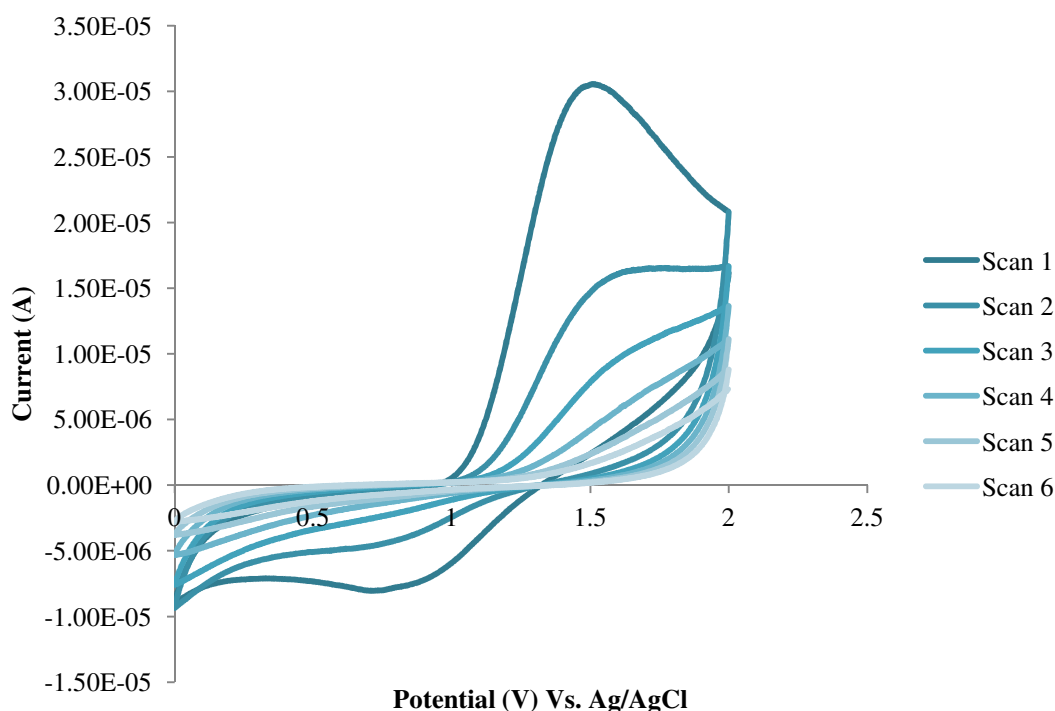


Figure 3.30. Characterisation of poly(tert-butyl thiophene-3-carboxylate).

Successful growth of poly(tert-butyl thiophene-3-carboxylate) demonstrates a key goal to the potential achievement of an activated ester deployed through the same electrochemical techniques. The characterisation of this sterically hindered polymer is an indication of the behaviour likely to be observed with the activated ester substituent.

3.3.2. Electrochemical Investigation of N-succinimido thiophene-3-acetate

Synthesis of the novel N-succinimido thiophene-3-acetate monomer was prepared using the well established carbodiimide reagent commonly employed within peptide synthesis details of which are described in chapter 2 section 2.0.3.

Polymerisation was initiated using a wide potential window of 0.0 V-2.5 V-1.0 V. A high positive potential was required which extended towards the negative potential region to ensure the complete reduction of the material. Interestingly only a slight increase in monomer concentration was required despite accommodating the large ester substituent indicating side reactions were minimal and the oxidised monomer was stable.

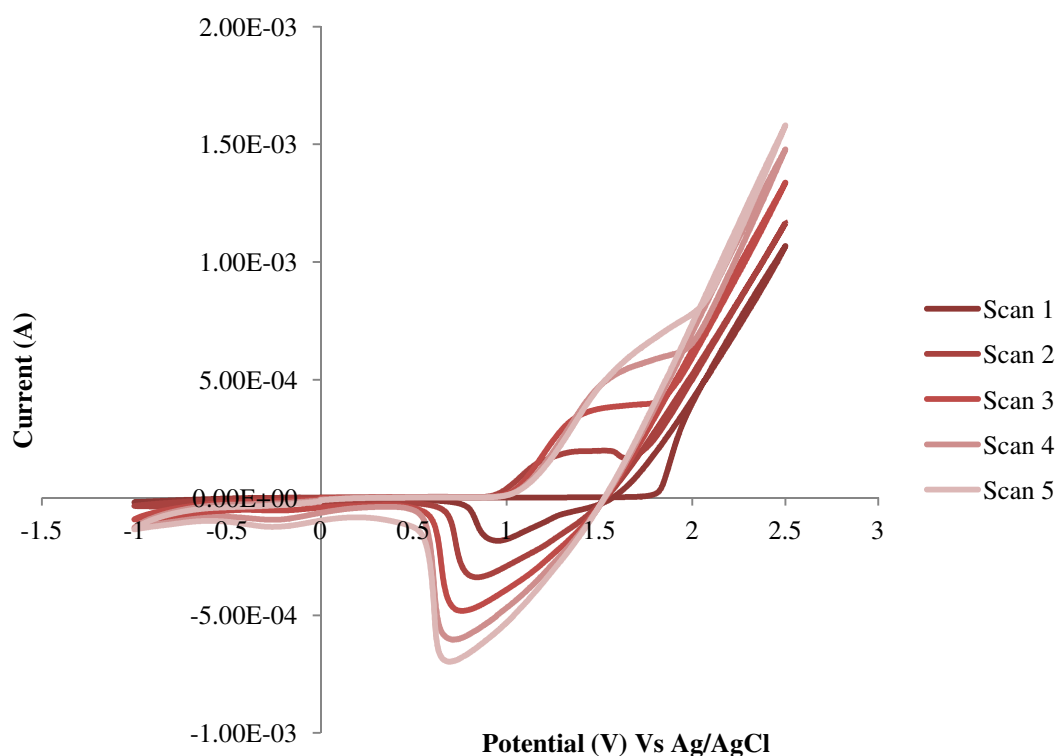


Figure 3.31. Growth of N-succinimido thiophene-3-acetate.

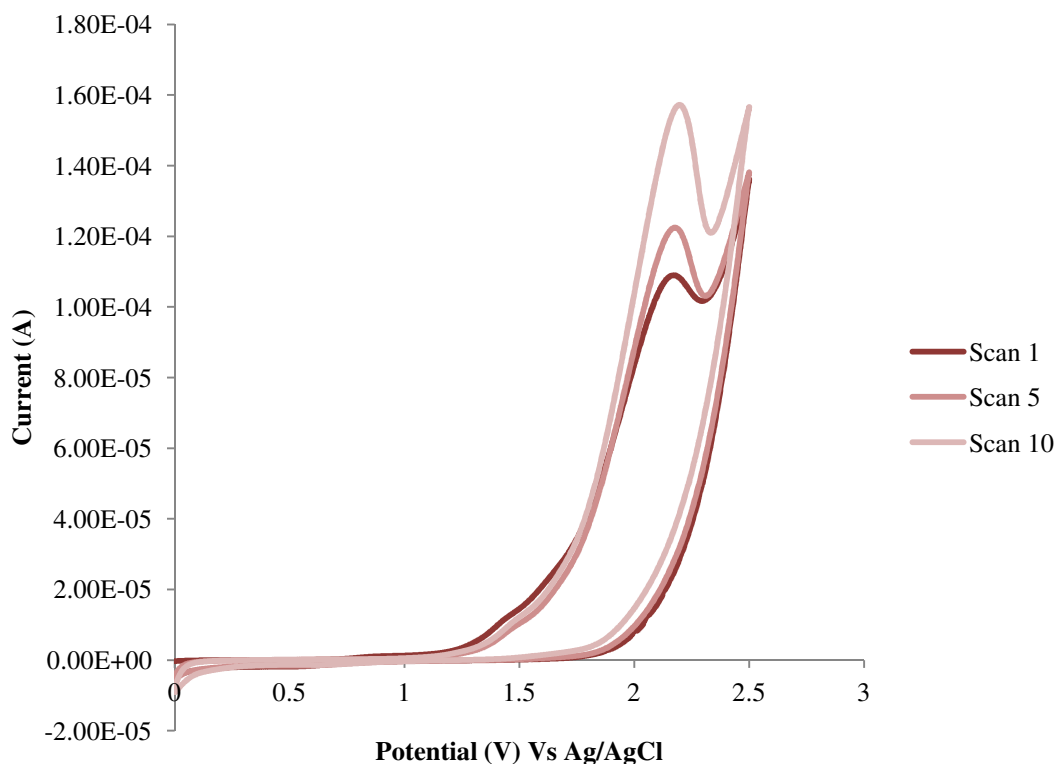


Figure 3.32. Characterisation of poly(N-succinimido thiophene-3-acetate).

Characterisation did not produce the redox responses expected. Although an oxidation peak was observed at +2.16 V the signal behaviour was unusual as the peak increased through the characterisation cycles. Peak decrease is generally observed for sterically hindered materials due to the difficulty of adjusting to the intercalation of dopant. Additionally there is complete absence of reduction therefore steric factors may well be affecting dopant release from the polymer even by extending the potential window to negative potentials reduction was not produced.

The poly(N-succinimido thiophene-3-acetate) behaviour was not typical of a conducting polymer film. Steric factors can be blamed for the redox responses observed, this however can easily be resolved through copolymerisation. A mixed polymer system will potentially neutralise the steric effect to generate a stable copolymer which can be repeatedly cycled with access to the conducting properties of the film.

3.4. Copolymerisation

Copolymerisation has worked successfully for a number of research groups with thiophene-3-acetic acid and 3-methylthiophene (T3AA-MT) frequently reported^{37,50-55}. Copolymerisation with 10% acid group content demonstrates enhanced responses to glucose which has been explained by the high conductivity achieved⁵⁴. Initial studies in this section include copolymerisation of thiophene-3-acetic acid and 3-methylthiophene (T3AA-MT) and also with tert-butyl thiophene-3-carboxylate (BTA-MT) investigated with increasing total concentration.

The incorporation of the functional species into a copolymer film was investigated by adjusting the monomer ratios to within a fixed total monomer concentration so the redox responses of the different compositions could be compared. This was successful for the novel N-succinimido thiophene-3-acetate and 3-methylthiophene (STA-MT) copolymerisation over a range of concentrations including the well documented thiophene-3-acetic acid and 3-methylthiophene (T3AA-MT) copolymer analysed for comparison purposes.

Copolymerisation of the trans-3-(3-thienyl) acrylic acid and its corresponding synthesised ester N-succinimido trans-3-(3-thienyl) acetate with 3-methylthiophene (TTA-MT), (STTA-MT) was also established. Solubility of these compounds were problematic however the recommended 10% functional content was achievable with a low monomer content and so all copolymer systems could be compared seen in figure 3.37.

Figure 3.33 demonstrates the electrochemical behaviour of films generated through the increase in concentration of the thiophene-3-acetic acid monomer in the polymerisation solution. As the total concentration increases the current response increases which would be expected as the higher concentration generates a thicker film. Signal intensity started to decrease with 0.4 M thiophene-3-acetic acid present in the solution. This can be explained due to the enhanced content of acid groups present in the film which affected the conjugation in the material. As more acid groups were incorporated into the structure the polymer chain flexibility became influenced by

steric effects increasing the difficulty to oxidise the polymer. This can be observed by the shift of the oxidation response to more positive potentials.

Figure 3.34 displays the copolymerisation of *tert*-butyl thiophene-3-carboxylate and 3-methylthiophene. Current increase is not as evident as the total concentration rises although copolymerisation is supported by the observed change in the voltammograms as redox responses are altered. The influence of the large butyl ester monomer is clear as increasingly higher potentials are needed to oxidise the film demonstrating the same anodic peak shift seen with the T3AA-MT system.

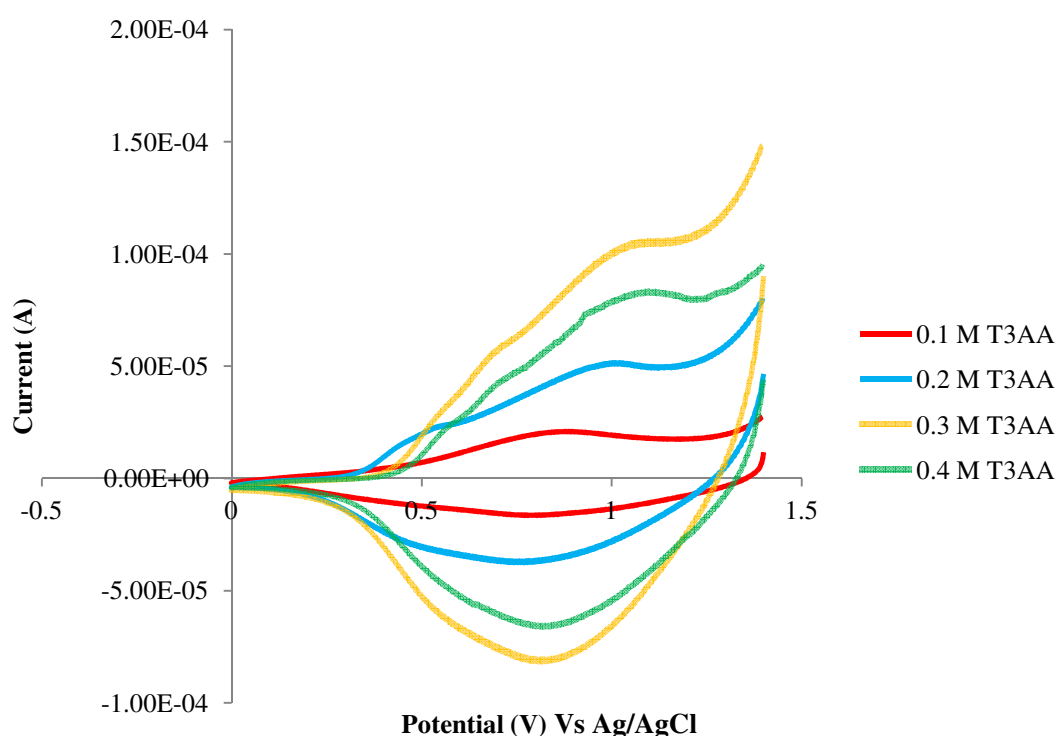


Figure 3.33. Copolymerisation of T3AA and MT with increasing concentration of the functional thiophene monomer (T3AA) characterised at 100 mV s^{-1} .

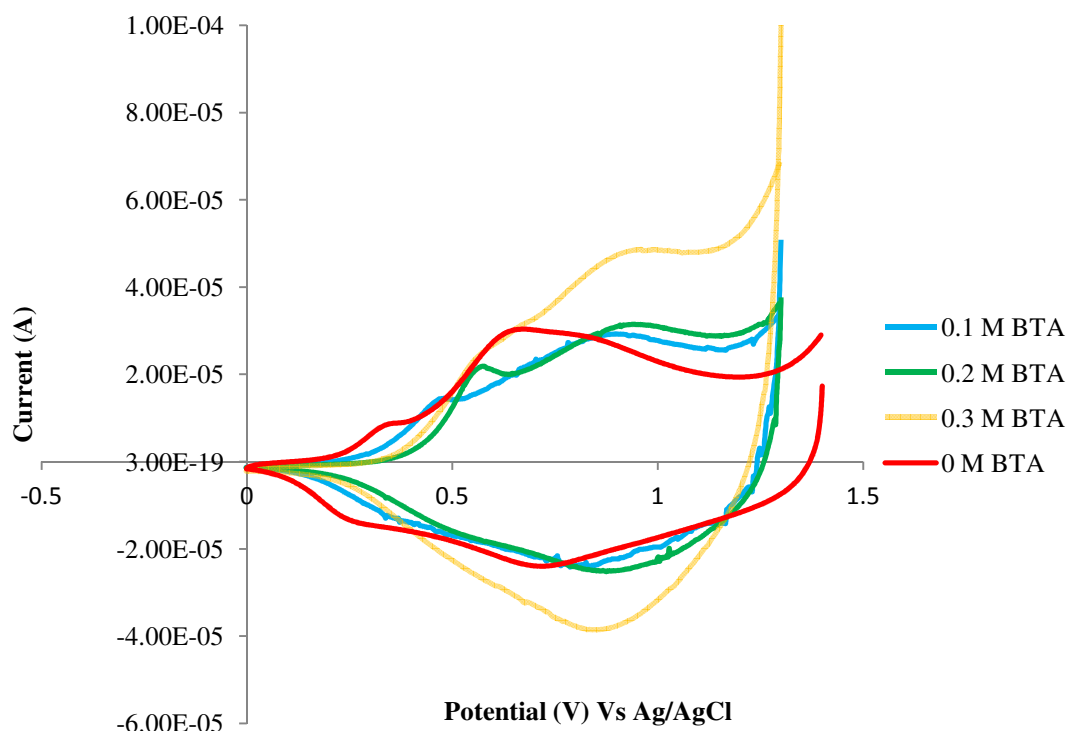


Figure 3.34. Copolymerisation of BTA and MT with increasing concentration of the tert-butyl thiophene-3-carboxylate monomer characterised at 100 mV s^{-1} .

The copolymerisation of T3AA-MT and BTA-MT with increasing T3AA and BTA concentration demonstrates a clear change in the characterisation voltammograms compared to poly(3-methylthiophene). Although the shape of the voltammogram indicates a change in the material generated, due to the increasing concentration it is difficult to determine optimum monomer ratio which is important for future biosensor investigations. Therefore T3AA and STA copolymerisation with MT has been performed with a total concentration which will also associate the redox responses generated to the successful integration of the monomers in the resulting material.

Tables 3.5 and 3.6 list the molar ratios used in the polymerisation solution and provides the corresponding functional monomer content for both T3AA and STA calculated through elemental analysis in chapter 4.

The voltammograms covering the range of concentrations investigated are displayed below in figures 3.35 and 3.36 and have been labelled with their relevant T3AA and STA content.

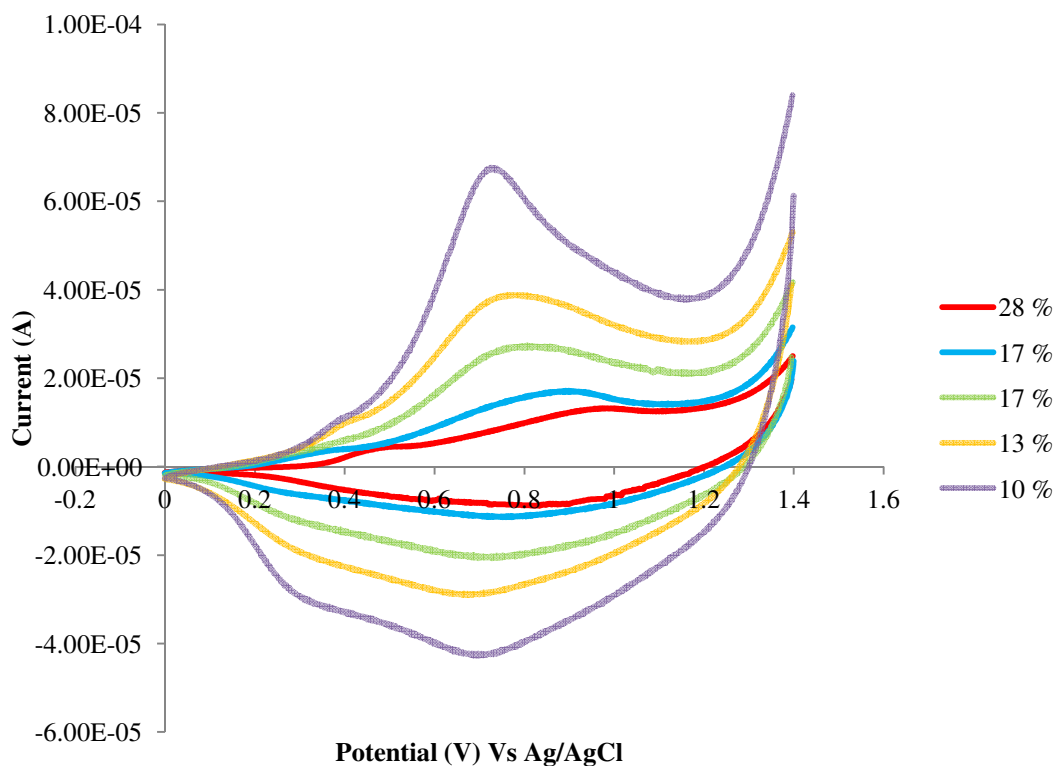


Figure 3.35. Copolymerisation of T3AA and MT with a total concentration of 0.6 M characterised at 50 mV s^{-1} .

Table 3.5. T3AA-MT Molar Ratio and Percentage Functional Monomer Content.

Molar Ratio T3AA-MT	Monomer Percentage Ratio	T3AA Content in Polymer
0.05-0.55 M	8.3-91.7%	10 %
0.1-0.5 M	16.7-83.3%	13 %
0.2-0.4 M	33.3-66.7%	17 %
0.3-0.3 M	50-50%	17 %
0.4-0.2 M	66.7-33.3%	28 %
0.5-0.1 M	83.3-16.7%	53 %

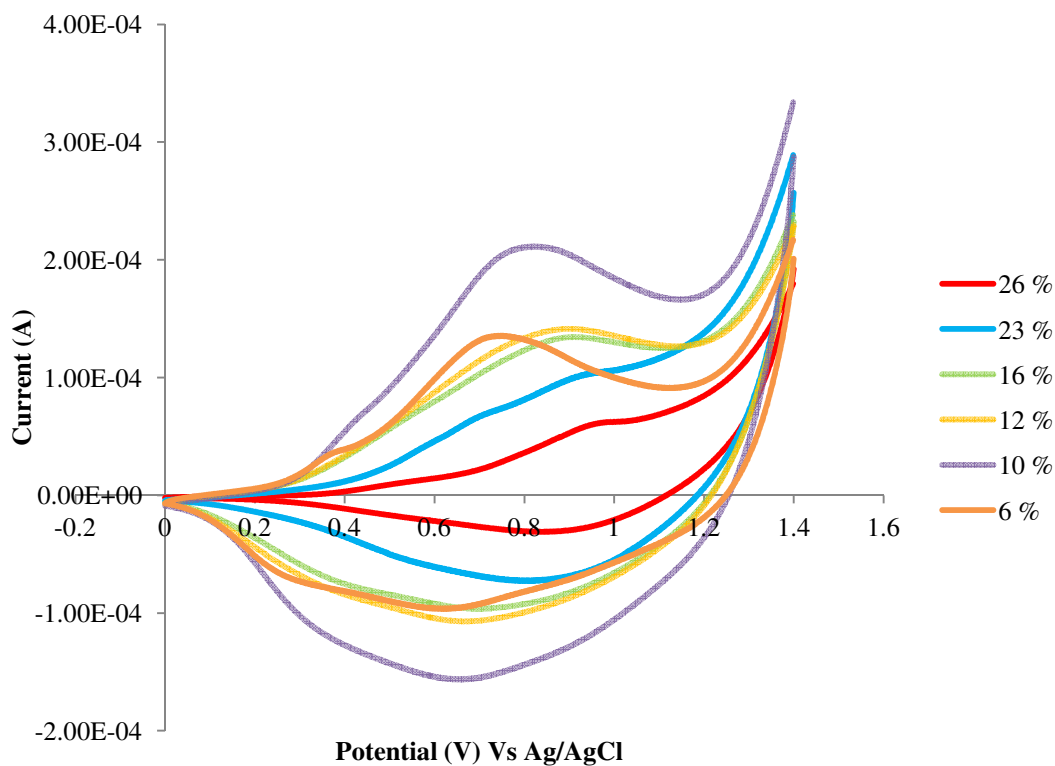


Figure 3.36. Copolymerisation of STA and MT with a total concentration of 0.3 M characterised at 50 mV s^{-1} .

Table 3.6. STA-MT Molar Ratio and Percentage Functional Monomer Content.

Molar Ratio STA-MT	Monomer Percentage Ratio	STA Content in Polymer
0.03-0.27 M	10-90%	6 %
0.06-0.24 M	20-80%	10 %
0.12-0.18 M	40-60%	12 %
0.15-0.15 M	50-50%	16 %
0.18-0.12 M	60-40%	23 %
0.24-0.06 M	80-20%	26 %

Table 3.7. Redox Data for 3-Methylthiophene and the Copolymer Materials.

Monomer Growth Solution	Monomer Conc. M	$E_p^{A'}, E_p^{A''}$ V		$I_p^{A'}, I_p^{A''}$ μA		$E_p^{C'}, E_p^{C''}$ V		$I_p^{C'}, I_p^{C''}$ μA	
MT	0.1	0.32	0.63	7.6	29.6	0.73	0.28	-23.9	-14.2
T3AA-MT	0.05-0.55	0.38	0.70	10.2	65.6	0.70	0.32	-42.3	-30.1
	0.1-0.5	0.39	0.75	10.6	38.7	0.69	0.29	-30.0	-19.2.
	0.2-0.4	0.77		27.0		0.73		-20.3	
	0.3-0.3	0.35	0.89	4.9	17.1	0.75		-11.5	
	0.4-0.2	0.46	0.97	4.76	13.1	0.82		-8.8	
STA-MT	0.03-0.27	0.35	0.72	31.3	134.0	0.64	-96.0	0.28	-71.1
	0.06-0.24	0.40	0.79	54.0	210.0	0.67	-156.0	0.37	-122.0
	0.12-0.18	0.87		141.0		0.67	-107	0.36	-79.0
	0.15-0.15	0.90		134.0		0.69	-96.3	0.39	-76.4
	0.18-0.12	0.69	0.91	65.5	100.0	0.86		-71.5	
	0.24-0.06	0.95		60.2		0.91		-28.9	

The voltammograms displayed for the copolymerisation study of T3AA and STA demonstrate a clear relationship between the amount of functional monomer incorporated into the polymer film and the redox responses obtained. Both copolymerisation voltammograms also indicate a relationship between the current signal generated and the different amounts of T3AA and STA in the electrogenerated film. Table 3.7 displays the corresponding redox data in which the observed relationships are confirmed.

Increasing the content of the functional monomers through copolymerisation demonstrates an increasing oxidation potential. The T3AA-MT copolymer shows the presence of a measureable anodic pre-peak within most of the voltammograms in figure 3.35 followed by a broad oxidation. The position of both oxidation peaks move to more positive potentials indicating the increased difficulty of oxidising the film where more T3AA monomers are incorporated. Interestingly as the total concentration remains the same an additional relationship can be observed reflecting a decrease in current response as the percentage content of T3AA increases. This is shown very

clearly in figure 3.35 with a broadening of the major oxidation peak as higher T3AA content is approached.

Copolymerisation of STA-MT demonstrates the same relationships through increasing STA content. Broader responses are evident within the characterisation of STA-MT copolymer films and therefore the pre-peak is not always measureable in the voltammograms produced. However it was still observed that both oxidation peaks became more positive as more STA was introduced into the polymer and the current decreased from 10% STA through the higher STA percentage content investigated.

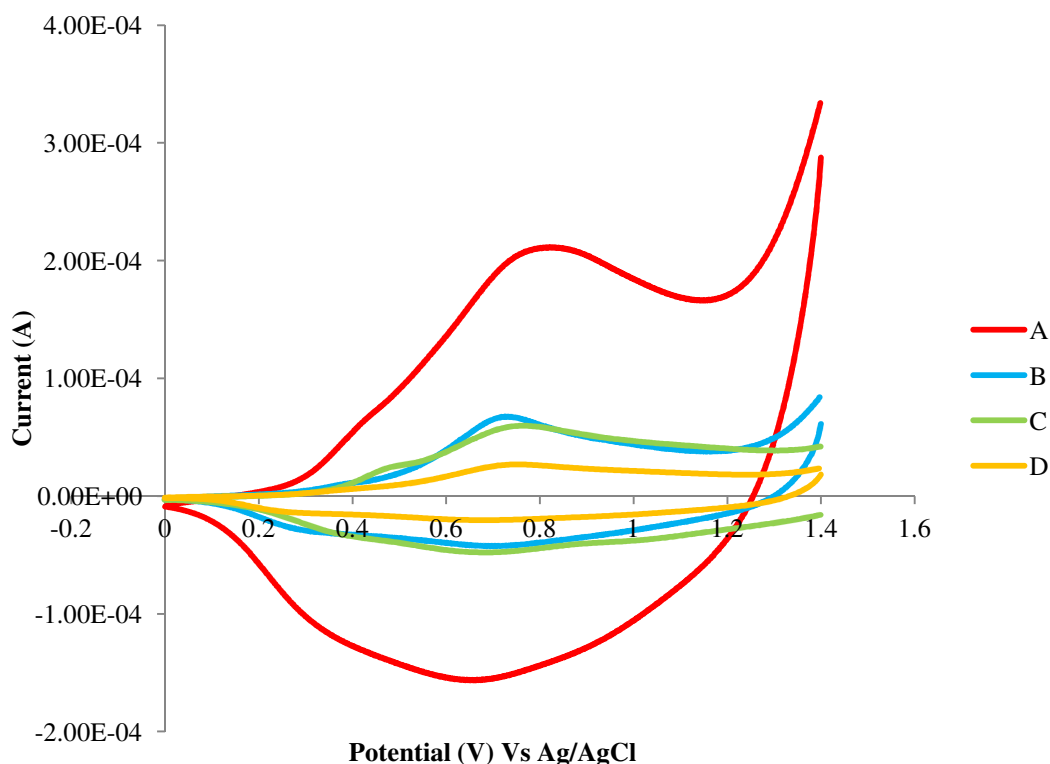


Figure 3.37. Comparison of the four copolymers with 10% functional content.
A STA-MT,(0.06-0.24 M) B T3AA-MT,(0.05-0.55 M) C STTA-MT, (0.04-0.26 M)
and D TTA-MT (0.05-0.55 M).

Copolymerisation of trans-3-(3-thienyl) acrylic acid and N-succinimido trans-3-(3-thienyl) acetate with 3-methylthiophene was performed in which 13% and 12% (respectively) was the maximum content achievable due to the restricted solubility of the compounds. A functional content of 10% was established for both copolymer materials and was combined for comparison with the T3AA-MT and STA-MT copolymers in figure 3.37.

Copolymerisation successfully provided a method of incorporating a monomer with polymerisation difficulties into a solid platform. Figure 3.37 displays the various copolymer systems all containing 10% functional monomer content in which clear differences can be seen in the voltammograms produced.

The major difference observed in figure 3.37 is the current signal generated for the 0.06-0.24 M STA-MT copolymer. The total concentration used is 0.3 M which is half the total concentration of the T3AA and TTA-MT series at 0.6 M and still generates a signal approximately four times the magnitude. Comparing this trace to the 0.04-0.26 M STTA-MT material it is clear that even at the same total concentration of 0.3 M the STA-MT copolymer produces an enhanced response. The structure of the functional monomer must therefore play a significant role and could potentially influence the current through different effects. The effectiveness of the polymerisation process is likely to impact the current obtained as sterically hindered monomers are more difficult to polymerise. Furthermore the presence of a rigid double bond linker chain provides increasing obstruction towards the coupling of radical species and electron withdrawing groups deactivate the alpha ring carbons needed for polymerisation. Therefore increasingly problematic species may lead to less material being generated at the electrode surface and as the concentration is directly related to the current low signals will correspond to the growth of thinner films. The properties of the films themselves maybe responsible for the difference in current obtained upon characterisation. Morphology is important as a structured polymer backbone that can compensate the movement of anions due to flexible side chains aid production of larger currents. Also side groups such as the carboxylic acid that possess a negative charge could potentially repel anions or permit self doping effectively neutralising the film¹⁸³⁻¹⁸⁴ therefore generating the small currents seen for the T3AA and TTA incorporated materials.

The increasing amount of functional monomer incorporated into the film generated increasingly positive oxidation potentials this was demonstrated clearly for both the T3AA-MT and STA-MT copolymers in figures 3.35 and 3.36. Higher oxidation potentials indicate the difficulty associated with oxidising the material and figure 3.37 was used to determine the major oxidation potentials of the copolymers which were T3AA +0.70 V, STA +0.79 V, TTA +0.72 V and STTA +0.73 V. This demonstrated

that the ester monomers required higher positive potentials due to the steric hindrance imparted by the substituent. Also the extended linker chain potentially alleviated the strain in the system indicated by the lower oxidation potential as the large group was now positioned further away from the main polymer chain. The oxidation potentials for the carboxylic acid functional monomers are similar indicating that a 10% content does not impart large steric effects and therefore lower potentials are not observed for the TTA monomer contributing the extended linker chain.

Overall good current response was seen with all copolymer materials especially STA-MT providing enhanced signals. Oxidation potentials remained in the region of hydrogen peroxide oxidation at 0.7 V therefore accessing conductivity through the film will aid oxidation at the polymer/solution boundary as well as at the electrode surface generating good response to glucose.

Introducing a simple thiophene monomer such as 3-methylthiophene into the polymerisation process generated radical cation species at low oxidation potentials which were capable of radical-monomer coupling aiding the growth of a conducting polymer film. In addition to facile polymerisation the introduction of a simple thiophene monomer imparted desirable properties to the resulting film. Copolymerisation with 3-methylthiophene effectively diluted the large functional species alleviating the steric hindrance within the polymer. This generated a stable conducting polymer platform essential for the electron transfer which will be generated to the electrode from the immobilised redox enzyme. Optimisation of the material through different copolymer ratios produced a film with low oxidation potential corresponding to the oxidation of hydrogen peroxide. Copolymerisation will therefore provide an important method to optimise enzyme loading for the biosensor system.

Chapter 4 Polymer Film Characterisation

Having shown in chapter 3 that combining different thiophene monomers in the polymerisation solution produces an observed variation in the electrochemistry it is evident that copolymerisation takes place to some extent. Investigating different ratios of thiophene compounds for copolymerisation generated a series of voltammograms displaying a clear change in the redox signals potentially demonstrating manipulation of the polymer content. Analysis of the polymer content is important and this is especially significant where the copolymer produced is to be incorporated into a biosensor format for the immobilisation of the essential biological recognition element.

The number of potential binding sites for the biological component is associated to the percentage content expressed for the functional thiophene monomer, in this case either the carboxylic acid species thiophene-3-acetic acid (T3AA) and trans-3-(3-thienyl) acrylic acid (TTA) or the activated ester form N-succinimido thiophene-3-acetate (STA) and N-Succinimido trans-3-(3-thienyl) acetate (STTA). Therefore by successful determination of the thiophene monomer content responsible for biological covalent attachment the copolymer ratio can be fine tuned to provide the optimum number of binding sites for achieving maximum sensor response.

Chapter 4 describes the different methods employed for the determination of the number of potential binding sites by exploiting the functionality of the thiophene ring. The polymer films were also characterised based on their doping capacity as they were electrochemically polymerised and further examined through SEM-EDX to determine the film morphology and anion content. Characterisation techniques included infrared spectroscopy, atomic absorption spectroscopy, surface bound electroactive species and SEM-EDX.

Investigation of the copolymer content was based upon the well studied T3AA-MT system and the activated ester monomer STA-MT. Past research performed upon the T3AA-MT system found that at 10% functional content the sensor achieved optimum performance⁵⁴. Therefore the aim was to not only produce a wide range of copolymer compositions but to produce the 10% available binding sites for both systems in order to maximise the sensor response. The range of copolymerisation compositions for the trans-3-(3-thienyl) acrylic acid and its activated ester compound was limited. The

solubility of both compounds was low and therefore only 10-13% functional group content was achievable.

The copolymer monomer ratios for thiophene-3-acetic acid and 3-methylthiophene were chosen based upon research by Shimomura *et al* and provided a good range of concentrations to investigate. N-succinimido thiophene-3-acetate and 3-methylthiophene copolymer demonstrated lower concentrations due to the synthesis procedure of the novel copolymer covering a wide concentration range.

4.0. Techniques Investigated for Functional Monomer Content

4.1. Infrared Spectroscopy

Infrared spectroscopy was used in order to analyse the compound ratio within the polymer film through excitation of the carbonyl species. The carbonyl group exists as a strong sharp peak in the region $1820 - 1660 \text{ cm}^{-1}$ and therefore should be clearly distinguishable and easily monitored for calculating the percentage content.

Ten individual polymer films were made starting with the 0.6 M thiophene-3-acetic acid (T3AA) homopolymer where 800 mC of passed charge at 2.2 V was used to develop a thick film that could be easily peeled away from the electrode surface for IR analysis. The spectra obtained for the homopolymer were good, displaying the carbonyl stretch at 1704 cm^{-1} as expected and reproducibility was calculated for the ten samples. The 0.5-0.1 M T3AA-MT copolymer was also analysed in which the carbonyl and hydroxyl groups were clearly reduced compared to the T3AA homopolymer. Further copolymer analysis was not successful as the lower T3AA content failed to be detected and the carbonyl stretch used for ratio calculation was absent. Therefore only data from the T3AA homopolymer and the 0.5-0.1 M T3AA-MT copolymer was obtained from this series and represented in figures 4.1 and 4.2 with tabulated carbonyl absorbance at 1704 cm^{-1} and reproducibility in table 4.1. Also displayed in table 4.1 is the data obtained from 0.2 M STA and 0.24-0.06 M STA-MT. The homopolymer demonstrates the carbonyl stretch occurring at 1733 cm^{-1} which is expected for an ester compound however the 0.24-0.06 M STA-MT copolymer analysis was problematic and a clear carbonyl absorbance peak was not observed however the carbonyl peak was measured as a broad response between 1731

cm^{-1} and 1715 cm^{-1} seen in figure 4.2. Due to the difficulty associated with measuring the carbonyl species further copolymer ratios could not be determined.

Table 4.1. Absorbance Data from the Carbonyl Species Present in Ten Polymer Films.

Sample Number	0.6 M T3AA	0.5-0.1 M T3AA-MT	0.2 M STA	0.24-0.06 M STA-MT
1	0.244	0.0657	0.237	0.0473
2	0.188	0.0244	0.248	0.0540
3	0.112	0.0486	0.0762	0.0280
4	0.132	0.0451	0.115	0.0344
5	0.0713	0.0627	0.146	0.0278
6	0.0871	0.0424	0.142	0.0351
7	0.0824	0.0877	0.369	0.0224
8	0.0736	0.0778	0.0933	0.0405
9	0.116	0.0833	0.121	0.0659
10	0.204	0.0473	0.0736	0.0374
Average	0.131	0.0585	0.162	0.0393
RSD	44 %	33%	55%	32%
% quantity	100%	45%	100%	24%

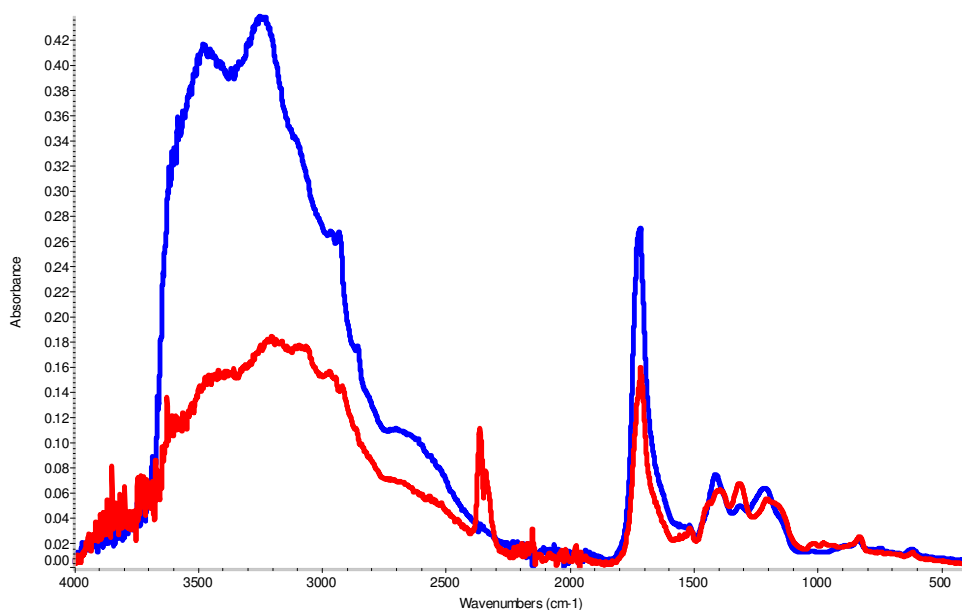


Figure 4.1. IR Spectrum of 0.6 M T3AA (blue) and 0.5 M-0.1 M T3AA-MT copolymer (red).

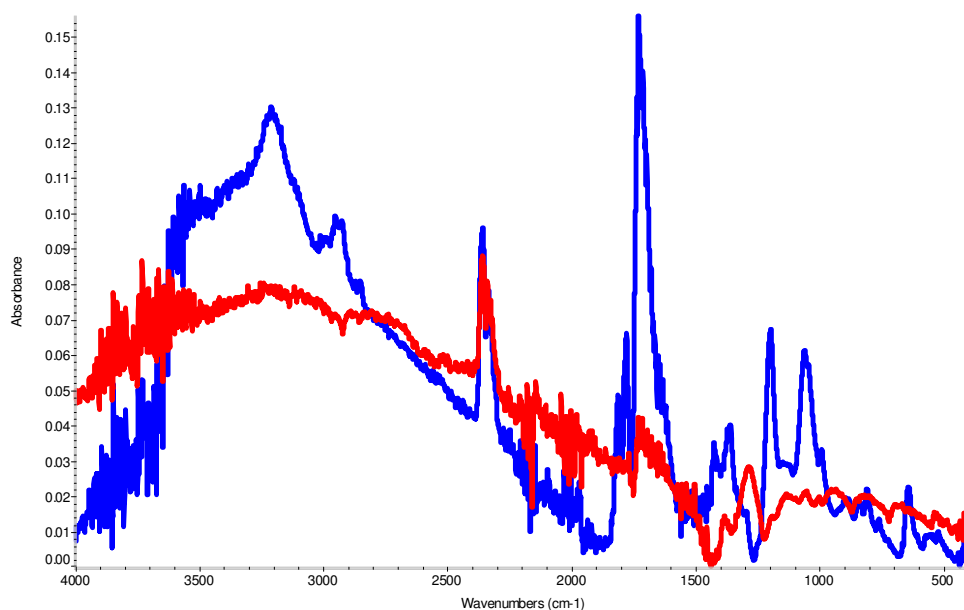


Figure 4.2. IR Spectrum of 0.2 M STA (blue) and 0.24 M-0.06 M STA-MT copolymer (red).

The results displayed in table 4.1 demonstrate a calculated ratio for the copolymers with a potential 45% functional content available for 0.5-0.1 M T3AA-MT and 24% available 0.24-0.06 M STA-MT. However the associated error is very large and unfortunately does not provide the precision required for accurately determining the polymer composition. In addition the failure to produce data for the majority of samples possibly due to morphological changes within the film causing reduced sensitivity leads the investigation of copolymer ratio onto alternative methods.

4.2. Atomic Absorption Spectroscopy

Atomic absorption is used for elemental analysis and therefore to use this technique the polymer materials needed adapting. This method was employed due to its high sensitivity and to overcome the difficulties surrounding film morphology. The objective was to first determine the concentration of the thiophene-3-acetic acid homopolymer and then use the results to calculate the percentage composition of thiophene-3-acetic acid within a range of copolymer materials at constant mass generated from known concentration ratios in the polymerisation solution.

In order to detect the amount of potential binding sites in the polymer the carboxylic acid groups were ion exchanged with sodium and then following acid exposure

dissociation of the sodium provided the concentration that was related to the thiophene-3-acetic acid content.

Although this method provided positive results from the initial investigations the reproducibility was poor and the technique required long and time consuming manipulation to the samples under study. Due to the lengthy nature of the method it was not applied for any further samples and a more efficient technique was sought out. The experimental details can be found in Chapter 2.

From this investigation it was determined that in order for the content of potential binding sites to be calculated a simpler technique was needed. This would eliminate large sources of error and reduce the analysis time required for the investigation.

4.3. Scanning Electron Microscopy with Energy-Dispersive X-ray Analysis (SEM-EDX)

SEM-EDX provided a successful technique that not only determined the copolymer ratio of the electrochemically grown films but generated data based upon the dopant inclusion through the same analysis. Morphological information was also obtained therefore generating data for several investigations. This technique was also non destructive as the polymers' inherent conductivity required no sputter coating treatment. The ease of sample preparation, quick analysis times and amount of information generated provided the large majority of data represented in chapter four.

Table 4.2 below displays the elemental data collected from the technique with most of the samples ranging in copolymer ratio in order to determine a wide range of functional content which can be further investigated in a sensor format. Two polymers were grown for each investigation with three sites analysed per sample. The average value of the six readings taken is displayed in the table below with their relative standard deviation. The analysis time was five minutes as previous experiments showed no change in the data obtained after extended periods of 30 minutes to an hour.

To determine the percentage of functional thiophene content a 0.6 M thiophene-3-acetic acid homopolymer was grown, rinsed in acetonitrile and then left in a desiccator overnight to dry. It was expected that the poly(thiophene-3-acetic acid) would produce an oxygen to sulphur ratio of two however the actual value was calculated at 2.38 in which residual oxygen can also be seen within the poly(3-methylthiophene) at similar content. This was most likely due to trapped oxygen from the solvent or evidence of over oxidation obtained during polymerisation and so provided a more reliable oxygen estimation and was therefore used to calculate the percentage content of thiophene-3acetic acid within the copolymer series.

The same process was performed for the N-succinimido thiophene-3-acetate series where an oxygen to sulphur ratio of four was anticipated however a value of 4.65 was determined and used in the following calculations.

Additional thiophene derivatives have also been investigated and were introduced within chapter 3 for their electropolymerisation capabilities and redox characteristics. Trans-3-(3-thienyl) acrylic acid and its synthesised activated ester counterpart have also been investigated with particular interest upon the generation of a 10% functional content. The low percentage is reported to provide enhanced response to glucose within a biosensor system⁵⁴ and is therefore determined at a concentration ratio of 0.04-0.26 M STTA-MT seen in table 4.2 however 0.06-0.24 M STTA-MT also produces a functional content close to 10% due to the calculated error.

The dopant ratio was also calculated for all samples in which poly(bithiophene) (PBT) and poly(3-dodecylthiophene) (PDDT) were also investigated for their dopant ratio and have been included at the end of the table for comparative purposes.

Percentage error is included for all dopant and functional thiophene calculations which vary considerably this demonstrates the variability of the films when small areas are investigated, however based upon the average measurements a clear trend can be seen.

Table 4.2. Elemental Data Representing Percentage Atomic Weight.

Polymer Sample	Average		RSD		Number of Thiophene rings TFB is distributed over	% Ratio of functional monomer
	F/S Dopant Ratio	O/S Ratio	F/S	O/S		
0.1 M MT	0.171	0.275	36%	38%	5.8	0%
0.6 M T3AA	0.0490	2.38	60%	14%	20.4	100%±7.0
0.5-0.1 M T3AA-MT	0.0894	1.27	26%	24%	11.2	53%±6.4
0.4-0.2 M T3AA-MT	0.0993	0.678	31%	19%	10.1	28%±2.7
0.3-0.3 M T3AA-MT	0.157	0.416	18%	20%	6.4	17%±1.7
0.2-0.4 M T3AA-MT	0.214	0.412	7%	15%	4.7	17%±1.3
0.1-0.5 M T3AA-MT	0.320	0.300	17%	32%	3.1	13%±2.0
0.05-0.55M T3AA-MT	0.375	0.241	14%	30%	2.7	10%±1.5
0.2 M STA	0.305	4.65	13%	17%	3.3	100%±8.5
0.24-0.06 M STA-MT	0.167	1.20	27%	48%	6.0	26%±6.2
0.18-0.12 M STA-MT	0.361	1.07	27%	31%	2.8	23%±3.6
0.15-0.15 M STA-MT	0.292	0.750	36%	26%	3.4	16%±2.1
0.12-0.18 M STA-MT	0.294	0.567	29%	40%	3.4	12%±2.4
0.06-0.24 M STA-MT	0.344	0.450	7%	15%	2.9	10%±0.75
0.03-0.27 M STA-MT	0.440	0.264	27%	54%	2.3	6%±1.6
0.05-0.55 M TTA-MT	0.491	0.230	13%	16%	2.0	10%±0.8
0.1-0.5 M TTA-MT	0.501	0.317	8%	6%	2.0	13%±0.39
0.04-0.26 M STTA-MT	0.281	0.472	21%	25%	3.6	10%±1.25
0.06-0.24 M STTA-MT	0.356	0.544	22%	31%	2.8	12%±1.86
0.1 M BT	0.148		14%		6.8	0%
0.1 M DDT	2.22		7%		0.5	0%

By decreasing the concentration of the functional thiophene monomer in the growth solution the functional content of the copolymer was also reduced. This was expected and can also be seen in the work published by Kuwahara *et al.* However the work

done by Kuwahara *et al* demonstrated little variation of the resulting thiophene-3-acetic acid content to the percentage in the growth solution where in this study a marked difference was seen.

Reducing the percentage of the thiophene-3-acetic acid monomer content in the growth solution from 100% to 83% decreases the content in the resultant copolymer by nearly 50% indicating the difficulty surrounding the polymerisation of this compound. However N-succinimido thiophene-3-acetate demonstrates an even larger drop in concentration within the electropolymerised material as an 80% N-succinimido thiophene-3-acetate content represents only 26% of the functional compound. This data supports the results generated in chapter 3 where a higher potential cycling limit of +2.5 V was needed to produce a film of N-succinimido thiophene-3-acetate compared to +2.0 V for the growth of thiophene-3-acetic acid this is also established by Li *et al* and can be explained by the steric influence imparted on the molecule coupled with the electron withdrawing effects of the substituent.

In conclusion a successful variation of functional content was established through both copolymer series and can be used for evaluation within the biosensor construction. The additional monomers of trans-3-(3-thienyl) acrylic acid and N-succinimido trans-3-(3-thienyl) acetate were established as copolymers with 10% functional content as it was envisaged a lower concentration of binding sites would increase sensor response⁵⁴ and unfortunately solubility issues limited the generation of a series of different compositions.

The dopant ratio was also investigated for the different thiophene derivatives. It is reported that polythiophene accommodates one charge for every 3-4 thiophene units which seems to be the accepted value. Interestingly a trend was observed through the thiophene-3-acetic acid copolymer series where increasing the acid concentration had a direct effect upon the level of doping associated with the material. It can be clearly seen by reducing the thiophene-3-acetic acid content the fractional dopant per thiophene unit increases. From the very low value of 0.049 charges per unit for a polymer comprised completely of acid groups to 0.375 for a copolymer with a 10% thiophene-3-acetic acid fraction. Interestingly upon esterification of the acid groups the variation of doping content with copolymerisation ratio no longer applies and a

fairly stable dopant value can be observed at around 0.3 charges per thiophene unit. The effect of decreasing dopant/charge associated with the copolymer film as more thiophene-3-acetic acid units are introduced could be evidence of self doping¹⁸³⁻¹⁸⁴.

Self doping represents a different mechanism of achieving charge neutrality within a conjugated polymer as the counterion is covalently bound to the polymer. Oxidation causes the film to become positively charged which is compensated by proton migration and balanced by the oppositely charged counterion attached to the polymer normally established by the electrolyte¹⁸⁵⁻¹⁸⁶. As the charge distribution over the polymer is reduced conductivity is observed to decrease^{14,183} in which there are several attributing factors. The charge carrier distribution over local polymer chains is restricted due to their increased distance caused by the bulky substituents. Additionally the self doping species such as CO_2^- and SO_3^- are also likely to decrease the conjugation in the material due to polymer twisting as the polymer attempts to compensate the large side groups¹⁵⁻¹⁷.

The evidence suggests that it is the influence of side group upon the thiophene ring that controls the degree of doping in the system. However it is not confirmed if these effects are entirely due to the self doping properties of the substituent or if a combination of factors such as steric or inductive effects exists.

Waltman *et al* concluded similar differences in doping content upon thiophene derivatives where β -substitution decreased the amount of charge associated with each thiophene unit³⁶. It was found that poly(3-methylthiophene) had only 0.12 of fractional charge per thiophene with polythiophene displaying a value of 0.22. However electrical conductivity evaluated for the polymer materials did not support the dopant values as poly(3-methylthiophene) demonstrated a 100-fold increased response against polythiophene and therefore suggests there are several parameters that effect electrical conductivity.

In contrast to the self doping concept dopant values for trans-3-(3-thienyl) acrylic acid were high at around 0.5 but upon esterification reverted to the 0.3 fractional charges per thiophene unit seen for the majority of the thiophene ester series. A rigid linker chain is reported to provide enhanced doping due to the increased porosity of the

polymer allowing facile anion movement in and out of the film³⁸. This may also be true for the trans-3-(3-thienyl) acrylic acid monomer as a double bond separates the side group from the polymer backbone therefore possibly increasing the charge calculated in the system.

Poly(bithiophene) and poly(3-methylthiophene) display similar dopant levels however with significant hydrocarbon chain influence seen with poly(3-dodecylthiophene) dopant levels dramatically increase to 2.22. Upon further examination of the data it can be seen that although the atomic percentage of the dopant is uniquely high the sulphur content of the film is significantly low. This maybe explained due to the extended hydrocarbon chain attached to the monomer effectively diluting the sulphur content and encouraging dopant integration due to the porous nature of the material.

Although interesting data can be observed for the dopant values it is difficult to fully evaluate this effect when a number of influential parameters maybe responsible. Without further investigation it can only be speculated that the side group demonstrates some control upon the charge capacity of the material.

4.4. Surface Coverage using Electrochemistry

A further method for the calculation of surface coverage was to be implemented in which the details can be found in chapter 2, however due to the capability of the SEM-EDX technique this was not required and thus removed the complex calculations associated with the method. Surface coverage was not the only information achievable through this procedure as confirmation of molecular attachment can also be provided with the possibility of determining experimental details that can be implemented within the biosensor fabrication step.

Examination of successful binding upon polymer substrates through cyclic voltammetry has been investigated⁵⁶ and attempted within this study.

The introduction of an electroactive species with amine groups was established in order to determine if covalent binding could be accomplished. The expected response using cyclic voltammetry would be to witness the redox properties of the chosen electroactive compound over the electrochemistry of the polymer material.

The electroactive species selected was 2,3,5,6-tetramethyl-1,4-phenylenediamine. This compound contains two amine groups that can be covalently bound to the activated ester group via a peptide bond with no additional reagents needed for the reaction to occur. The compound was dissolved in acetonitrile generating a 0.1 M solution and was used under stirring to soak the copolymer materials generated from a solution containing a large concentration of potential binding sites and a second solution with only a small concentration of binding sites. The percentage of available binding positions was calculated at 26% with a ratio corresponding to 0.24-0.06 M STA-MT in the polymerisation solution and 10% associated with 0.06-0.24 M STA-MT this was determined from the data obtained by elemental analysis in section 4.3.

Investigations start with the 0.06-0.24 M STA-MT polymerisation solution comprising of 10% binding sites. The material was grown potentiostatically at 2.2 V obtaining a film after using 2.5 mC of charge. The copolymer was then exposed to the diamine compound for 30 minutes then rinsed and cycled in a monomer and diamine free solution. The results can be seen in figure 4.3 below.

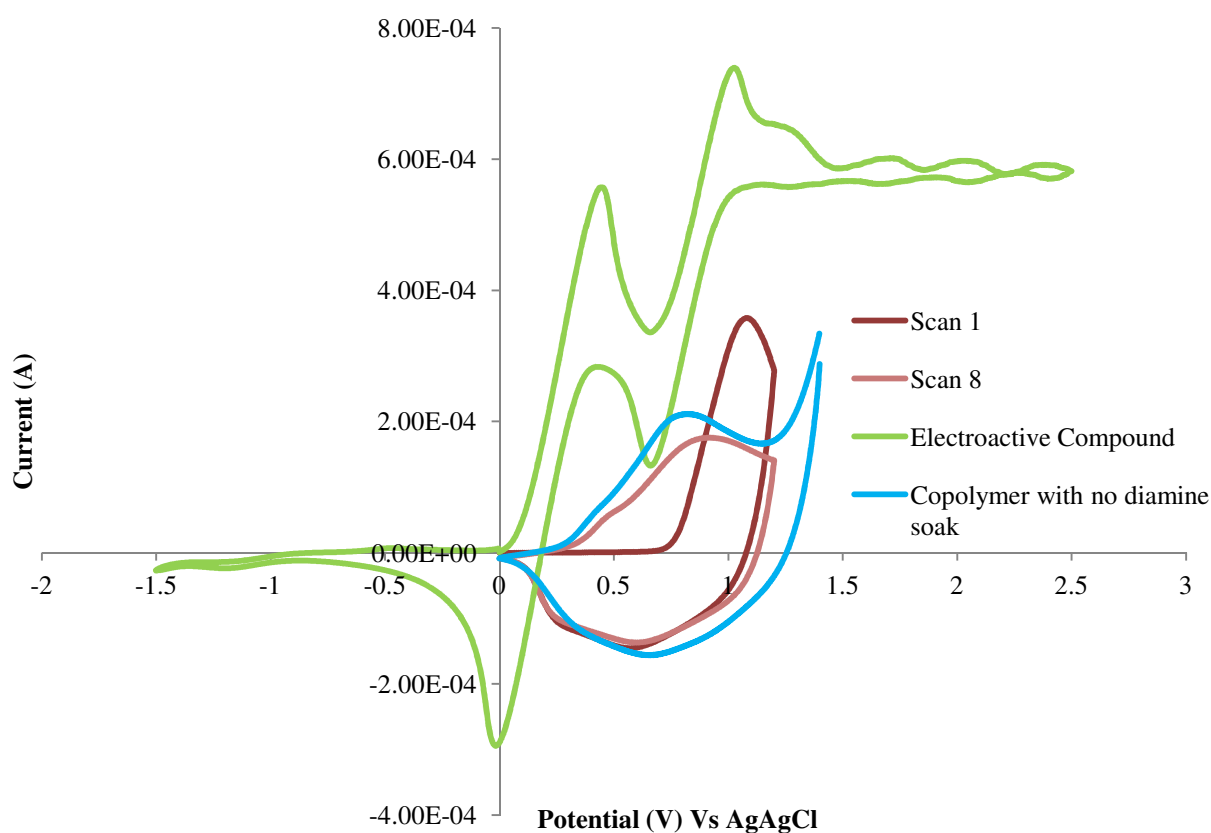


Figure 4.3. Comparison of redox properties established within the electroactive film and the copolymer materials with and without diamine exposure at 30 minutes.

Two well defined redox processes can be seen at approximately -0.0156 V and +0.45 V and +1.0 V and +0.67 V for the 3,5,6-tetramethyl-1,4-phenylenediamine which should therefore be seen when bound to the copolymer film. The initial scan 1 of the copolymer exposed to the diamine solution shows a possible anodic response corresponding to the second oxidation of the diamine compound however upon subsequent scans the redox responses revert to the electrochemistry seen for the film with no diamine exposure seen at scan 8. As figure 4.3 shows covalent binding did not take place this could be due to the short 30 minute exposure time and therefore increasing the time may promote binding of the electroactive diamine species.

After three hours of diamine exposure the copolymer film was extracted from solution and rinsed with acetonitrile to remove all unbound species. The electrodes were again cycled in a 0.1 M TBATFB acetonitrile solution free from the diamine compound and thiophene monomer.

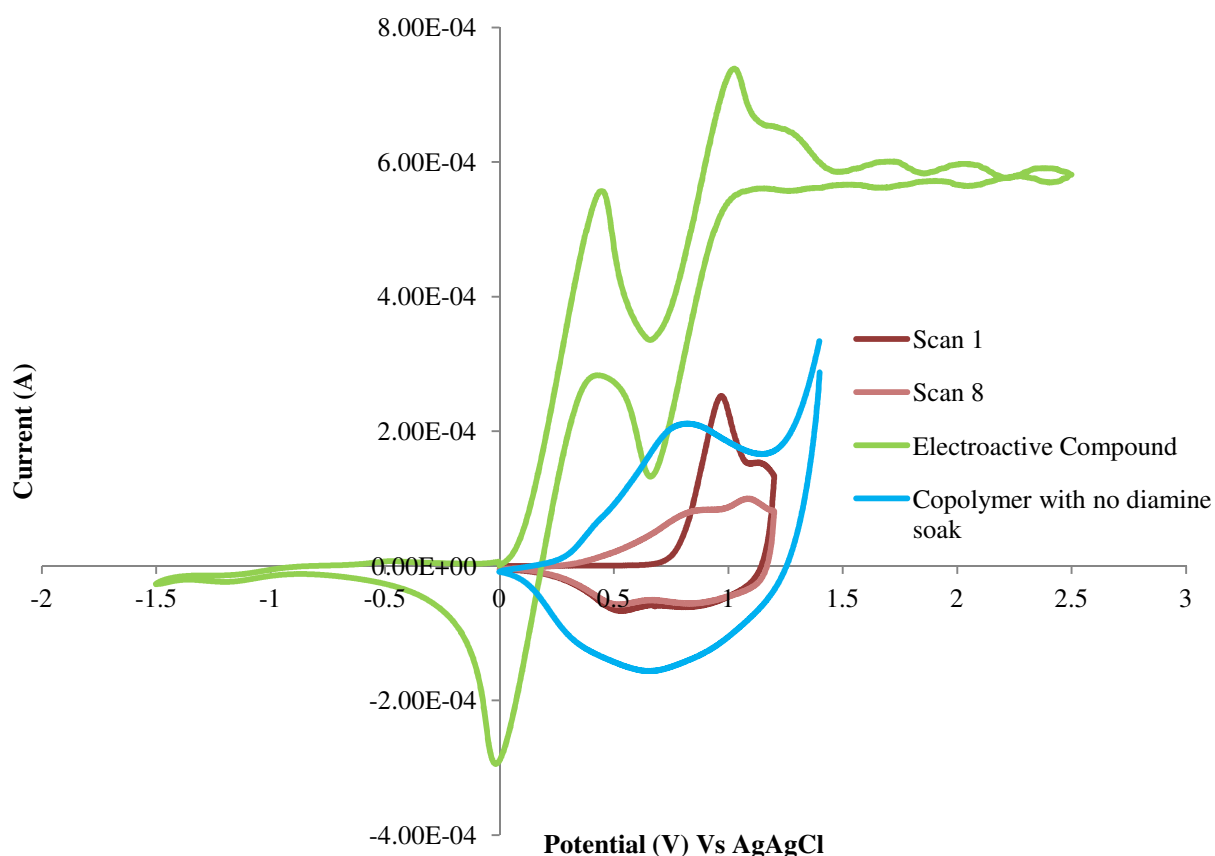


Figure 4.4. Comparison of redox properties established within the electroactive film and the copolymer materials with and without diamine exposure at three hours.

Scan 1 demonstrates an anodic response corresponding to the entrapped diamine with a possible shoulder oxidation also seen within the diamine scan. As the copolymer was further cycled both anodic responses decreased. Compared with no diamine soak it was possible that covalent attachment had not taken place as reduction responses were absent. It was possible that the number of available binding sites was too low to be detected over the electrochemistry of the material or the exposure time was not sufficient to enable efficient binding.

Infrared analysis was performed on a thicker film with the same composition 0.06-0.24 M STA-MT with 3 hours diamine exposure to confirm that amine groups had not been covalently bound.

The number of binding sites was increased to 26% (0.24-0.06 M STA-MT) and an exposure time of three hours was implemented in order to achieve the redox responses of the diamine.

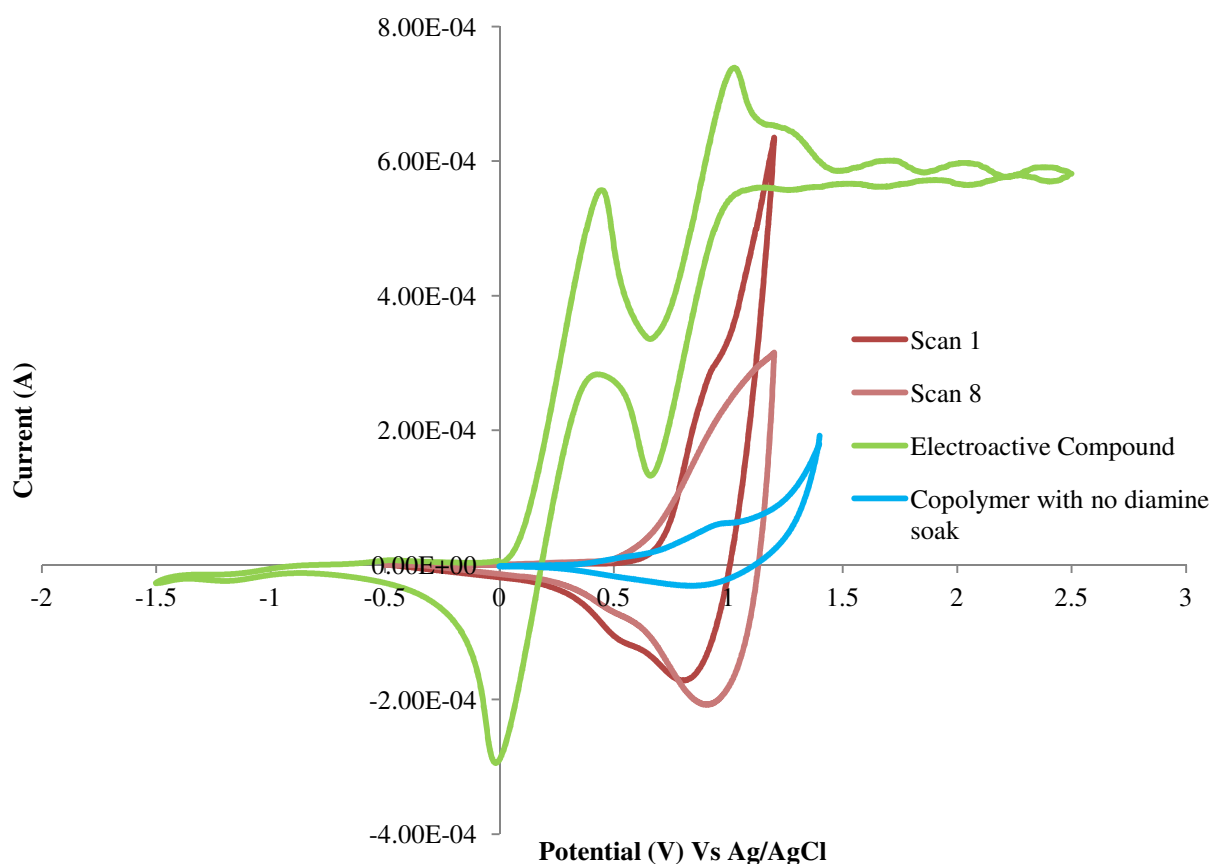


Figure 4.5. Comparison of redox properties established within the electroactive film and the copolymer materials with and without diamine exposure at three hours.

Figure 4.5 demonstrates clearly the effect of covalently bound 3,5,6-tetramethyl-1,4-phenylenediamine. Both the oxidation and reduction responses can be seen over the electrochemistry of the film and continue to be evident upon the 8th scan.

Infrared analysis verified the shift of the carbonyl stretch from 1731-1715 cm^{-1} to 1644 cm^{-1} which was consistent with the formation of an amide bond. A primary amine at 3405 cm^{-1} was present which corresponded to the unbound amine located on the para position on the ring. Figure 4.6 demonstrates the appearance of these peaks with the retained carbonyl peak at 1715 cm^{-1} indicating that not all the ester groups reacted and therefore 3 hours may not have been long enough for complete amine attachment upon thicker films of 800 mC with 26% potential binding sites.

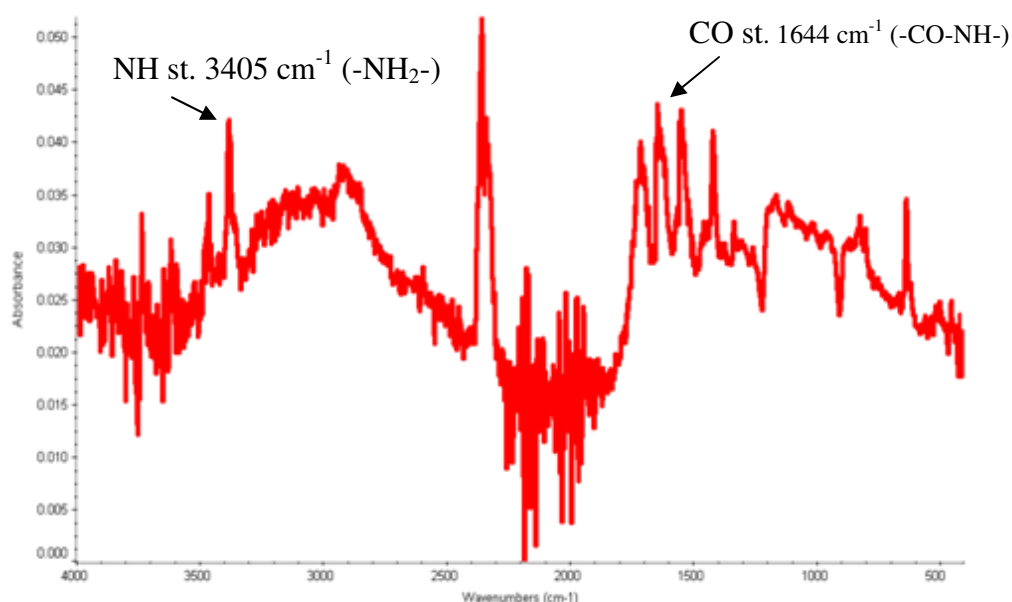


Figure 4.6. IR spectrum of 0.24-0.06 M STA-MT after 3 hours of diamine exposure.

One issue regarding the results displayed for all copolymer ratios and exposure times was the absence of the first redox couple of the 3,5,6-tetramethyl-1,4-phenylenediamine. This observation is also acknowledged through the work of Li *et al*. The research of Li *et al* followed a similar approach using the same functional monomer of N-succinimido thiophene-3-acetate and obtained the same difficulty surrounding the generation of redox responses corresponding to the electroactive compound employed. As stated by Li *et al* the conductivity of the film was limited to oxidative regions where electrical transport was accommodated and we see redox

processes of the copolymer material. The electroactive compound used by Li was a naphthoquinone derivative, which displayed very negative redox potentials and subsequently was not electrochemically accessible. The electroactive compound used in this study did possess a positive redox couple and demonstrated this effect successfully in figure 4.5 upon a copolymer with 26% potential binding sites although the first redox response of the diamine was not successfully accessed due to the redox potentials occurring in the reduced region of the material. However it is also possible that as covalent binding takes place through one or both amine groups the electrochemistry of the electroactive diamine compound could change, thereby producing only one redox response which can be seen in figure 4.5.

Upon analysis of the diamine soaked copolymer 0.06-0.24 M with 10% binding sites seen in figures 4.3 and 4.4 the first potential sweep of the amine exposed copolymer showed that the first redox couple was absent which corresponded to the reduced region of the film however upon film oxidation the second oxidation response of the diamine was clearly observed over the anodic portion of the conducting copolymer. Upon subsequent scans the disappearance of the anodic signal was evident and indicated absorption of the species rather than the covalent link initially anticipated. This could be explained by the fully occupied ring structure of the diamine compound with the amine groups effectively hidden amongst the methyl substituents. The accessibility to the activated ester groups is reduced further due to the obstruction generated by the short side chain to the polymer backbone and therefore covalent immobilisation is obstructed. Also due to the low percentage of binding sites three hours may not have been sufficient to allow covalent binding to take place and therefore longer times may be required, alternatively if binding did occur it may be possible that it was not enough to be detected over the redox chemistry of the film.

By employing more binding sites and a three hour diamine soak covalent binding was possible; this finding can be used as a guide for the determination of enzyme immobilisation with considerations regarding enzyme exposure time to the percentage of binding sites present.

4.5. Film Morphology

As already mentioned SEM-EDX provided detailed images of the polymer materials aiding characterisation through visual representation of the film morphology. Each thiophene compound where possible was studied through the high magnification available with the microscope and clear differences were seen between the various homopolymers. For copolymer determination the images established a facile method of obtaining confirmation of structural changes expected through the influence of compounds with different spatial characteristics.

All films generated for the scanning electron micrographs were potentiostatically grown at the monomers corresponding oxidation potential until 800 mC of charge was passed. Such growth conditions were developed in order to obtain a thick enough film which could be extracted without damaging the polymer surface. The films were then rinsed with acetonitrile and left to dry in a desiccator overnight. The insets show the polymer at higher magnification.

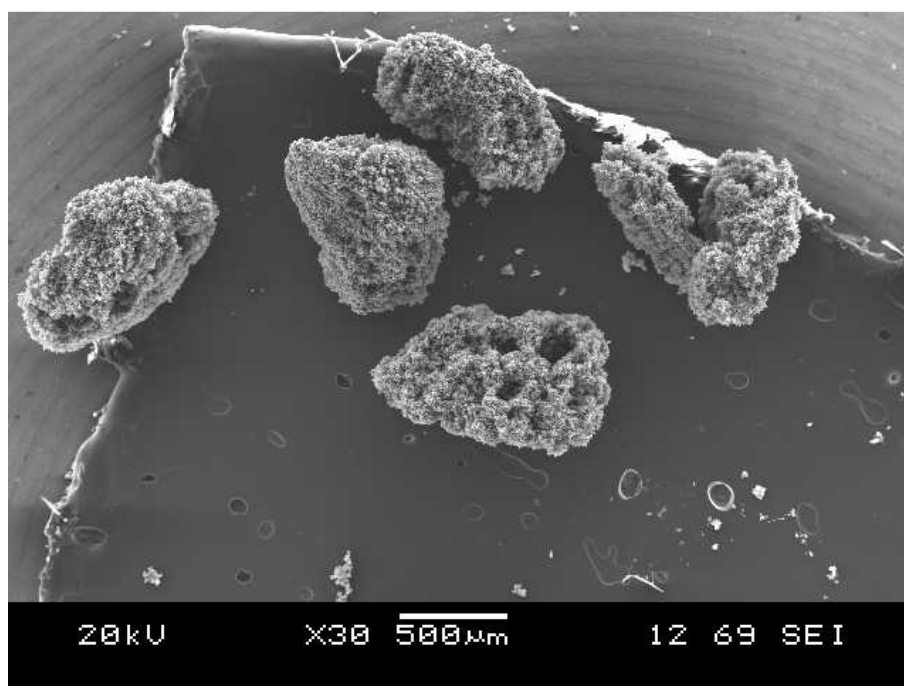


Figure 4.7. Poly(bithiophene) grown from a 0.1 M solution with TBATFB as electrolyte at +1.2 V.

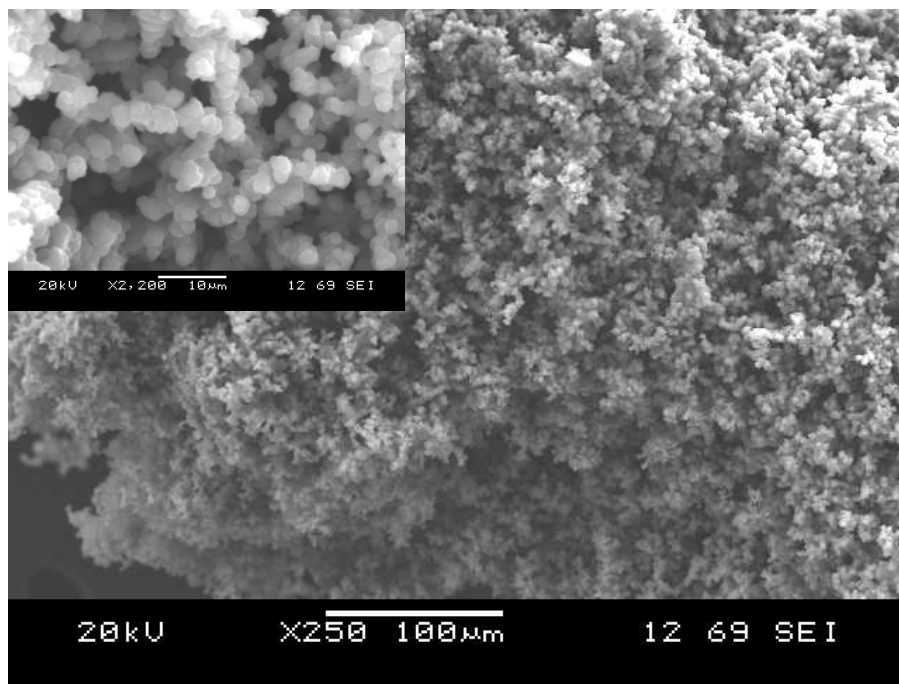


Figure 4.8. Poly(bithiophene) grown from a 0.1 M solution with TBATFB as electrolyte at +1.2 V.

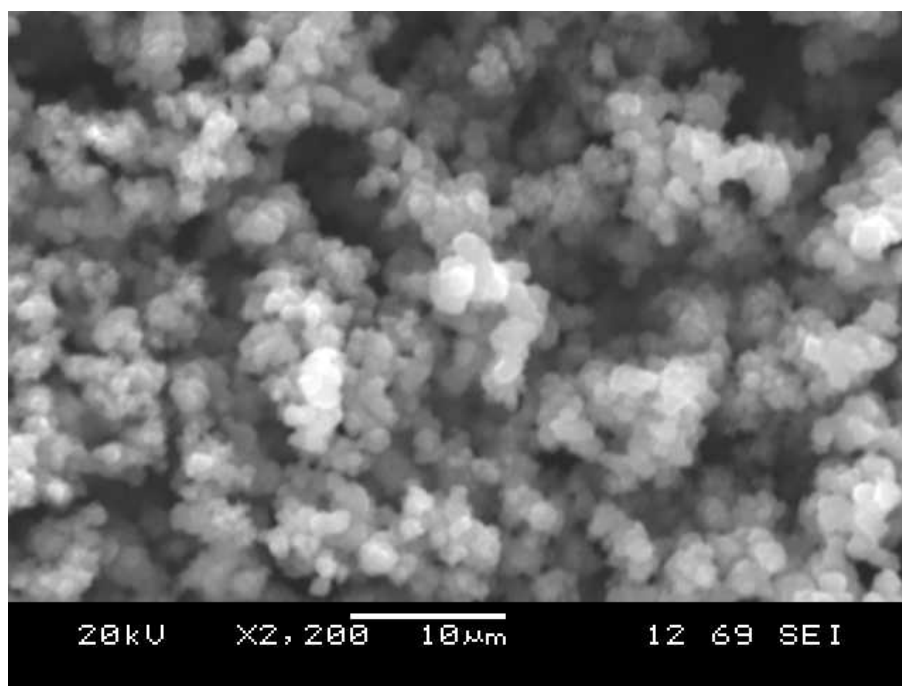


Figure 4.9. Poly(bithiophene) grown from a 0.1 M solution with TBATFB as electrolyte at +2.2 V.

Information regarding the film quality is initially determined simply from the transfer of the material from the electrode surface to the microscope. Poly(bithiophene) represented a brittle polymer that did not form a strong film and therefore can be seen in several fragments in figure 4.7. The images seen upon higher magnification show a bead structure with the growth of the polymer beads at uniform size. Interestingly generation of the polymer at increased potential displayed in figure 4.9 produced a decrease in the bead size and a less porous morphology with an observed deterioration in the image quality. The potential applied at +2.2 V for poly(bithiophene) exceeds the oxidation limit and introduces overoxidation. Overoxidation is known to disrupt polymer growth alignment and therefore the conductivity of the material. The poor image quality is the result of overoxidation as it is the conducting nature of the polymers that produces good useful images without the requirement of sputter coating. With simple ring substituents the film characteristics can change significantly seen with poly(3-methylthiophene) below.

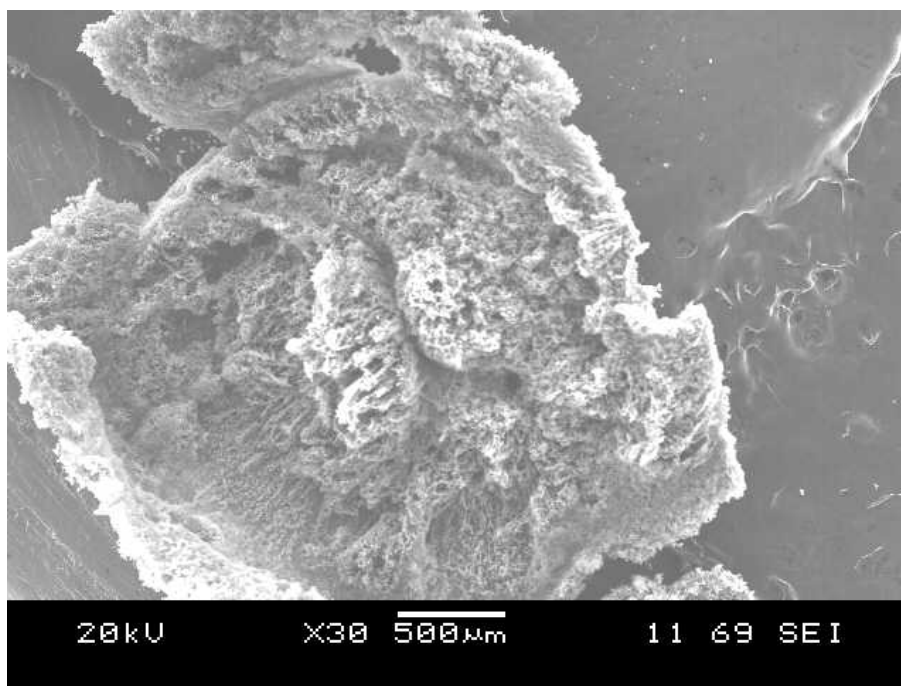


Figure 4.10. Poly(3-methylthiophene) grown from a 0.1 M solution with TBATFB at +1.7 V.

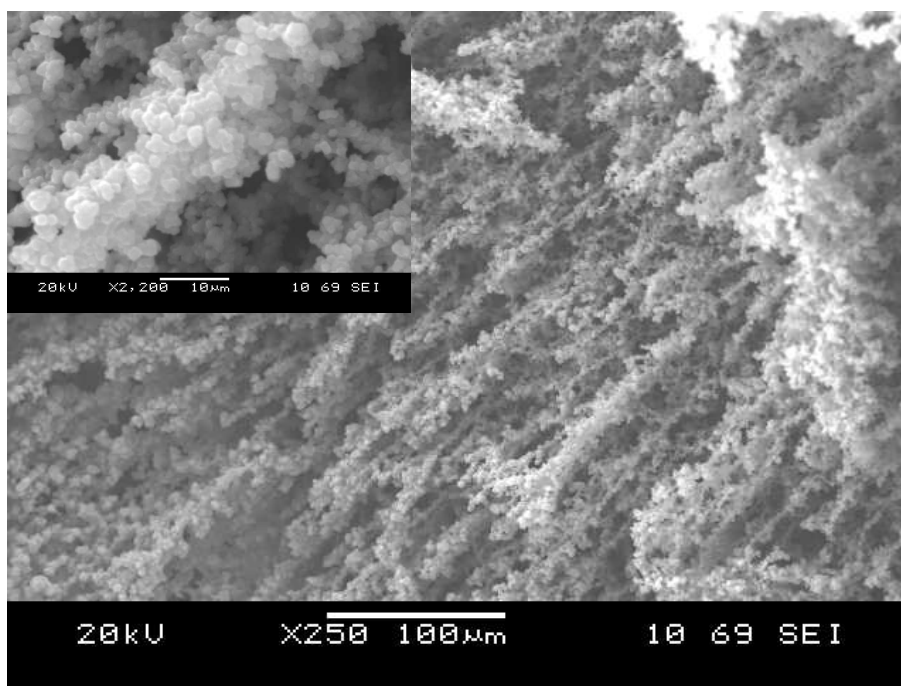


Figure 4.11. Poly(3-methylthiophene) grown from a 0.1 M solution with TBATFB at +1.7 V.

Poly(3-methylthiophene) demonstrates very different film quality compared to poly(bithiophene) with the successful removal of the complete polymer film from the electrode surface seen in figure 4.10. The film was stronger suggesting uniform growth with a defined growth pattern observed through higher magnification in figure 4.11. The material displays a polymer bead arrangement with densely populated 3-dimensional rope-like formations extending outward from the polymer base. The difference in film morphology is clearly influenced by the nature of the side group, in this case the methyl substituent imparted advantageous qualities to the polymer producing a stronger intact film with potentially greater surface area that would be desirable within a biosensor format.

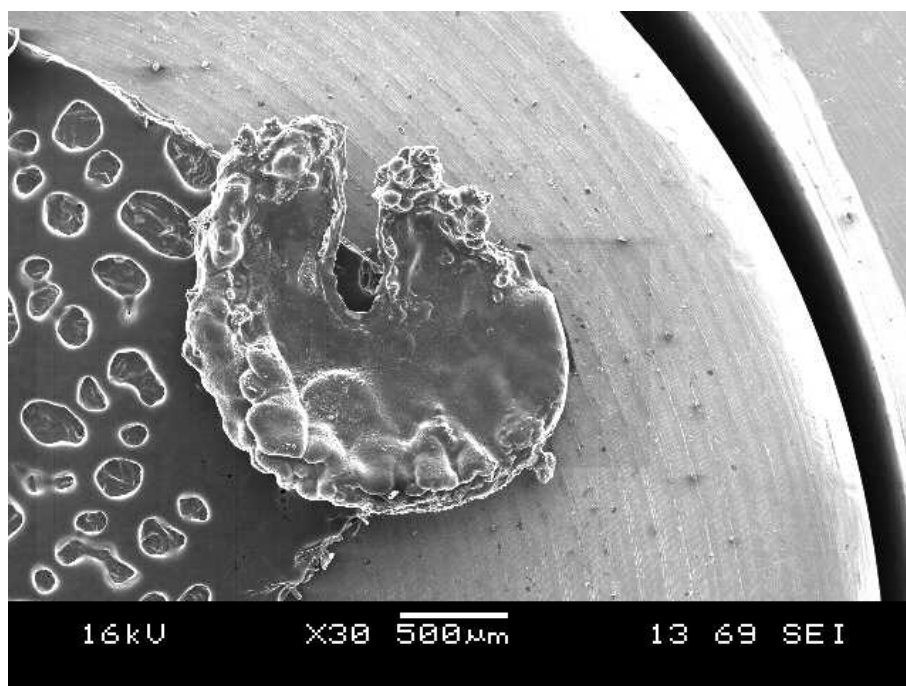


Figure 4.12. Poly(3-dodecylthiophene) grown from a 0.1 M solution with TBATFB at +2.0 V.

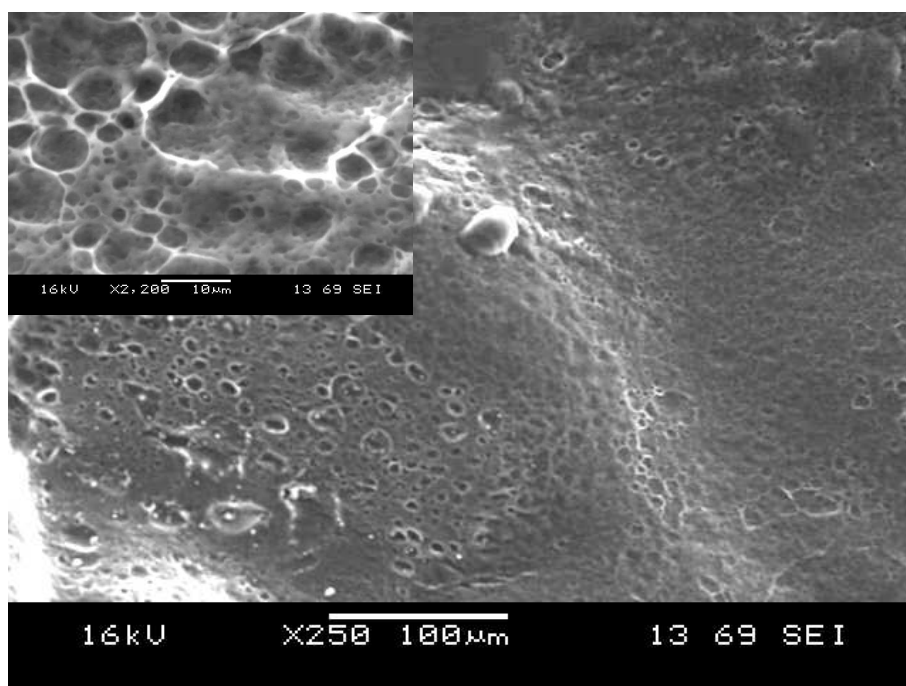


Figure 4.13. Poly(3-dodecylthiophene) grown from a 0.1 M solution with TBATFB at +2.0 V.

Poly(3-dodecylthiophene) is a thiophene monomer that has a 12 carbon chain substituent. By extending the alkyl chain associated with the thiophene ring the film strength was further increased which can be seen in figure 4.12 due to the ease of removal and its durability through the sample preparation. The significant changes to the film topography is clear, a compact 2-dimensional film is produced without the typical bead-like composition seen with the poly(bithiophene) and poly(3-methylthiophene) materials. Closer inspection revealed a smooth surface arranged in a mesh network displaying considerable porosity, again this would provide good properties for an immobilisation matrix however oxidation of the polymer becomes increasingly difficult with +1.3 V needed to oxidise the film determined in chapter 3 section 3.1.3.

Introducing bulky side groups again alters the film morphologies seen. Poly(thiophene-3-acetic acid) was grown using a concentration of 0.6 M the high concentration employed was necessary for initiating film growth as lower concentrations did not produce a polymer film which was investigated in Chapter 3 section 3.2.4.

Poly(thiophene-3-acetic acid) is particularly important as it provides the necessary functionality required for peptide linkage, and therefore a durable film is desirable.

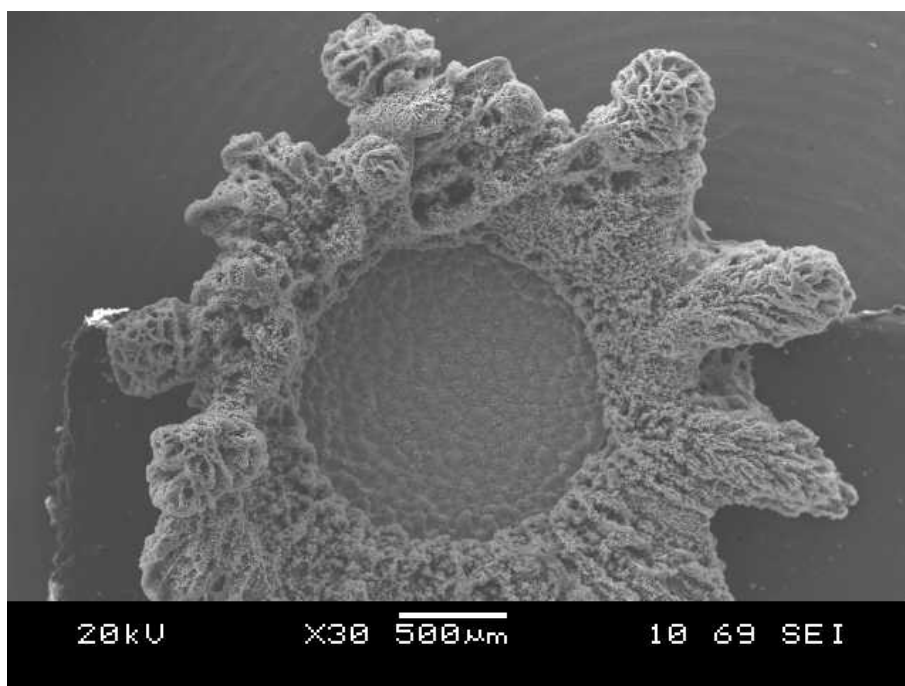


Figure 4.14. Poly(thiophene-3-acetic acid) grown from a 0.6 M solution with TBATFB at +2.2 V.

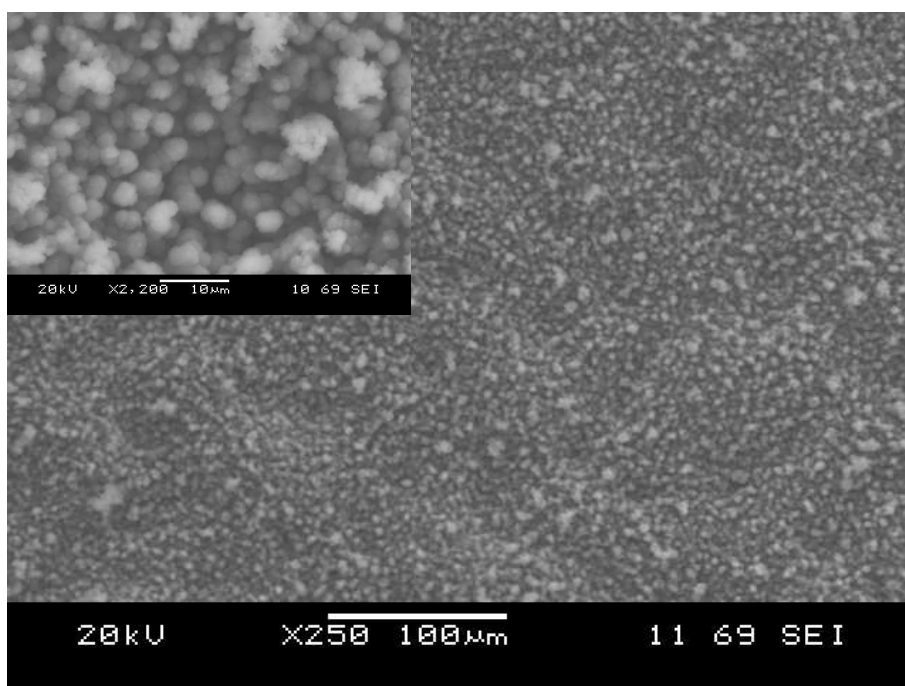


Figure 4.15. Poly(thiophene-3-acetic acid) grown from a 0.6 M solution with TBATFB at +2.2 V.

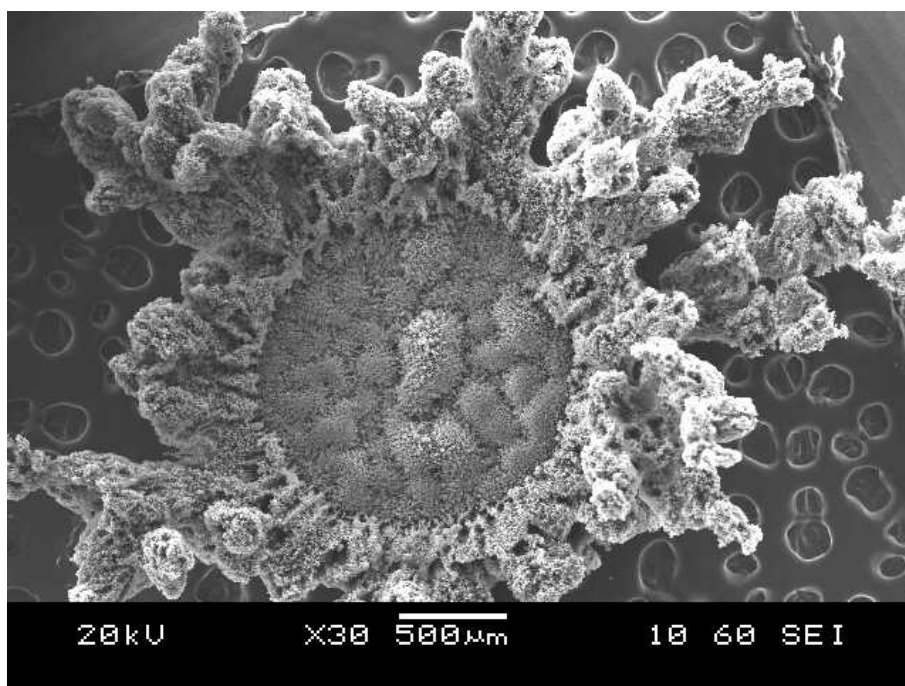


Figure 4.16. 0.4 M thiophene-3-acetic acid and 0.2 M 3-methylthiophene grown with 0.1 M TBATFB at +2.2 V.

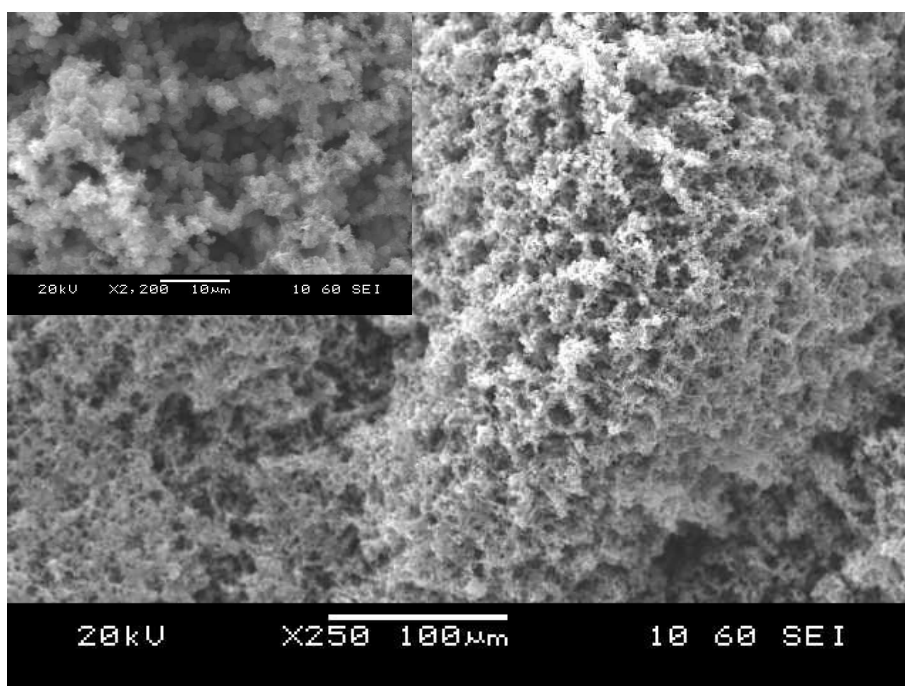


Figure 4.17. 0.4 M thiophene-3-acetic acid and 0.2 M 3-methylthiophene grown with 0.1 M TBATFB at +2.2 V.

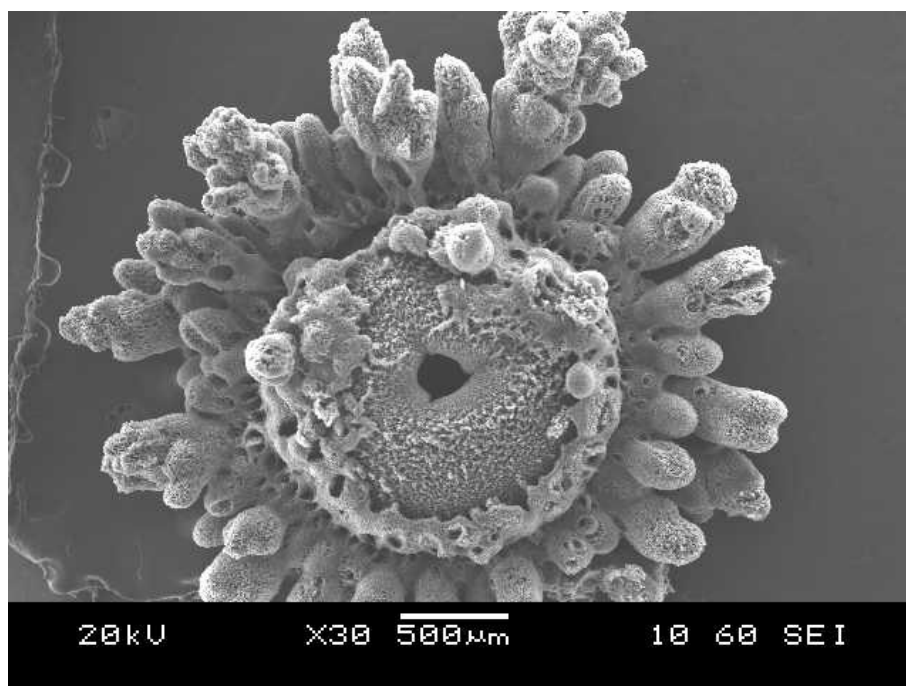


Figure 4.18. 0.3 M thiophene-3-acetic acid and 0.3 M 3-methylthiophene grown with 0.1 M TBATFB at +2.2 V.

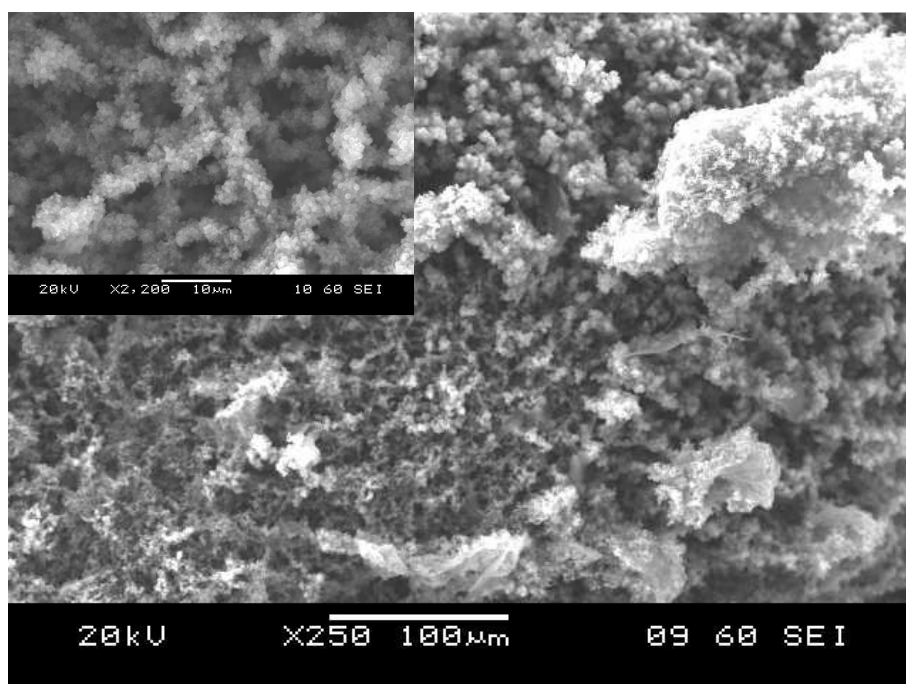


Figure 4.19. 0.3 M thiophene-3-acetic acid and 0.3 M 3-methylthiophene grown with 0.1 M TBATFB at +2.2 V.

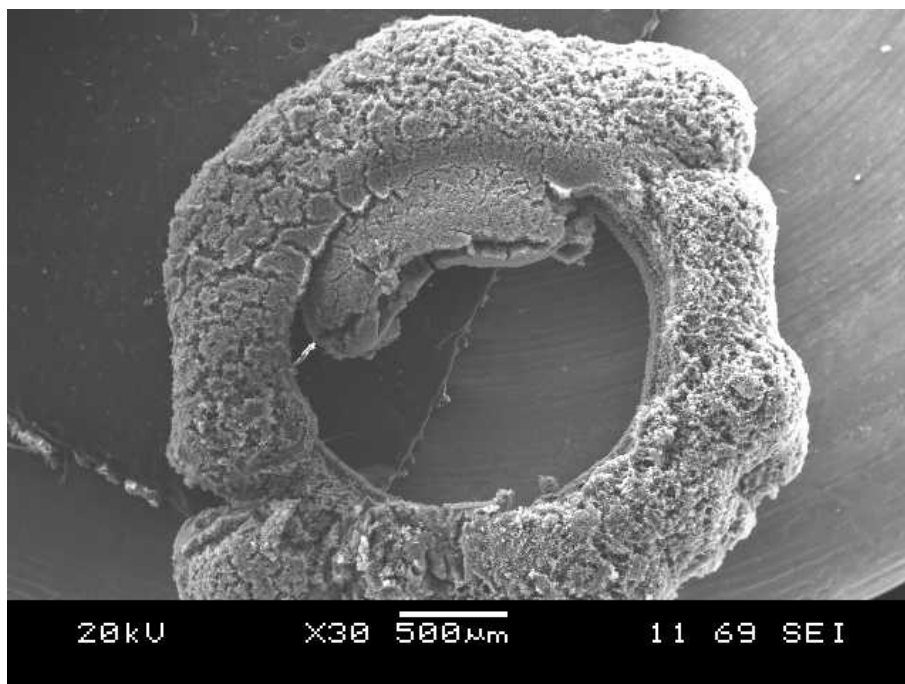


Figure 4.20. 0.05 M thiophene-3-acetic acid and 0.55 M 3-methylthiophene grown with 0.1 M TBATFB at +2.2 V.

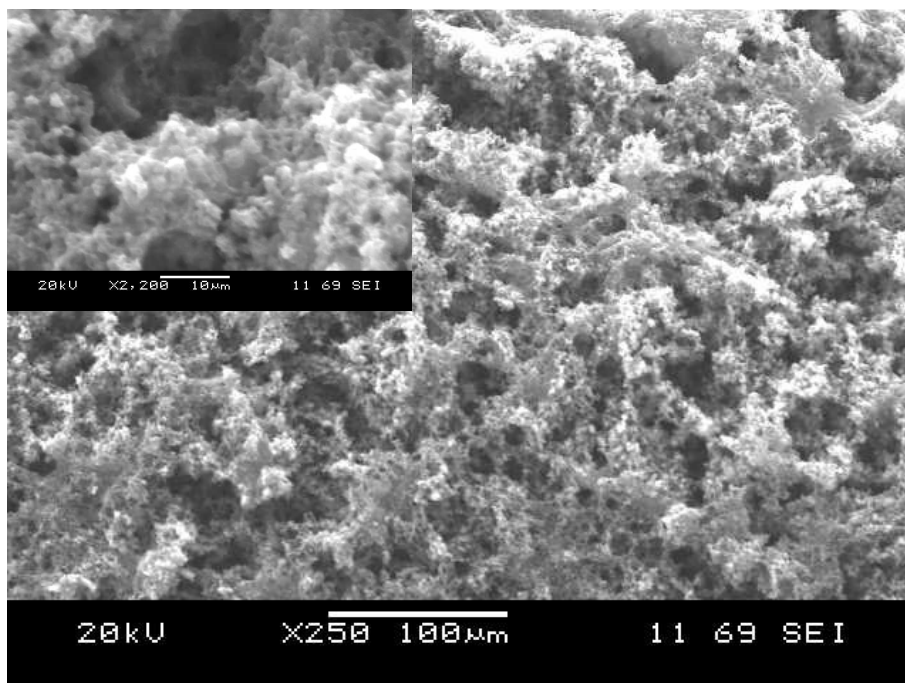


Figure 4.21. 0.05 M thiophene-3-acetic acid and 0.55 M 3-methylthiophene grown with 0.1 M TBATFB at +2.2 V.

Poly(thiophene-3-acetic acid) produces a very interesting growth pattern seen in figure 4.14. Combinations of 2-dimensional and 3-dimensional growth formations are

observed producing what resembles a flower pattern. Such growth has been studied in metal deposition¹⁸⁷ where both mechanisms have been observed¹⁸⁸ and the deposition pattern controlled through electrolyte concentration and voltage obtaining either dendritic or fractal formations¹⁸⁹. Similar studies have been extended to conducting polymers following their discovery with mixed results. Different thiophene compounds^{188,190} including the investigated poly(thiophene-3-acetic acid) have been examined and deposition in a two-dimensional layer-by-layer process has been evidenced in contrast to the 3-dimensional models of nucleation and growth reported in earlier research. Both models have been reported and therefore support the 2-dimensional and 3-dimensional growth seen in the micrograph. The clear patterns that can be seen in figure 4.14 are characterised by the open, random and chain like structures that seem to have no natural length scale and can be well described as fractals¹⁹¹. Examination of the 2-dimensional arrangement that has adhered to the electrode surface at X250 magnification represents a very compact grain structure homogenous in nature and upon higher magnification a close packed polymer bead formation is evident. Interestingly when the copolymer ratio is altered a clear change in the morphology can be observed. Even at low magnification a visible difference in the films can be seen where the polymer attached directly on the electrode surface demonstrates the generation of larger colonies of polymer material in figure 4.16 until it becomes securely fixed on the electrode and cannot be removed in its entirety (figures 4.18 and 4.20). Additionally the fractal growth changes displaying more layers with rounded ends until no fractal growth is present with lower thiophene-3-acetic acid concentration seen in figure 4.20. The higher magnifications at X250 demonstrate a more porous morphology as less thiophene-3-acetic acid is incorporated into the film this can be observed more clearly at X2000 magnification displayed as the smaller images.

The lower concentrations of thiophene-3-acetic acid and higher concentrations of 3-methylthiophene used to produce the copolymer increased the adherence of the film to the electrode surface. Upon equal ratios of monomer in the polymerisation solution the material generated was more strongly attached to the electrode surface as extraction was more difficult and some polymer broke away. When only 0.05 M of thiophene-3-acetic acid was present most of the polymer remained on the electrode leaving only the outer ring. Similar results have been reported by Minett *et al*¹¹⁹.

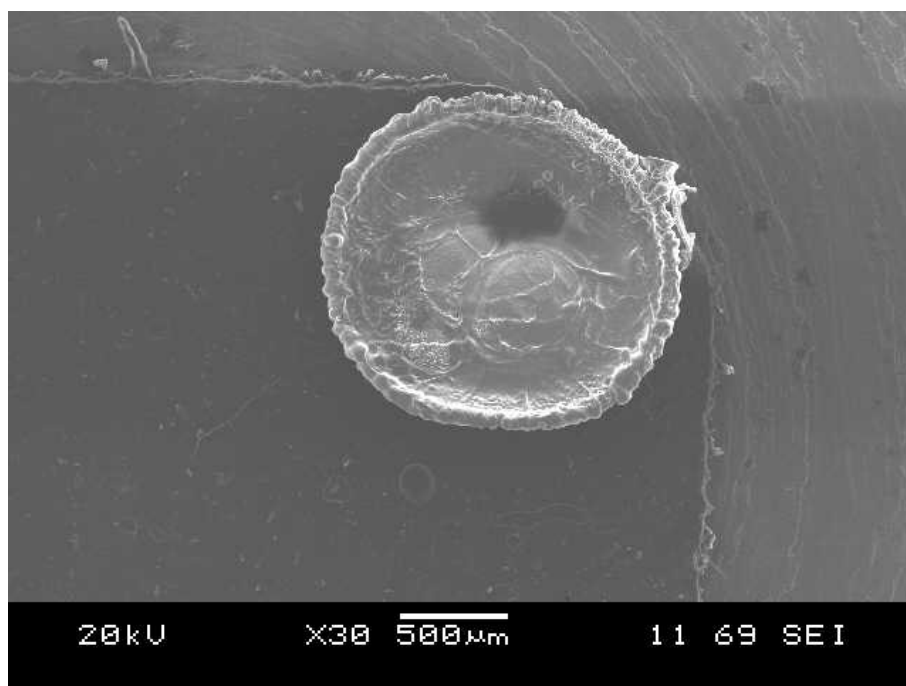


Figure 4.22. Poly(N-succinimido thiophene-3-acetate) grown from a 0.2 M solution with TBATFB at +2.2 V.

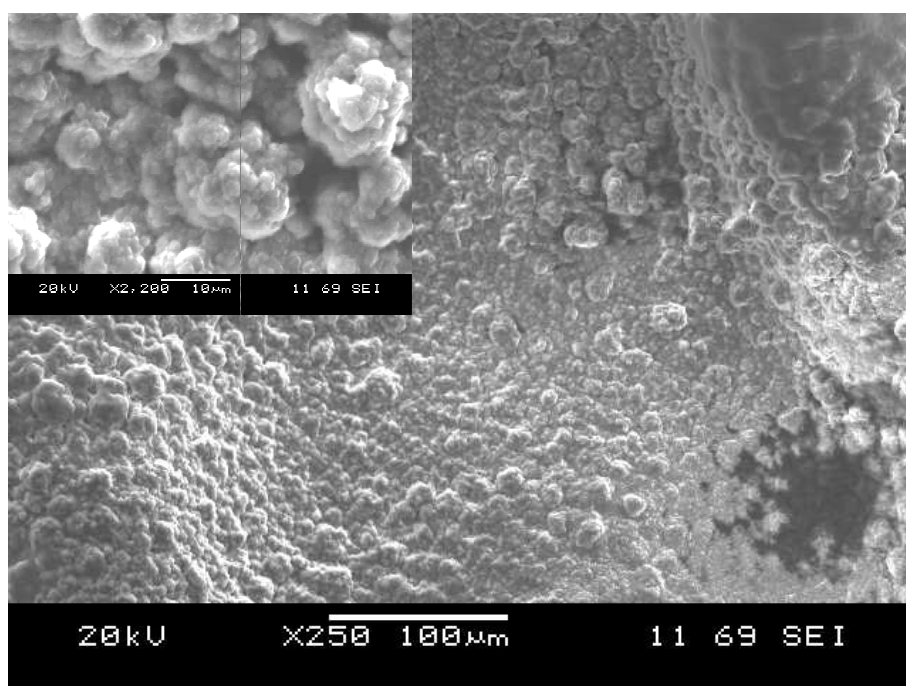


Figure 4.23. Poly(N-succinimido thiophene-3-acetate) grown from a 0.2 M solution with TBATFB at +2.2 V.

The micrographs of the novel poly(N-succinimido thiophene-3-acetate) display a very different morphology in comparison to the poly(thiophene-3-acetic acid) material. By extending the spacial requirement of the side group through esterification a highly compact film is developed forming the material only upon the electrode surface. The film is two-dimensional with no evidence of fractal growth surrounding the material although an outer frame is defined by a procession of bulbous formations. Film properties are enhanced indicating improved durability with a degree of flexibility and therefore the film remained intact through its characterisation. Closer observations at X250 magnification show large beaded clusters in contrast to the grain arrangement of the poly(thiophene-3-acetic acid) and further magnification demonstrates the solid structure as cauliflower compositions demonstrating multiple, large and more complex constructions.

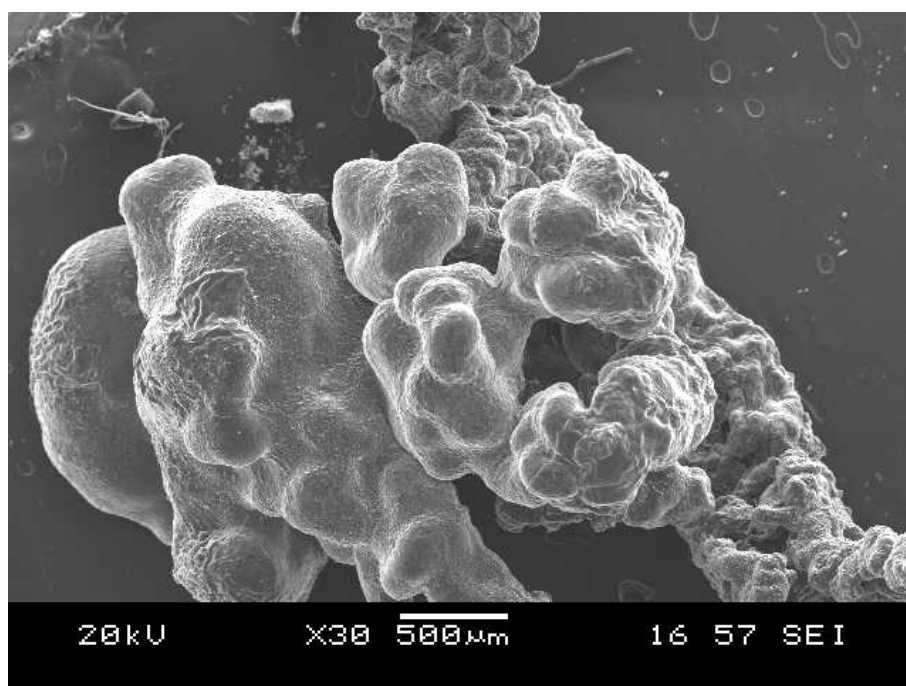


Figure 4.24. Poly(N-succinimido thiophene-3-acetate) grown from a 2.0 M solution with TBATFB at +2.2 V.

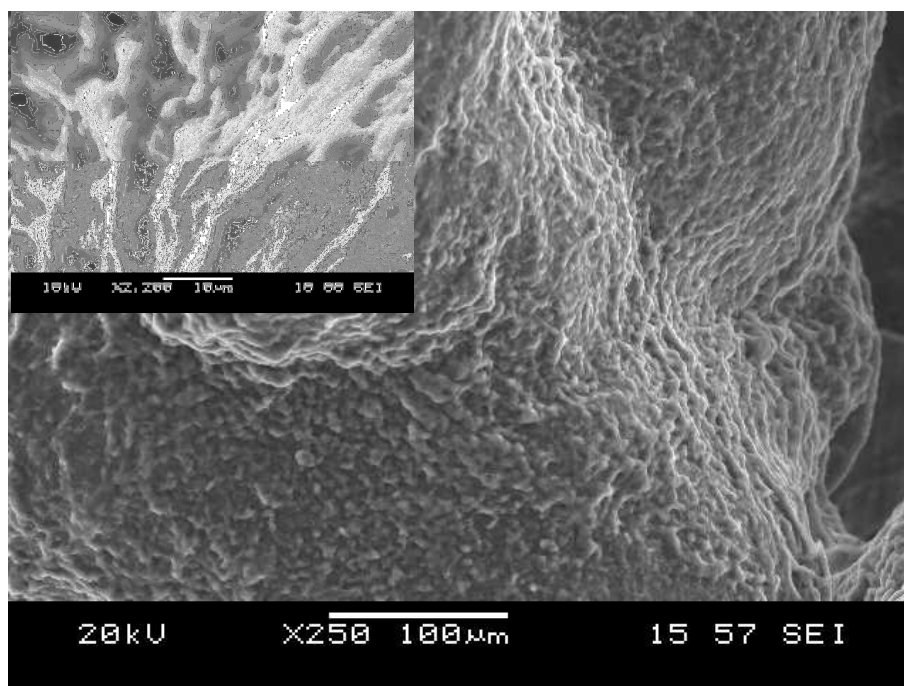


Figure 4.25. Poly(N-succinimido thiophene-3-acetate) grown from a 2.0 M solution with TBATFB at +2.2 V.

Polymer growth from a high concentration of N-succinimido thiophene-3-acetate generates a three-dimensional mass of material with developed bulbous regions that seem to decrease in size through the polymer. A flat polymer film does not form and therefore the resulting material would be difficult to assemble as an immobilisation platform. Increasing the magnification reveals a dense rope formation resembling a very different structure to the cauliflower clusters seen at lower monomer concentration.

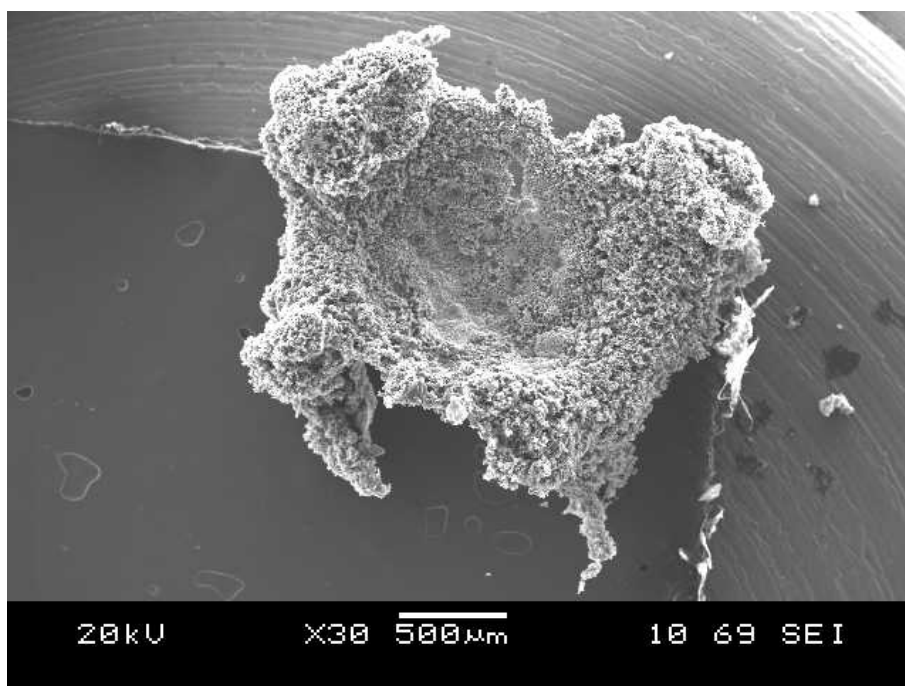


Figure 4.26. 0.24 M N-succinimido thiophene-3-acetate and 0.06 M 3-methylthiophene copolymer grown with TBATFB at +2.2 V.

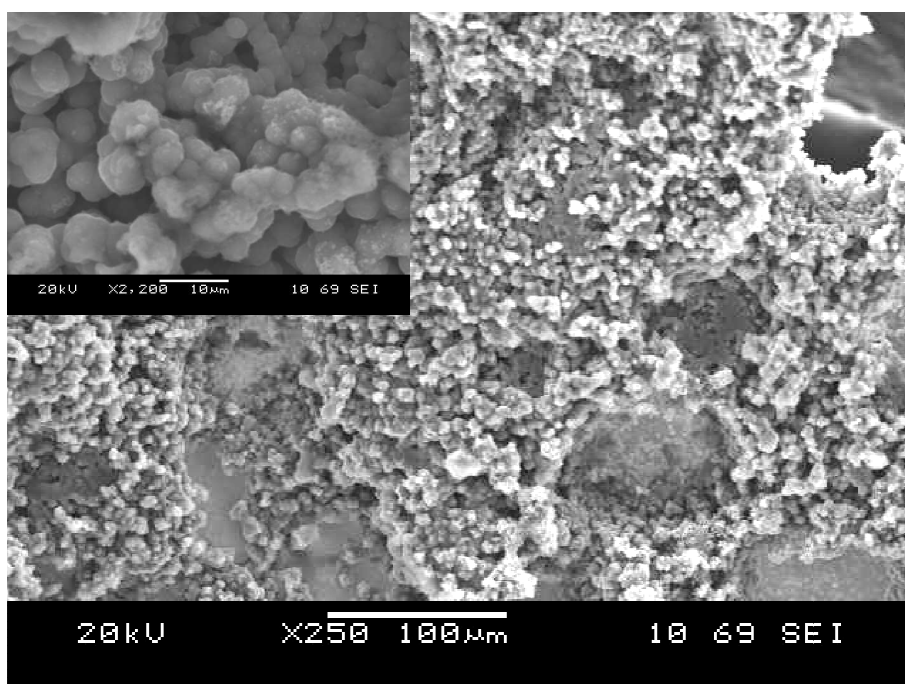


Figure 4.27. 0.24 M N-succinimido thiophene-3-acetate and 0.06 M 3-methylthiophene copolymer grown with TBATFB at +2.2 V.

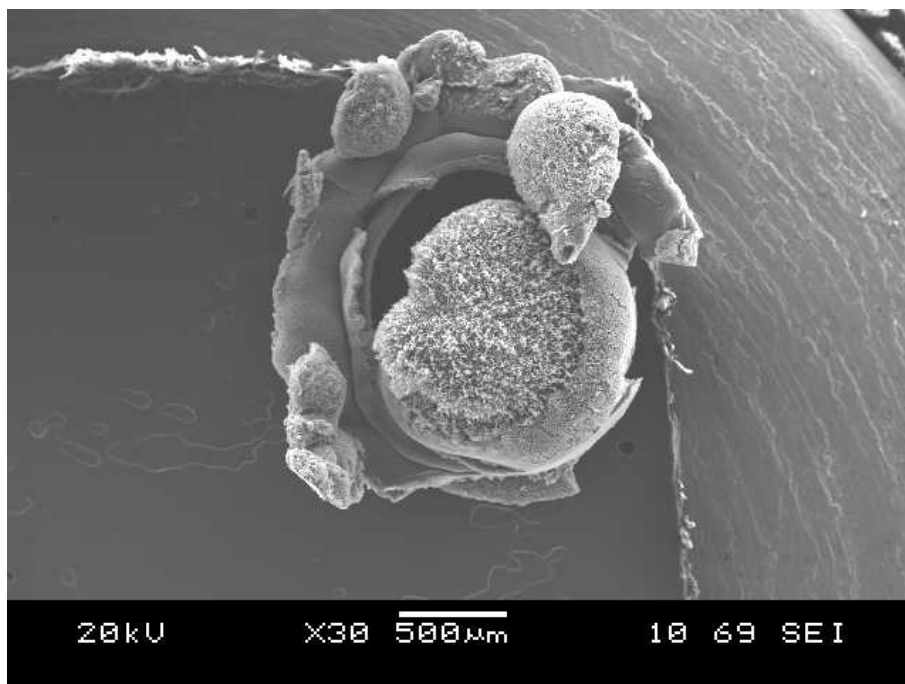


Figure 4.28. 0.06 M N-succinimido thiophene-3-acetate and 0.24 M 3-methylthiophene copolymer grown with TBATFB at +2.2 V.

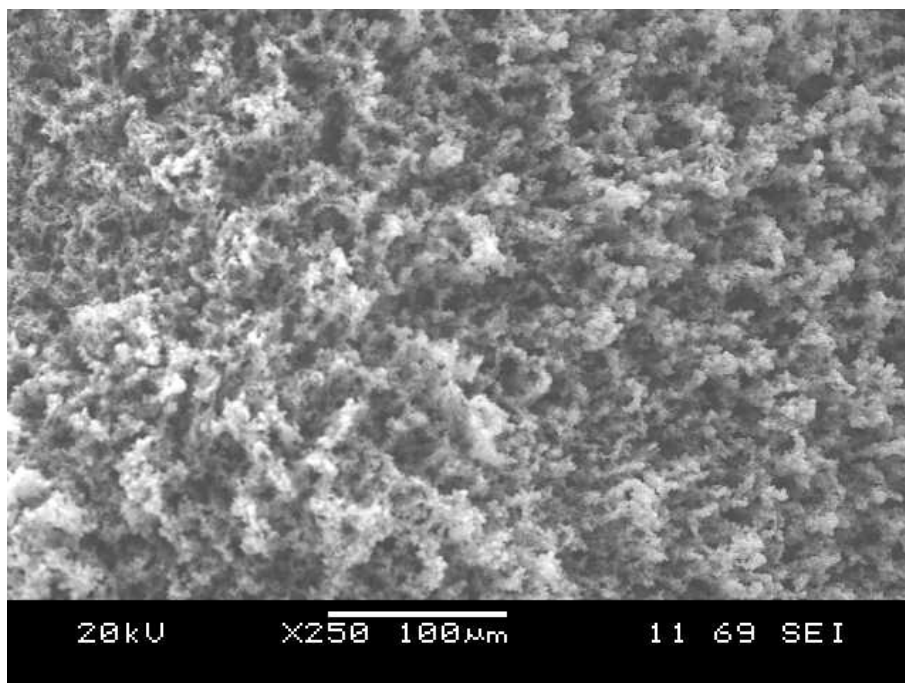


Figure 4.29. 0.06 M N-succinimido thiophene-3-acetate and 0.24 M 3-methylthiophene copolymer grown with TBATFB at +2.2 V.

The copolymerisation of N-succinimido thiophene-3-acetate and 3-methylthiophene could be visually identified by the SEM technique. By introducing a small amount of 3-methylthiophene the flat film grown through the polymerisation of N-succinimido thiophene-3-acetate in figure 4.22 resembled a more three-dimensional structure and was brittle. These qualities were directly imparted through the incorporation of the 3-methylthiophene with morphological characteristics representing both polymers. This can be seen in the higher magnification micrographs with a combination of smaller cauliflower clusters embedded in a more porous bead-like matrix. As more 3-methylthiophene was introduced the sterically hindered N-succinimido thiophene-3-acetate became more diluted and the material grown was less brittle and more compact with a fibrillar structure.

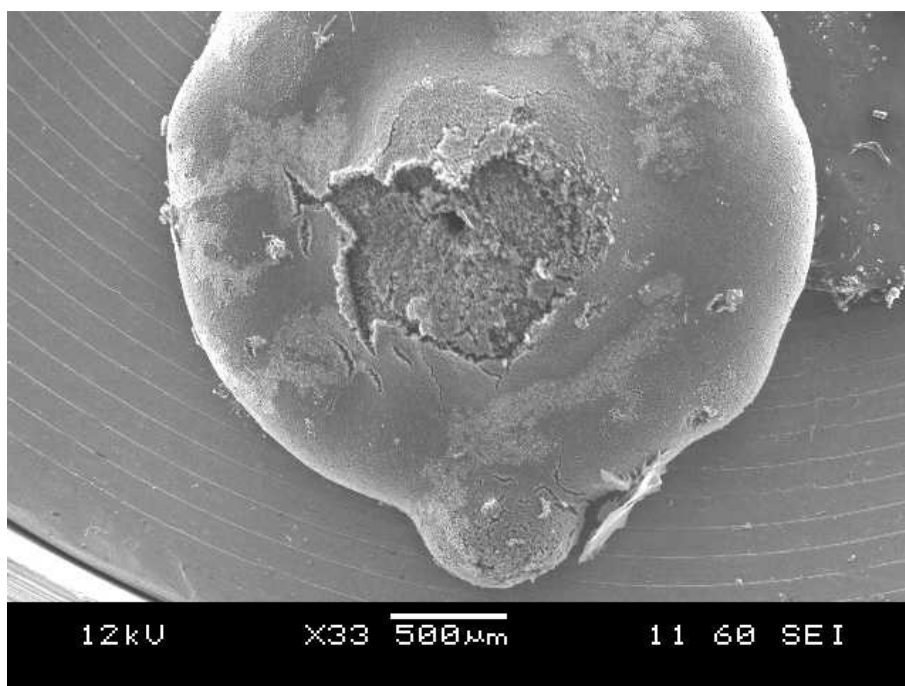


Figure 4.30. 0.06 M N-succinimido trans-3-(3-thienyl) acetate and 0.24 M 3-methylthiophene grown with TBATFB at +2.2 V.

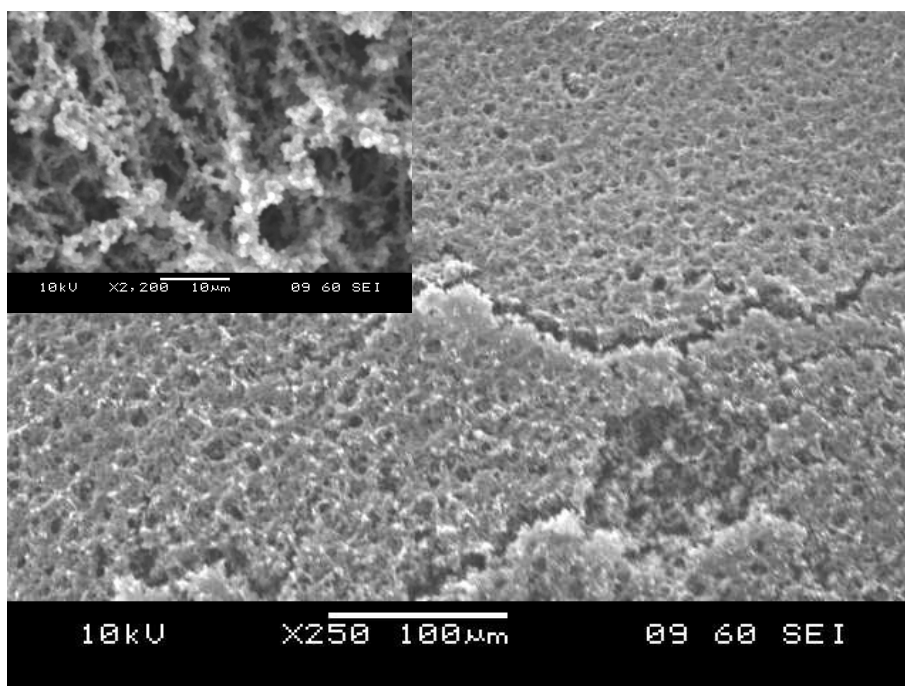


Figure 4.31. 0.06 M N-succinimido trans-3-(3-thienyl) acetate and 0.24 M 3-methylthiophene grown with TBATFB at +2.2 V.

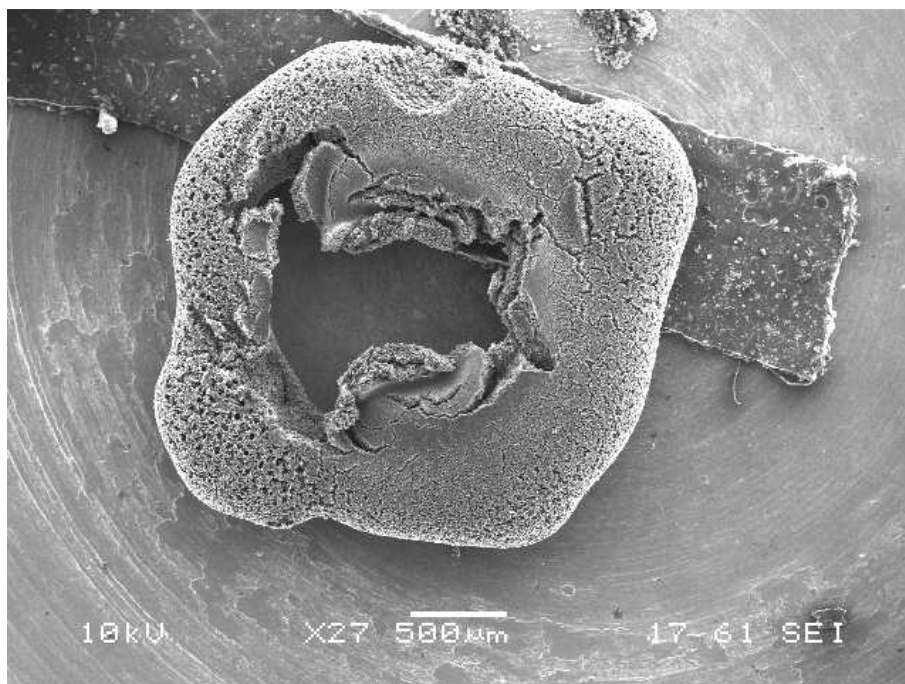


Figure 4.32. 0.05 M trans-3-(3-thienyl) acrylic acid and 0.55 M 3-methylthiophene grown with TBATFB at +2.2 V.

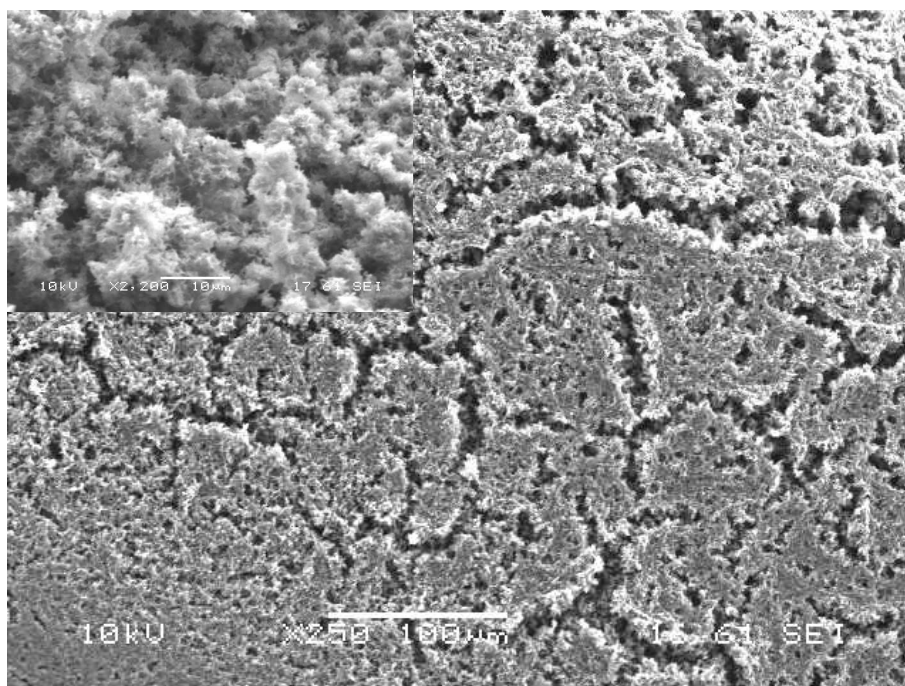


Figure 4.33. 0.05 M trans-3-(3-thienyl) acrylic acid and 0.55 M 3-methylthiophene grown with TBATFB at +2.2 V.

Copolymer films of trans-3-(3-thienyl) acrylic acid and N-succinimido trans-3-(3-thienyl) acetate with 3-methylthiophene were grown with a 10% functional monomer

content. Both demonstrated compact films at low magnification however higher magnification showed more detail. STTA-MT resembled a porous morphology at X2000 magnification displaying linear polymer clusters like a string of beads. TTA-MT demonstrated dense polymer morphology for the outer ring formation. Interestingly the polymer located at the electrode surface became detached from the rest of the material indicating a strong adherence to the platinum surface.

In conclusion all polymers grown from mixed monomer solutions demonstrated successful copolymerisation. Excellent examples can be seen from the electromicrographs displayed particularly for the T3AA-MT and STA-MT materials.

The introduction of increasingly smaller concentrations of T3AA led to a more porous film that was well adhered to the electrode surface and STA-MT changed the highly compact and rigid film of STA into a thicker film displaying some 3D character which was less dense. STTA-MT and TTA-MT materials also revealed different morphology to the poly(3-methylthiophene) displaying more compact and solidly formed structures.

SEM is a very powerful and useful tool that has contributed significantly to the characterisation of conducting polymer films. Morphological changes can be seen through the manipulation of the polymer backbone by introducing sterically impeding and inductive substituents producing a range of film qualities. Brittle intractable polymer materials to durable and flexible films can be obtained with micrographs demonstrating the associated structural changes. Copolymerisation is evident as homopolymer materials are combined to demonstrate the characteristics of two morphologies in one polymer material. The visual representation of the materials generates useful information for their use as immobilisation platforms. Uniform polymer growth, thickness and porosity have direct effects upon sensor behaviour and contribute to its operation influencing diffusion rates and response times. Therefore by using SEM for characterisation the morphology can be tailored through side group incorporation or copolymerisation allowing different properties to be generated.

SEM-EDX also allowed the functional monomer content to be calculated for the full range of copolymer materials. The instrument was quick, simple and non destructive

proving to be the most effective technique available therefore avoiding long preparation and high source of error with atomic absorption and limited data through FTIR. Importantly copolymerisation was determined and a wide range of copolymer ratios were established for further analysis within a biosensor format investigated within chapter 5.

Chapter 5 Biosensor Analysis

Within this study polythiophenes have been chosen as the conducting polymer materials to be investigated as the immobilisation matrix for glucose oxidase through covalent attachment. It was envisaged that the conducting nature of the polymer would enable facile signal detection; however, efforts to exploit this property proved problematic, and this was due to the signal being operated at a potential which produced a partially oxidised polymer. Since the exact degree of oxidation was unknown and apparently highly variable, the subsequent attempts to obtain reproducible biosensor data were unsuccessful. This is not uncommon with conducting polymer sensors where in the past options such as over oxidation of the material has been employed to produce consistent material and hence reproducible analytical data¹⁹². In this instance a mediated system was designed which employed a potential value at which the polymer was mostly reduced producing a stable and reliable background signal for subsequent analytical measurements. In this case *p*-benzoquinone was used within all investigations instigating facile electron transport to the electrode surface. A deoxygenated solution was employed aiding mediation through the electroactive compound and therefore limiting reaction to oxygen.

The novel copolymer materials studied for their biosensor properties in this chapter were all grown to include approximately 10% functional content for potential enzyme attachment. The copolymers studied were trans-3-(3-thienyl) acrylic acid and 3-methylthiophene (TTA-MT), N-succinimido thiophene-3-acetate and 3-methylthiophene, (STA-MT) and N-succinimido trans-3-(3-thienyl) acetate and 3-methylthiophene (STTA-MT). As data comparison is important when assessing new models included within this chapter is the study of previous work reported by Kuwahara *et al.* A polythiophene copolymer platform containing an optimum 10% yield of thiophene-3-acetic acid electropolymerised with 3-methylthiophene was explored for its response to glucose in which the published parameters were followed closely in order to replicate the results generated by Kuwahara *et al.* *p*-Benzoquinone was the mediator employed within Kuwahara's work and therefore it was also chosen as the mediator within this study. The pH used for the investigation of sensor performance was pH 7.0 which is commonly implemented due to the shift in pH optimum observed in immobilised systems^{51,54,113,117}. Kinetic data is displayed for the novel biosensor systems and the replicated thiophene-3-acetic acid and 3-

methylthiophene copolymer generated using Hanes plots. All the results for the copolymer materials are compared and displayed in section 5.1.5 table 5.13.

5.0. Sensor Response in a Non-Mediated Environment

5.0.1. Investigation of The Novel N-succinimido thiophene-3-acetate and 3-Methylthiophene Copolymer

Before the analysis of the prepared biosensor systems was initiated a blank was tested. The blank consisted of electropolymerised 3-methylthiophene with no functional monomers present to enable covalent immobilisation. The amount of charge passed was 100 mC in a 0.1 M monomer solution. The electrode was then exposed to an enzyme buffer solution under stirring for 8 hours after which the electrode was washed with buffer solution and analysed for its response to glucose.

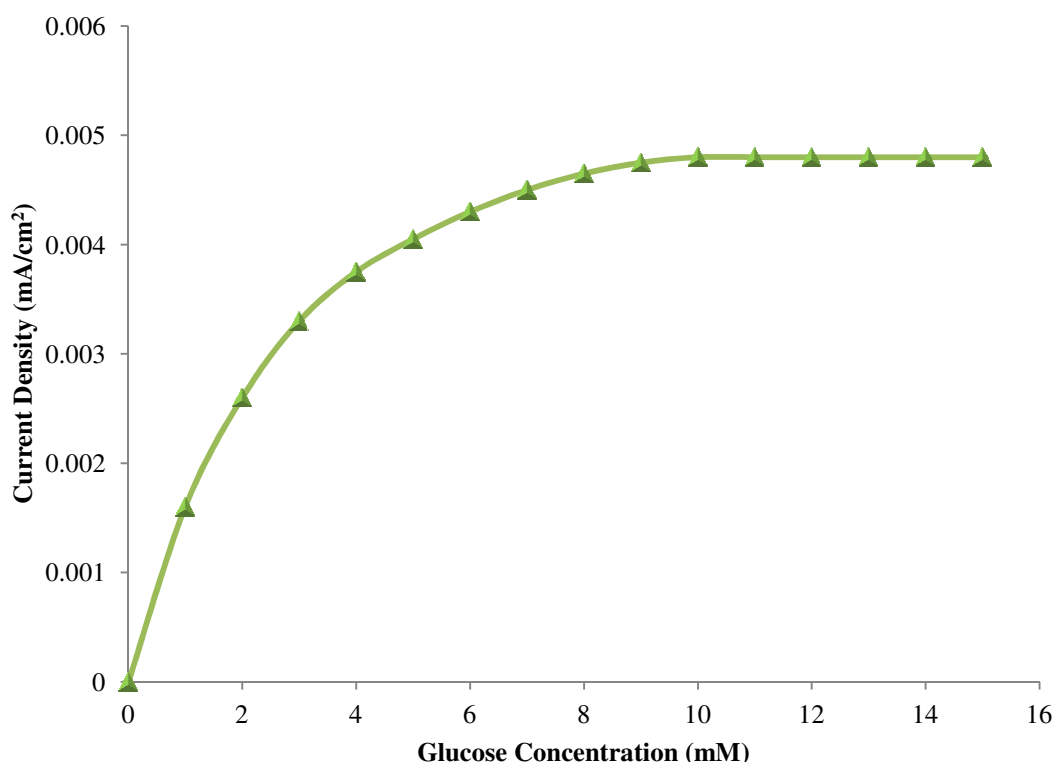


Figure 5.1. Response to glucose for the poly(3-methylthiophene) blank.

The plot resembles Michaelis-Menten behaviour which can be explained by the absorption of free enzyme trapped within the polymer matrix. Covalent immobilisation cannot be implemented within this material due to the absence of functional monomers, and therefore the signal generated in figure 5.1 is likely to originate from absorbed enzyme. This is supported by the low K_m value of 1.99 mM

calculated using Hanes plots and a V_{\max} of 0.00011 mA/cm^2 indicating good enzyme activity with no adverse immobilisation effects influencing the kinetic data. Although a response was detected it was over 100 times lower than the average response of an enzyme electrode generated with covalent binding sites and therefore did not interfere with the analysis of the following biosensor investigations.

5.0.1.1. Reproducibility

The enzyme electrodes were produced with 400 mC of charge at +2.2 V and exposed to enzyme buffer solution for 24 hours. The 10% N-succinimido thiophene-3-acetate content is responsible for the covalent immobilisation of the glucose oxidase within the copolymer and therefore was the assumed method of enzyme incorporation.

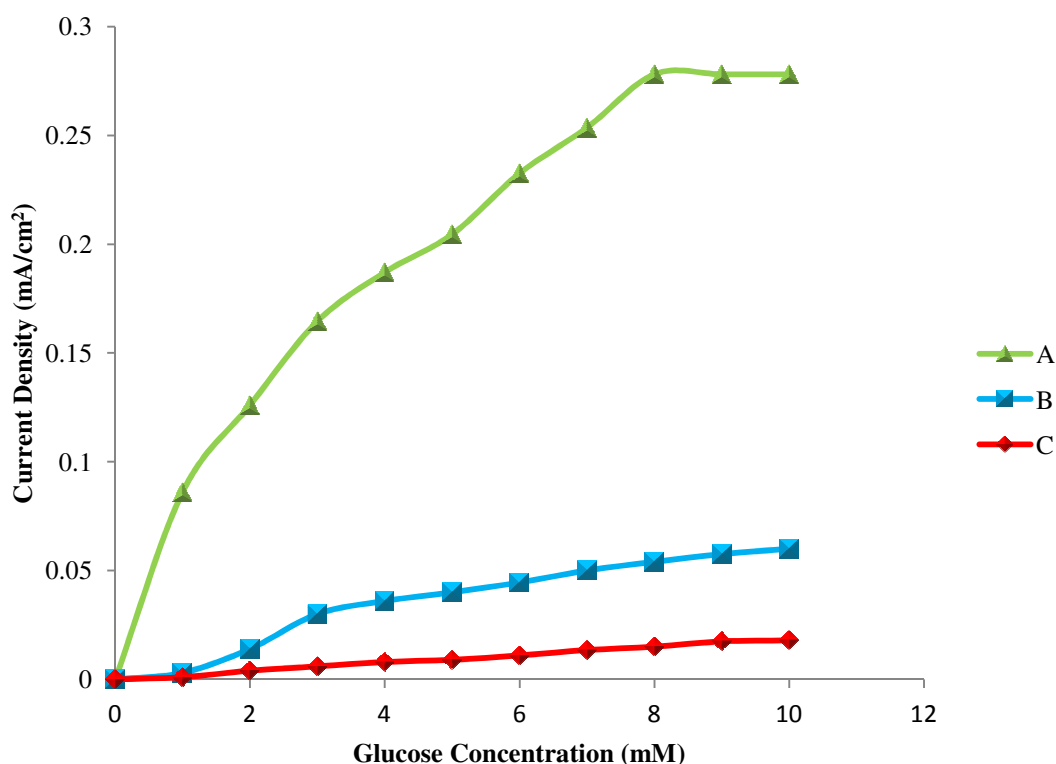


Figure 5.2. Reproducibility of three 400 mC enzyme electrodes.

Reproducibility was extremely low for enzyme electrodes without a mediator as not all enzyme electrodes provided a measureable response. Three enzyme electrodes generated with 400 mC of charge were analysed and a coefficient variation (% RSD) of the responses obtained was calculated at 127%. The large reproducibility error could be explained due to problems associated with substrate diffusion and electron transport difficulties. Furthermore the fabrication process could introduce error as thicker films extending away from the electrode surface are less robust and are more

likely to be damaged through enzyme immobilisation and sensor analysis therefore loss of polymer material may be responsible for the variation in biosensor response observed.

5.0.1.2. Investigation of Length of Enzyme Exposure upon Sensor Response

Copolymer films were generated through passage of 100 mC of charge at a potential of +2.2 V. A range of enzyme immobilisation times were chosen in which they are generally quoted in hours and are found to range considerably. Figure 5.3 displays large current responses at short exposure times with a decreasing response to glucose as the time period for enzyme immobilisation becomes longer.

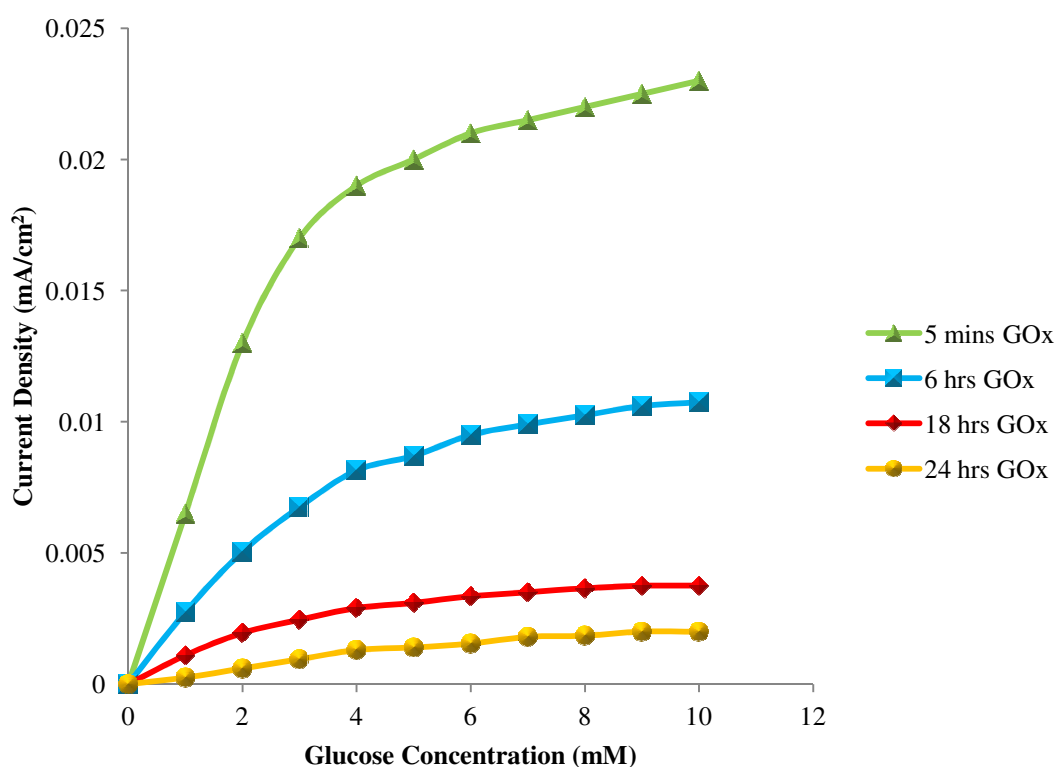


Figure 5.3. Current response generated for varying enzyme exposure times.

The kinetic data for the various enzyme exposure times in figure 5.4 were determined using Hanes plots and can be seen in table 5.1 where V_{\max} and K_m values are presented. V_{\max} represents the maximum reaction rate at a particular enzyme concentration and K_m is the Michaelis constant. The K_m value is an indication of the activity of the enzyme as it defines the substrate concentration required to achieve a given rate. Due to various factors such as immobilisation that can influence the enzyme behaviour the kinetic data is often affected and therefore K_m is termed the apparent K_m .

Figure 5.3 demonstrates the response to glucose mainly over long exposure times (6-24 hours) however a five minute enzyme exposure time was implemented to investigate the response generated. Interestingly after only five minutes current response was very high compared to the 6, 18 and 24 hour investigations.

The kinetic data displayed in table 5.1 for the five minute immobilisation period can be compared to free unbound enzyme as determined for the poly(3-methylthiophene) material and therefore longer immobilisation times were needed to generate covalent bonding. Six hours resulted in a good signal to glucose and represented a slightly higher K_m value implying possible structural changes of the enzyme as covalent attachment took place. The longer exposure times of 18 and 24 hours suggested unfavourable conditions affecting the sensor behaviour due to the reduced current signals. Introducing extended immobilisation times may lead to the incorporation of more enzyme. If there are unoccupied sites more covalent binding will occur but the polymer thickness will increase affecting substrate and product diffusion. Also the enzymes may become anchored at multiple sites, either obstructing access to the substrate binding site or forcing the protein to adapt a less active conformation.

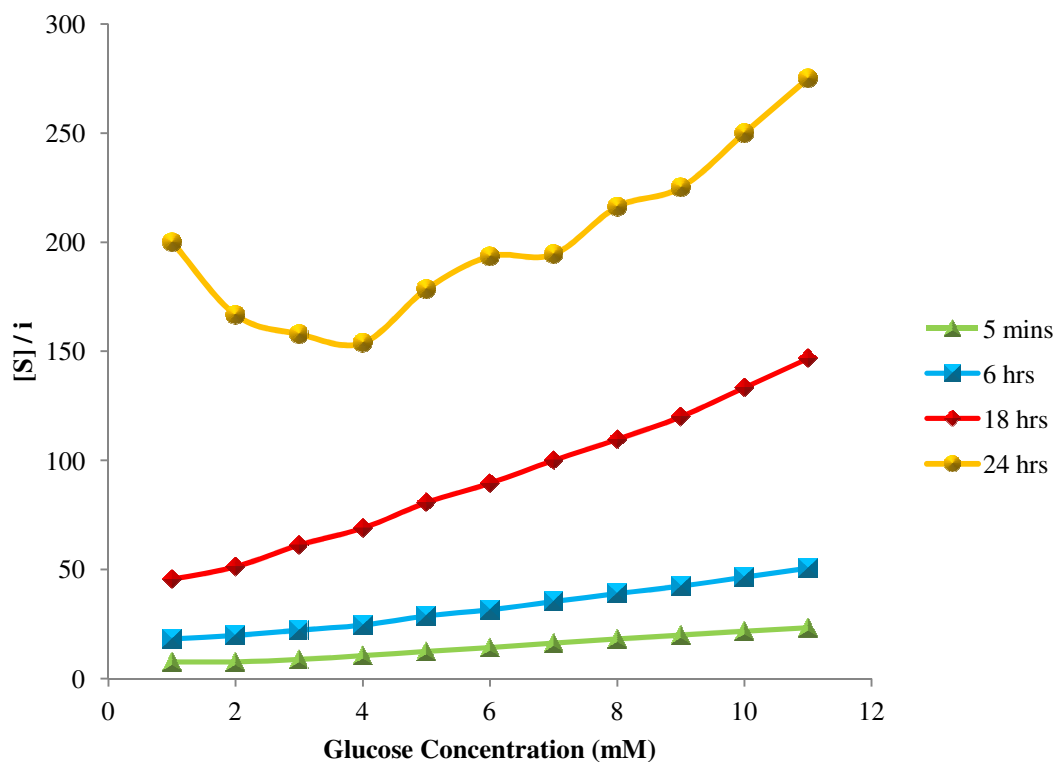


Figure 5.4. Hanes plots for enzyme electrodes with varying enzyme exposure times.

Table 5.1. Kinetic Data for Different Enzyme Immobilisation Times.

Enzyme Exposure Time	V_{\max} (mM/A)	Apparent K_m (mM)
5 minutes	0.0005	1.6
6 hours	0.00025	2.4
18 hours	0.0001	2.4
24 hours	0.00005	4.6

The Hanes plots for solution enzyme kinetics are associated by a straight line, however as immobilisation causes the enzyme kinetics to change a shallow gradient can be observed at the low substrate concentrations referred to as the lag phase. The Hanes plots above in figure 5.4 demonstrate the lag phase which corresponds to the slow transport of glucose into the polymer and are significant at longer enzyme immobilisation times. This provides an indication into the permeability and diffusion limitation of the polymer film as more enzyme is incorporated into the matrix.

5.0.1.3. Examination of the Effects of Copolymer Thickness

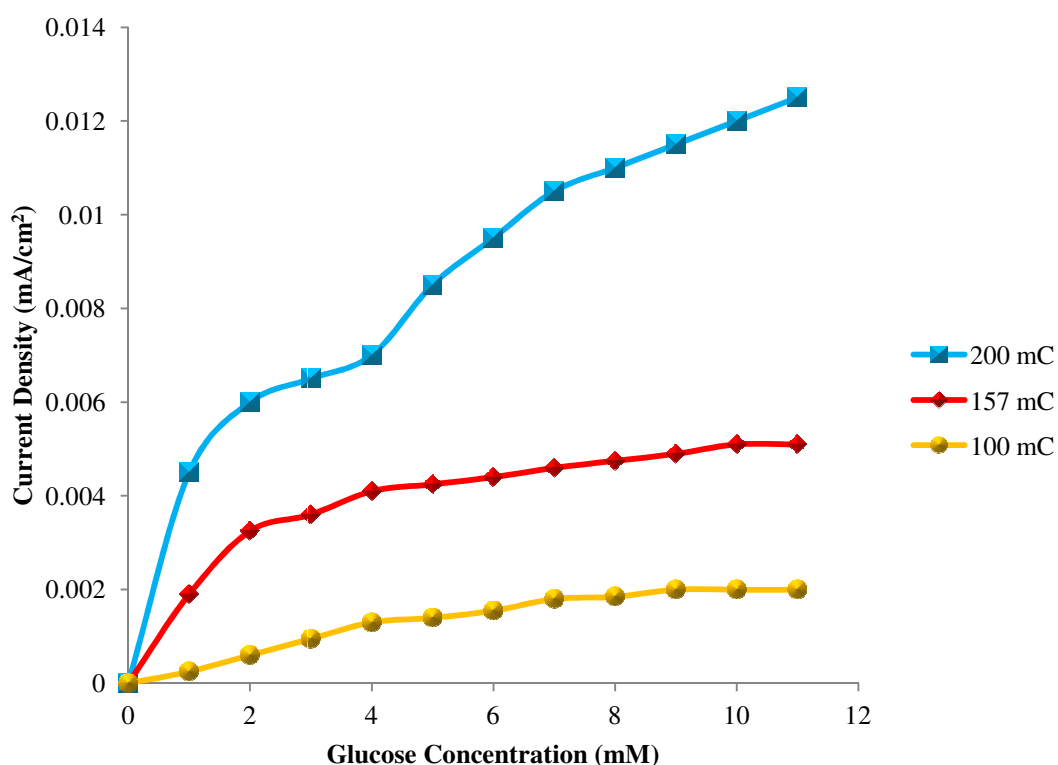


Figure 5.5. Current response generated for 24 hours of enzyme exposure.

As the amount of charge passed for film generation was increased the response to glucose increased. It is difficult to conclude trends seen within the non-mediated systems due to the absence of reproducibility seen in figure 5.2 with a calculated coefficient variation of 127%. However increasing the amount of material produced is likely to increase the copolymer surface area as the film extends away from the electrode surface and produces a very porous, surface rich copolymer matrix. Increased surface exposure is likely to aid more enzyme binding and therefore more possible reaction sites generating a larger current response.

Table 5.2. Kinetic Data for Increasing Polymer Thickness.

Film Thickness (mC)	V_{\max} (mM/A)	Apparent K_m (mM)
100	0.00005	4.6
157	0.000125	2.2
200	0.0005	7.5
400	0.0037	5.3

Although V_{\max} increased in figure 5.5 with the use of more charge for film growth the K_m data demonstrated little change in the sensor behaviour compared to the previous investigation of the length of enzyme exposure at 24 hours. Therefore increasing the amount of polymer film with longer enzyme exposure did not achieve optimum sensor performance and due to low reproducibility, investigations involving thinner films over shorter immobilisation times were not successful.

5.0.1.4. Investigation of the Effects of Analyte Diffusion

Due to the irreproducibility of the glucose sensors highlighted in section 5.0.1.1 figure 5.2, diffusion through the polymer matrix was investigated. Two electrodes were prepared both with electrogenerated polymers encompassing 400 mC of passed charge. One electrode was placed in an enzyme phosphate buffer solution and one in the phosphate buffer without enzyme, both were exposed to the solutions for 24 hours under stirred conditions. Diffusion was therefore monitored through a matrix immobilised with enzyme and without the bound species with equal buffer exposure to eliminate factors due to polymer swelling affecting diffusion properties.

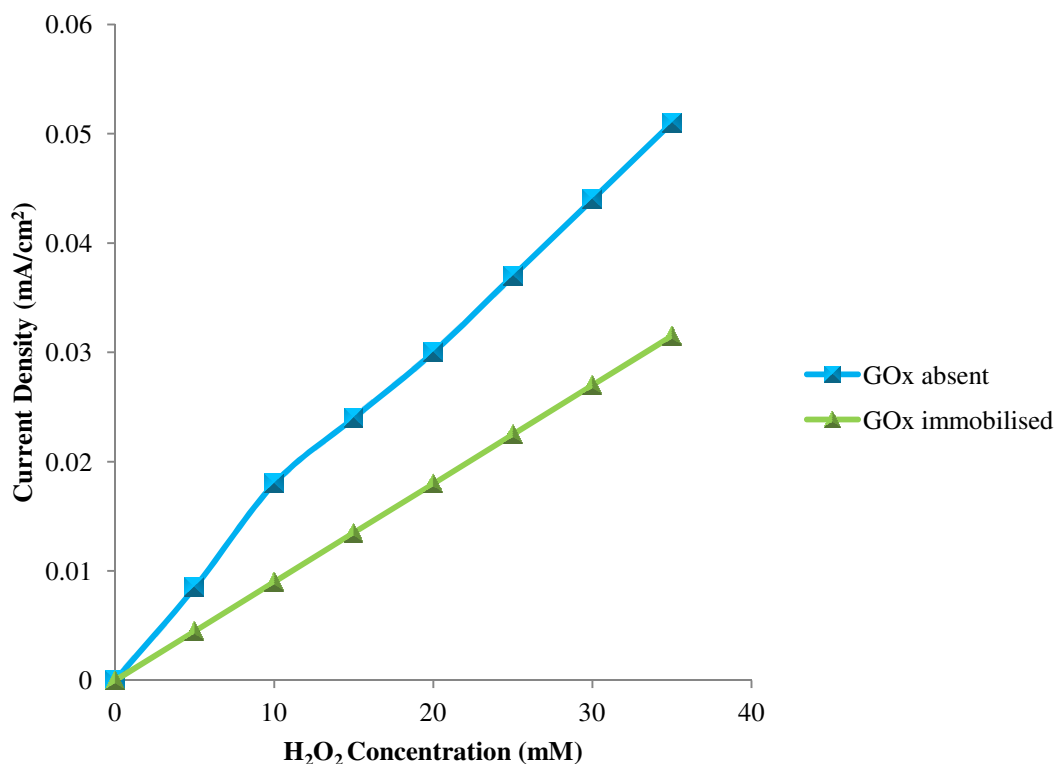


Figure 5.6. Investigating the response to H₂O₂ upon thick copolymer films.

A significant difference was observed between diffusion within a matrix occupied by enzyme species and a matrix free of enzyme. Larger responses were detected where no enzyme was present approaching an increase of 40% indicating a possible obstruction to the diffusion of the hydrogen peroxide when enzyme was present. Although a decreased response was seen the hindered species still achieves access to the electrode surface albeit at reduced concentration therefore explaining the low current signals observed under non mediated systems and also the irreproducibility associated with the sensor performance.

5.1. Sensor Response in a Mediated Environment

5.1.1. Investigation of The Novel N-Succinimido thiophene-3-acetate and 3-Methylthiophene Copolymer

The mediator *p*-benzoquinone was chosen in the following experiments due to its incorporation in the work of Kuwahara *et al.* The parameters published in this work were followed closely in order to compare the optimised biosensor electrodes in both studies.

As a mediated environment was employed, nitrogen was used to eliminate the oxygen in the solution. Oxygen acts as a natural mediator generating hydrogen peroxide which becomes oxidised primarily at the electrode surface. Removing the oxygen competition increased the current response to glucose by 16% seen in figure 5.7 for the novel copolymer. Due to the enhanced signals attainable with deoxygenation this method was employed through all *p*-benzoquinone mediated systems.

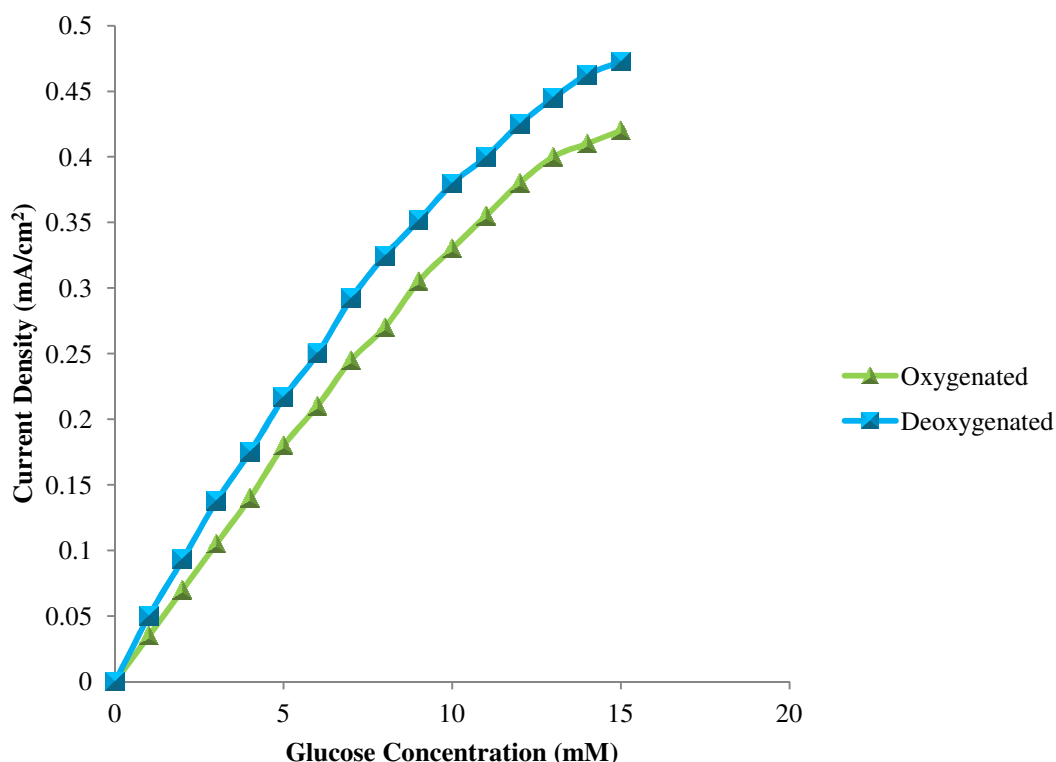


Figure 5.7. Sensor response in oxygenated and deoxygenated systems.

Incorporating a mediator into the system provided a sustained response to glucose throughout the various parameter changes identified for biosensor development. The elimination of oxygen in the system by nitrogen flushing increased the current signals upon glucose addition and was used throughout the study incorporating the mediator. Response to glucose, absent through non-mediated systems, indicated the difficulty associated with diffusion limitation and electron transport through the film.

5.1.1.1. Altering Potential Binding Sites through Copolymerisation

The literature concerning conducting polymers and the optimum content for potential enzyme immobilisation is stated at 10%⁵⁴. The previous non-mediated investigations performed incorporated a 10% content of the functional thiophene monomer based

upon the literature findings. Alteration of the copolymer ratio along with many other biosensor studies could not be performed due to irreproducibility associated with the non-mediated environment. Through a mediated system these investigations were accomplished starting with the investigation of the optimum content of N-succinimido thiophene-3-acetate for sensor response.

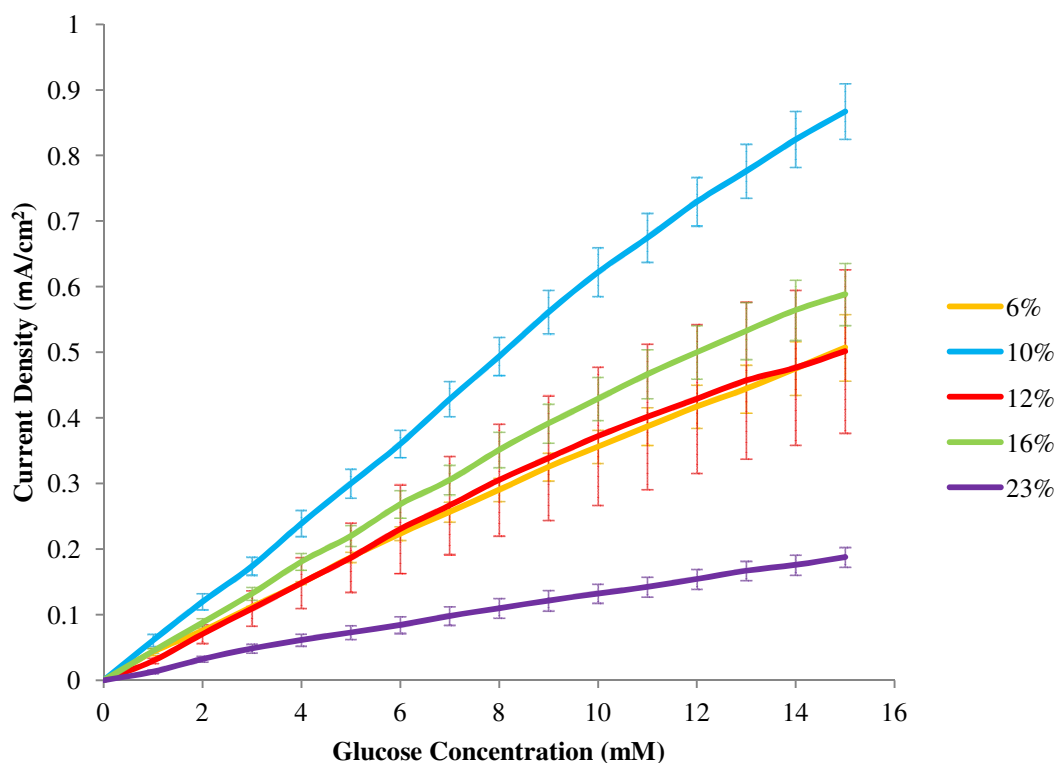


Figure 5.8. STA content in the copolymerisation ratio employing a 50 mC film.

As the novel functional monomer differs in structure compared to the thiophene-3-acetic acid monomer it is important to establish if the same percentage content provides the greatest signal response.

From the results generated it was observed that at 10% N-succinimido thiophene-3-acetate content the current signal to glucose reached a maximum response. The lower ester content of 6% provided decreased current response to glucose with high apparent K_m . Therefore indicating that the lower concentration of activated ester compounds was not sufficient in order to produce improved current response to glucose. The decrease in response to glucose upon the addition of more potential binding sites is explained in the literature through different reasoning. Kuwahara *et al* conclude that the reduction of the amperometric response is a result of decreasing

conductivity within the copolymer film. This implies that the functional groups of the carboxylic acid and the activated ester have a direct effect upon the conductivity of the matrix and that the conducting nature of the immobilisation platform is an important aspect in the biosensor performance. Comparing the biosensor signals in figure 5.8 to the current response generated at +0.4 V obtained upon cyclic voltammetry characterisation in chapter 3 a relationship can be observed.

Table 5.3. Comparison of current generated at 0.4 V to the average current obtained upon biosensor analysis for the copolymers with different ester content.

Copolymer STA Content (%)	Current Response at +0.4 V (μA)	Average Current Obtained for the Biosensor. (mA/cm^2)
6	39.1	0.28
10	54.6	0.48
12	33.7	0.29
16	32.4	0.34
23	12.0	0.11

At +0.4 V the polymer films are mostly in their reduced state; however the pre-peak observed in several of the copolymers occurs at this potential and therefore some oxidation of the film exists. At +0.4 V the current response generated for the copolymer and the biosensor with 10% ester content is the largest with 23% ester content representing the lowest signals for both the copolymer characterisation and the analysis of the biosensor. All remaining compositions produce similar current response at +0.4 V within the film characterisation and the corresponding biosensor system.

The level of oxidation of the copolymer films could in part explain the trend in current response seen due to the potential conductivity imparted to the modified enzyme electrode. However conductivity is not the only parameter that affects the response of the biosensor and therefore the results generated in figure 5.8 require further explanation.

Li *et al* have probed the behaviour of a polyaniline (PANI) conducting polymer platform for glucose oxidase attachment through surface grafted acrylic acid (AAc)⁴⁸. The results generated through the amount of AAc deployed describes a linear increase in enzyme activity with increasing binding sites until a plateau is reached. Li *et al* conclude a number of factors that remain potentially responsible for the cease in activity increase involving diffusion, cofactor accessibility and enzyme conformation which are also likely to be associated with the change in copolymer ratio of the N-succinimido thiophene-3-acetate biosensor system.

Larger K_m values are typically observed with all immobilised enzyme systems due to the reduced substrate accessibility to the reaction site, as the enzyme is no longer free. However the large apparent K_m values with decreasing response to glucose upon greater STA content indicates a more complex effect than accessibility issues and therefore requires a different explanation.

Diffusion limitation of the material could be responsible for the decrease in sensor behaviour indicated by the high apparent K_m and low V_{max} values as more functional monomer is incorporated into the immobilisation platform. Increasing the available binding sites will potentially increase the amount of enzyme immobilised introducing a thicker film with limited substrate and product diffusion¹⁵⁷. In addition enzyme activity can be inhibited through multiple binding likely to be found within greater functional monomer content affecting the enzyme structure and causing damage to the reaction site.

With 23% occupancy of N-succinimido thiophene-3-acetate the response to glucose decreased significantly. This can be attributed to the multiple covalent bonding and overcapacity imparting steric effects, increased polymer thickness and therefore diffusion limitation. Furthermore the low conductivity of the material may provide a contributing factor.

Although diffusion of the substrate was affected, a build up of product in the film was generated; causing constant detection at the electrode surface, resulting in a linear graph at higher glucose concentrations, ideal for a biosensor system¹⁹³⁻¹⁹⁴, observed clearly in figure 5.8.

Table 5.4. Kinetic Data Associated with a Varying Monomer Ratio.

STA Monomer Content (%)	Molar Ratio (M) STA-MT	V_{\max} (mM/A)	Apparent K_m (mM)
6	0.03-0.27	0.08	81
10	0.06-0.24	0.08	56
12	0.12-0.18	0.04	40
16	0.15-0.15	0.05	44
23	0.18-0.12	0.01	44

Further investigations considering response optimisation features the novel copolymer at a 10% content regarding the functional monomer species. This value was chosen as the optimum enzyme binding through the investigation upon the copolymer ratio which supported the maximum response to glucose stated in the literature at around 10%⁵⁴.

5.1.1.2. Effects of Film Thickness and Enzyme Exposure on the Biosensor Response.

There are many parameters that can be altered through the various stages of fabrication and these parameters can impart great influence upon the performance of the sensor. It was therefore decided to first investigate the amount of material deposited and the enzyme exposure period that would generate a practical sensor before determination of repeatability and reproducibility.

A range of film thicknesses were generated potentiostatically using coulometry with a defined potential of +2.2 V employing 16, 50, 100 and 400 mC to the working electrode corresponding to charge densities of 800, 2500, 5000, and 20000 mC/cm². Enzyme exposure times included 2, 6, 9, 18 and 24 hours.

The results displayed below in figures 5.9-5.13 coupled with the tabulated data in table 5.5 indicate an evident relationship between the amount of polymer material employed for the biosensor established through the amount of passed charge and the time period implemented for enzyme immobilisation.

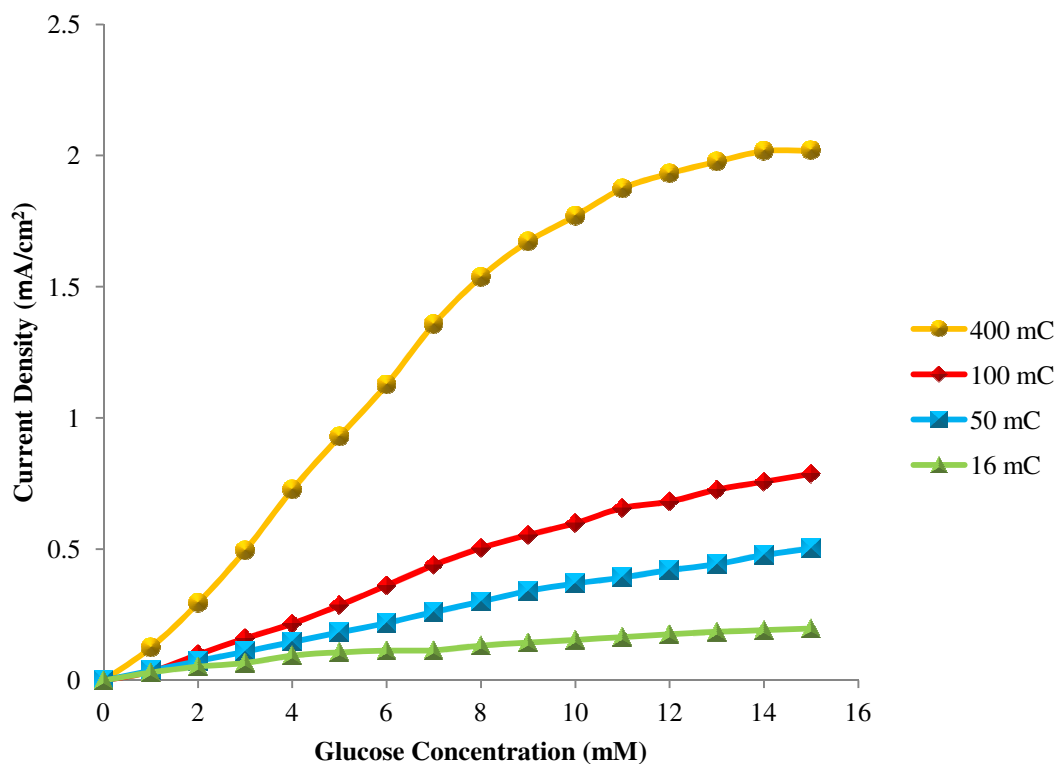


Figure 5.9. Current response generated after 2 hours of enzyme exposure.

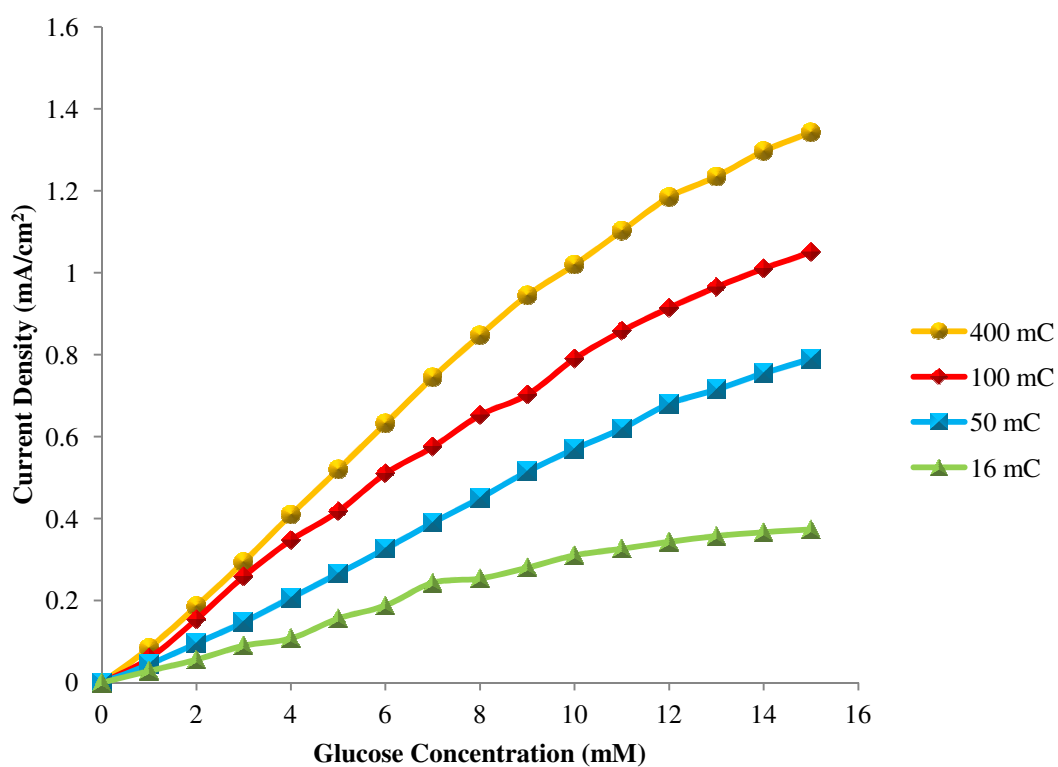


Figure 5.10. Current response generated after 6 hours of enzyme exposure.

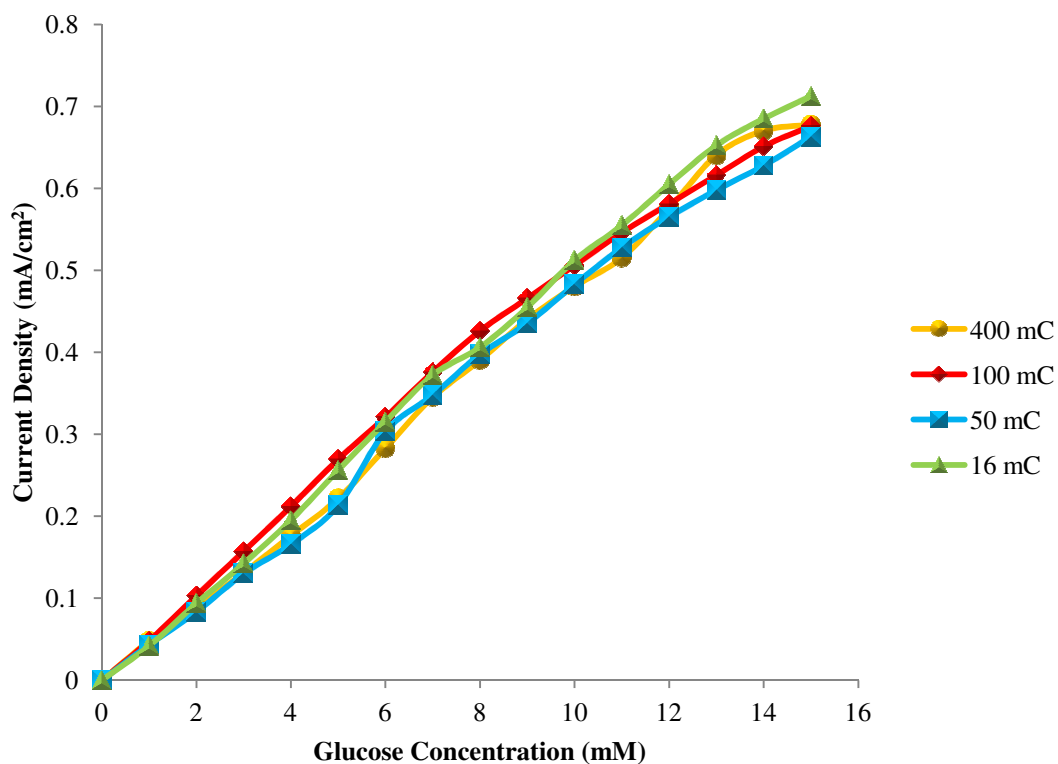


Figure 5.11. Current response generated after 9 hours of enzyme exposure.

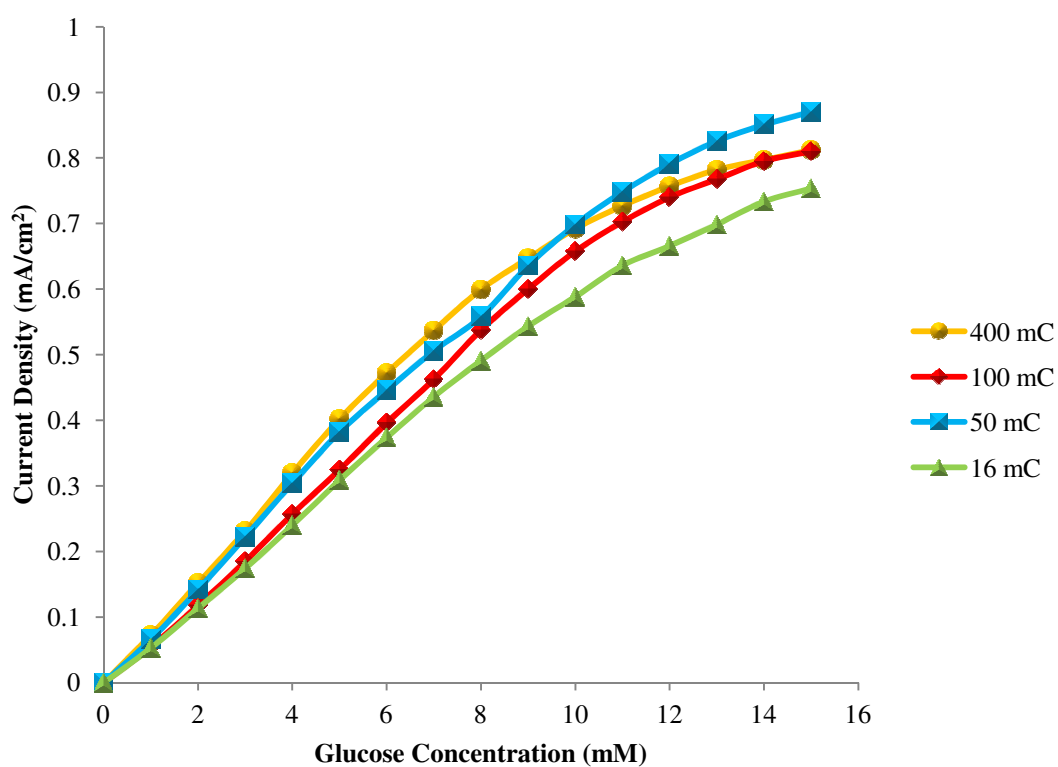


Figure 5.12. Current response generated after 24 hours of enzyme exposure.

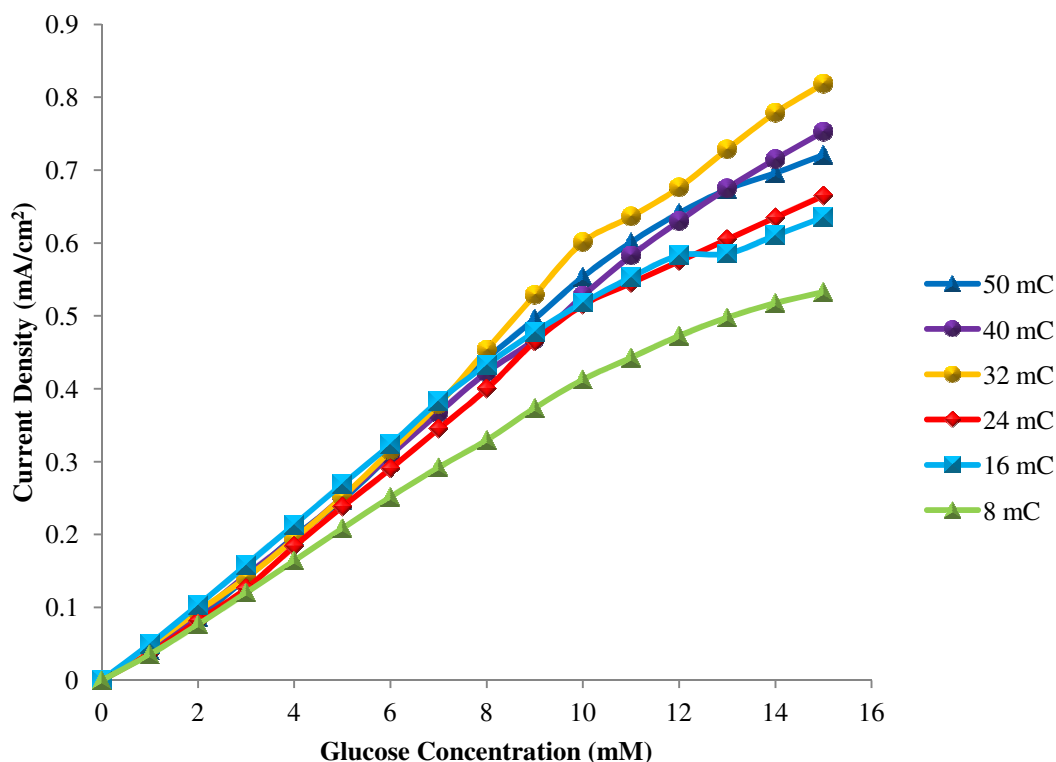


Figure 5.13. Current response generated after 24 hours of enzyme exposure employing lower charge for film growth.

Employing shorter immobilisation times of 2 and 6 hours demonstrated amplified current signals for 1 mM glucose additions as more charge was implemented for the resulting films seen in figures 5.9 and 5.10. Larger currents were also generated at shorter immobilisation times within a non-mediated system, figure 5.3. However as the enzyme immobilisation time was increased to 9 and 24 hours in figures 5.11 and 5.12 respectively the response to glucose remained constant despite the differences in charge applied for film growth. A similar response for the same investigation was seen in figure 5.5 within the non-mediated system where the apparent K_m demonstrated little variation indicating no change in the sensor behaviour over the same extended immobilisation times.

The limited signal response at longer enzyme exposure was explored further to incorporate thinner polymer films of 8, 16, 24, 32, 40 and 50 mC seen in figure 5.13. Examination of the response to glucose over lower concentrations up to 8 mM clearly showed very limited variation for most of the polymer thicknesses investigated. However the sensor developed with the smallest amount of charge at 8 mC when

compared with the rest of the polymer films clearly demonstrated a reduced signal. Examination over the whole concentration range displays larger signal variation indicating a slight response increase as more charge is used for the film growth until possible stabilisation is reached. At 32 mC the largest response to glucose is observed however increasing the charge to 40 mC and 50 mC fails to generate enhanced current signals demonstrating a potential plateau of signal response at increasing film thickness over a 24 hour immobilisation period.

At longer enzyme immobilisation times of 18 and 24 hours the response to glucose does not differ significantly when compared to the current response plots over shorter immobilisation times of 2, 6 and 9 hours. The data has been re-plotted to include the whole range of exposure times for both a thin copolymer film of 16 mC plotted as figure 5.14 and the thickest film produced at 400 mC seen in figure 5.15.

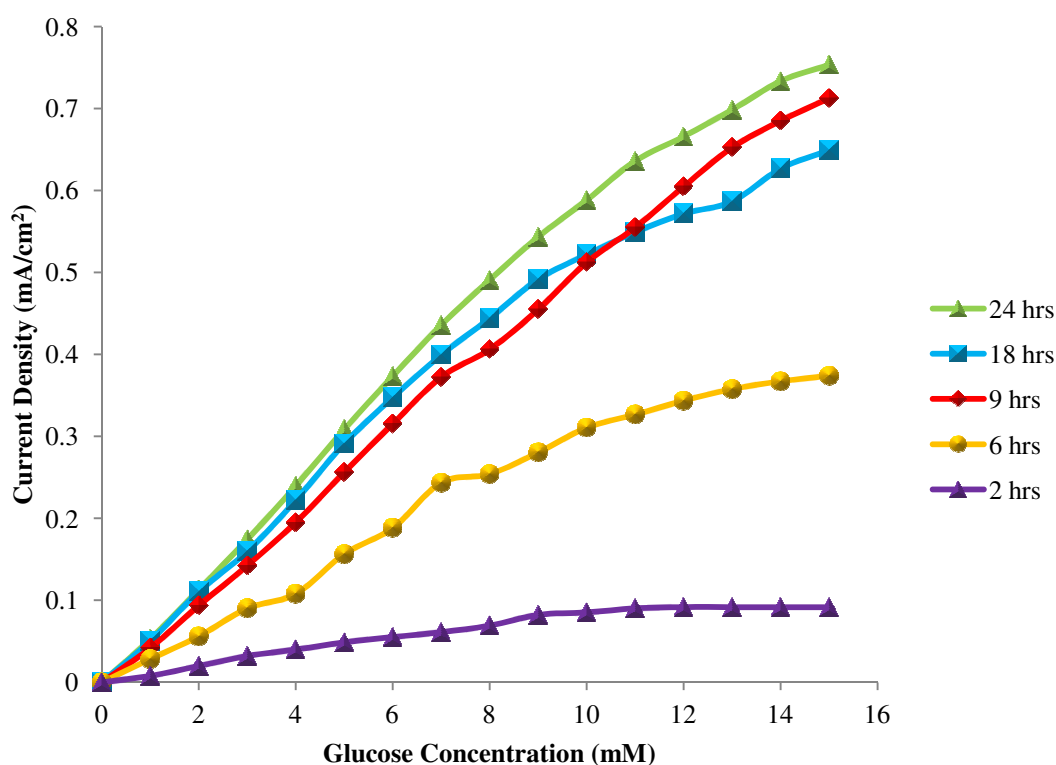


Figure 5.14. Stabilisation of signal at longer immobilisation times for a 16 mC film.

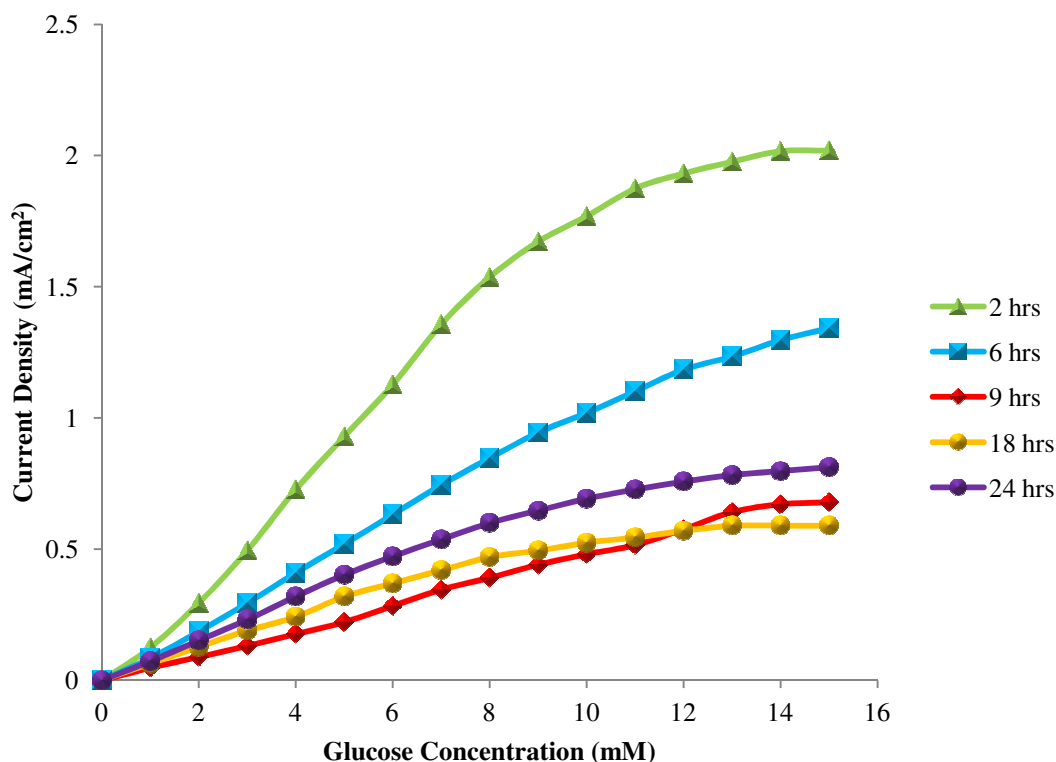


Figure 5.15. Stabilisation of signal at longer immobilisation times for a 400 mC film.

The responses obtained for the 16 mC film demonstrated an increase in current signal with increasing apparent K_m values over the range of enzyme exposure times. Thinner films represent less exposed surface area and therefore an increased enzyme exposure time was required to reach maximum loading as displayed in figure 5.14. Response to glucose increased greatly over the 9 hour period with considerable slowing after 24 hours. The 16 mC thin polymer film took longer to stabilise than the other polymer films as the response to glucose was still increasing after 24 hours, although the increase was small. A possible reason for this considers the polymer structure. The growth of the thin 16 mC film produced a very even polymer with no three dimensional growth; therefore access to the binding sites was likely to be more difficult and as more sites were occupied more time was needed for the enzymes to bind to available groups. After 24 hours it is likely that most sites are occupied by enzyme, slowing diffusion and elevating the apparent K_m data seen in table 5.6.

Polymer films produced from 400 mC show a reverse order for current signal enhancement in relation to enzyme exposure. By employing a thicker film for the immobilisation layer, shorter time periods stimulated greater response to glucose, this

could be associated with the ease of immobilisation upon a larger surface area and therefore less time was needed for covalent binding to occur upon the polymer surface. It is also likely that the large current signals after two hours of immobilisation time were generated due to enzyme absorption as a low apparent K_m of 8 mM is observed. The thicker films resembled growth in a three dimensional form extending away from the electrode surface with a porous composition. Enzyme molecules may have been absorbed in the matrix and therefore trapped without generating covalent attachment. Absorbed enzymes react to substrate more effectively and therefore large current signals and small apparent K_m values were produced and are displayed in table 5.6. Increasing the enzyme exposure time demonstrated a significant change to the large signals achieved over 2 and 6 hours of enzyme immobilisation representing an overall reduction in current response and increased apparent K_m .

The results obtained can be explained in part regarding diffusion properties associated with the immobilisation matrix. Thicker films exhibited diffusion limitation supported by the results obtained in figure 5.6 in which lower current signals were generated in response to hydrogen peroxide additions for a 400 mC film immobilised with glucose oxidase over 24 hours compared to a film exposed to only buffer solution. Increasing the amount of enzyme that was immobilised through the extension of the enzyme exposure time increased the difficulty associated with the diffusion of the generated product to the electrode surface. This was seen more predominantly with thicker films as more enzyme was able to immobilise over the extended time frame imparting a greater diffusion barrier and therefore decreased the current signal seen in figure 5.15. In addition the porous nature of the film with the increased thickness coupled with the longer immobilisation times was likely to generate enzyme binding deeper within the polymer therefore restricting substrate access and affecting the response generated.

The stability associated with the signal observed in figures 5.9-5.12 over a range of polymer thickness and immobilisation times of 9 and 24 hours demonstrated the maximum signal generated where species diffusion limited thicker films¹⁵⁷ and fully occupied binding sites limited the thinner films producing current responses of equal intensity.

Table 5.5. Maximum Response Determined after 15 mM.

Film Thickness	Current Response Achieved after 15 mM (mA/cm ²)			
	Enzyme Exposure Time			
	2 Hours	6 Hours	9 Hours	24 Hours
16 mC	0.198	0.374	0.713	0.753
50 mC	0.503	0.790	0.663	0.870
100 mC	0.786	1.050	0.676	0.810
400 mC	2.019	1.342	0.678	0.812

Table 5.6. Kinetic Data for Film Thickness and Enzyme Exposure Time.

Film Thickness	Enzyme Exposure Time							
	2 Hours		6 Hours		9 Hours		24 Hours	
	Kinetic Data (mM)							
	V _{max}	K ^{App} _m	V _{max}	K ^{App} _m	V _{max}	K ^{App} _m	V _{max}	K ^{App} _m
16 mC	0.0068	11	0.013	11	0.004	60	0.04	26
50 mC	0.035	38	0.08	56	0.064	58	0.06	35
100 mC	0.049	31	0.09	49	0.04	32	0.03	16
400 mC	0.063	8	0.08	27	0.14	138	0.03	13

From the examination of varying film thickness and enzyme exposure time further studies were carried out upon both a 50 mC and 400 mC film after 6 hours of enzyme interaction. The 50 mC film represented good response to glucose and produced a good even film covering the electrode surface with quick, facile growth. A thicker film of 400 mC generates longer growth times however the response to glucose was greatly enhanced.

5.1.1.3. Repeatability and Reproducibility

Repeatability and reproducibility are two important factors that were investigated. Repeatability is an evaluation of how precise measurements are for a single electrode which is related to the behaviour of the biosensor within the experimental set up.

Reproducibility focuses upon the fabrication of the biosensor from polymer deployment to enzyme attachment this determines how reproducible the process is which is important for the generation of multiple enzyme electrodes.

Reproducibility is also affected by the performance of the individual electrode. The electrodes available varied in age and as they are used the area and quality of the platinum surface is likely to change therefore the current signal variation was calculated between the six platinum electrodes employed within the study. The associated error was found to be 6% and so current signal variation up to this value can be associated with the reproducibility of the electrode used.

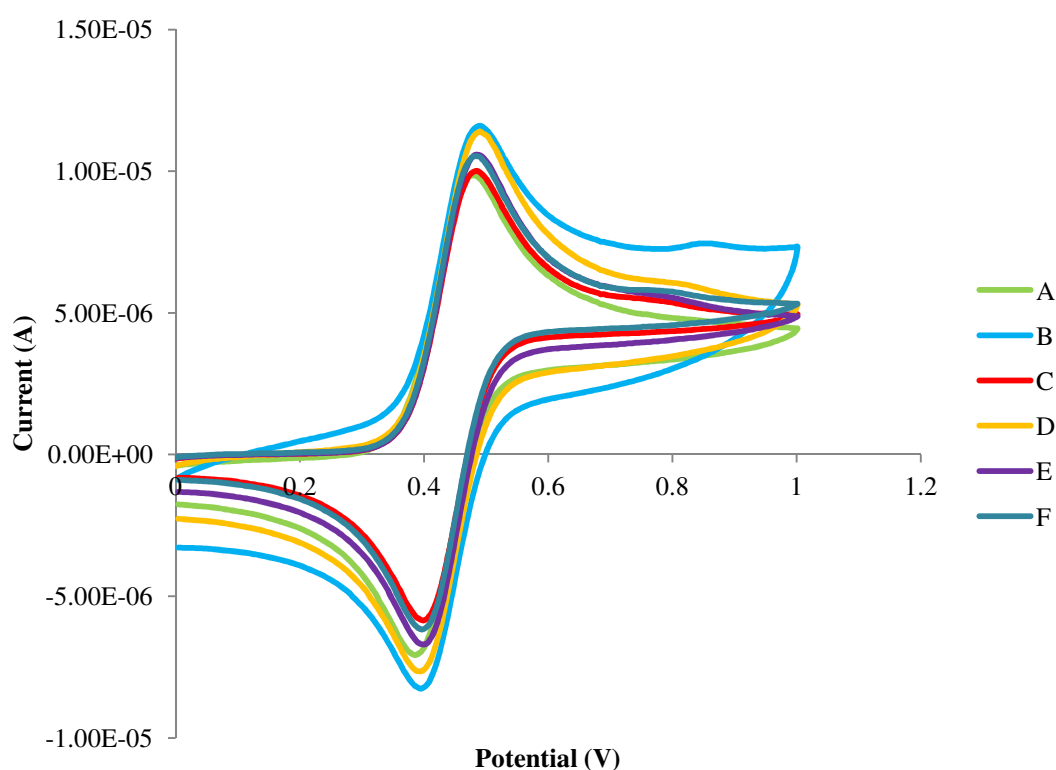


Figure 5.16. Cyclic voltammograms of 1 mM ferrocene scanned at 100 mVs^{-1} .

Reproducibility calculated for all biosensor systems considered the 6% error involved with the electrodes used and where error was greater possible causes were given.

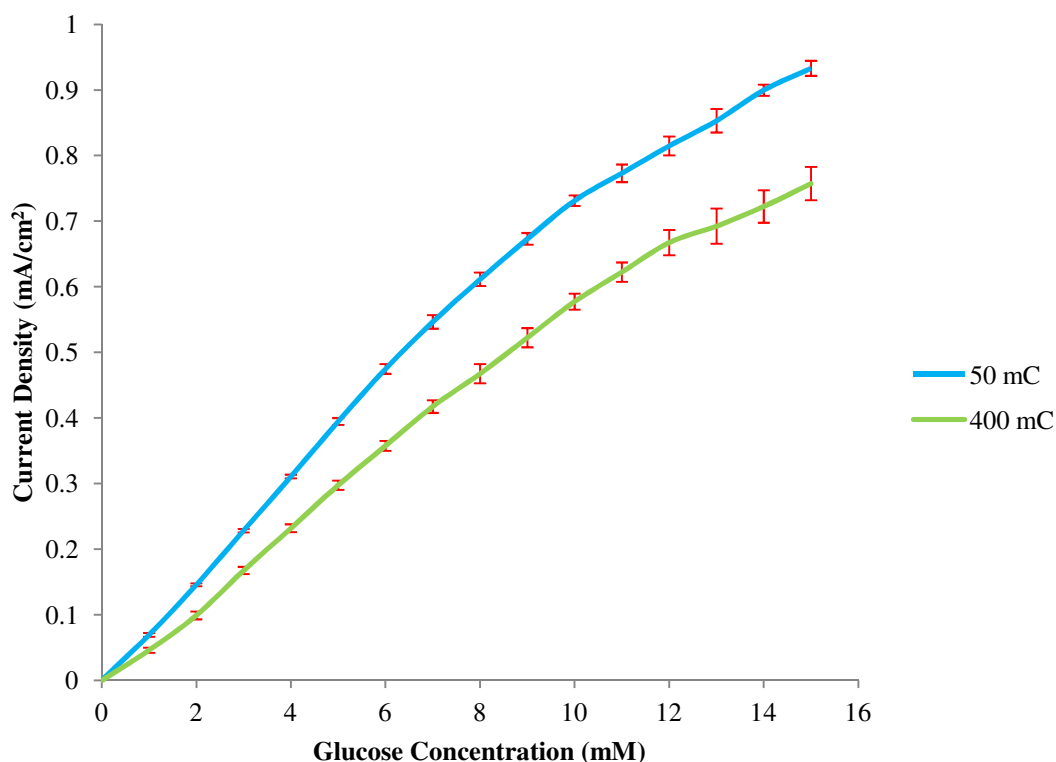


Figure 5.17. Repeatability of a 50 mC and 400 mC enzyme electrode.

The repeatability error for the 50 mC enzyme electrode analysed was calculated at 3% which was sufficiently low and can most likely be associated with experimental error such as introducing the correct volume of glucose, measuring buffer volumes and measurement analysis.

The increase in error for the 400 mC enzyme electrode calculated at 6% is approximately double the error involved with the 50 mC film. In this particular investigation the large current responses at 6 hours enzyme exposure displayed in table 5.5 are absent which indicates significant variation within thicker films. The error increase and current response decrease compared to the 50 mC film may be explained by the variability that larger amounts of material can impart. As more material is deposited upon the electrode surface an increase in the proportion of defects is probable^{25,35,178,195} affecting the conjugation within the polymer and the outward growth of the film becomes problematic as this can contribute to the loss of material throughout the fabrication process affecting the behaviour of the biosensor.

The reproducibility was determined using the average error calculated for two sets of three enzyme electrodes in which each set was performed upon different days. Combining the six data sets was avoided due to the variation in signal response generated upon the different days. This was due to the laboratory temperature change which occurred between winter and summer months, and therefore the errors were calculated separately for the data sets and averaged to provide an overall reproducibility error quoted as % RSD.

The average error associated with the analysis of three enzyme electrodes in each of the two data sets upon copolymer films of 50 mC was determined at 15% which incorporates the reproducibility of the electrodes used calculated previously at 6% leaving 9% variation accountable to the error associated with the fabrication process as different solutions were made for the biosensors on different days.

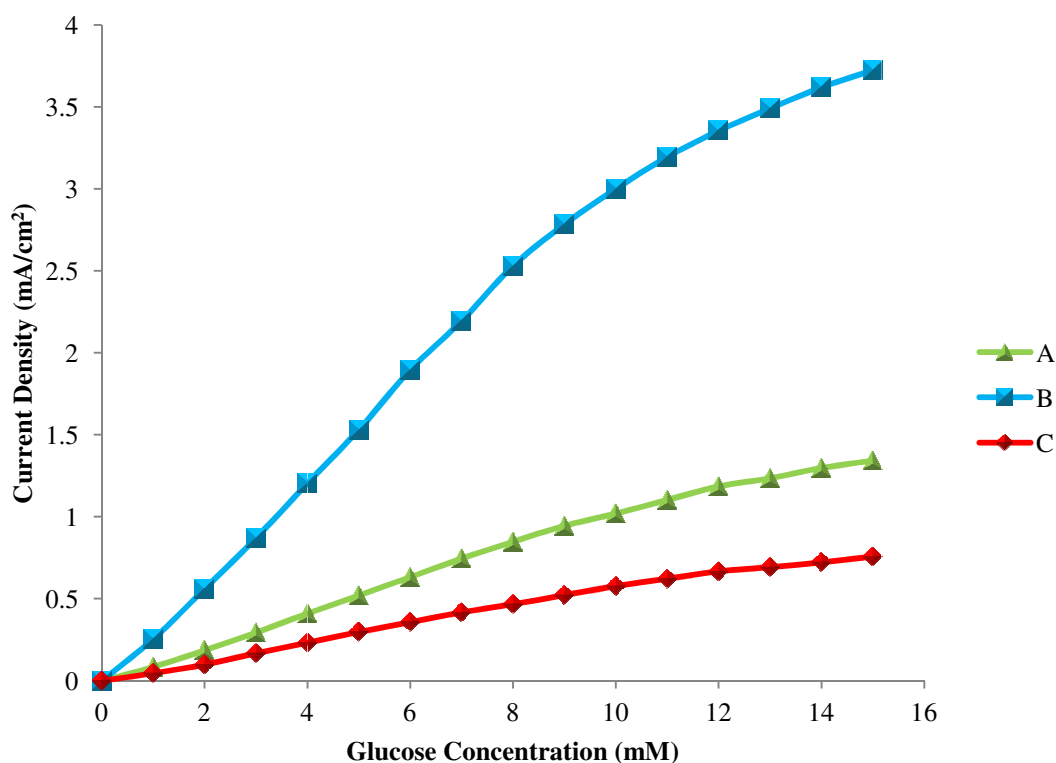


Figure 5.18. Reproducibility of three 400 mC enzyme electrodes.

The assessment of three 400 mC enzyme electrodes produced some difficulty. Due to the enhanced loading of the copolymer and its related physical properties the polymer film would not remain intact and therefore suffered loss of material through the fabrication stages. The error associated with the 400 mC film was 84%. The large

variation upon each prepared enzyme electrode demonstrates the low practical application of a thick film.

5.1.1.4. Investigation of the Effects of Buffer Exposure Time upon Current Response

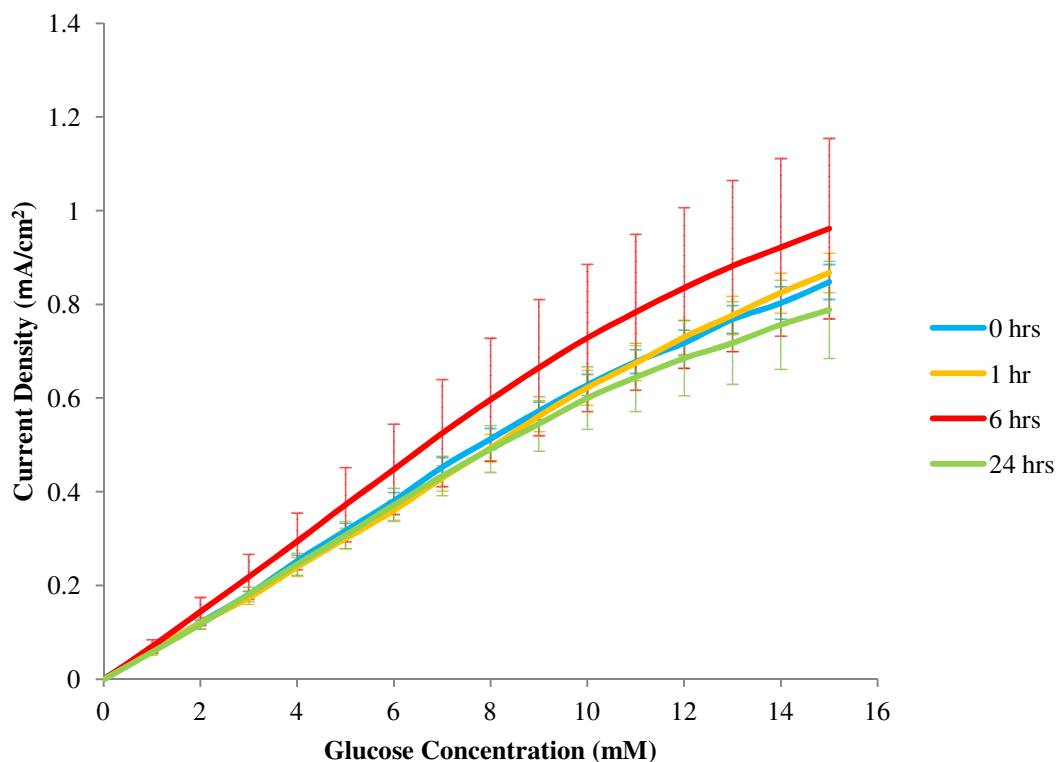


Figure 5.19. Investigation of the effects of buffer exposure upon 50 mC copolymer films.

The three 50 mC enzyme electrodes investigated for each of the buffer exposure times investigated demonstrated significant variation in signal over 24 hours. The spread of results was greatest upon leaving the enzyme electrodes at extended periods of time and therefore the limited storage time of up to one hour reduced the response variation. For the 6 and 24 hour buffer exposure, average error was calculated at 31.5% in which 6% was accountable for the error within electrode reproducibility therefore the variation represented 25.5%. Electrode storage between 0 and 1 hour generated an average variation of 4.5% taking electrode reproducibility into account therefore demonstrating that longer buffer soaking leads to increased variation in glucose response. Therefore the enzyme electrodes were not left in buffer for any extended period of time.

The average responses for the various buffer soak times seen in table 5.7 demonstrated the increase in deviation between values at longer storage times in buffer solution. This can possibly be explained due to the limited polymer swelling over shorter buffer exposure times influenced by the hydrophobic nature of the film, however over longer periods some buffer interaction may occur due to the fibrillar structure and level of film porosity¹⁷ causing the very large variation of response at 6 hours until the signal begins to stabilise at 24 hours.

The low variation in the biosensor response at shorter buffer exposure times was surprising as it was expected through eliminating the buffer soak greater current signals would be observed contributing to a larger error. The expected heightened response would have been explained through the presence of unbound enzyme and the fact that responses were precise demonstrated that the copolymer material did not excessively retain unbound species and therefore the rinsing of the electrodes and storage in between analysis presented little issue. However it was concluded that storage time was limited where possible due to the increase in response variation seen considerably at 6 hours and moderately at 24 hours.

Table 5.7. Error Associated with Each Set of Sensors for Various Buffer Soak Times.

	0 hours	1 hour	6 hours	24 hours
Average CV	7 %	14 %	42 %	21 %

5.1.1.5. Stability Over 72 Hours

Three enzyme electrodes were prepared for the following study each one was analysed with the resulting data representing the average obtained.

The stability of the enzyme electrodes for both the N-succinimido thiophene-3-acetate and the thiophene-3-acetic acid copolymers were investigated over 72 hours as a measure of stability. The first analysis was carried out after 1 hour of buffer interaction with the subsequent results obtained after three 24 hour intervals. The enzyme electrodes were stored in pH 7.0 phosphate buffer at room temperature in between data collection.

Repeated use over 72 hours demonstrated the stability provided by films employing differing thicknesses. Table 5.8 displays the average signal retained as a percentage over 15 mM of glucose through 72 hours with graphical representations of stability demonstrating a 50 mC copolymer film and a thicker film generated by employing 400 mC to the electrode surface.

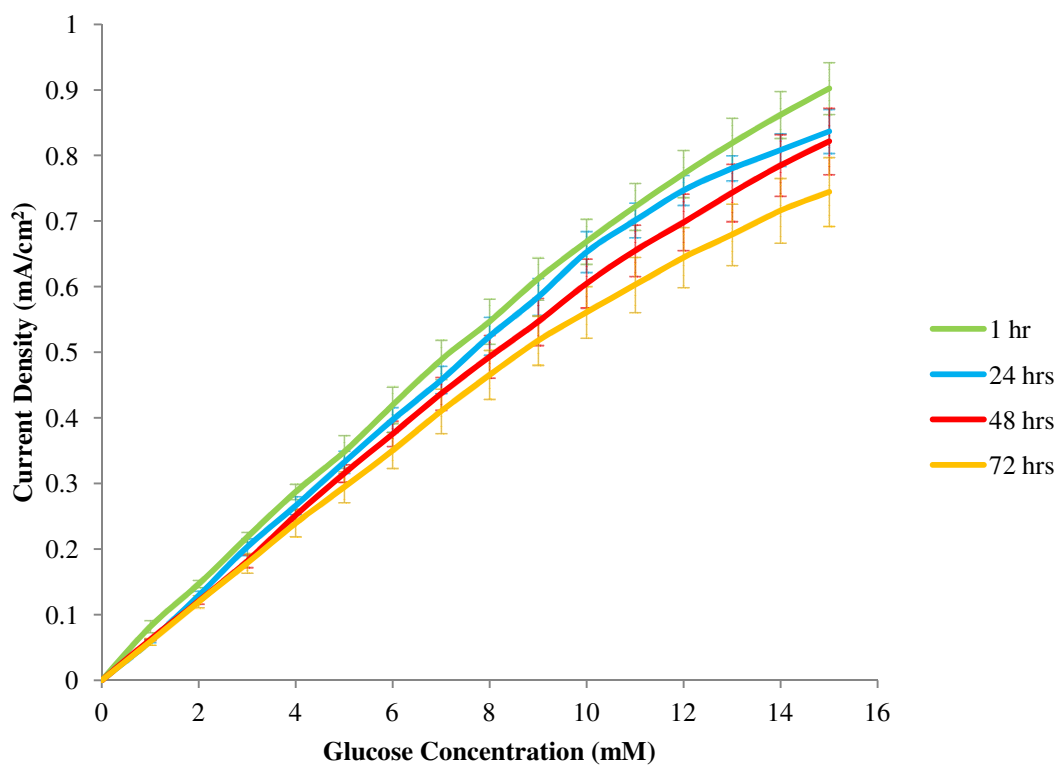


Figure 5.20. Average response of three 50 mC N-succinimido thiophene-3-acetate film exposed to 6 hours of GOx and analysed over 72 hours.

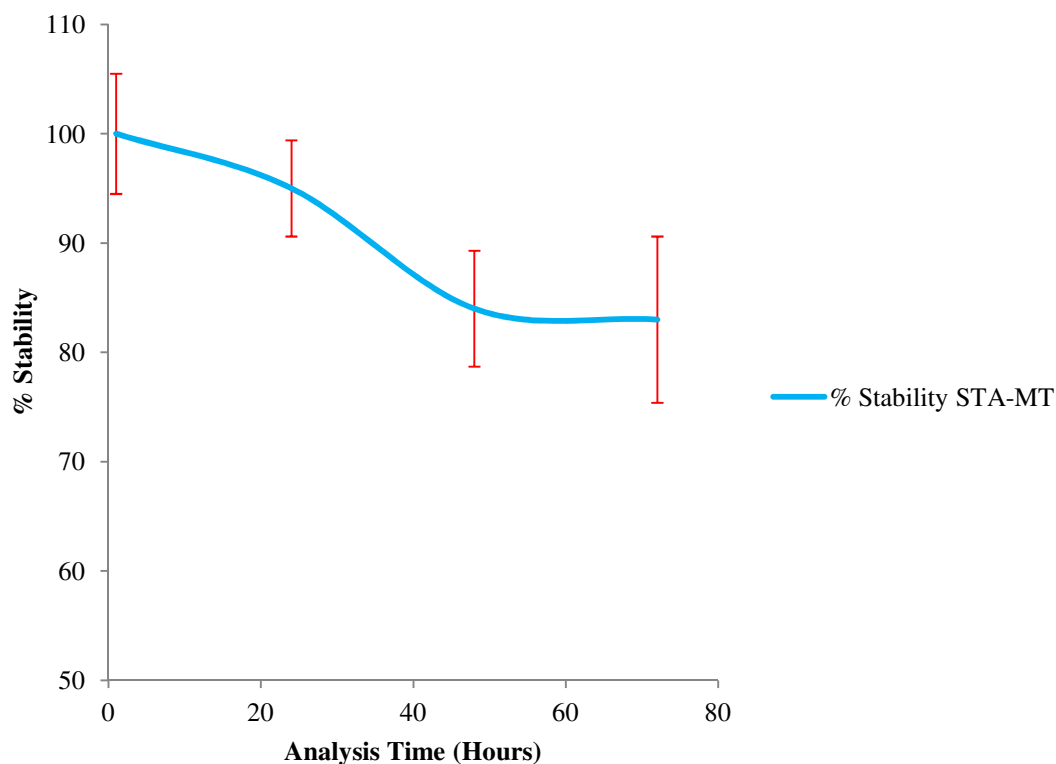


Figure 5.21. Average response of three 50 mC N-succinimido thiophene-3-acetate copolymer films exposed to 6 hours of GOx and analysed over 72 hours.

The stability of the film is seen clearly in figures 5.20 and 5.21 and demonstrates a small deviation of 17% from the original analysis. However as the enzyme electrodes were stored in buffer over the 72 hour time frame the variation in response could in part be attributed to the effects of extended buffer interaction associated with the film up to 24 hours as depicted in the buffer soak study represented in figure 5.19. If after 24 hours the variation in signal is associated to the stabilisation of polymer swelling only a 12% error can be related to loss of biosensor performance.

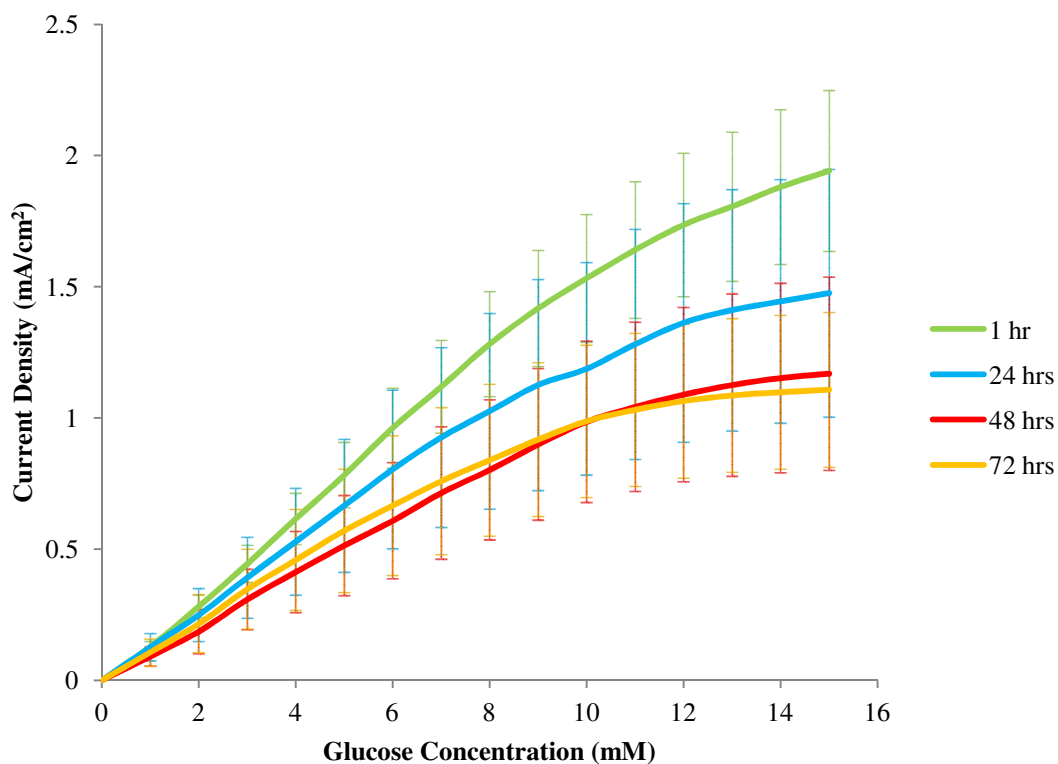


Figure 5.22. Average response of three 400 mC N-succinimido thiophene-3-acetate films exposed to 6 hours of GOx and analysed over 72 hours.

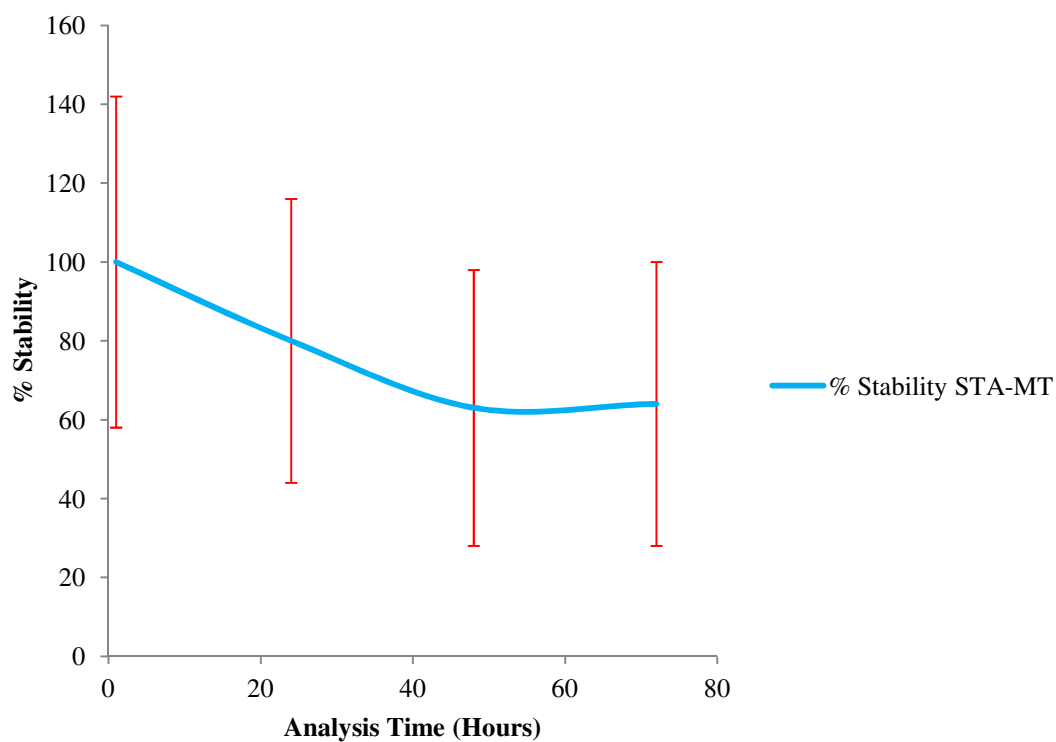


Figure 5.23. Average response of three 400 mC N-succinimido thiophene-3-acetate copolymer films exposed to 6 hours of GOx and analysed over 72 hours.

The thicker film demonstrated a 36 % variation from the original analysis, more than double the loss of signal compared to the 50 mC film. It was likely that absorbed enzyme was more difficult to remove when thicker films were used for immobilisation and the large signal loss could be explained predominantly through enzyme leaching. As the buffer soak investigation did not include thicker films it was also expected that the signal variation was likely to be influenced by a degree of polymer swelling in which stabilisation may have taken longer to achieve.

The 400 mC film in this case generated a larger response to glucose which is desirable for a biosensor device however as the stability is greatly affected due to possible enhanced enzyme absorption, swelling and film fragility analysis of different copolymer formats did not include thicker films.

Table 5.8. Percentage Signal Retained Over 72 Hours.

Time (hours)	Enzyme Exposure; 16 mC Film					Enzyme Exposure; 50 mC Film				
	2 hours	6 hours	9 hours	18 hours	24 hours	2 hours	6 hours	9 hours	18 hours	24 hours
1	100%					100%				
24	65%	100%	82%	103%	62%	67%	95 %	73%	100%	49%
48	37%	78%	56%	113%	42%	37%	84%	45%	67%	52%
72	51%	43%	33%	26%	41%	13%	83%	35%	61%	33%

Time (hours)	Enzyme Exposure; 100 mC Film					Enzyme Exposure; 400 mC Film				
	2 hours	6 hours	9 hours	18 hours	24 hours	2 hours	6 hours	9 hours	18 hours	24 hours
1	100%					100 %				
24	107%	97 %	107%	100%	74%	44%	80 %	53%	89%	77%
48	58%	87 %	100%	45%	80%	14%	63 %	51%	49%	21%
72	55%	69 %	97%	44%	69%	26%	64 %	43%	57%	17%

The stability study over 72 hours was implemented for all film thicknesses and enzyme immobilisation times previously investigated. Only the 50 mC and 400 mC films at 6 hours enzyme exposure were reproduced in triplicate as the remaining

studies were performed to determine other possible beneficial formats for further investigation.

The thin films of 16 mC were least stable after 72 hours retaining biosensor performance at only approximately 50% and lower. The average stability at 72 hours for both the thin (16 mC) and thick (400 mC) films were low representing 39% and 36% respectively, employing 50 mC and 100 mC of charge for film growth provided enhanced stability in which 50 mC retained an average 45% of the original signal and 100 mC retained 67%. Upon closer comparison it can be observed that for the 50 mC film exposed to 6 hours of enzyme solution stability was high at 83% over 72 hours of storage at room temperature. Furthermore the 100 mC film at 9 hours of enzyme immobilisation represents virtually no loss in signal. The biosensor demonstrated an increase in response to glucose after 24 hours where usually reduced responses were observed. This behaviour was possibly the result of established diffusion channels in the material¹⁵⁶. It was therefore concluded that investigations would continue with the thinner 50 mC film at shorter enzyme immobilisation of 6 hours as this format was successful in retaining enzyme stability with excellent repeatability, reproducibility and signal response.

5.1.1.6. Stability Over Four Weeks

Stability of the enzyme electrodes stored over 72 hours at room temperature generated very positive results with only a 12% loss of signal after the effects of buffer exposure were taken into account. Enzymes are generally considered as unstable species however upon immobilisation enzyme stability typically increases. A further stability study was employed in which three 50 mC enzyme electrodes were stored at 4 °C in between measurements over 4 weeks. By storing the enzyme at reduced temperature the lifetime of the enzyme biomolecule will be prolonged¹⁹⁶. It is expected that stability will be enhanced and the enzyme electrodes can be stored for longer periods of time without significant decrease in biosensor performance.

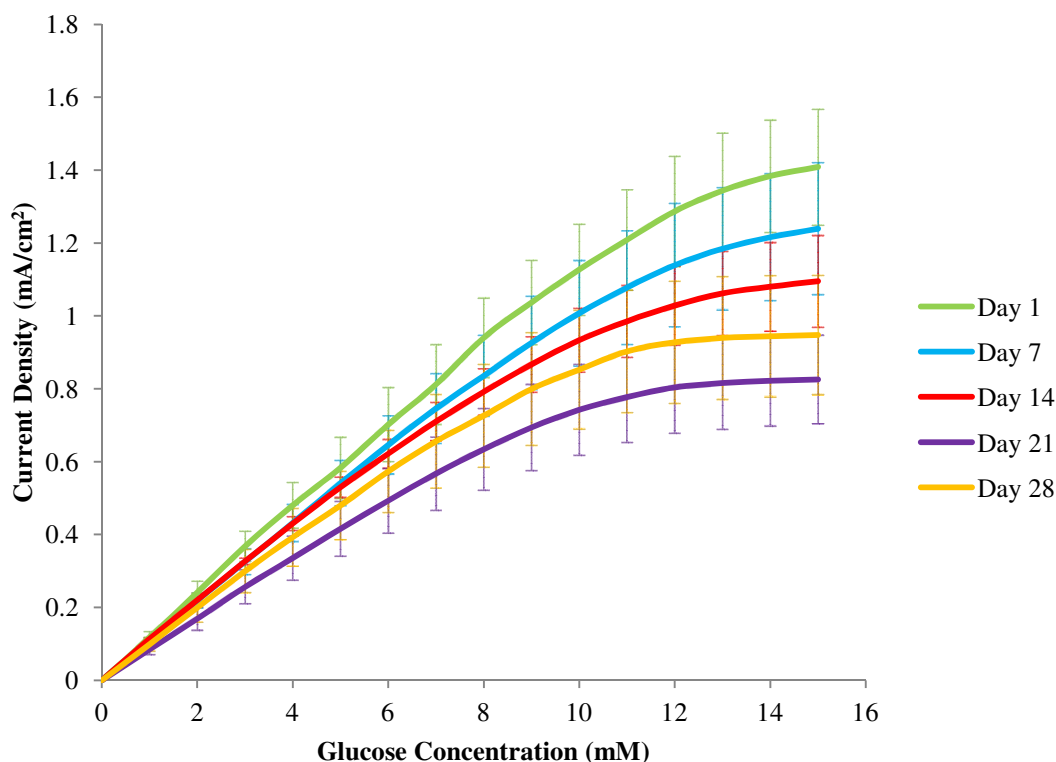


Figure 5.24. Average response of three 50 mC N-succinimido thiophene-3-acetate copolymer films exposed to 6 hours of GOx and analysed over 4 weeks.

Stability over 4 weeks was good with a relatively constant decrease in response observed through the weekly analysis using the average of the three averaged responses. The storage temperature influenced the stability of the immobilised enzyme providing a retained signal of 75% from the original analysis after 1 month at 4 °C in phosphate buffer solution.

Over the 1-8 mM range of substrate, stability of the enzyme electrode was improved seen in table 5.9. Less degradation was seen; however the response still continued to fall as it is well known that enzymes denature over time. At higher substrate concentration saturation of the biosensor was observed in which saturation started to occur at lower concentrations over the following weeks. As less active enzyme remained the current responses decreased which can be observed clearly in figure 5.24.

Table 5.9. Stability of the N-succinimido thiophene-3-acetate Copolymer Sensors
Analysed over Four Weeks.

STA-MT	1 Hour	1 Week	2 Weeks	3 Weeks	4 Weeks
1-15 mM	100%	89%	83%	65%	75%
1-8 mM	100%	91%	88%	70%	81%

The signal retained through each 7 day period can be seen in table 5.9. Interestingly a 10% increase is observed over weeks 3 and 4 this may correspond to a stabilisation of signal over longer storage times however further stability measurements would be required to confirm this.

5.1.2. Investigation of the Thiophene-3-acetic acid and 3-Methylthiophene Copolymer

The thiophene-3-acetic acid and 3-methylthiophene copolymer is a biosensor system which is well explored. The work by Kuwahara *et al* was incorporated into this study and provided a guide for successful biosensor analysis. Where possible the experimental conditions were followed closely in order to replicate data and compare biosensor performance to the parameters found to be optimal for the new biosensor system employing N-succinimido thiophene-3-acetate.

The results generated for the T3AA/MT copolymer were comparable to the STA/MT system with analytical assessment of signal response and stability displaying close agreement. Reproducibility for the two biosensor formats differed considerably with the novel biosensor system providing greater signal reproducibility. Response to glucose for both copolymer systems indicated a measureable signal to glucose in under four seconds.

Employing the conditions found in the literature⁵⁴ thiophene-3-acetic acid and 3-methylthiophene monomers were copolymerised to provide a polymer film consisting of a 10% content of the acid substituted monomer specifically for enzyme binding. The amount of charge deployed for the immobilisation matrix differed from the literature due to difficulty obtaining even polymer coatings upon the electrode surface. Alternatively a thicker film of 2500 mC/cm² was used with an enzyme

exposure time of 6 hours employing optimum parameters generated from the N-succinimido thiophene-3-acetate copolymer. The mediator *p*-benzoquinone was used within the study.

By deoxygenating the buffer solution with nitrogen the response to glucose increased up to 44% within a mediated environment. A larger increase was seen with the thiophene-3-acetic acid copolymer through the removal of oxygen highlighting the competition against *p*-benzoquinone.

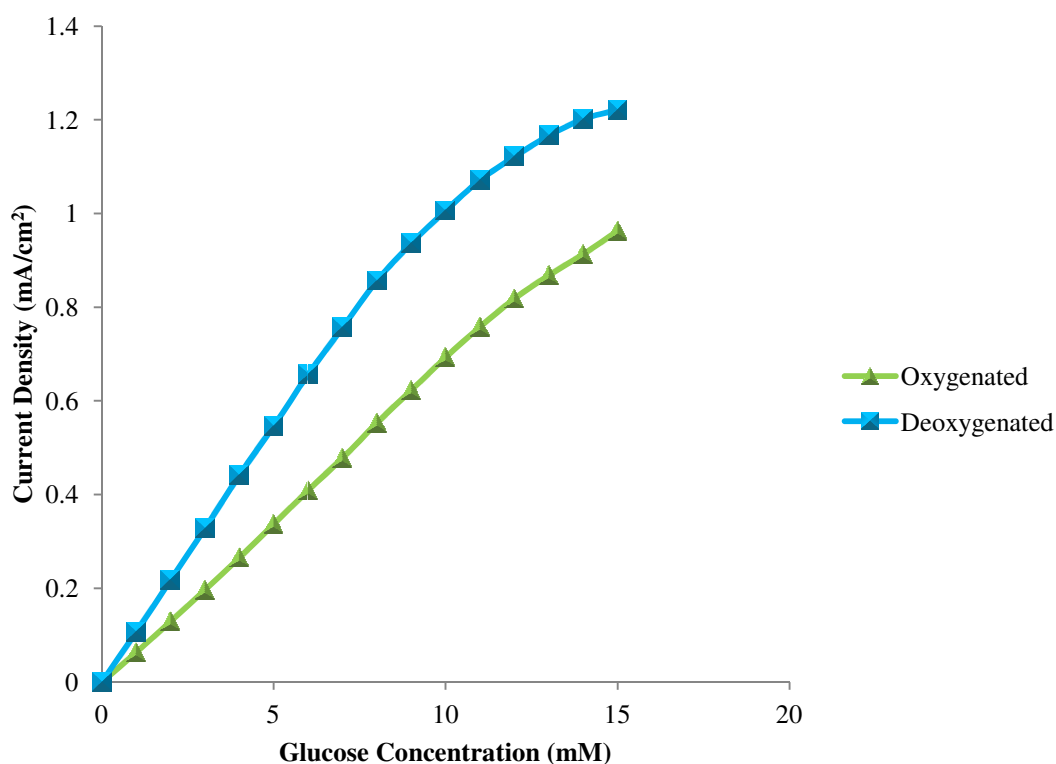


Figure 5.25. Sensor response within a deoxygenating environment using nitrogen.

The method of oxygen removal by nitrogen bubbling over 20 minutes was seen to considerably enhance signal response and was therefore employed through the rest of the biosensor investigations in order to gain maximum response to glucose and provide consistency for both copolymer assessments.

5.1.2.1. Repeatability and Reproducibility

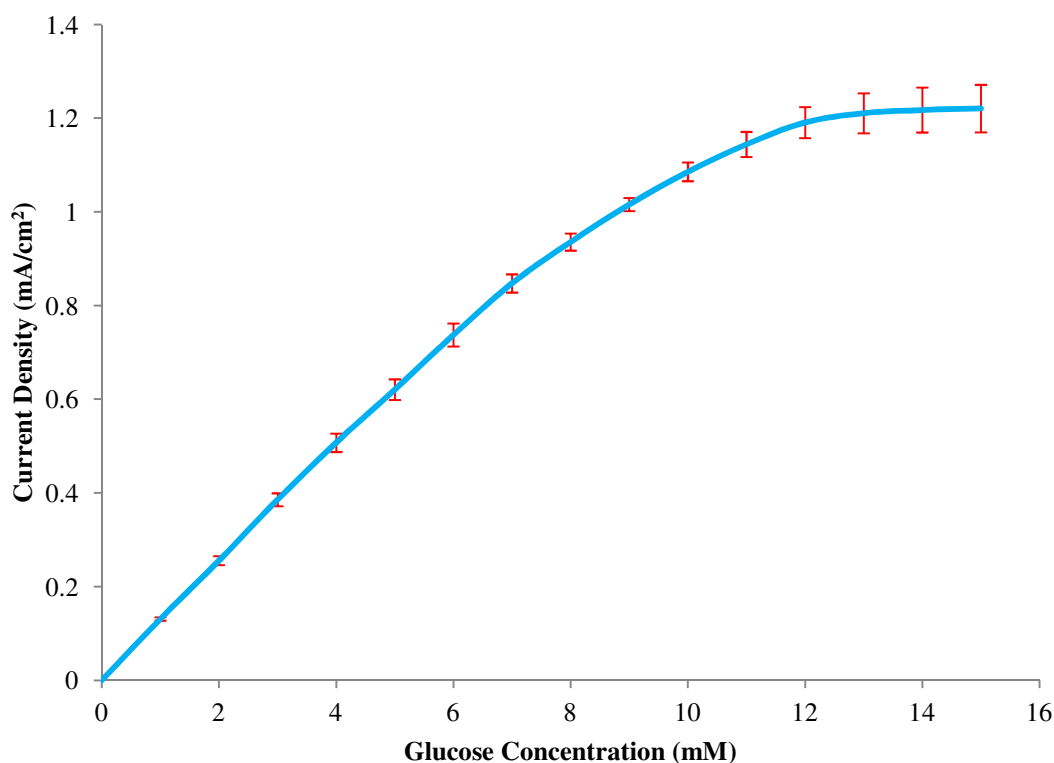


Figure 5.26. Repeatability of 50 mC enzyme electrodes (n=3).

The error associated with three repeat analysis of the thiophene-3-acetic acid and 3-methylthiophene copolymer was 6%. The error was double that of the novel copolymer and may be less stable than the ester copolymer.

Reproducibility represents a variation of 16% calculated as an average over two sets of three different enzyme electrodes. The error involved requires an explanation other than the 6% variation calculated between the working electrodes as a 10% error still remains. This large error can be associated with the variation produced by buffer soak times between 0-1 hours at 10.5% and the fabrication process where different batches of monomer solution, and enzyme solution were prepared on different days.

5.1.2.2. Stability Over 72 Hours

The 50 mC film was chosen to investigate the thiophene-3-acetic acid copolymer stability due to the good, steady responses to glucose obtained over a four day period with the novel copolymer.

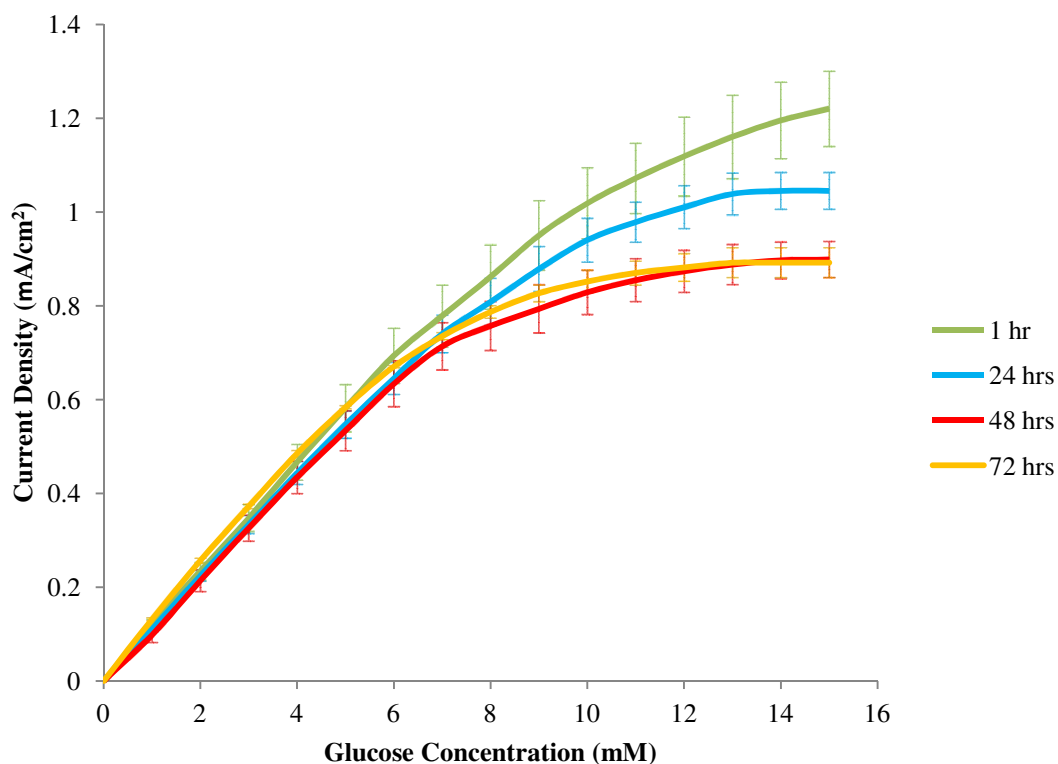


Figure 5.27. Average response of three 50 mC thiophene-3-acetic acid copolymer films exposed to 6 hours of GOx and analysed over 72 hours.

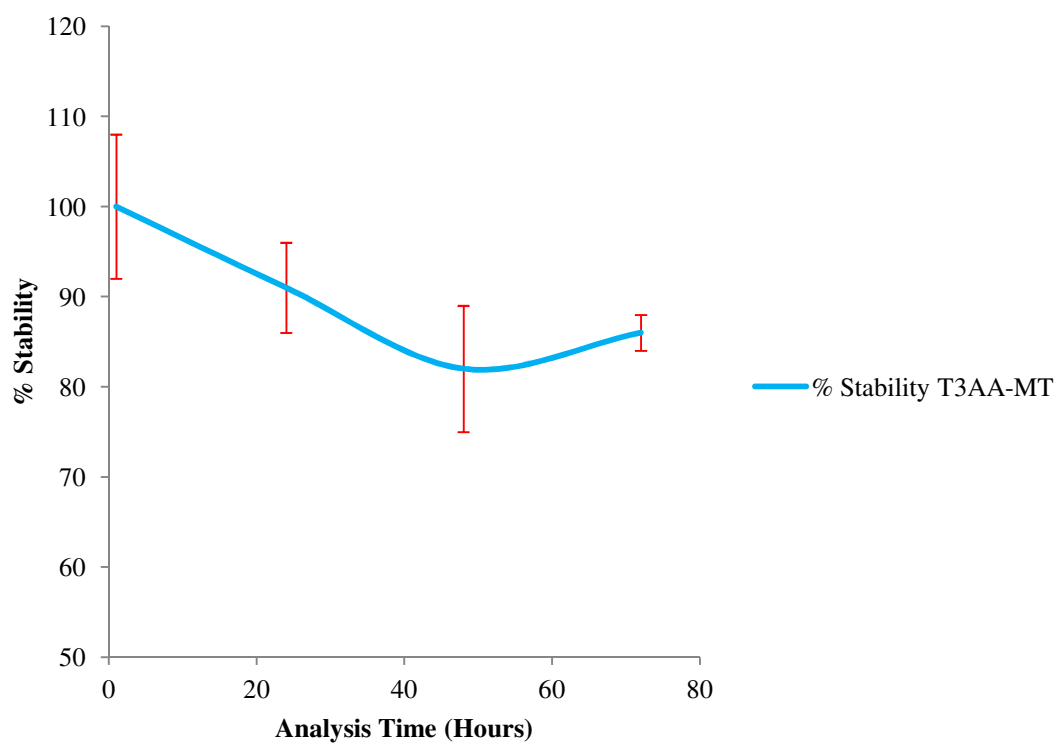


Figure 5.28. Average response of three 50 mC thiophene-3-acetic acid copolymer films exposed to 6 hours of GOx and analysed over 72 hours.

Glucose response for the thiophene-3-acetic acid copolymer over 72 hours at room temperature presented a stable film demonstrating a comparable 86% response to the original analysis after 72 hours. Increased deactivation can be seen more clearly at higher glucose concentrations where saturation was observed with very little variation in response over the 72 hour period up to 7 mM of glucose.

5.1.2.3. Stability Over Four Weeks Stored at 4 °C

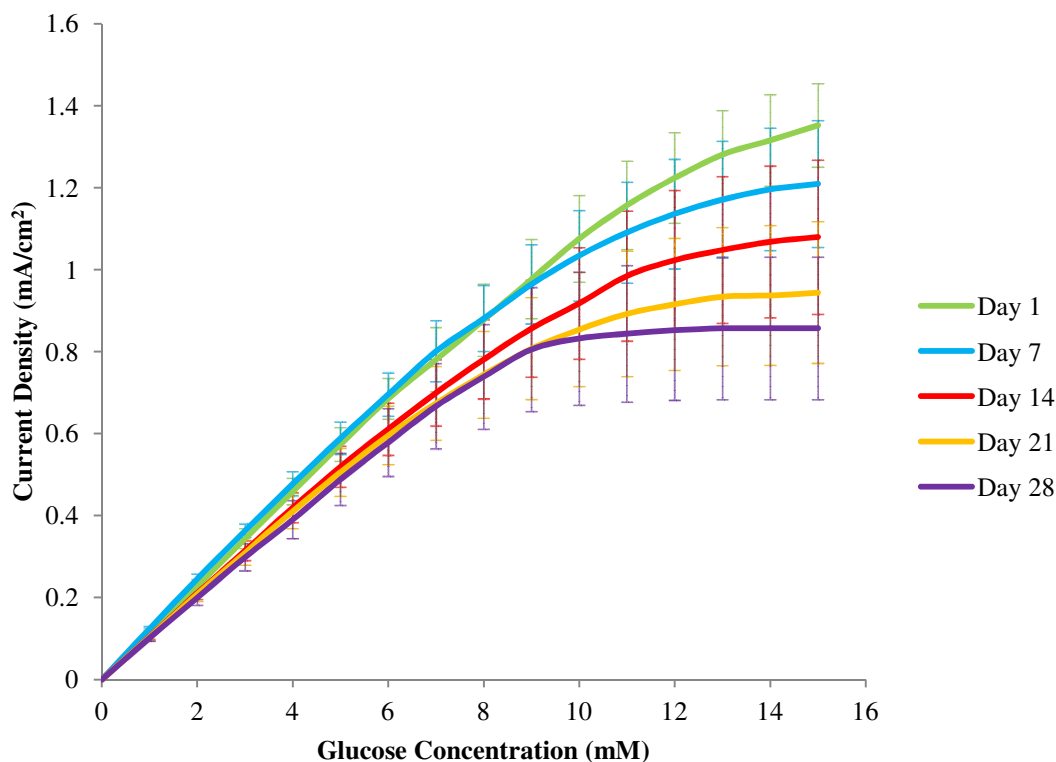


Figure 5.29. Average response of three 50 mC thiophene-3-acetic acid copolymer films exposed to 6 hours of GOx and analysed over four weeks.

Although room temperature stability was successful over a four day period stability can be increased by storing the enzyme electrodes at 4 °C between analysis. After one month 78% of the original response was retained with only a 1% decrease between weeks three and four indicating a lower rate of deactivation after longer storage periods. Response to glucose over 1-8 mM showed increased stability as saturation of the immobilised enzyme had not yet been reached. A slight 2% increase in stability after one week is seen and may possibly be due to the formation of diffusion channels within the material or a preferred and more stable rearrangement in enzyme conformation¹⁹⁷.

Table 5.10. Stability of the 3-thiophene acetic acid Copolymer Sensors Analysed over Four Weeks.

T3AA-MT	1 Hour	1 Week	2 Weeks	3 Weeks	4 Weeks
1-15 mM	100%	96%	85%	79%	78%
1-8 mM	100%	102%	90%	90%	85%

Biosensor investigations have so far incorporated the well established thiophene-3-acetic acid and 3-methylthiophene copolymer and the novel N-succinimido thiophene-3-acetate and 3-methylthiophene copolymer. The novel N-succinimido thiophene-3-acetate compound was synthesised within this study to monitor the effects that a preactivated thiophene monomer would produce within a biosensor format. The investigations provided encouraging results especially where signal response, repeatability and reproducibility were enhanced and therefore prompted further investigation.

Copolymers were studied with the identical functionality of the carboxylic acid and activated ester groups but differed by an extension between the thiophene ring and the functional group through a double bond provided by an additional methylene species. The compound trans-3-(3-thienyl) acrylic acid is readily available and was modified by the same condensation reaction with carbodiimide reagent to yield the activated ester species. It was envisaged that the double bond linkage would impart enhanced electron transport due to the extended conjugation provided and would increase the current signals produced.

The investigations performed for both the novel trans-3-(3-thienyl) acrylic acid and 3-methylthiophene copolymer and N-succinimido trans-3-(3-thienyl) acetate and 3-methylthiophene copolymer follow the same studies of repeatability, reproducibility, stability, limit of detection, signal response and enzyme kinetics and are tabulated in table 5.13 with data extracted for all copolymer biosensors investigated.

5.1.3. Investigation of the Novel Trans-3-(3-thienyl) acrylic acid and 3-Methylthiophene Copolymer

5.1.3.1. Repeatability and Reproducibility

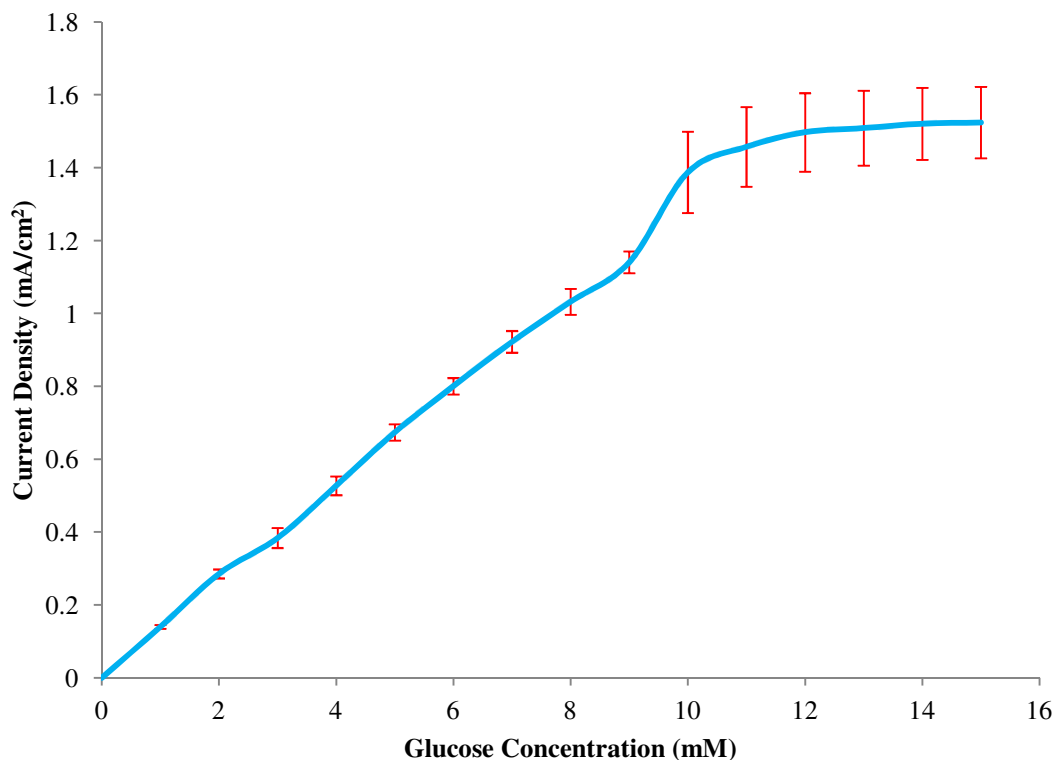


Figure 5.30. Repeatability of a 50 mC enzyme electrode.

The error calculated between the triplicate measurements was determined at 10% RSD. This represents a large variation between repeat analysis upon the same enzyme electrode and may signify stability issues.

A 10% signal reproducibility error was calculated over three different enzyme electrodes of trans-3-(3-thienyl) acrylic acid and 3-methylthiophene in which a 4% variation was established once the 6% electrode error was subtracted. This represented a lower variation compared to the thiophene-3-acetic acid and 3-methylthiophene copolymer in which the 4% signal variability occurred within the 0-1 hour buffer soak error margin of 10.5%.

5.1.3.2. Stability Over 72 Hours

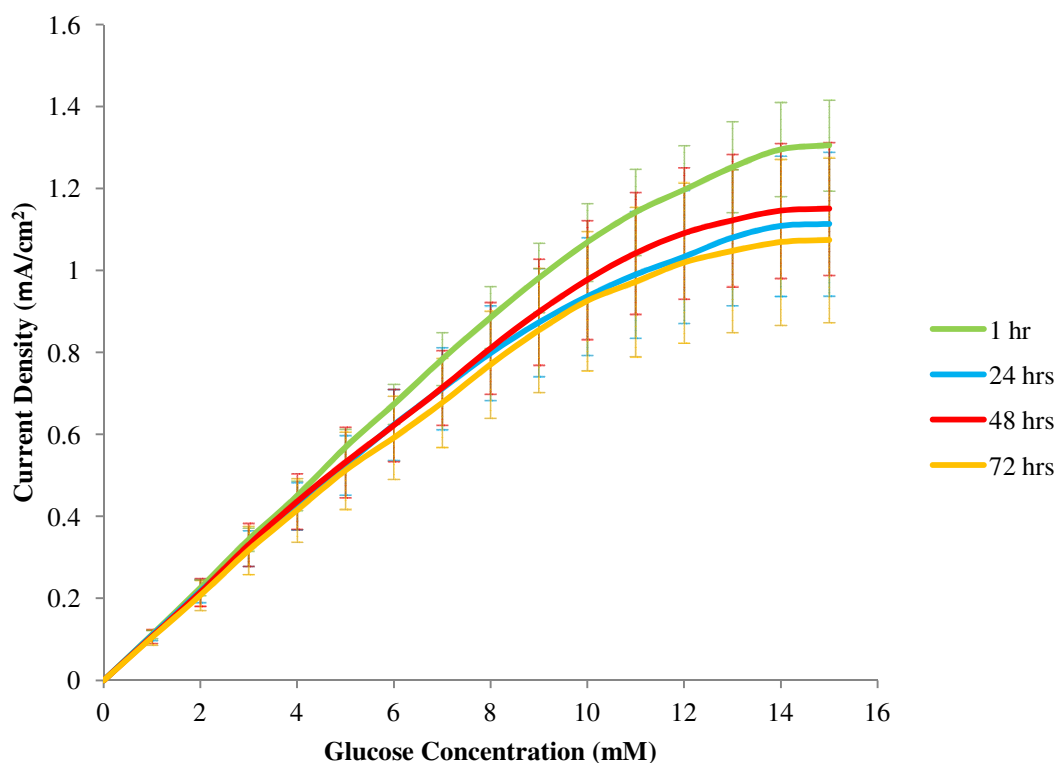


Figure 5.31. Average response of three 50 mC trans-3-(3-thienyl) acrylic acid copolymer films exposed to 6 hours of GOx and analysed over 72 hours.

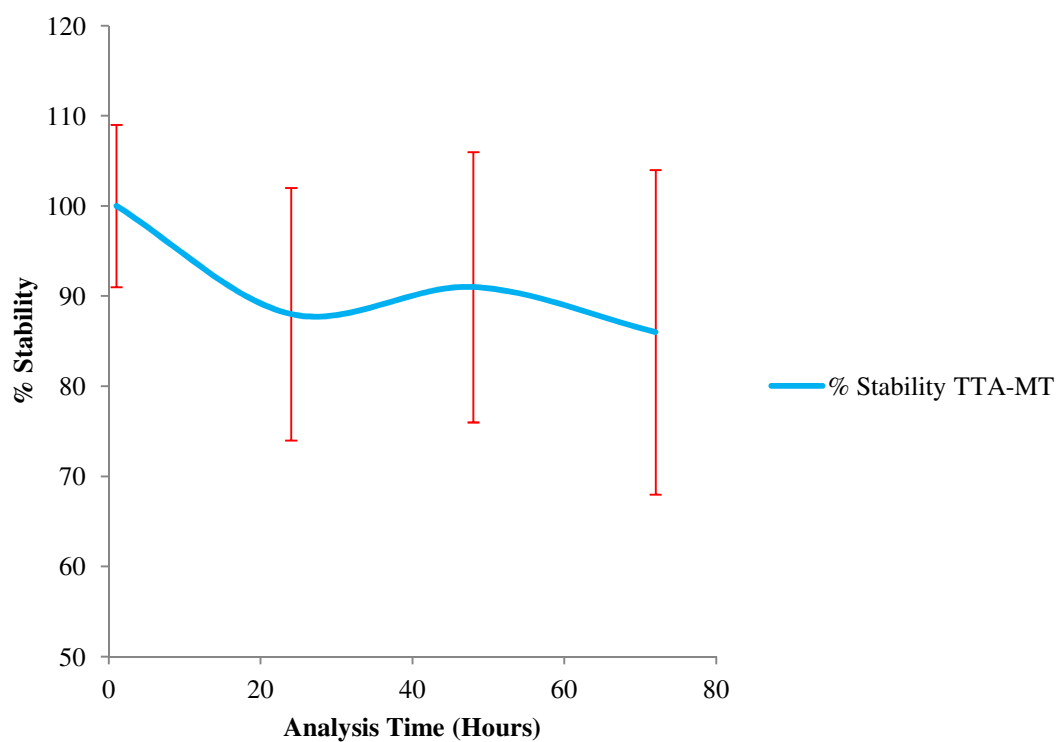


Figure 5.32. Average response of three 50 mC trans-3-(3-thienyl) acrylic acid copolymer films exposed to 6 hours of GOx and analysed over 72 hours.

Stability over three days at room temperature was good with 86% of the original signal retained after 72 hours. This stability study demonstrated the same level of precision for thiophene-3-acetic acid after 72 hours. Therefore stability over four days does not reflect the high error associated with the biosensor repeatability indicating successive measurements may have a large effect on the biosensor performance. Stability is further investigated over a longer analysis period of 28 days at 4 °C where a large decrease in current response is determined.

5.1.3.3. Stability Over Four weeks

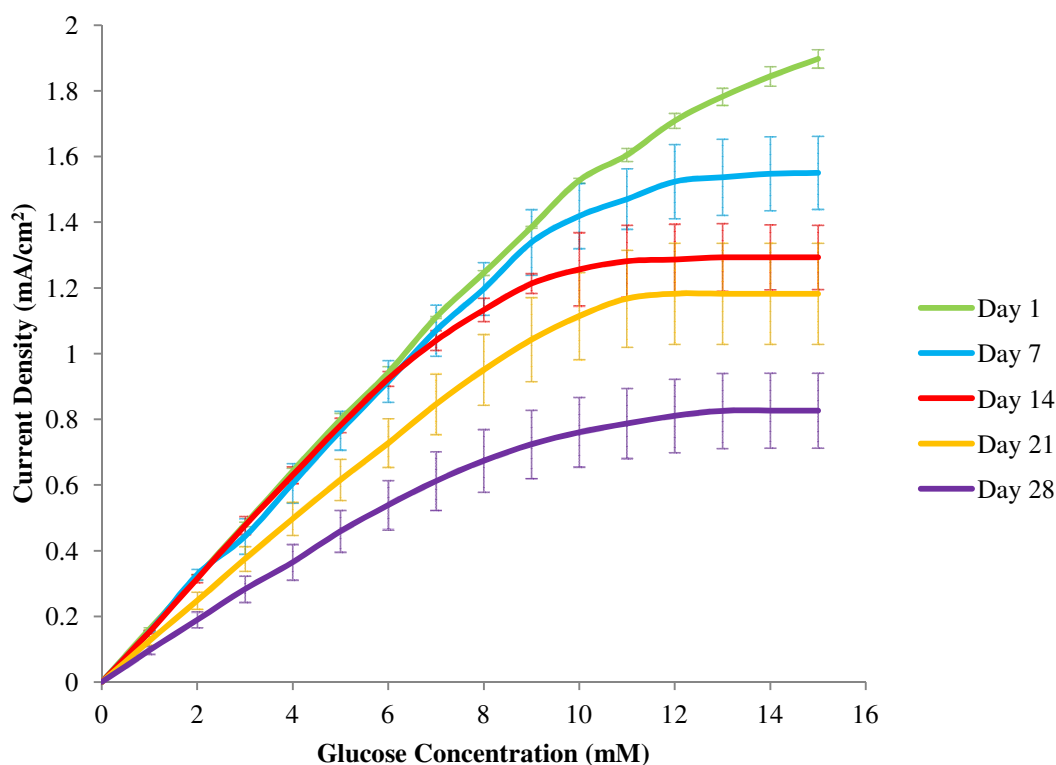


Figure 5.33. Average response for three 50 mC trans-3-(3-thienyl) acrylic acid copolymer films exposed to 6 hours of GOx and analysed over four weeks.

Stability is excellent at lower glucose concentrations where analysis is performed over two weeks as 96% of the original electrode signal is retained. However after 14 days stability of the enzyme electrode diminishes considerably as the current response calculated for 1-8 mM glucose additions decreased by approximately 20% by week three with a further decline of 20% by week four leaving the sensor with only 56% of its original performance. Large reductions in current response was also observed at high glucose concentrations where only 50% of the signal remained.

Table 5.11. Stability of the Trans-3-(3-thienyl) acrylic acid Copolymer Sensors
Analysed over Four Weeks.

TTA-MT	1 Hour	1 Week	2 Weeks	3 Weeks	4 Weeks
1-15 mM	100%	91%	82%	71%	50%
1-8 mM	100%	96%	96%	77%	56%

5.1.4. Investigation of The Novel N-succinimido trans-3-(3-thienyl) acetate and 3-Methylthiophene Copolymer

5.1.4.1. Repeatability and Reproducibility

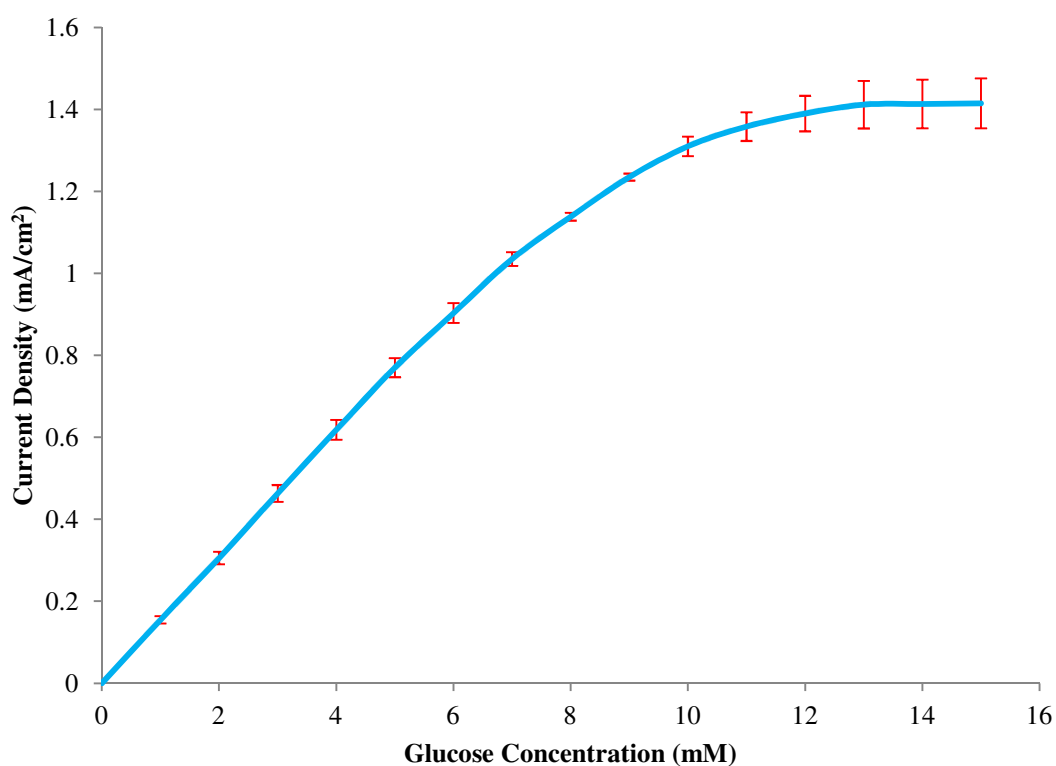


Figure 5.34. Repeatability of three 50 mC N-succinimido trans-3-(3-thienyl) acetate and 3-methylthiophene enzyme electrodes.

The repeatability error of the novel N-succinimido trans-3-(3-thienyl) acetate and 3-methylthiophene copolymer was calculated at 6%. Repeatability was affected with the introduction of the double bond linker chain compared to N-succinimido thiophene-3-acetate as the response variation doubled. Therefore the stability of the sensor between successive measurements was observed to decrease and may require an extended analysis period.

An error value of 11% RSD was calculated in which a 5% variation in reproducibility was established over the average of the two sets of three enzyme electrodes developed with the N-succinimido trans-3-(3-thienyl) acetate copolymer. The error was low and comparable to the trans-3-(3-thienyl) acrylic acid copolymer of 4% and may be related to the same structural properties of TTA affecting the sensor behaviour. The extension of the chain length between the polymer backbone and the enzyme provides enhanced access for the substrate potentially lowering signal variability associated with obstruction from the polymer material. Conjugation present in the linker chain should in theory facilitate electron transfer through the system generating better reproducibility.

5.1.4.2. Stability Over 72 Hours

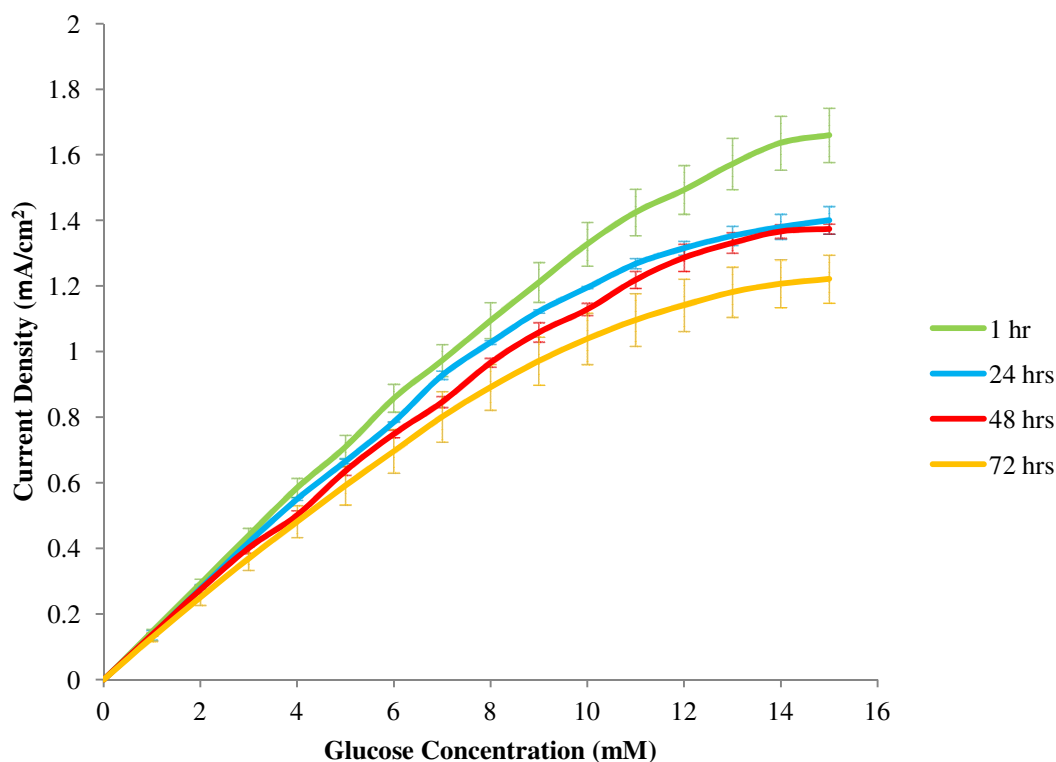


Figure 5.35. Average response for three 50 mC N-succinimido trans-3-(3-thienyl) acetate copolymer films exposed to 6 hours of GOx and analysed over 72 hours.

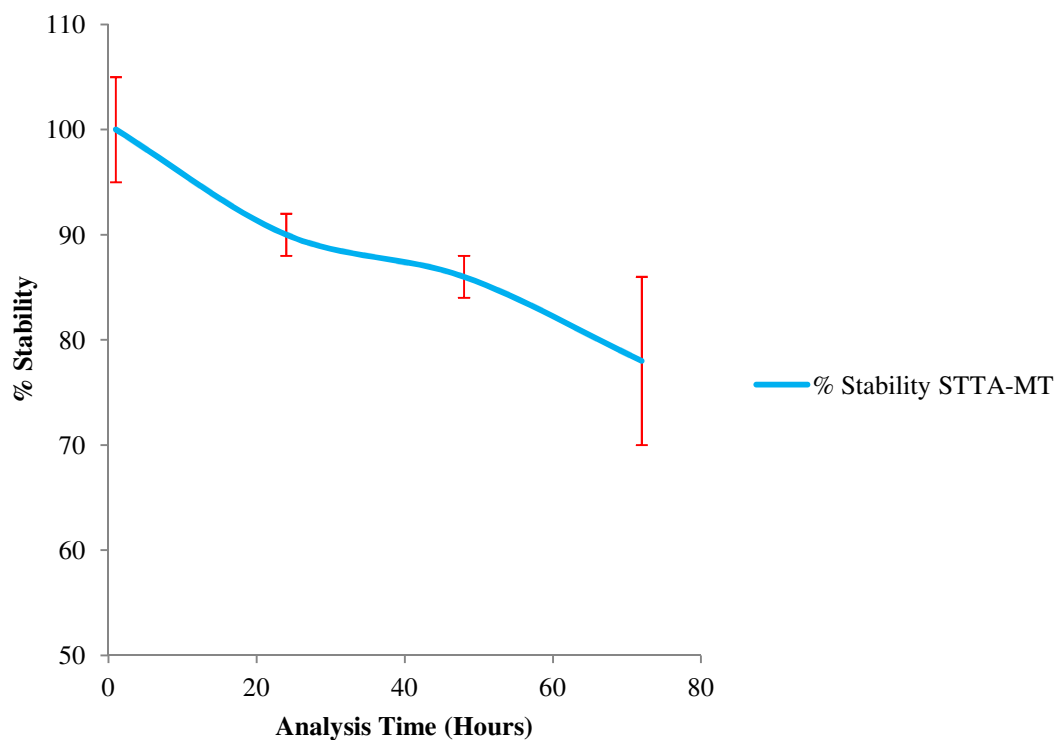


Figure 5.36. Average response for three 50 mC N-succinimido trans-3-(3-thienyl) acetate copolymer films exposed to 6 hours of GOx and analysed over 72 hours.

Over a 72 hour period signal response to glucose remained relatively high at 78% when stored at room temperature. This level of stability is comparable to the other biosensor formats demonstrating little difference in stability at this stage.

5.1.4.3. Stability Over Four Weeks

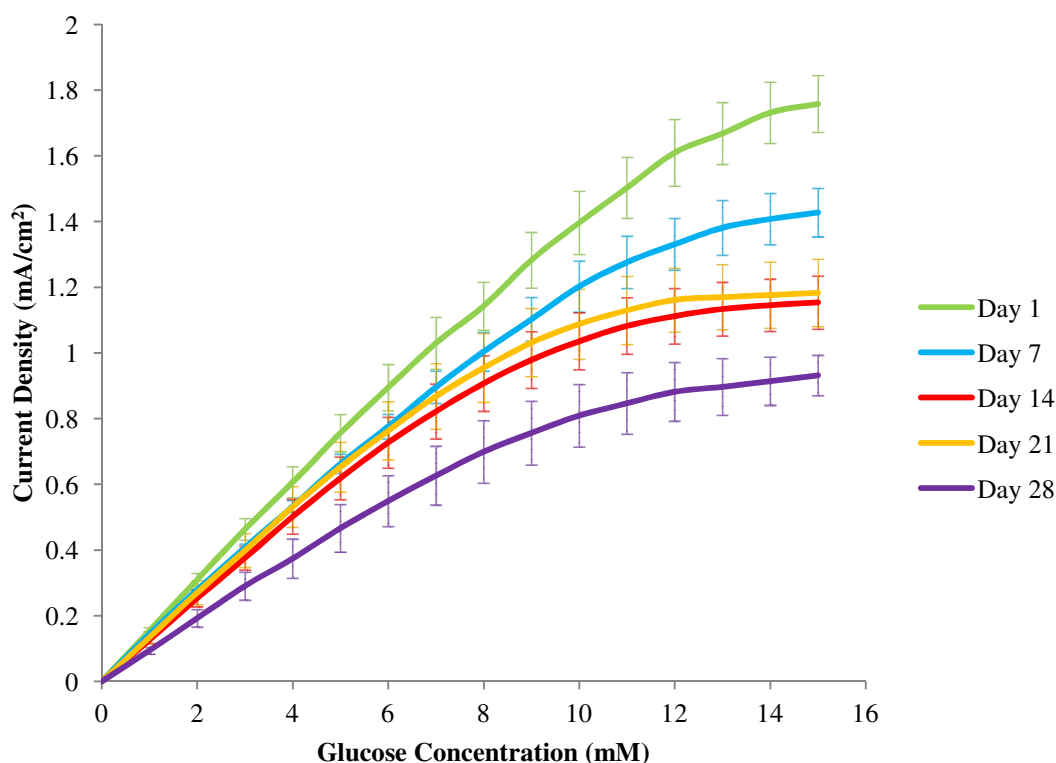


Figure 5.37. Average response for three 50 mC N-succinimido trans-3-(3-thienyl) acetate copolymer films exposed to 6 hours of GOx and analysed over four weeks.

After one month of storage in buffer solution at 4 °C and measurements taken every seven days a significant change in stability is observed. The stability decrease is large compared to the biosensor formats previously investigated and therefore was less able to retain enzyme activity over longer periods of analysis.

The same structural characteristics of the copolymer that seem to enhance the reproducibility may also be responsible for the decrease seen in stability. Although the extended chain allows the glucose oxidase to be easily accessed, the polymer matrix may not be able to provide the same degree of protection to the enzymes exposed position. Therefore bacterial growth is likely to denature the enzyme with less difficulty over the longer storage period.

Table 5.12. Stability of the N-succinimido trans-3-(3-thienyl) acetate Copolymer
Sensors Analysed over Four Weeks.

STTA-MT	1 Hour	1 Week	2 Weeks	3 Weeks	4 Weeks
1-15 mM	100%	85%	73%	77%	57%
1-8 mM	100%	88%	81%	85%	61%

5.1.5. Data Comparison of Each Biosensor System

Table 5.13. Examination of Data Obtained from a 10% Functional Monomer Content.

	Functional Monomer Copolymerised with Methyl Thiophene			
	STA	T3AA	STTA	TTA
Response after 15 mM. (mA/cm ²)	1.4 ± 13%	1.4 ± 14%	1.8 ± 10%	1.9 ± 10%
Stability after 24 hours at r.t. (%)	95% ± 4%	91% ± 8%	90% ± 2%	88% ± 14%
Stability after 3 days at r.t. (%)	83% ± 8%	86% ± 2%	78% ± 8%	86% ± 18%
Stability after 7 days at 4 °C (%)	89% ± 13%	96% ± 9%	85% ± 5%	91% ± 7%
Stability after 28 days at 4 °C (%)	75% ± 19%	78% ± 14%	57% ± 12%	50% ± 14%
Upper limit linear range (mM)	7	4	6	7
LOD (mM)	0.50 ± 0.1	0.53 ± 0.006	0.48 ± 0.15	0.50 ± 0.01
Response to Glucose (seconds)	3.8 ± 0.6	2.9 ± 0.5	3.1 ± 0.7	2.6 ± 0.6
Repeatability (%)	97%	94%	94%	90%
Reproducibility (%)	85%	84%	89%	90%
K _m	20 ± 7.5%	13 ± 8%	13 ± 5.5%	15 ± 5%
V _{max}	0.07 ± 7.5%	0.05 ± 8%	0.07 ± 5.5%	0.08 ± 5%

Table 5.13 demonstrates some interesting results with clear differences seen between the copolymers that incorporated the use of the extended double bond linker arm and the thiophene monomers that employed only a single methylene group between the ring and the functional species.

One apparent difference is the current response generated with the extended side group associated with the trans-3-(3-thienyl) acrylic acid. This can be observed below in figure 5.38 where the reproducibility errors for the two copolymer series are clearly isolated demonstrating the effect of the structure upon the enhanced signals seen.

The difference in current response between the two copolymer structures including the variability associated with the error was calculated at 14%. This demonstrated a significant difference in the biosensor performance with the copolymers bearing the double bond linker producing enhanced response to glucose.

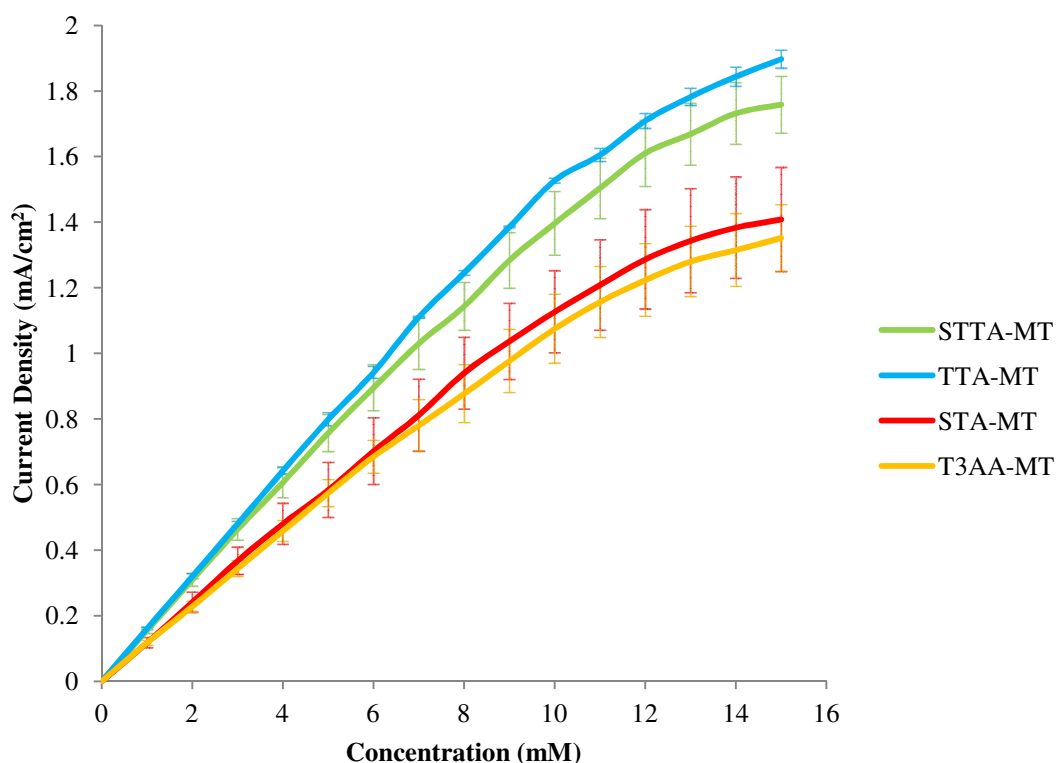


Figure 5.38. Average response to glucose for four different copolymer materials containing approximately 10% enzyme binding sites.

The influence upon reproducibility can also be observed as the error produced was low between the biosensors that incorporated the double bond linker. Both current

response to glucose and reproducibility are important within biosensor systems and although all the copolymer materials studied provided workable formats the introduction of an extended double bond linker between the polymer backbone and the biological recognition element enhanced these properties which are desirable within a biosensor device.

Repeatability was good for all biosensor formats achieving 90% and above for three repeat measurements carried out in succession on the same day. However a noticeable decrease in repeatability was observed with the STTA-MT and TTA-MT copolymers compared to the STA-MT and T3AA-MT formats. It was concluded that successive analysis upon these biosensors significantly affected the biosensor performance and therefore in future measurements for repeatability should not be taken immediately after each analysis.

Stability of the biosensors was investigated over two experiments in which both demonstrated good response throughout the analysis period. The first stability experiment monitored response to glucose over 72 hours with biosensor storage in phosphate buffer at room temperature. The second stability study was carried out over an extended period of time of four weeks where the enzyme electrodes were stored at 4 °C. By storing the sensors in the fridge in between analysis the stability of the enzyme electrodes were extended. The enhanced stability at 4 °C compared to the investigation at room temperature is observed after seven days. Although stability for the four biosensors over four weeks was good a significant difference was seen between the two copolymer formats. A noticeable decrease in stability was identified for the copolymers supporting the double bond linker where approximately only 50% of the signal was retained after four weeks compared to over 70% for the single methylene linker. The substantial loss in signal after 28 days was associated with the difference in enzyme location from the main polymer matrix. It is assumed that the increase in access to the enzyme will assist enzyme-substrate complex formation producing efficient signal detection but will be susceptible to denaturation from bacterial growth. Therefore reproducible results may be obtained but at the cost of long term stability.

Glucose response times were all below four seconds with signal stabilisation occurring within 90 seconds. The rapid response to glucose and short intervals between measurements demonstrated a practical biosensor system.

The working linear range for most formats was good only T3AA-MT displayed a narrow range to 4 mM. The extended linear range is likely to be formed through slow diffusion of product to the electrode surface. Diffusion limitation is generated through the use of thicker films or less porous material which exerts a certain degree of control over product diffusion. Due to the build up of product a steady response to glucose is obtained allowing the biosensor to perform over a larger concentration range. As only one of the copolymers is affected by a narrow linear range it is likely that the morphology of the copolymer materials is responsible. As T3AA bears the smallest substituent it is possible that the resulting morphology does not impede diffusion of the product therefore extension of the linear range is not observed.

The limit of detection was performed for each biosensor and was defined as the concentration of glucose that gave a signal equal to three times the noise level of the baseline. The limit of detection for all biosensors analysed were comparable where approximately 0.5 mM provided the lowest concentration of glucose accurately measureable. Large background currents were present in all biosensor investigations and are generally associated with the conducting nature of the film. As the measurement of glucose was performed at a low potential where the thiophene copolymer is mainly in a reduced form the large background currents could not be generated entirely by the polymer film. Overoxidation of the film is reported to improve the detection limit by reduction of the background current which was attempted but did not significantly decrease the background signal. The heavy baseline noise that was still present may be explained by the mechanical stirring of the solution possibly vibrating the electrode.

Kinetic data for the biosensor systems are displayed in table 5.13 in which the maximum reaction rates V_{\max} and the apparent Michaelis constants K_m are determined from Hanes plots where substrate concentration was divided by the initial velocity (current values). The clear difference observed across all the apparent K_m values was the value obtained for the N-succinimido thiophene-3-acetate and 3-methylthiophene

copolymer. The Michaelis constant for this copolymer was larger than the other K_m values for the other biosensor systems and can be attributed to the limited accessibility of the substrate to the active sites of the immobilised enzyme. Although all the copolymer matrices cause this same affect the morphology of the film may help to explain the observed behaviour. Upon examination of the polymer topography through scanning electron microscopy the copolymerisation of N-succinimido thiophene-3-acetate and 3-methylthiophene looked to provide a more compact film with fibrillar structure seen in figure 5.39. Without the aid of the extended link between the thiophene ring and the binding site the immobilised enzyme was possibly trapped within the dense structure leading to difficulty accessing the enzyme. The thiophene-3-acetic acid copolymer produces a more porous structure and the trans-3-(3-thienyl) thiophene species provided the extended link both allowing easy access to the glucose oxidase and generated lower apparent K_m constants.

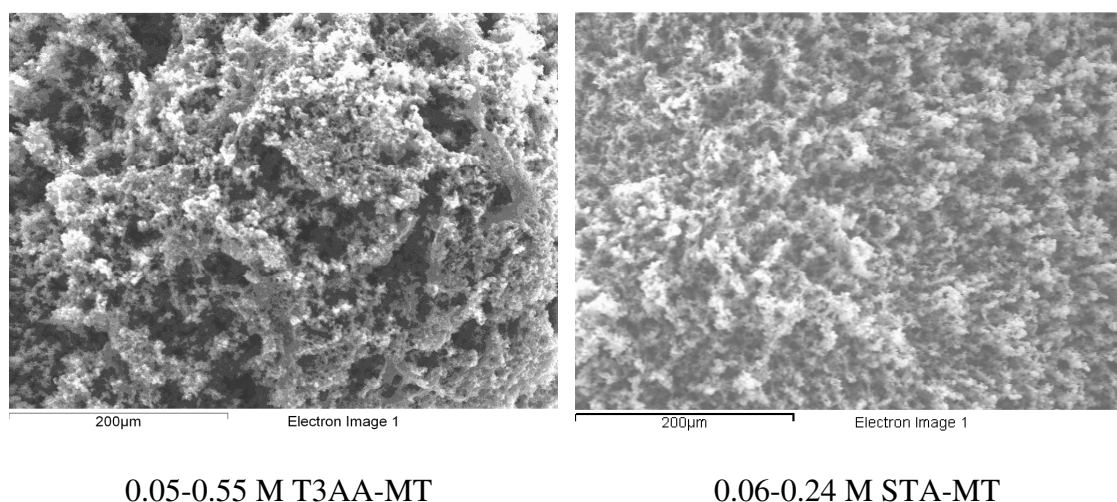


Figure 5.39. SEM pictures comparing the two copolymer morphologies grown with TBATFB at 2.2 V at X250 magnification.

5.1.6. Effect of Temperature and pH upon the Sensor Response

All copolymer formats were investigated for the effect of pH and reaction temperature upon the biosensor performance. The average response of the glucose additions (1-15 mM) were plotted against a temperature range of 30 to 70 °C and pH values 4 to 9.

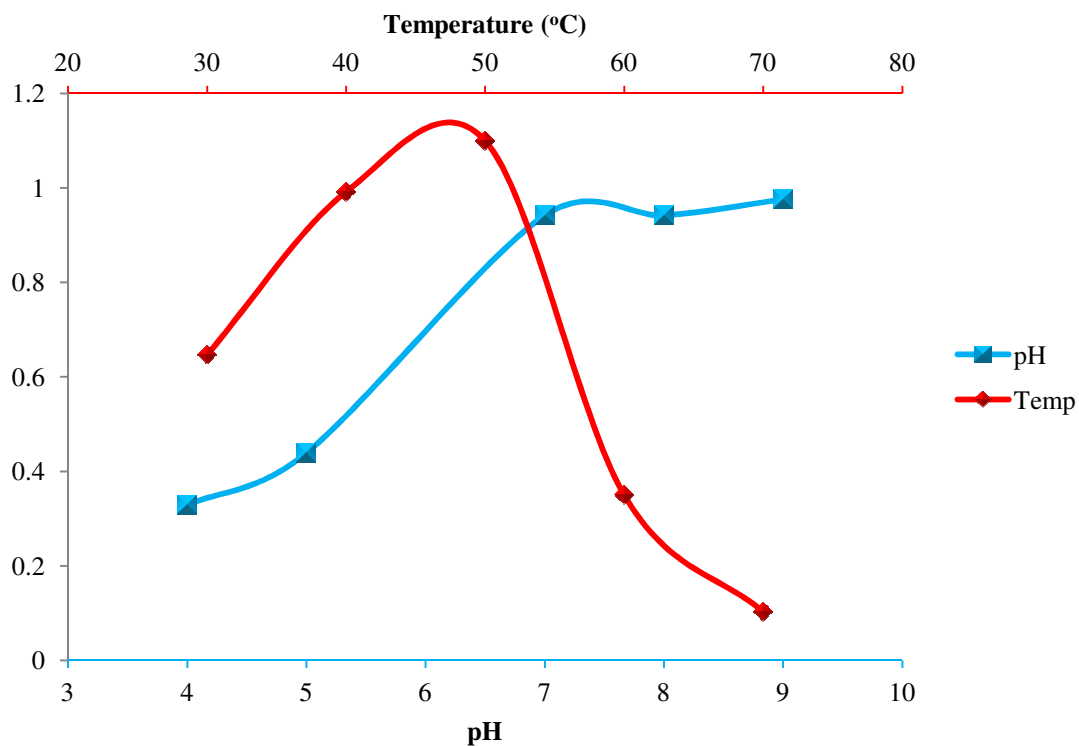


Figure 5.40. Affect of temperature and pH upon the average sensor response of N-succinimido thiophene-3-acetate and 3-methylthiophene copolymer.

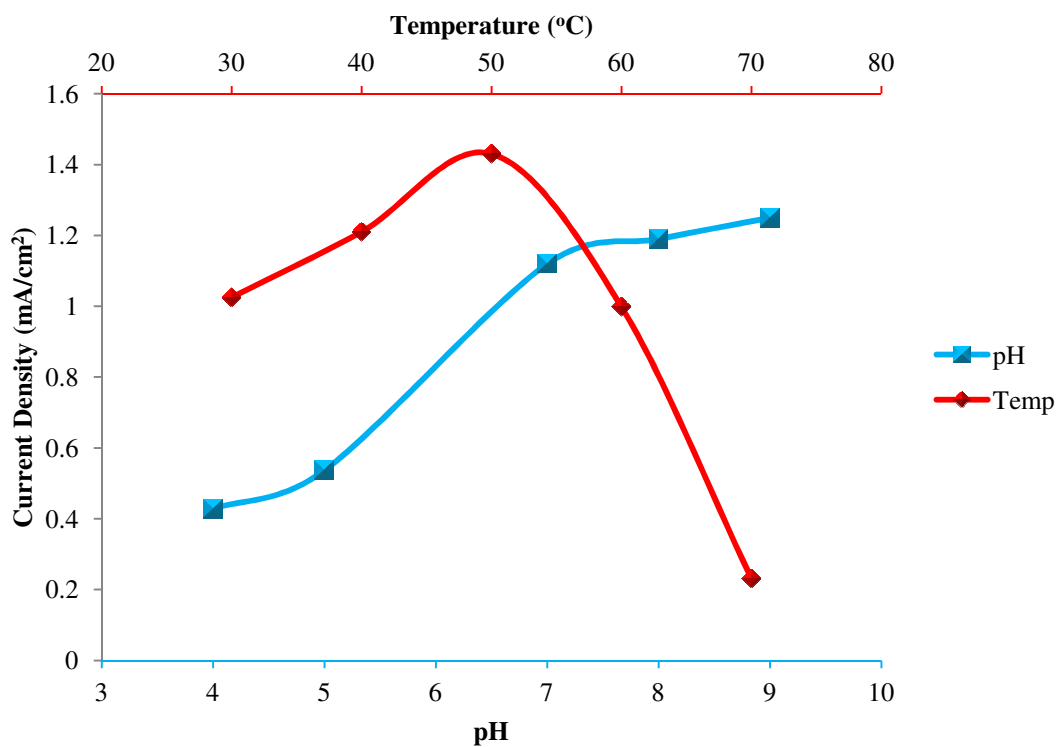


Figure 5.41. Affect of temperature and pH upon the average sensor response of 3-thiophene acetic acid and 3-methylthiophene copolymer.

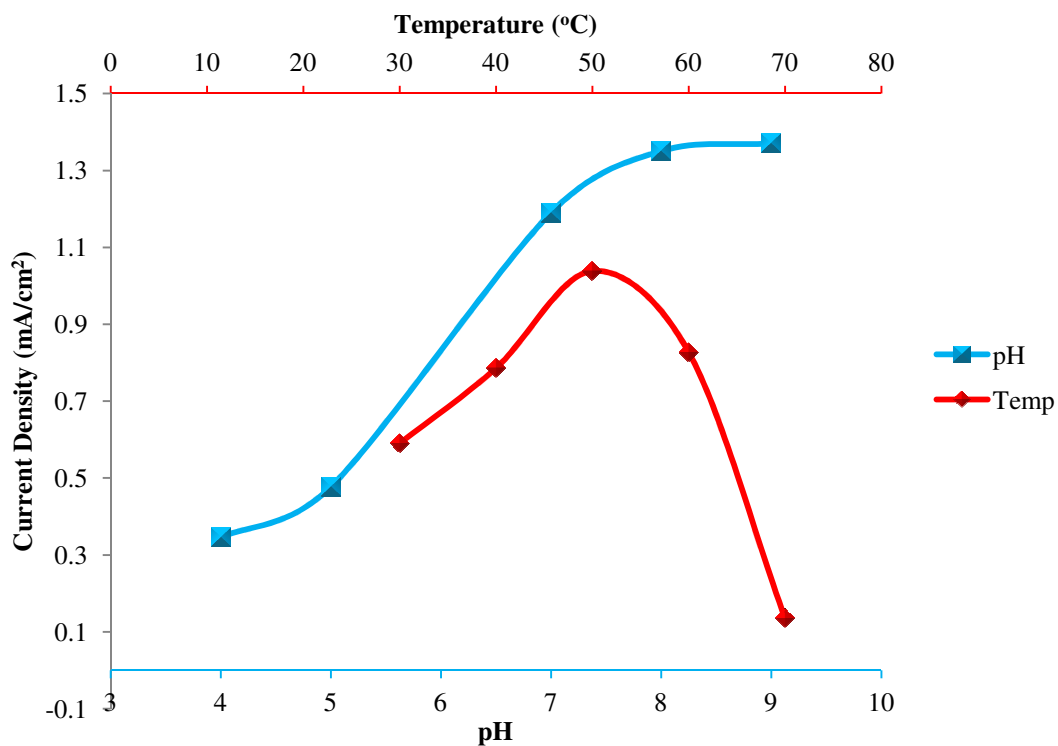


Figure 5.42. Affect of temperature and pH upon the average sensor response of N-succinimide trans-3-(3-thienyl) acetate and 3-methylthiophene copolymer.

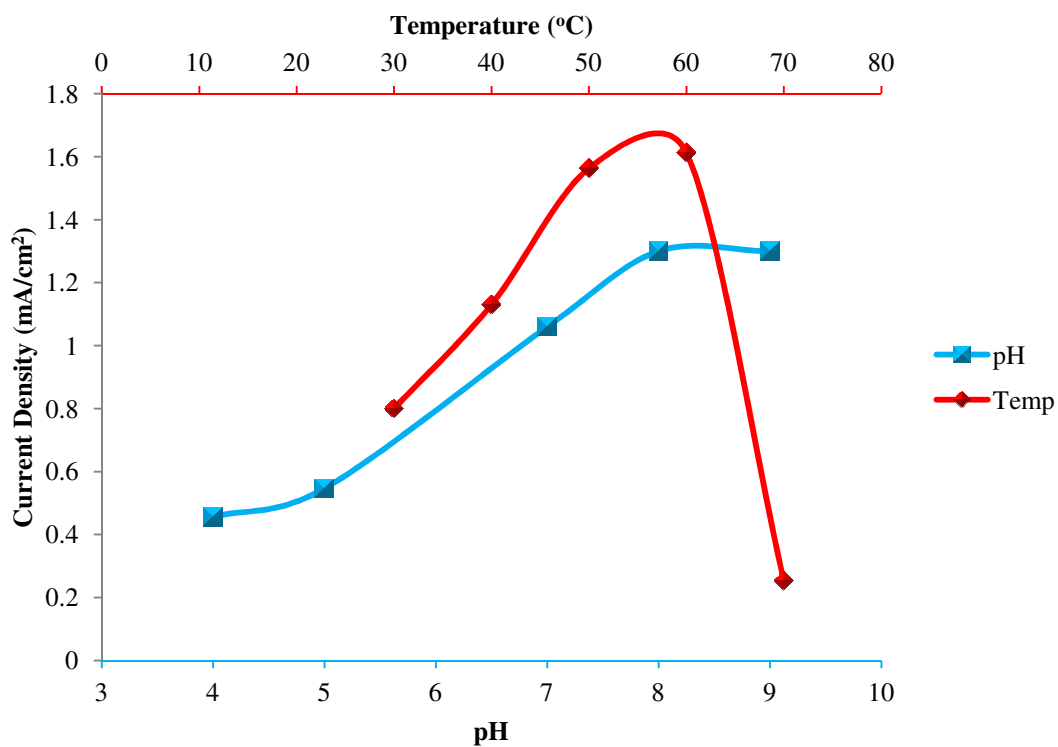


Figure 5.43. Affect of temperature and pH upon the average sensor response of Trans-3-(3-thienyl) acrylic acid and 3-methylthiophene copolymer.

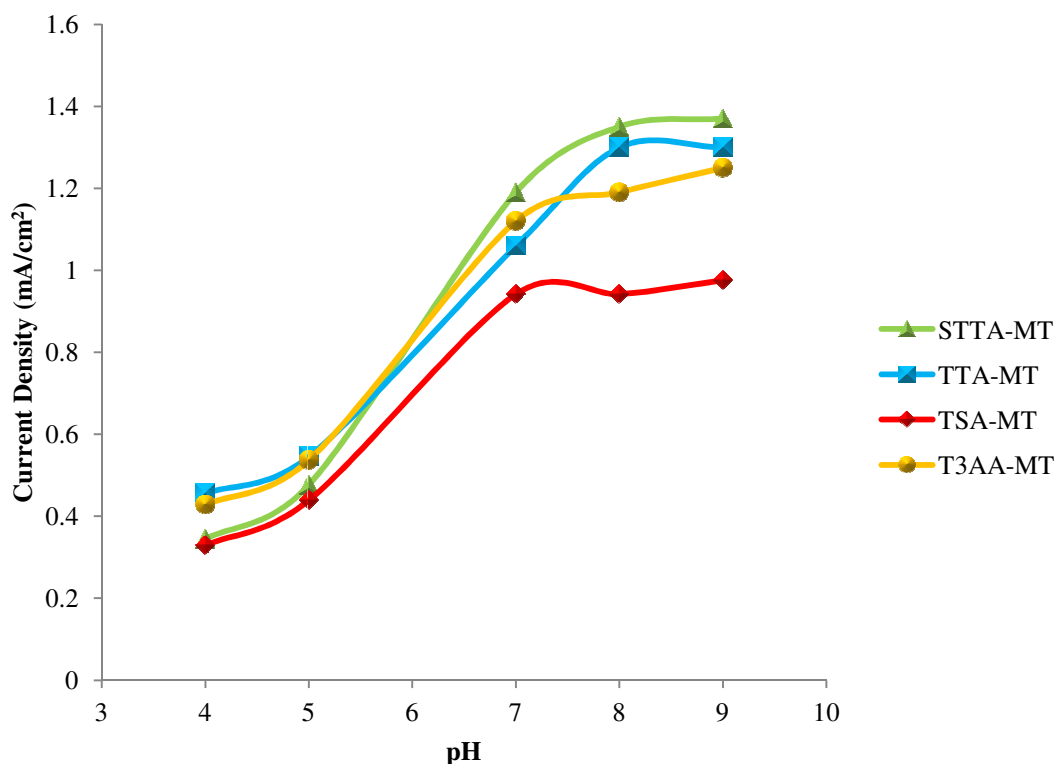


Figure 5.44. pH comparison of the four biosensor formats.

The pH and temperature profiles are separately combined for the four different biosensors. The pH profiles for the four biosensors demonstrate the optimal and stable current signals generated through the change in pH. Each enzyme has an optimum pH where it demonstrates its highest activity however this value often differs from an enzyme in solution to one which is immobilised and for fast response times it is advised to use the optimum pH¹⁹⁸⁻¹⁹⁹. The biosensor system may however perform poorly at such pH values and it is important not to force the enzyme system to conform with the requirements of the sensor as this may lead to loss in activity and instability where high pH values are employed¹⁵⁸.

Figure 5.44 shows that the T3AA-MT and STTA-MT copolymers provide an optimum working range across pH 7 to 9. The optimum pH shifts to more positive pH values of 8 and 9 when the TTA and STTA copolymers are analysed. pH shifts to higher values have been explained by the negative charge associated with the matrix. Yamauchi *et al.*, explains the shift in pH through the presence of residual carboxyl groups in the T3AA-MT copolymer¹⁵² which can also be attributed to the novel copolymer system of TTA-MT. Another possible source of negative charge could potentially include the increase in electron density provided by the double bond linking group²⁰⁰. The

increase in electronegativity from either source may attract a high concentration of positively charged ions (H^+) and due to the lack of polymer oxidation at +0.4 V the ions will migrate in the vicinity of the matrix and solution boundary influencing a drop in pH compared to that of the bulk solution²⁰⁰⁻²⁰¹. In this case the apparent pH of the enzyme can be increased as the pH environment surrounding the enzyme is in fact much lower²⁰¹.

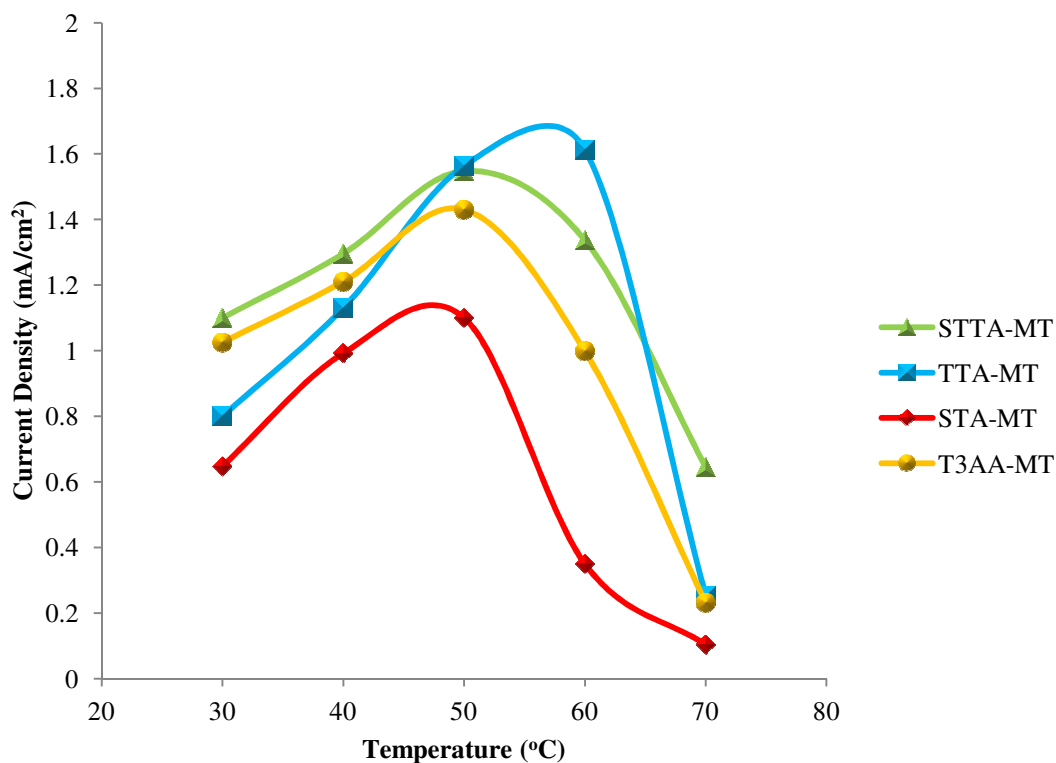


Figure 5.45. Temperature comparison of the four biosensor formats.

Immobilisation is reported to enhance the stability of the enzyme when influenced by extreme conditions it is reported that the inactivation of free glucose oxidase occurs at lower temperatures^{48,201}. Immobilisation on different biosensor formats showed maximum current response is influenced by different temperatures. Overall an increase in current response was seen upon higher working temperatures of the enzyme sensors. Optimum current signals were achievable approximately between 50-60 °C but rapidly decreased with increase in analysis temperature. A subtle increase in optimum temperature was seen for the copolymer systems in the order; STA-MT, T3AA-MT and STTA-MT as they approach 50 °C. TTA-MT demonstrated a higher response to glucose over a broader temperature range from 50 °C and reached

maximum response at approximately 60 °C. All biosensors exhibited rapid loss of signal when analysed at 70 °C with most formats representing less than 15% of the optimum signal.

The four biosensor formats demonstrated improved response to glucose over higher pH and temperature. The enhanced stability is associated with the covalent immobilisation on the polymer matrix restricting the unfolding of the protein which destroys the enzyme activity. Therefore extreme conditions can be tolerated up to a certain degree before the biosensor becomes inoperative.

Chapter 6 Conclusions

This section of the report aims to outline the key objectives that were the focus of this research project and to describe the methods implemented to achieve these goals. Each chapter of the report has been summarised in detail and conclusions have been drawn based upon the findings determined from the experimental data and supporting information from the literature.

The intension of this study was to develop and evaluate a range of biosensor systems incorporating novel conducting thiophene derivatives for the covalent immobilisation of enzyme species. The aim was to improve the biosensor performance with specific consideration to the reproducibility of the biosensor format and its lifetime. The biosensor was based upon the well documented and familiar glucose oxidase system for the amperometric detection of glucose.

Biosensors have a huge potential which is yet to be fully achieved in areas such as diagnostic, industrial and environmental analysis. The combination of selectivity and sensitivity within a portable and robust device remains in demand however improved systems are desirable where the boundaries of such devices need to be pushed to their limits and therefore biosensors continue to be researched.

Conventional biosensor formats generally incorporate crosslinking, covalent binding or entrapment within a gel or behind a membrane for the immobilisation of biological species. The problems generated within such fabrication techniques involve uniform enzyme loading and poor reproducibility¹¹¹. Conducting polymers provide a promising material for biological attachment due to their intrinsic properties and their wide scope for adaptation. Their conducting nature allows the precise generation of polymer controlling the size and shape of the immobilisation platform and the thickness through the electrode dimensions and amount of current applied to the electrochemical cell by simply switching on and off the electrical supply. Furthermore conductivity within the biosensor structure has generated improved biosensor performance in terms of the speed and magnitude of the current response to substrate and the ability to entrap the biological recognition element in a single electropolymerisation process distributing the biological species throughout the polymer matrix.

Various conducting polymer formats have been investigated for their application in biosensor devices many of which have provided promising results. Polypyrrole and PEDOT have been studied extensively due to their solubility in aqueous solution. This provides the advantageous properties previously mentioned for entrapping the biomolecule within the generation of the film. However polypyrrole has a low oxidation potential and is known to undergo film degradation as a high potential is needed for the detection of hydrogen peroxide¹⁸. Also polypyrrole has few commercially available derivatives making manipulation more difficult and therefore introducing desirable qualities into the polymer structure is not a simple process¹³⁷. PEDOT belongs to the thiophene family and unlike most thiophene compounds is soluble in aqueous solution. This has enabled the thiophene conducting polymers to be more adaptable and extensively studied where entrapment of the biomolecule is possible. Although a one step process is achieved and enhanced stability is observed due to the higher oxidation potential of the polymer⁹² disadvantages of the PEDOT system are recognised. Covalent immobilisation of biological compounds upon the polymer backbone cannot be pursued due to both beta positions on the ring being occupied. Although this has been reported to increase the regioregularity and hence conductivity within the film, as defects such as alpha-beta linkages are avoided, long term biosensor stability is problematic as entrapment suffers from enzyme leaching. Covalent attachment is the method that provides enhanced biosensor lifetime and is an important feature of a biosensor device required to perform multiple analysis⁴⁹.

The enzyme immobilisation copolymer thiophene-3-acetic acid and 3-methylthiophene was included in this study for comparison as this enzyme system has been reported to demonstrate good biosensor performance⁵⁰⁻⁵⁴. The parameters were followed closely to the literature in order to establish a working biosensor system. Alterations to the method were made when the activated ester STA-MT copolymer exhibited improved response. As a result both biosensor formats were prepared with the same consideration ensuring compatibility.

Several copolymer formats were proposed for the generation of novel immobilisation matrices within a biosensor system. N-succinimido thiophene-3-acetate and 3-methylthiophene was the first proposed copolymer. The N-succinimido thiophene-3-acetate monomer represents an activated ester which rapidly loses the ester group

upon reaction with an amide such as the lysine residues surrounding the enzyme glucose oxidase. The peptide bond formed is a covalent attachment imparting enhanced stability between the biomolecule needed for substrate recognition and the polymer matrix. It was expected that efficient immobilisation would take place through the activated species reducing the long immobilisation times generally observed. A different thiophene derivative was chosen trans-3-(3-thienyl) acrylic acid in which the spacer arm separating the carboxylic acid functional group from the monomer ring was one methine group longer and incorporated a double bond. This functional monomer was copolymerised with 3-methylthiophene and was expected to generate improved amperometric response to glucose due to enhanced conjugation affecting the conductivity of the film and higher reproducibility due to the longer spacer arm influencing facile enzyme-substrate complex formation. The same improved responses were envisaged for the activated ester synthesised from the trans-3-(3-thienyl) acrylic acid with possible changes to the biosensor behaviour potentially influenced by morphological differences between the copolymer films developed with monomers of different spacial requirement.

Chapter three demonstrates the electrochemical characterisation of various conducting polymer films. Cyclic voltammetry was mainly used to generate even polymer films upon a platinum electrode surface from a bithiophene solution containing a dopant. Using the same electrochemical technique the redox properties of the resulting films were probed gaining valuable information upon the reversible nature of the polymer and the ease of polymerisation and subsequent polymer oxidation.

From the bithiophene study it was concluded that thin films were required in order to successfully characterise the material which generally involved one full potential cycle. Slow scan rates of 20 mV s^{-1} enhanced the details associated with the redox processes of the film and provided better comparison to other polymer characterisations. The influence of solvent and dopant were investigated and acetonitrile with LiClO_4 for film growth and TBATFB for film characterisation generated the largest current responses upon cycling the potential and were therefore implemented for the rest of the study unless otherwise stated.

Bithiophene provided a good starting compound to develop the electrochemical methods required to obtain successful polymer characterisation. The alkyl substituted thiophene monomers generated a good understanding of the electrochemical properties associated with the extension of the linear alkyl chain in the beta ring position. It was determined that increasing the alkyl chain increased the polymerisation potential of the monomer in which higher potentials were also observed for the oxidation of the resulting polymer film. This is associated with the difficulty of polymerising a monomer with a large side group due to obstruction of the alpha reaction site. The same steric hindrance is responsible for high polymer oxidation potentials as anion movement through the matrix is restricted. Flexibility of the film aids the intercalation of the anions providing charge neutrality whilst doping the polymer. Therefore 3-methylthiophene having the shortest alkyl substituent provided low polymerisation and film oxidation potentials, its affordability and reported conductivity all desirable for further study within a copolymer format.

The determination of functional monomers capable of covalent immobilisation were investigated these included T3AA, STA, TTA and STTA. The functional compounds all presented polymerisation difficulties with TTA and STTA homopolymerisation prevented by low solubility. Both T3AA and STA were successfully polymerised employing elevated potentials and increased monomer concentration to overcome the steric and inductive effects of the functional substituent. Although polymer films were generated characterisation of the redox processes produced undesirable film properties. High potentials were required to oxidise both T3AA and STA polymers with T3AA demonstrating irreversible damage to the polymer alignment due to forcing dopant into the polymer matrix. The following reduction response is therefore much smaller indicating the difficulty of anion expulsion due to the possible structural change to the film. STA bears a larger functional group in which the steric influence is observed upon characterisation as there is complete absence of a reduction response possibly affected by poor dopant release from the polymer film.

Copolymerisation was investigated as a method of incorporating functional monomers with polymerisation difficulties into a polymer film. Furthermore the homopolymers of T3AA and STA associated with undesirable film properties were easily modified by the incorporation of the simple 3-methylthiophene monomer. Ultimately

copolymerisation provided a method of controlling the percentage of functional units in the film. This demonstrated an effective technique that generated a series of copolymer ratios where cyclic voltammetry clearly illustrated the significant influence of the functional monomer content upon the electrochemistry of the film.

3-methylthiophene provided beneficial properties desirable within a copolymer material for the support of a functionalised thiophene monomer ready for enzyme immobilisation. A low polymerisation potential of +1.35 V provided readily available radical cations aiding copolymerisation of the problematic monomers of T3AA, STA TTA and STTA. A low polymer oxidation of +0.8 V influenced the corresponding copolymers generating reduced polymer oxidation and stable copolymer films demonstrating reversible redox processes.

The bulky functional groups copolymerised with 3-methylthiophene were effectively alleviated as the steric influence associated with the material was diluted. Oxidation of the film became easier indicated by the increasingly low oxidation potentials of the copolymers supporting less functionality. A 10% functional content associated with T3AA and the STA monomer provided enhanced current response which is reported to provide improved biosensor performance by Kuwahara *et al* and confirmed within the biosensor analysis chapter of this study. 10% TTA and STTA functionality was achieved although low solubility was an issue. The oxidation potentials of the films demonstrated that the ester monomers required higher positive potentials due to the steric hindrance imparted by the very bulky substituent. The similar oxidation potentials of the carboxylic acid substituted copolymers suggests that steric effects in this case do not dominate the electrochemistry of the film as lower potentials are not observed for the TTA monomer contributing the extended linker chain.

Thiophene compounds have been successfully investigated using electrochemical techniques to generate polymer films and to determine their stability for their use as an immobilisation platform within a biosensor device. Copolymerisation with 3-methylthiophene enabled the incorporation of various functional thiophene monomers generating the stable films necessary for enzyme immobilisation and therefore provided an important method to optimise enzyme loading for the biosensor system.

Functional monomer content was the next important investigation into the development of a workable biosensor format which was evaluated in chapter 4. The calculation of copolymer ratio and dopant content was successful with information gathered upon the morphological composition and evidence of covalent binding on the functionalised films.

Functional group content was investigated as it was important to identify the amount of available reaction sites for enzyme attachment. Various monomer ratios were investigated for T3AA-MT and STA-MT and used for polymerisation and elemental analysis. The percentage compositions from the resulting films were successfully determined providing a range of T3AA content where the highest and lowest monomer percentage ratios in the polymerisation solution were approximately 80% and 10% respectively. The functional monomer content for T3AA in the resulting copolymer was therefore 10-53% and STA content provided a range of 6-26% .

The findings concluded that the functional monomer content in the copolymer film was significantly lower than the percentage ratio in the monomer mixture. Similar conclusions were made by Shimomura *et al* upon the investigation of the copolymer ratio T3AA-MT¹⁴¹. In this case IR was employed with the KBr disk method to calculate the T3AA content. The absorbance corresponding to the stretching of the carbonyl groups allowed the T3AA percentage to be determined. Again a smaller percentage ratio of T3AA was determined in the copolymer film compared to the polymerisation solution however the difference was considerably lower than the findings in this report. A deviation from this relationship was observed for the T3AA-MT copolymer where a percentage content of over 8% was used in the monomer mixture and a higher 10% content was calculated in the copolymer film. In all other cases where higher T3AA concentrations were introduced large differences in T3AA content was seen between the monomer solution and resulting copolymer. This was supported by IR data obtained through the determination of the carbonyl absorbance using the ATR attachment. Copolymer films with high functional group content were successfully analysed where a T3AA ratio of 83.3% in the monomer solution gave a 45% T3AA content in the copolymer. Analysis of further copolymer compositions was unsuccessful due to the low concentration of carbonyl groups on the polymer surface. Therefore the difference in T3AA content reported here and in the work of

Shimomura *et al* can be explained through the different methods used for the investigation.

The samples obtained for characterisation were grown as thick films this was necessary in order to be able to extract the polymer material from the electrode surface however in most cases the thick films were difficult to grind. Due to the durable films produced and the method used, characterisation was limited to the polymer film surface. Elemental analysis employing SEM-EDX will only detect surface composition to a depth of a few microns and similarly IR (ATR) generates a small penetration depth between 0.6-2.0 μm and therefore confirms the same T3AA percentage²⁰²⁻²⁰³. Shimomura *et al* used IR (KBR-disk) allowing the T3AA content to be determined throughout the sample therefore as analysis was not surface restricted higher T3AA content was calculated in all samples. The calculation of the functional species content in this study was important for the determination of an optimised composition for use within a biosensor format. As enzyme immobilisation is only considered to take place on the polymer surface¹³⁰⁻²⁰⁴ the percentage compositions calculated can potentially be related to the percentage occupancy of enzyme essential for the response current generated. Therefore a more accurate determination of enzyme loading was established with elemental analysis providing a quick, non destructive technique that required minimal sample preparation and time.

The novel copolymer system STA-MT was also investigated for the generation of various copolymer compositions. Due to the synthesis procedure lower concentrations were employed in order to reduce the number of reactions and therefore sample batches that were used in the study. A total concentration of 0.3 M was used which was half that of the T3AA-MT system. The lower concentrations used did not show any adverse effects upon film formation or biosensor performance compared to the copolymer systems employing higher total concentrations. The influence of lower monomer concentration has been reported where a total concentration of only 0.12 M was used. This was described for a T3AA-MT copolymer by Liu *et al* in which slight morphological changes were reported and biosensor performance suffered where low polymerisation currents of 2 mA were implemented⁵⁰. Although the polymerisation currents generated for film formation in this study were considered low 1-3 mA the total concentration of the monomer solution at 0.3 M was sufficient for achieving a

good range of copolymer ratios. The difference observed for the generation of the novel copolymer films was associated with a lower functional group content compared to the copolymer films of T3AA-MT. All monomer solutions containing 40% STA and above provided less than half the STA percentage content in the resulting copolymer films. At 80% STA monomer content only 26% activated ester sites were generated compared to over 50% for the T3AA functional monomer. This can be explained by the size of the functional group attached to thiophene ring. The carboxylic acid group is much smaller than the ester formed by the N-hydroxysuccinimide reagent and therefore polymerisation is not heavily restricted by its obstruction to the alpha carbon reaction site. Steric hindrance is however associated with the ester monomer due to its large size and short spacer leading to polymerisation difficulties and therefore lower STA content.

Doping of the conducting films provided interesting results. SEM-EDX was used for the determination of fluorine as TBATFB was the electrolyte chosen for film growth within this study. The copolymer films bearing carboxylic acid groups demonstrated an increasing dopant inclusion as the percentage content of T3AA decreased. Several explanations have been determined for this phenomenon in which results have been found to support the doping difficulties of the T3AA monomer. The work of Shimomura and Kuwahara⁵⁴ demonstrated the use of UV analysis upon 100% T3AA polymer films in doped and dedoped condition. Interestingly the same spectra for both doped and dedoped polymers were determined and was suggested that doping of the films was prevented by the carboxyl groups. In addition self doping and weak side arm rigidity have been postulated for low dopant levels which are explained in the following paragraphs.

Self doping of the T3AA compound is reported to be generated through the COO⁻ species covalently bound to the ring. The calculated dopant / thiophene ratio for the T3AA-MT copolymer range in chapter 4, table 4.2 demonstrates this well. As the ratio of T3AA groups increase more COO⁻ species are likely to be associated with the polymer. The negative charge required to neutralise the film upon oxidation is therefore provided by the COO⁻ species causing a decrease in the anion content from the electrolyte to be seen. Although doping was low until approximately 10% T3AA content was established, the same dopant content was not observed for the TTA

copolymer. A slightly higher doping level of 0.5 was established with polymer containing 10-13% TTA groups however a higher percentage of TTA could not be achieved due to poor solubility. It is likely that the self doping effect of the carboxylic acid group is influenced by the thiophene compound. Lower dissociation of the ionic species may be associated with TTA and therefore comparable dopant levels were not seen. Due to the difficulty of generating a range of TTA compositions a relationship based upon the effect of self doping could not be established. The presence of the carboxylic acid group could therefore not be determined as the influential factor upon dopant content. Another explanation involves the rigidity of the linker chain where the more rigid the side chain the more dopant that can be incorporated into the film due to increased porosity³⁸. The double bond associated with TTA may therefore have some influence upon the enhanced dopant values.

Kabasakaloglu *et al*⁷² Skotheim *et al*¹² Tourillon and Garnier¹⁸⁰ and Waltman *et al*³⁶ provide conflicting reviews regarding dopant levels where conductivity is concerned. In addition Kuwahara *et al* describes an increase in conductivity as the content of T3AA decreases. As conductivity was not fully explored within this study the association between dopant level, T3AA content and conductivity cannot be made. The dopant variation is difficult to explain and the only conclusion that can be made describes the T3AA influence upon the material limiting dopant interaction.

Substituents attached to the thiophene ring generated a range of doping levels. DDT supports a 12 carbon flexible alkyl chain which in this study generated a polymer with significantly elevated dopant inclusion of over 2 anions per thiophene ring. Such a large dopant ratio is unlikely and can be explained due to the entrapment of solvent and electrolyte in the film. Due to the enhanced porosity of the material caused by the long alkyl substituent entrapment is likely to occur. Poly(3-methylthiophene) generated a dopant fraction of 0.17 which was lower than the accepted value for thiophene compounds and may be influenced by the less mobile methyl species and the different conditions employed in this study.

Copolymerisation was elucidated visually by the morphological changes of the copolymers with varying monomer content. This was coupled with the physical

properties of the films determined upon ease of extraction from the electrode and their overall robustness.

The integration of 3-methylthiophene within the copolymer films provided a more robust material compared to the brittle properties observed for poly(bithiophene). The low cost and low oxidation potential made 3-methylthiophene the first choice for copolymerisation with a monomer carrying bulky groups for covalent bonding. The low steric requirement of 3-methylthiophene enabled successful dilution of the functionalised thiophene monomers which included T3AA, STA, TTA and STTA.

T3AA-MT with low T3AA content of 10% generated a porous film with strong adhesion to the electrode surface. STA-MT at 10% ester content was denser and thicker than T3AA-MT with less surface adherence. TTA-MT with the same functional content showed similar cohesion to the electrode surface as T3AA-MT whereas STTA-MT was extracted from the electrode with less difficulty and displayed a very porous structure upon higher magnification.

The investigation upon copolymerisation was extended further to verify the covalent attachment of diamine species by exposing STA-MT functionalised films to a solution of 2,3,5,6-tetramethyl-1,4-phenylenediamine. After a reaction time of 3 hours with 26% reaction sites cyclic voltammetry demonstrated altered redox signals that were stable over successive cycles. Covalent attachment was confirmed using FTIR where the carbonyl stretch was observed at both $1731\text{--}1715\text{ cm}^{-1}$ and 1644 cm^{-1} verifying the formation of an amide bond with remaining unreacted ester groups. This provided useful information for the optimisation of biosensor fabrication. As it was expected that employing short immobilisation times of less than 3 hours was likely to only retain enzyme molecules through absorption, this was demonstrated in chapter 5.

Chapter 5 incorporates the copolymer materials characterised in chapters 3 and 4 for use as immobilisation platforms into a biosensor format for the evaluation of biosensor performance. All novel formats were compared to the well documented T3AA-MT copolymer in which the enzyme electrode construction was followed closely to allow a direct comparison. A mediated system was utilised by Kuwahara *et al* however it was expected that the enzyme electrodes would generate current

response to glucose within both a mediated and non-mediated environment. However this was not the case and analysis was unsuccessful over several attempts in a non mediated system. A diffusion study was implemented to better understand the difficulty in obtaining reproducible data. The current response to 5 mM additions of hydrogen peroxide was monitored for two electrodes in which one was immobilised with enzyme. A 40% decrease in amperometric response was observed for the electrode that had been immobilised with enzyme demonstrating the diffusion limitation of the obstructed film. In addition the small platinum surface area coupled with thick film growth most likely contributed to a low concentration of hydrogen peroxide diffusion through the matrix in cases where diffusion had not already occurred into the bulk of the solution. Employing the mediator *p*-benzoquinone in solution established efficient electrical communication from the redox enzyme to the electrode surface. Developing the analysis method to achieve maximum current response involved the removal of oxygen from the solution. Nitrogen flushing was required to generate an enhanced amperometric response to glucose therefore eliminating competition for oxygen mediation. Furthermore the potential used for biosensor analysis was reduced from +0.8 V to +0.4 V due to a lower oxidation potential associated with *p*-benzoquinone. This also provides an advantage to a mediated system where interferants are present. The low working potential will be unable to oxidise any interfering species in solution therefore increasing sensitivity and avoiding false measurement.

Many parameters were investigated to optimise the fabrication steps such as polymer thickness through the applied charge, immobilisation time of the enzyme, copolymer ratio and the extent of buffer exposure before analysis. The copolymer ratio for STA-MT was investigated for the amperometric response to glucose. As concluded by Kuwahara *et al* a 10% functional content in the grown polymer presented the optimum amount for response to glucose based upon the conductivity of the film. Conductivity was not monitored in this study but the current was examined at +0.4 V during the characterisation of the copolymer films using cyclic voltammetry. Although the copolymers were mostly reduced a trend was seen where 10% STA content provided the largest current at +0.4 V. Currents were then observed to decrease upon increasing STA content which could also be seen for the copolymers investigated in a biosensor format. Diffusion properties of the copolymers provided

the best explanation for the difference in biosensor performance. Increasing the amount of functional sites in the polymer will potentially bind more enzyme causing an increased thickness of the material and therefore causing greater diffusion limitation of both the substrate and product. Diffusion effects can be confirmed due to the extended linear range produced upon biosensor analysis caused by an accumulation of product near the electrode surface.

It was found that polymer films grown with 50 mC (2500 mC/cm^2) of charge generated an even polymer distributed over the platinum surface. The relatively thick polymer endured the various immobilisation times and sample preparation without damage to the film. An immobilisation time of 6 hours was found to produce good responses to glucose which differed to the 18-24 hours normally implemented^{48,50,53-55,140-141,151}. The extended times were investigated and it was found that in general the response to glucose demonstrated little change at the longer immobilisation times. Interestingly at 24 hours of enzyme exposure the response to glucose for all copolymer thicknesses were of equal intensity. This can be explained in terms of diffusion limitation affecting thicker films and saturated binding sites limiting the response of the thinner films. Implementing a 6 hour enzyme exposure period reduced the time needed for biosensor preparation in comparison to methods found in the literature⁵⁰⁻⁵⁵.

Buffer exposure on the polymer films indicated a possible swelling effect although any noticeable influence only occurred after extended periods of 6-24 hours. A small margin of error was present at short exposure times of 0-1 hour demonstrating the polymers resistance to trapping absorbed enzyme and buffer interaction over short time periods. Further studies are required for the determination of possible swelling effects on the film and therefore were not conclusive in this case. From the results of the investigation it was decided where possible to maintain a short exposure time to buffer when analysing the enzyme electrodes.

From the preliminary investigations where biosensor fabrication was optimised producing good signal responses with faster preparation methods sensor evaluation provided the next step. Repeat analysis was performed upon all biosensor evaluation studies where three measurements were taken for each investigation and the mean

response was tabulated. Evaluating each biosensor system for repeatability and reproducibility is important when determining biosensor precision. Additional analytical determinations include amperometric response to analyte, sensitivity, linear range and stability studies. Table 5.13 in chapter 5 summarises the data clearly with graphical illustration in figure 5.31 demonstrating an improved amperometric response to glucose with the potential effect of the extended double bond spacer arm.

In summary from the four copolymers investigated for application in a biosensor format TTA-MT (10% TTA) generated the maximum response to glucose, good linear range up to 7 mM, rapid response to glucose in under 3 seconds, 90% in both repeatability and reproducibility and indication of good affinity to glucose with an apparent K_m of 15 mM. In nearly all areas the 10% content of TTA copolymerised with MT generated improved performance, however stability of the enzyme electrode was limited. Only 50% of the original response was retained after 28 days stored at 4 °C in pH 7.0 phosphate buffer solution. Comparable results are observed for STTA-MT and it can be seen clearly that there is little difference in analytical assessment for copolymers of identical structure where enzyme immobilisation has taken place. Response to glucose, stability at 4 °C over 28 days and reproducibility are comparable for the carboxylic acid functionalised copolymers (T3AA and TTA) against their corresponding activated esters of STA and STTA. Therefore the morphology of the polymer seems to demonstrate little influence in these areas however where results seem to deviate away from this trend morphology of the film presents a feasible explanation. Differences in enzyme activity for the STA-MT copolymer and linear range for T3AA-MT are observed. A high Michaelis value of 20 mM was determined for the STA-MT format where all other copolymers produced lower K_m values of around 15 mM. The observed increase was attributed to the limited accessibility of the substrate to the active sites of the immobilised enzyme due to the compact morphology of the polymer. The opposite effect was related to the short linear range of 4 mM for the T3AA-MT copolymer as a more porous morphology was concluded from the SEM images in chapter 4. The product generated from the enzyme-substrate reaction did not accumulate in the matrix to any significant extent due to the porosity of the polymer. The facile diffusion produced no control of the product concentration released to the electrode surface and therefore a short linear range was generated.

Response to temperature and pH provided the expected shift in optimum conditions associated with immobilised enzymes. The covalent method of enzyme attachment improved the stability of all the biosensors tolerating extreme conditions not normally withstood by solution based enzyme. The optimum pH and temperature showed only slightly different results when comparing the two different biosensor formats whereas the copolymer TTA-MT demonstrated the greatest affect to pH and temperature variation explained by the associated negative charge on the TTA monomer²⁰⁰⁻²⁰¹.

From the evaluation of all four biosensor composites a distinct improvement was observed with the copolymers incorporating the extended double bond spacer within the functional monomer. Enhancement of amperometric response to glucose and reproducibility are important factors which are desirable within a biosensor device. Stability is also an essential aspect of biosensor design and although TTA-MT and STTA-MT systems demonstrated successful operation after one month biosensor activity had decreased by 50%. The T3AA-MT and STA-MT copolymers provided improved sensor stability retaining over 70% of the original response however generated lower response to glucose and reproducibility. It is therefore clear that the improvements observed form the different biosensor systems and indeed the biosensor fabrication and optimisation steps are influenced by several parameters.

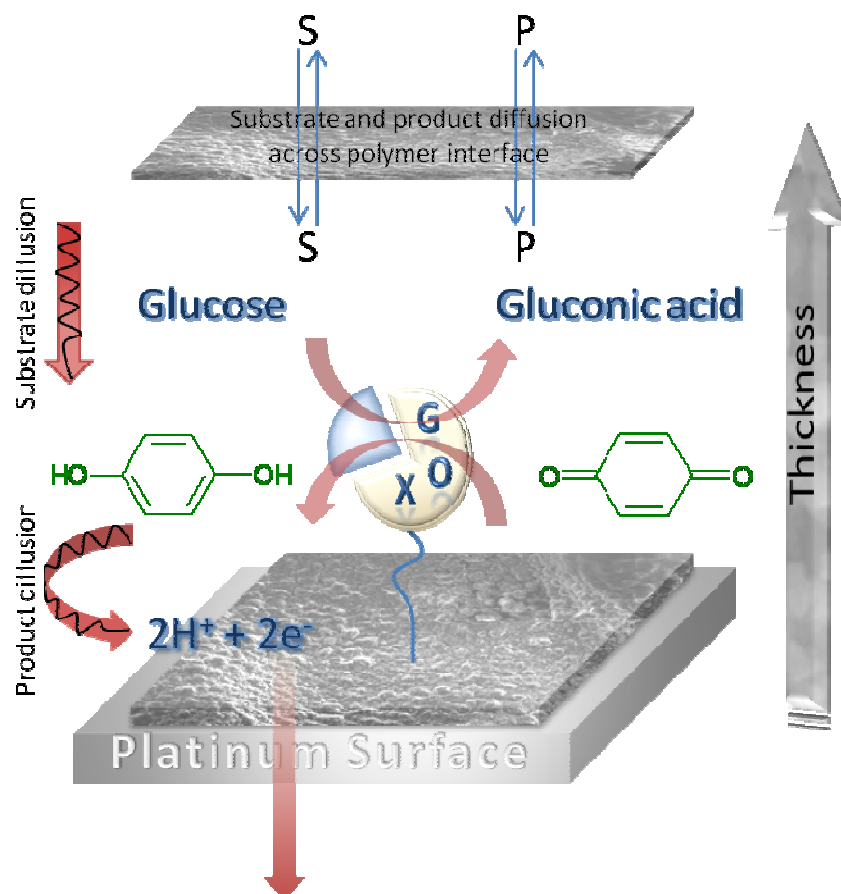


Figure 6.1. A mediated biosensor system highlighting influential parameters upon the biosensor performance.

The diagram above illustrates the dynamic biosensor system demonstrating the wide range of influencing effects that can alter the performance of the biosensor. Defining each effect is difficult due to the complex relationship of the parameters involved as changing a single parameter is likely to affect the outcome of several controlling factors. Understanding the diverse requirements of the biosensor system aid the advancement of improved biosensor formats. Modification of the parameters that control amperometric response by increasing the enzyme concentration such as polymer thickness, immobilisation time and copolymer ratio also affect product and substrate diffusion therefore limiting the maximum current response obtainable. The fabrication of the biosensor was focused upon the conducting material employed for enzyme immobilisation to maximize essential biosensor properties without significant loss to other important parameters determining biosensor performance. The four copolymer systems illustrate the ease of fabrication through the simple control of an electrochemical cell. Polymer thickness and the area can be easily manipulated due to the conducting nature of the polymer therefore providing a reproducible method that

generates reproducible enzyme electrodes. Copolymer conductivity was envisaged to enhance response to glucose and provide rapid response times without the side effect of increased copolymer thickness. Although this potential property of the polymer was not exploited as difficulty arose in the initial biosensor investigations the introduction of the mediator *p*-benzoquinone generated enhanced amperometric response to glucose operating at low potential which is known to further improve the biosensor system when measurement is required in an environment containing interfering species.

This study therefore concludes the evaluation of four biosensor systems. T3AA-MT was repeated from the literature and STA, TTA and STTA-MT copolymers are novel formats demonstrating successful immobilisation matrices with improved biosensor performance for the determination of glucose.

References

1. Shirakawa H, Louis E J, McDiarmid A J, Chaing C K, Heeger A J. 'Synthesis of electrically conducting organic polymers: halogen derivatives of polyacetylene, $(CH)_x$ '. *J. Chem. Soc., Chem. Commun*, **578**, (1977), 578-560.
2. Hatano M, Kambara S, Okamoto S. 'Paramagnetic and electric properties of polyacetylene'. *Polymer Science*, **51**, (1961), 26-29.
3. Ahuja T, Mir I A, Kumar D, Rajesh. 'Biomolecular immobilization on conducting polymers for biosensing applications'. *Biomaterials*, **28**, (2007), 791-805.
4. Natta G, Mazzanti G, Corradini P. *Atti. Acad. Naz. Lincei Cl. Sci. Fis. Mater. Nat. Rend.*, **8**, (3), (1958), 25.
5. Shirakawa H. 'The discovery of polyacetylene film the dawning of an era of conducting polymers'. *Synthetic Metals*, **125**, (2002), 3-10.
6. Nalwa H S. 'Handbook of advanced electronic and photonic materials and devices'. Academic Press, London, (2001), 132, 105-106.
7. Margolis J. 'Conductive polymers and plastics'. Chapman and Hall Ltd, London, (1989), 2-11.
8. Cambell I M. 'Introduction to synthetic polymers'. Oxford Science Publications, (1994), 196.
9. Huang W S, Humphrey B D, MacDiarmid A G. 'Polyaniline, a novel conducting polymer, morphology and chemistry of its oxidation and reduction in aqueous electrolytes'. *J. Chem. Soc., Faraday Trans. 1*, **82**, (1986), 2385-2400.
10. Min G. 'Conducting polymers and their applications in the film industry polyaniline/polyimide blended films '. *Synthetic Metals*, **102**, (1999), 1163-1166.
11. Guimard N K, Gomez N, Schmidt C E. 'Conducting polymers in biomedical engineering'. *Progress in Polymer Science*, **32**, (2007), 876-921.
12. Skotheim T A, Pochan J M. 'Handbook of conducting polymers'. Volume 2. Marcel Dekker, New York, (1986), 1384.
13. Billingham N C, Calvert P D, Foot P J S, Mohammad F. 'Stability and degradation of some electrically conducting polymers'. *Polymer Degradation and Stability*. **19**, (1987), 323-341.
14. Skotheim T A, Pekker S, Jánossy A, Tourillon G. 'Handbook of conducting polymers'. Volume 1. Marcel Dekker, New York, (1986), 60-62, 323-326.

15. Udum Y A, Pekmez K, Yıldız A. 'Electropolymerization of self-doped polythiophene in acetonitrile containing FSO_3H '. *Synthetic Metals*, **142**, (2004), 7–12.
16. Lee R-O, Lai H-H, Wang J-J, Jeng R-J, Lin J-J. 'Self-doping effects on the morphology, electrochemical and conductivity properties of self-assembled polyanilines'. *Thin Solid Films*, **517**, (2008), 500–505.
17. Tourillon G, Garnier F. 'Structural effect on the electrochemical properties of polythiophene and derivatives'. *Electroanalytical Chemistry*, **161**, (1984), 51–58.
18. Bidan G. 'Electroconducting conjugated polymers; new sensitive matrices to build up chemical or electrochemical sensors. A review'. *Review Sens. Actuators B*, **6**, (1992), 45–56.
19. Clayden J, Greeves N, Warren S, Wothers P. 'Organic chemistry'. Oxford University Press, (2001), 156–171.
20. Skotheim T A, Feast W J. 'Handbook of conducting polymers'. Volume 1. Marcel Dekker, New York (1986), 2.
21. Dewick P M. 'Essentials of organic chemistry'. John Wiley and sons Ltd, (2006), 37–38.
22. Brown, LeMay, Bursten. 'Chemistry the central science'. Eighth edition, (2000), 303–342.
23. Brett C M A, Brett A M O. 'Electrochemistry principles, methods and applications'. Oxford Science Press, (1993).
24. McCullough R D. 'The chemistry of conducting polythiophenes'. *Advanced Materials*, **10**, (1998), 93–116.
25. Waltman R J, Bargon J. 'Electrically conducting polymers: a review of the electropolymerization reaction, of the effects of chemical structure on polymer film properties, and of applications towards technology'. *Can J Chem*, **64**, (1986), 76–95.
26. Barsch V, Beck F. 'Anodic overoxidation of polythiophenes in wet acetonitrile electrolytes'. *Electrochimica Acta*, **41**, (1996), 1761–1771.
27. Diaz A F, Kanazawa K K, Gardini G P. 'Electrochemical polymerization of pyrrole'. *J. Chem. Soc., Chem. Commun.*, **635**, (1979).
28. Diaz A F. 'Electrochemical preparation and characterization of conducting polymers'. *Chemica Scripta*, **17**, (1981), 145–148.
29. Tourillon G, Garnier F. 'New electrochemically generated organic conducting polymers'. *Electroanalytical Chemistry*, **135**, (1982), 173–178.

30. Bargon J, Mohamand S, Waltman R J. 'Electrochemical synthesis of electrically conducting polymers from aromatic compounds'. *IBM Journal of Research and Development*, **27**, (1983), 330-331.
31. Delamer M, Lacaze P C, Dumousseau J Y, Dubois J E. 'Electrochemical oxidation of benzene and biphenyl in liquid sulfur dioxide: formation of conductive deposits'. *Electrochim. Acta*, **27**, (1982), 61-65.
32. Diaz A F, Logan J A. 'Electroactive polyaniline films'. *Electroanalytical Chemistry*, **111**, (1980), 111-114.
33. Kao J, Radom L. 'Conformations, stabilities, and charge distributions in 2- and 3-monosubstituted thiophenes. An ab initio molecular orbital study'. *American Chemical Society*, **101**, (1979), 311-318.
34. Watchers A J H, Davies D W. 'A theoretical study of the UV spectra of dithienyls and thiophene'. *Tetrahedron*, **20**, (1964), 2841-2849.
35. Roncali J. 'Synthetic principles for bandgap control in linear π -conjugated systems'. *Chemical Review*, **97**, (1997), 173-205.
36. Waltman R J, Bargon J, Diaz A F. 'Electrochemical studies of some conducting polythiophene films'. *Physical Chemistry*, **87**, (1983), 1459-1463.
37. Welzel H-P, Kossmehl G, Stein H-J, Schneider J, Plieth W. 'Reactive groups on polymer electrodes-I. Electrochemical copolymerisation of thiophene-3-acetic acid with 3-methylthiophene'. *Electrochimica Acta*, **40**, (1995), 577-584.
38. Marchand G, Pilard J-F, Fabre B, Rault-Berthelot J, Simonet J. 'Synthesis and electrochemical behaviour of new polythiophenes branched with sulfonamides for solid phase synthesis'. *New J. Chem.*, **23**, (1999), 869-875.
39. Skotheim T A, Diaz A F, Bargon J. 'Handbook of conducting polymers'. Volume 1. Marcel Dekker, New York, (1986), 100-101.
40. Dietrich M. 'Electrochemical and spectroscopic characterisation of polyalkylenedioxythiophenes'. *Electroanalytical Chemistry*, **369**, (1994), 87-92.
41. Krische B, Zagorska M. 'Overoxidation in conducting polymers'. *Synthetic Metals*, **28**, (1989), 257-262.
42. Krische B, Zagorska M. 'The polythiophene paradox'. *Synthetic Metals*, **28**, (1989), 263-268.
43. Gratzl M, Hsu D-F, Riley A M, Janata J. 'Electrochemically deposited polythiophene. 1. Ohmic drop compensation and the polythiophene paradox'. *Physical Chemistry*, **94**, (1990), 5973-5981.

-
44. Albery W J, Li F, Mount A R. 'Electrochemical polymerisation of poly(thiophene-3-acetic acid), poly(thiophene-co-thiophene-3-acetic acid and determination of their molar mass'. *Electroanalytical Chemistry*, **310**, (1991), 239-253.
45. Chen H S O, Toh C-S, Gan L-M. 'Use of polythiophene and poly(thiophene-3-acetic acid) as charge-selective films for amperometric flow-cell detectors'. *Materials Chemistry*, **5**, (4), (1995), 631-637.
46. Roncali J, Garreau R, Yassar A, Marque P, Garnier F, Lemaire M. 'Effects of steric factors on the electrosynthesis and properties of conducting poly(3-alkylthiophenes)'. *Physical Chemistry*, **91**, (1987), 6706-6714.
47. Li G, Kossmehl G, Welzel H-P, Engelmann G, Hunnius W-D, Plieth W, Zhu H. 'Reactive groups on polymer electrodes, 7. New electrogenerated electroactive polythiophenes with different protected carboxyl groups'. *Macromol. Chem. Phys.*, **199**, (1998), 525-533.
48. Li Z F, Kang E T, Neoh K G, Tan K L. 'Covalent immobilization of glucose oxidase on the surface of polyaniline films graft copolymerized with acrylic acid'. *Biomaterials*, **19**, (1998), 45-53.
49. Rajesh, Bisht V, Takashima W, Kaneto K. 'An amperometric urea biosensor based on covalent immobilization of urease onto an electrochemically prepared copolymer poly(N-3-aminopropyl pyrrole-co-pyrrole) film'. *Biomaterials*, **26**, (2005), 3683-3690.
50. Liu C, Kuwahara T, Yamazaki R, Shimomura M. 'Covalent immobilization of glucose oxidase on films prepared by electrochemical copolymerization of 3-methylthiophene and thiophene-3-acetic acid for amperometric sensing of glucose: effects of polymerization conditions on sensing properties'. *European Polymer Journal*, **43**, (2007), 3264-3276.
51. Liu C, Ohta H, Kuwahara T, Shimomura M. 'Amperometric glucose-responding property of enzyme electrodes fabricated by covalent immobilization of glucose oxidase on conducting polymer films with macroporous structure'. *European Polymer Journal*, **44**, (2008), 1114-1122.
52. Welzel H P, Kossmehl G, Engelmann G. 'Reactive groups on polymer covered electrodes, 4a. Lactate-oxidase-biosensor based on electrodes modified by polythiophene'. *Macromol. Chem. Phys.*, **197**, (1996), 3355-3363.
53. Kuwahara T, Oshima K, Miyauchi S, Shimomura M. 'Immobilization of glucose oxidase and electron-mediating groups on the film of 3-methylthiophene/thiophene-3-acetic acid copolymer and its application to reagentless sensing of glucose'. *Polymer*, **46**, (2005), 8091-8097.
54. Kuwahara T, Oshima K, Miyauchi S, Shimomura M. 'Glucose sensing with glucose oxidase immobilised covalently on the films of thiophene copolymers'. *Synthetic Metals*, **152**, (2005), 29-32.

-
55. Kojima K, Yamauchi T, Shimomura M, Miyauchi S. 'Covalent immobilisation of glucose oxidase on poly[1-(2-carboxyethyl)pyrrole] film for glucose sensing'. *Polymer Papers*, **39**, (1998), 2079-2082.
56. Li G, Koßmehl G, Welzel H-P, Engelmann G, Hunnius W-D, Plieth W, Zhu H. 'Reactive groups on polymer coated electrodes, 8. Novel conducting polymer interfaces produced by electrochemical copolymerization of functionalized thiophene activated esters with 3-methylthiophene'. *Macromol. Chem. Phys.*, **199**, (1998), 2255-2266.
57. Roncali J. 'Conjugated poly(thiophenes): synthesis, functionalisation and applications'. *Chemical Reviews*, **92**, (1992), 711-738.
58. Hotta S, Rughooputh S D D V, Heeger A J, Wudl F. 'Spectroscopic studies of soluble poly(3-alkylthienylenes)'. *Macromolecules*, **20**, (1987), 212-215.
59. Sato M, Tanaka S, Kaeriyama K. 'Soluble conducting polythiophenes'. *J. Chem. Soc., Chem. Commun.*, **235**, (1986), 873-874.
60. Jen K Y, Miller G G, Elsenbaumer R L. 'Highly conducting, soluble, and environmentally-stable poly(3-alkylthiophenes)'. *J. Chem. Soc., Chem. Commun.*, **729**, (1986), 1346-1347.
61. Lee C, Kim K J, Rhee S B. 'The effects of ester substitution and alkyl chain length on the properties of poly(thiophene)s'. *Synthetic Metals*, **69**, (1995), 295-296.
62. Szkurlat A, Palys B, Mieczkowski J, Skompska M. 'Electrosynthesis and spectroelectrochemical characterization of poly(3,4-dimethoxy-thiophene), poly(3,4-dipropoxythiophene) and poly(3,4-dioctyloxythiophene) films'. *Electrochimica Acta*, **48**, (2003), 3665-3676.
63. Vignali M, Edwards R, Cunnane V J. 'Characterisation of doping and electropolymerization of free standing films of polyterthiophene'. *Electroanalytical Chemistry*, **592**, (2006), 37-45.
64. Ballarin B, Lanzi M, Paganin L, Cesari G. Electrosynthesis of valuable conducting polymers from the anodic coupling of β -substituted oligothiophenes'. *Electrochimica Acta*, **52**, (2007), 7849-7856.
65. Smie A, Synowczyk A, Heinze J, Alle R, Tschuncky P, Götz G, Bäuerle P. ' β,β -Disubstituted oligothiophenes, a new oligomeric approach towards the synthesis of conducting polymers'. *Electroanalytical Chemistry*, **452**, (1998), 87-95.
66. Lee T-Y, Shim Y-B, Shin S C. 'Simple preparation of tertiophene-3'-carboxylic acid and characterisation of its polymer'. *Synthetic Metals*, **126**, (2002), 105-110.

-
67. Peng H, Zhang L, Spires J, Soeller C, Travas-Sejdic J. 'Synthesis of a functionalised polythiophene as an active substrate for a label-free electrochemical genosensor'. *Polymer*, **48**, (2007), 3413-3419.
68. Chen W, Xue G. 'Low potential electrochemical syntheses of heteroaromatic conducting polymers in a novel solvent system based on trifluoroborate-ethyl ether'. *Progress in Polymer Science*, **30**, (2005), 783-811.
69. Ewbank P C, Loewe R S, Zhai L, Reddinger J, Sauv   G, McCullough R D. 'Regioregular poly(thiophene-3-alkanoic acids): water soluble conducting polymers suitable for chromatic chemosensing in solution and solid state'. *Tetrahedron*, **60**, (2004), 11269-11275.
70. Tourillon G, Garnier F. 'Morphology and crystallographic structure of polythiophene and derivatives'. *Mol. Cryst. Liq. Cryst.*, **121**, (1985), 349-355.
71. Skotheim T A, Tourillon G. 'Handbook of conducting polymers'. Volume 1. Marcel Dekker, New York, (1986), 310.
72. Kabasakaloglu M, Kiyak T, Toprak H, Aksu M L. 'Electrochemical properties of polythiophene depending on preparation conditions'. *Applied Surface Science*, **152**, (1999), 115-125.
73. Chen T-A, Wu X, Rieke R D. 'Regiocontrolled synthesis of poly(3-alkylthiophenes) mediated by rieke zinc: their characterization and solid-state properties'. *Journal of the American Chemical Society*, **117**, (1995), 233-244.
74. Wallace G G, Spinks G M, Kane-Maguire L A P, Teasdale P R. 'Conductive electroactive polymers, intelligent materials systems'. Second edition, CRC Press LLC, (2003), 97.
75. Tsai E W, Basak S, Ruiz J P, Reynolds J R, Rajeshwar K. 'Electrochemistry of some β -substituted thiophenes'. *J. Electrochem. Soc.*, **136**, (1989), 3683-3689.
76. Brillas E, Oliver R, Estrany F, Rodr  guez E, Tejero S. 'Anodic polymerization of α -tetrathiophene in organic medium. Doping with perchlorate ion and properties of conducting polymer with anionic species providing electrical neutrality at these sites'. *Electrochimica Acta*, **47**, (2002), 1623-1631.
77. Foot P J S, Merchant J. 'Annealing behaviour of conductive poly(3-hexylthiophene) films'. *Polymer*, **38**, (1997), 1749-1751.
78. Dass A, Mulik S, Sotiriou-Leventis C, Leventis N. 'Protection of 2-(3-thienyl) ethanol with 3-thienylacetic acid and hard cross-linked conducting films by electropolymerization of the ester'. *Synthetic Metals*, **156**, (2006), 966-972.
79. Wang J. 'Analytical electrochemistry'. Third edition, John Wiley & sons, Inc Hoboken New Jersey, (2006), 32.

-
80. Monk P M S. 'Fundamentals of electroanalytical chemistry'. John Wiley & sons Ltd, Baffins Lane, Chichester, West Sussex, (2001), 161-166.
81. <http://www.cheng.cam.ac.uk/research/groups/electrochem/JAVA/electrochemistry/ELEC/l4html/cv.html>
82. Zoski C G. 'Handbook of electrochemistry'. Elsevier, Kidlington, Oxford, (2007), 830.
83. Hall C E. Cyclic voltammetry lecture notes 2005/6.
84. <http://web.nmsu.edu/~snsm/classes/chem435/Lab13/intro.html>
85. Skotheim T A, Tourillon G. 'Handbook of conducting polymers'. Volume 1. Marcel Dekker, New York, (1986), 330.
86. Thompson B C, Schottland P, Zong K, Reynolds J R. 'In situ colorimetric analysis of electrochromic polymers and devices'. *Chem. Mater.* **12**, (2000), 1563-1571.
87. Lévesque I, Leclerc M. 'Chromism in polythiophene derivatives'. *Synthetic Metals*, **84**, (1997), 203-204.
88. Murray K A, Holmes A B, Moratti S C, Rumbles G. 'Conformational changes in regioregular polythiophenes due to crosslinking'. *Materials Chemistry*, **9**, (1999), 2109-2115.
89. Heeger A J. 'Semi conducting and metallic polymers: the fourth generation of polymeric materials'. *Synthetic metals*, **125**, (2002), 23-42.
90. Kumar A, Rajesh, Chaubey A, Grover S K, Malhotra B D. 'Immobilization of cholesterol oxidase and potassium ferricyanide on dodecylbenzene sulfonate ion-doped polypyrrole film'. *Applied Polymer Science*, **82**, (2001), 3486-3491.
91. Zeng H, Jiang Y, Yu J, Xie G. 'Choline oxidase immobilized into conductive poly(3,4-ethylenedioxythiophene) film for choline detection'. *Applied Surface Science*, **254**, (2008), 6337-6340.
92. Kros A, Sommerdijk N A J M, Nolte R J M. 'Poly(pyrrole) versus poly(3,4-ethylenedioxythiophene): implications for biosensor applications'. *Sensors and Actuators B*, **106**, (2005), 289-295.
93. Atta N F, Galal A, Mark Jr. H B, Yu T, Bishop P L. 'Conducting polymer ion sensor electrodes-III. Potentiometric sulfide ion selective electrode'. *Talanta*, **47**, (1998), 987-999.
94. Migdalski J, Blaz T, Lewenstam A. 'Conducting polymer-based ion-selective electrodes'. *Analytica Chimica Acta*, **322**, (1996) 141-149.

-
95. Ram M K, Yavuz O, Aldissi M. 'NO₂ gas sensing based on ordered ultrathin films of conducting polymer and its nanocomposite'. *Synthetic Metals*, **151**, (2005), 77-84.
96. Ram M K, Yavuz O, Lahsangah V, Aldissi M. 'CO gas sensing from ultrathin nano-composite conducting polymer film'. *Sensors and Actuators B*, **106**, (2005), 750-757.
97. Dhawan S K, Singh N, Venkatachalam S. 'Shielding effectiveness of conducting polyaniline coated fabrics at 101 GHz'. *Synthetic Metals*, **125**, (2002), 389-393.
98. Bhadra S, Singha N K, Khastgir D. 'Semiconductive composites from ethylene 1-octene copolymer and polyaniline coated nylon 6: studies on mechanical, thermal, processability, electrical and EMI shielding properties'. *Polymer Engineering and Science*, **48**, (2008), 995-1006.
99. Trung V Q, Tung D N, Huyen D N. 'Polypyrrole/Al₂O₃ nanocomposites: preparation, characterisation and electromagnetic shielding properties'. *Experimental Nanoscience*, **4**, (2009), 213-219.
100. Subba Reddy Ch V, Jin A-P, Zhu Q-Y, Mai L-Q, Chen W. 'Preparation and characterization of (PVP + NaClO₄) electrolytes for battery applications'. *The European Physical Journal E*, **19**, (2006), 471-476.
101. Croce F, Appetecchi G B, Persi L, Scrosati B. 'Nanocomposite polymer electrolytes for lithium batteries'. *Letters to Nature*, **394**, (1998), 456-458.
102. Chen J, Too C O, Burrell A K, Collis G E, Officer D L, Wallace G G. 'Photovoltaic devices based on poly(bis-tertiophenes) and substituted poly(bisterthiophene)'. *Synthetic Metals*, **137**, (2003), 1373-1374.
103. Collis G E, Campbell W M, Officer D L, Burrell A K. 'The design and synthesis of porphyrin/oligothiophene hybrid monomers'. *Org. Biomol. Chem.*, **3**, (2005), 2075-2084.
104. Cremer J, Mena-Osteritz E, Pschierer N G, Müllen K, Bäuerle P. 'Dye-functionalized head-to-tail coupled oligo(3-hexylthiophenes)— perylene-oligothiophene dyads for photovoltaic applications'. *Org. Biomol. Chem.*, **3**, (2005), 985-995.
105. Kuwahara T, Homma T, Kondo M, Shimomura M. 'Fabrication of enzyme electrodes with a polythiophene derivative and application of them to a glucose fuel cell'. *Synthetic Metals*, **159**, (2009), 1859-1864.
106. Kuwahara T, Ohta H, Kondo M, Shimomura M. 'Immobilisation of glucose oxidase on carbon paper electrodes modified with conducting polymer and its application to a glucose fuel cell'. *Bioelectrochemistry*, **74**, (2008), 66-72.

-
107. Camurlu P, Cirpan A, Toppare L. 'Conducting polymers of octanoic acid 2-thiophen-3-yl-ethyl ester and their electrochromic properties'. *Materials Chemistry and Physics*, **92**, (2005), 413–418.
108. Ho P K H, Kim J-S, Burroughes J H, Becker H, Li S F Y, Brown T M, Cacialli F, Friend R H. 'Molecular-scale interface engineering for polymer light-emitting diodes'. *Letters to Nature*, **404**, (2000), 481-484.
109. Clark Jr. L C, Lyons C. 'Electrode systems for continuous monitoring in cardiovascular surgery'. *Annals of the New York Academy of Science*, **102**, (1962), 29-45.
110. Rechnitz G A, Kobos R K, Riechel S J, Gebauer C R. 'A bio-selective membrane electrode prepared with living bacterial cells'. *Analytica Chimica Acta*, **94**, (1977), 357-365.
111. Gerard M, Chaubey A, Malhotra B D. 'Application of conducting polymers to biosensors'. *Biosensors and Bioelectronics*, **17**, (2002), 345-359.
112. Wen Z, Ye B, Zhou X. 'Direct electron transfer reaction of glucose oxidase at bare silver electrodes and its application in analysis'. *Electroanalysis*, **9**, (8), (1991), 641-644.
113. Wang G, Thai N M, Yau S T. 'Preserved enzymatic activity of glucose oxidase immobilized on an unmodified electrode'. *Electrochemistry communications*, **8**, (2006), 987-992.
114. Lu Q, Li C M. 'One-step co-electropolymerized conducting polymer–protein composite film for direct electrochemistry-based biosensors'. *Biosensors and bioelectronics*, **24**, (2008), 773-778.
115. Zhang S, Wright G, Yang Y. 'Materials and techniques for electrochemical biosensor design and construction'. *Biosensors & Bioelectronics*, **15**, (2000), 273–282.
116. Iwakura C, Kajiya Y, Yoneyama H. 'Simultaneous immobilization of glucose oxidase and a mediator in conducting polymer films'. *J. Chem Soc., Chem. Commun.*, (1988), 1019-1020.
117. Guilbault G G. 'Analytical uses of immobilized enzymes'. Marcel Dekker, INC New York, (1984), 163.
118. Korri-Yousoufi H, Richard C, Yassar A. 'A new method for the immobilisation of antibodies in conducting polymers'. *Materials Science and Engineering C*, **15**, (2001), 307–310
119. Minett A I, Barisci J N, Wallace G G. 'Immobilisation of anti-Listeria in a polypyrrole film'. *Reactive and Functional Polymers*, **53**, (2002), 217-227.

-
120. Peng H, Zhang L, Soeller C, Travas-Sejdic J. 'Conducting polymers for electrochemical DNA sensing' *Biomaterials*, **30**, (2009), 2132–2148.
121. Béra-Abérem M, Ho H-A, Leclerc M. 'Functional polythiophenes as optical chemo- and biosensors'. *Tetrahedron*, **60**, (2004), 11169–11173.
122. Uygun A. 'DNA hybridization electrochemical biosensor using a functionalized Polythiophene'. *Talanta*, **79**, (2009), 194-198.
123. Korri-Youssoufi H, Makrouf B. 'Electrochemical biosensing of DNA hybridization by ferrocenyl groups functionalized polypyrrole' *Analytica Chimica Acta*, **469**, (2002), 85–92.
124. Raba J, Mottola H A. 'Glucose oxidase as an analytical reagent'. *Critical Reviews in Analytical Chemistry*, **25**, (1995), 1-42.
125. Berry D R, Paterson A. 'Enzymes in the food industry', *Enzyme Chemistry, Impact and Applications*, Second edition, Suckling C J, Chapman and Hall, London, (1990), 319.
126. Zoldák G, Zubrik A, Musatov A, Stupák M, Sedlák E. 'Irreversible thermal denaturation of glucose oxidase from *Aspergillus niger* is the transition to the denatured state with residual structure'. *Biological Chemistry*, **279**, (2004), 47601-47609.
127. Hecht H J, Kalisz H M, Hendle J, Schmid R D, Schomburg D. 'Crystal structure of glucose oxidase from *Aspergillus niger* refined at 2.3 Å resolution'. *Molecular Biology*, **229**, (1993), 153-172.
128. Bankar S B, Bule M V, Singhal R S, Ananthanarayan L. 'Glucose oxidase-an overview'. *Biotechnology Advances*, **27**, (2009), 489-501.
129. Guilbault G G. 'Analytical uses of immobilized enzymes'. Marcel Dekker, INC New York, (1984), 15.
130. Palmer T. 'Enzymes biochemistry, biotechnology, clinical chemistry'. Horwood Publishing Ltd (2001), 107.
131. Eienthal R, Danson M J. 'Enzyme assays a practical approach'. Oxford University Press, (1993), 281.
132. Palmer T. 'Enzymes biochemistry, biotechnology, clinical chemistry'. Horwood Publishing Ltd (2001), 107-118.
133. Palmer T. 'Enzymes biochemistry, biotechnology, clinical chemistry'. Horwood Publishing Ltd (2001), 70-71.
134. Bisswanger H. 'Enzyme kinetics: principles and methods'. Second edition, Wiley-VCH Verlag GmbH & Co. KGaA, Weinheim, Germany, (2008), 169.

-
135. Cosnier S. 'Biosensors based on electropolymerised films: new trends'. *Analytical and Bioanalytical Chemistry*, **377**, (2003), 507-520.
136. Vedrine C, Fabiano S, Tran-Minh C. 'Amperometric tyrosinase based biosensor using an electrogenerated polythiophene film as an entrapment support'. *Talanta*, **59**, (2003), 535-544.
137. Hiller M, Kranz C, Huber J, Bauerle P, Schuhmann W. 'Amperometric biosensors produced by immobilization of redox enzymes at polythiophene-modified electrode surfaces'. *Advanced Materials*, **8**, (1996), 219-222.
138. Vidal J-C, Garcia-Ruiz E, Castillo J-R. 'Recent advances in electropolymerized conducting polymers in amperometric biosensors'. *Microchim. Acta*, **143**, (2003), 93-111.
139. Cosnier S, Ionescu R E, Herrmann S, Bouffier L, Demeunynck M, Marks R S. 'Electroenzymatic polypyrrole-intercalator sensor for the determination of west Nile virus'. *Analytical Chemistry*, **78**, (2006), 7054-7057.
140. Oshima K, Nakamura T, Matsuoka R, Kuwahara T, Shimomura M, Miyauchi S. 'Immobilisation of alcohol dehydrogenase on poly[1-(2-carboxyethyl)pyrrole] film for fabrication of ethanol responding electrode'. *Synthetic Metals* **152** (2005), 33-36.
141. Shimomura M, Miyata R, Kuwahara T, Oshima K, Miyauchi S. 'Immobilization of glucose oxidase on the films prepared by electrochemical copolymerization of pyrrole and 1-(2-carboxyethyl)pyrrole for glucose sensing'. *European Polymer Journal*, **43**, (2007), 388-394.
142. Emge A, Bäuerle P. 'Molecular recognition properties of nucleobase-functionalized polythiophenes'. *Synthetic Metals*, **102**, (1999), 1370-1373.
143. Li Z F, Kang E T, Neoh K G, Tan K L. 'Covalent immobilisation of glucose oxidase on the surface of polyaniline films graft copolymerised with acrylic acid'. *Biomaterials*, **19**, (1998), 45-53.
144. Li G, Kößmehl G, Welzel H-P, Engelmann G, Hunnius W-D, Plieth W, Zhu H. 'Reactive groups on polymer coated electrodes, 7 new electrogenerated electroactive polythiophenes with different protected carboxyl groups'. *Macromol. Chem. Phys.*, **199**, (1998), 525-533.
145. Li G, Kößmehl G, Hunnius W, Zhu H, Kautek W, Plieth W, Melsheimer J, Doblhofer K. 'Reactive groups on polymer coated electrodes 10. Electrogenerated conducting polyalkylthiophenes bearing activated ester groups'. *Polymer*, **41**, (2000), 423-432.
146. Godillot P, Korri-Youssoufi H, Srivastava P, El Kassmi A, Gamier F. 'Direct chemical functionalization of as-grown electroactive polypyrrole film containing leaving groups'. *Synthetic Metals*, **33**, (1996), 117-123.

-
147. Bäuerle P, Hiller M, Scheib S, Sokolowski M, Umbach E. 'Post-polymerization functionalization of conducting polymers: novel poly(alkylthiophene)s substituted with easily replaceable activated ester groups'. *Advanced Materials*, **8**, (1996), 214-218.
148. Benoit N. 'Chemistry of peptide synthesis'. Taylor and Francis, CRC Press, (2006), 36.
149. Shelkov R, Nahmany M, Melman A. 'Selective esterifications of alcohols and phenols through carbodiimide couplings'. *Org. Biomol. Chem.*, **2**, (2004), 397-401.
150. Albericio F. 'Developments in peptide and amide synthesis'. *Current Opinion in Chemical Biology*, **8**, (2004), 211-221.
151. Kojima K, Unuma T, Yamauchi T, Shimomura M, Miyauchi S. 'Preparation of polypyrrole covalently attached with glucose oxidase and its application to glucose sensing'. *Synthetic Metals*, **85**, (1997), 1417-1418.
152. Yamauchi T, Kojima K, Oshima K, Shimomura M, Miyauchi S. 'Glucose-sensing characteristics of conducting polymer bound with glucose oxidase'. *Synthetic Metals* **102**, (1999), 1320.
153. Kates S A, Albericio F. 'Solid phase synthesis: a practical guide'. Marcel Dekker, INC, New York, (2000), 278.
154. Nakajima N, Ikada Y. 'Mechanism of amide formation by carbodiimide for bioconjugation in aqueous media'. *Bioconjugate Chemistry*, **6**, (1995), 123-130.
155. Iwasawa T, Wash P, Gibson C, Rebek J. 'Reaction of an introverted carboxylic acid with carbodiimide'. *Tetrahedron*, **63**, (2007), 6506-6511.
156. Guilbault G G. 'Analytical uses of immobilized enzymes'. Marcel Dekker, INC, New York, (1984), 143.
157. Lu W, Zhou D, Wallace G G. 'Enzymatic sensor based on conducting polymer coatings on metallised membranes'. *Analytical Communications*, **35**, (1998), 245-248.
158. Guilbault G G. 'Analytical uses of immobilized enzymes'. Marcel Dekker, INC, New York, (1984), 150.
159. Bartlett P N, Whitaker R G. 'Electrochemical immobilisation of enzymes part 1 theory'. *Electroanalytical Chemistry*, **224**, (1987), 27-35.
160. Rahmann M A, Kwon N, Won M, Choe E S, Shim Y. 'Functionalized conducting polymer as an enzyme-immobilizing substrate: an amperometric glutamate microbiosensor for in vivo measurements.' *Analytical Chemistry*, **77**, (2005) 4854-4860.

161. Kim H-J, Choi S-H, Lee K-P, Gopalan A I, Oh S-H. Woo J-C. 'Fabrication of functional poly(thiophene) electrode for biosensors'. *Ultramicroscopy*, **108**, (2008), 1360-1364.
162. Çil M, Büyükbayram A E, Kiralp S, Toppare L, Yağci Y. 'Various applications of immobilised glucose oxidase and polyphenol oxidase in a conducting polymer matrix'. *International Journal of Biological Macromolecules*, **41**, (2007), 49-55.
163. Yilmaz F, Cianga L, Guner Y, Toppare L, Yagci Y. 'Synthesis and characterisation of alternating copolymers of thiophene-containing N-phenyl maleimide and styrene by photoinduced radical polymerisation and their use in electropolymerisation'. *Polymer*, **45**, (2004), 5765-5774.
164. Abasıyanık M F, Şenel M. 'Immobilization of glucose oxidase on reagentless ferrocene-containing polythiophene derivative and its glucose sensing application'. *Electroanalytical Chemistry*, **639**, (2010), 21-26.
165. Hall C E. 'Functional dopants in conducting polymers'. Coventry Polytechnic, (1991).
166. Ganapathy H S, Kima J S, Jin S-H, Gal Y-S, Lim K T. 'Synthesis and properties of novel fluorinated ester substituted polythiophenes'. *Synthetic Metals*, **156**, (2006), 70-74.
167. Ruff E L, Abenas F J. 'Acid-catalyzed rearrangement of cyclobutanols. A novel rearrangement'. *Canadian Journal of Chemistry*, **65**, (1987), 1663-1667.
168. INCA Microanalysis Suite, (2004).
169. Experiment 9 kinetic methods of analysis, enzymatic determination of glucose'. Department of Chemistry, University of Kentucky, (2006), 51-61. http://www.chem.uky.edu/courses/che226/Labs/090-Glucose_Kinetics.pdf
170. Li J, Aoki K. 'Electrochemically pH-controllable 3-substituted polythiophene films'. *Electroanalytical Chemistry*, **458**, (1998), 155-160.
171. Pringle J M, Forsyth M, MacFarlane D R, Wagner K, Hall S B, Officer D L. 'The influence of the monomer and the ionic liquid on the electrochemical preparation of polythiophene'. *Polymer*, **46**, (2005), 2047-2058.
172. Wallace G G, Spinks G M, Kane-Maguire L A P, Teasdale P R. 'Conductive electroactive polymers, intelligent materials systems'. Second edition, CRC Press LLC, (2003), 13.
173. Zanardi C, Scanu R, Pigani L, Pilo M I, Sanna G, Seeber R, Spano N, Terzi F, Zucca A. 'Electrochemical and spectroelectrochemical characterisation of poly(3'-hydroxymethyl-2,2':5',2''-terthiophene'. *Synthetic Metals*, **156**, (2006), 984-989.

-
174. Aoki S, Imanishi K, Satoh M, Yasuda Y, Tsushima R. 'Solvent effect on electrochemical polymerisation of aromatic compounds'. *Electroanalytical Chemistry*, **242**, (1988), 203-208.
175. Diaz A F, Castillo J I, Logan J A, Lee W-Y. 'Electrochemistry of conducting polypyrrole films'. *Electroanalytical Chemistry*, **129**, (1981), 115-132.
176. Marque P, Roncali J, Garnier F. 'Electrolyte effect on the electrochemical properties of poly(3-methylthiophene) thin films'. *Electroanalytical Chemistry*, **218**, (1987), 107-118.
177. Sahin E, Sahmetlioglu E, Akhmedov I M, Tanyeli C, Toppare L. 'Synthesis and characterisation of a new soluble conducting polymer and its electrochromic devices'. *Organic Electronics*, **7**, (2006), 351-362.
178. Sezai Sarac A, Evans U, Serantoni M, Clohessy J, Cunnane V J. 'Electrochemical and morphological study of the effect of polymerization conditions on poly(terthiophene)'. *Surface and Coatings Technology*, **182**, (2004), 7-13.
179. Lukachova L V, Shkerin E A, Puganova E A, Karyakina E E, Kiseleva S G, Orlov A V, Karpacheva G P, Karyakin A A. 'Electroactivity of chemically synthesized polyaniline in neutral and alkaline aqueous solutions. Role of self-doping and external doping'. *Electroanalytical Chemistry*, **544**, (2003), 59-63.
180. Garnier F, Tourillon G. 'Effect of dopant on the physicochemical and electrical properties of organic conducting polymers'. *Physical Chemistry*, **87**, (1983), 2289-2292.
181. Faid K, Leclerc M. 'In situ conductivity and spectroelectrochemistry of asymmetrically disubstituted polybithiophenes: a multistep behaviour'. *Chem. Mater.*, **6**, (1994), 107-109.
182. Guay J, Kasai P, Diaz A. 'Chain-length dependence of electrochemical and electronic properties of neutral and oxidized soluble α,α -coupled thiophene oligomers'. *Chem. Mater.* **4**, (1992), 1097-1105.
183. Wang R S, Wang L M, Fu Y J, Su Z M, 'The influence of different substituent on polymer self-doping substituent property'. *Synthetic Metals*, **69**, (1995), 1713-1714.
184. Wallace G G, Spinks G M, Kane-Maguire L A P, Teasdale P R. 'Conductive electroactive polymers, intelligent materials systems'. Second edition, CRC Press LLC, (2003), 66.
185. Patil A O, Ikenoue Y, Basescu N, Colaneri J, Wudl F, Heeger A J. 'Self doped conducting polymers'. *Synthetic Metals*, **20**, (1987), 151-159.

-
186. Ikenoue Y, Uotani N, Patil A O, Wudl F, Heeger A J. 'Electrochemical studies of self-doped conducting polymers: verification of the 'cation-popping' doping mechanism'. *Synthetic Metals*, **30**, (1989), 305-319.
187. Sander L M. 'Fractal growth processes'. *Nature*, **322**, (1986), 789-793.
188. Li F, Albery J. 'A novel mechanism of electrochemical deposition of conducting polymers: two dimensional layer-by-layer nucleation and growth observed for poly(thiophene-3-acetic acid) *Electrochimica Acta*, **37**, (1992), 393-401.
189. Sawada Y, Dougherty A, Gollub J P. 'Dendritic and fractal patterns in electrolytic metal deposits'. *Physical Review Letters*, **56**, (1986), 1260-1263.
190. Kontturi K, Pohjakallio M, Sundholm G, Vieil E. 'Potential controlled electrosynthesis of poly(thiophene-3-methanol): application of the two-dimensional layer-by-layer nucleation and growth model'. *Electroanalytical Chemistry*, **384**, (1995), 67-75.
191. Matsushita M, Sano M, Hayakawa Y, Honjo H, Sawada Y. 'Fractal structures of zinc metal leaves grown by electrodeposition'. *Physical Review Letters*, **53**, (1984), 286-289.
192. Arrigan D W M, Gray D S. 'Electrochemical study of electroactive reagent retention in overoxidised polypyrrole films'. *Analytica Chimica Acta*, **402**, (1999) 157-167.
193. Schuhmann W. 'Electron-transfer pathways in amperometric biosensors. Ferrocene modified enzymes entrapped in conducting polymer layers'. *Biosensors and Bioelectronics*, **10**, (1995), 181-193.
194. Park J, Kyu Kim H, Son Y. 'Glucose biosensor constructed from capped conducting microtubules of PEDOT'. *Sensors and Actuators B*, **133**, (2008), 244-250.
195. Roncali J, Yassar A, Garnier F. 'Electrochemical synthesis of highly conducting poly(thiophene) thin films'. *Synthetic Metals*, **28**, (1989), 275-280.
196. Guilbault G G. 'Analytical uses of immobilized enzymes'. Marcel Dekker, INC New York, (1984), 33.
197. Guilbault G G. 'Analytical uses of immobilized enzymes'. Marcel Dekker, INC New York, (1984), 114.
198. Fabiano S, Tran-Minh C, Piro B, Dang L A, Pham M C, Vittori O. 'Poly 3,4-ethylenedioxythiophene as an entrapment support for amperometric enzyme sensor'. *Materials Science and Engineering C*, **21**, (2002), 61-67.

- 199.Yildiz H B, Toppare L. 'Biosensing approach for alcohol determination using immobilized alcohol oxidase'. *Biosensors and Bioelectronics*, **21**, (2006), 2306–2310.
- 200.Yildiz H B, Kiralp S, Toppare L, Yagci Y. 'Immobilization of tyrosinase in poly(ethyleneoxide) electrodes and determination of phenolics in red wines'. *Reactive & Functional Polymers*, **63**, (2005), 155–161.
- 201.Guilbault G G. 'Analytical uses of immobilized enzymes'. Marcel Dekker, INC, New York, (1984), 96-97.
- 202.Hauser M, Oelichmann J. 'A critical comparison of solid state preparation techniques in infrared spectroscopy'. *Mikrochimica Acta*, **1**, (1988), 39-43.
- 203.Rintoul L, Panayiotou H, Kokot S, George G, Cash G, Frost R, Bui T, Fredericks P. 'Fourier transform infrared spectrometry: a versatile technique for real world samples'. *Analyst*, **123**, (1998), 571–577.
- 204.Cosnier S. 'Biomolecule immobilization on electrode surfaces by entrapment or attachment to electrically polymerized films. A review'. *Biosensors and Bioelectronics*, **14**, (1999), 443-456.